# New Tools for Target Identification by Affinity Chromatography


**Felicetta Landi**

A thesis submitted for the degree of

Doctor of Philosophy

University of Edinburgh

**February 2011**

## Contents

## Declaration

This thesis is submitted in part fulfilment of the requirements for the degree of Doctor of Philosophy at the University of Edinburgh. Unless otherwise stated the work described in this thesis is original and has not been submitted previously in whole or in part for any degree or other qualification at this, or any other university. In accordance with the regulations this thesis does not exceed 70,000 words in length.

Felicetta Landi

## Acknowledgements

I would like to thank Dr. Alison N. Hulme for her supervision and encouragement throughout my PhD and for proofreading this manuscript. Coping with young children and a research group at the same time must be a really arduous job!

Many thanks to the other people who proofread parts of this document: Emiliano, Tendai, Paul, Sarah and the hippo.

I'm extremely grateful to all the people who made these last three years in UK very enjoyable. In this country, I learnt that the seasons are not necessarily 4 and above all I discovered the fine art of queuing.

Thanks to all the past members of the Hulme group: Dr. Odile Meyer, Dr. Sandra Fanjul, Dr. Philip Dorgan, Dr. Lauren Donaldson and Dr. Emiliano Gemma. Emiliano, I honestly spent all my first year fighting with you and the rest of my PhD missing you!
Big thanks to all the current members of the Hulme group: Helen, Nico, sugar Sarah, Kevin, Heather, Lore and especially to my fellow 4$^{th}$ year PhD students Jill and Sarah, it has been tough girls, but we made it!

I would like to express my gratitude to my fabulous supramolecular friends: the Leigh group. Guys, you are the best neighbours ever! Many thanks to: Aurelien, Bea, Victor, Adam, Ara, the Lewandowskis, Marcus, Jhenyi, Kathleen, Sarah & Max von Delius and Paul for all your kindness and the great nights out! Special thanks to Dr. Marius Kroll, Dr. Armando Carlone and Dr. Daniel D' Souza for helping me keeping my fume hood in one piece during my PhD.

Many thanks to Conny Johansson for helping me with the preliminary affinity experiments and to the Barlow group for letting me use their facilities. Conny, I had the most fun working with you, all the best for your new job!

I would like to thank our NMR hero: Juraj Bella. Thanks for all the help with running the NMR of the agarose gels and for being always so approachable even when busy. Thanks for the weekly Badminton games and for having such a lovely wife, Slata. You are probably the kindest people I met here in Edinburgh!

Thanks to the methodology dudes, the Lam group for their kindness and for the great chats at lunch time (often about organic materials?!): Charlene, Sam, Serghei, Graham, Darryl, Aakarsh, Donna, Yi, Claire and Mairi and Benoit and Myriam. Special thanks to Benoit and Darryl for running my samples at the chiral HPLC. Many thanks to Myriam for being an awesome cook and a very nice person.

Many thanks to Dina, my Badminton mate, for the great chats and shopping sessions and Dr. Volfango Bertola for the coffee breaks and the nights out!

I also would like to thank my lovely flatmate and "wife" Mary. Thanks for being always so encouraging and a dynamic full of life person. Thanks for coping with me during my long, annoying "final year PhD student" phase.

Finally, I would like to thank my favourite scientist, Dr. Hippo, for being a controversial yet amazing person and for bringing into my life so much joy and IT skills.

## Abstract

The recovery of the selected biological material in affinity-based separations relies on reversing the biological interaction responsible for the binding. General elution methods which are independent of the bioaffinity interaction have attracted increasing attention. The first three chapters of this thesis describe the development of a novel “click” functionalised azobenzene-based linker for affinity-independent elution protocols and the preliminary affinity studies using this linker. Ligands functionalised with a bioorthogonal propargyl label were readily attached to the terminal azide of the linker using the copper(I) catalysed Huisgen cycloaddition (or "click" reaction). Following separation, the linker was cleaved under mild non-denaturing conditions using $Na_2S_2O_4$.

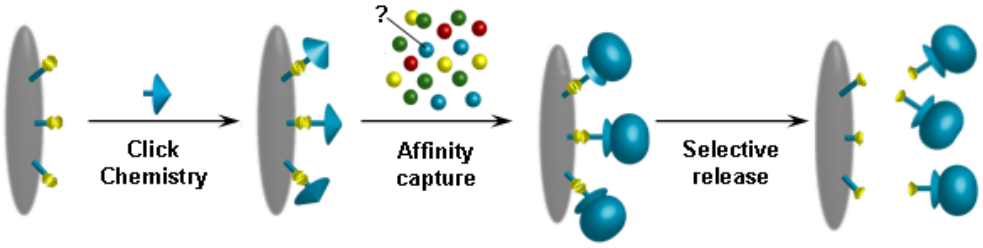


In the last three chapters a novel approach towards the synthesis of the 4-methyl proline fragment of the cytotoxic natural product bisebromoamide (a potential affinity target) is proposed.

**Bisebromoamide**

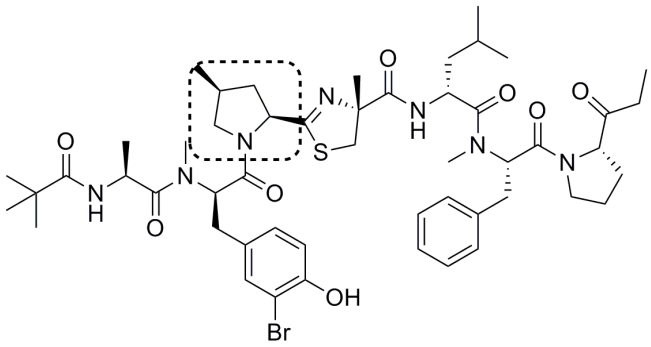


For the pyrrolidine ring construction an enamide-olefin ring-closing metathesis (RCM) approach has been attempted. The installation of the required absolute stereochemistry has been achieved using a phase-transfer catalyst for the enantioselective alkylation of Schiff bases derived from glycine esters.

# 1 Affinity Chromatography

## 1.1 Theoretical aspects

The term affinity chromatography is used to describe a procedure aimed at the purification of one or more components of a biochemical mixture, based on the reversible adsorption of biomolecules using highly specific biological interactions.[1] The technique is ideal for a capture or intermediate step in a purification protocol and can be used whenever a suitable ligand is available for the biomolecule of interest.[2] Biological interactions between a ligand and a target molecule can be a result of electrostatic or hydrophobic interactions, van der Waals' forces and/or hydrogen bonding. To elute the target molecule from the affinity medium the interaction has to be reversed, either specifically using a competitive ligand, or non-specifically, by changing the pH, ionic strength or polarity of the mobile phase. Successful affinity separation requires a biospecific ligand that can be covalently attached to a chromatography matrix. The coupled ligand must retain its specific binding affinity for the target molecule(s) and, after washing away unbound material, the binding between the ligand and target molecule(s) must be reversible to allow the target molecule(s) to be removed in an active form (Fig. **1**). Enzyme/substrate or inhibitor; antibody/antigen or virus; lectin/polysaccharide or glycoprotein; nucleic acid/ complementary base sequence or histones; hormone or vitamin/receptor or carrier protein are among the most frequently used biological interactions in affinity chromatography. Although most of the ligands are of biological origin, the term "affinity chromatography" has also been used over the years to describe some chromatography matrices that contain selective ligands of non-biological origin. Terms such as "bioaffinity chromatography" and "biospecific adsorption" are occasionally used to specify that the affinity ligand is biological in nature.[3] The type of ligand can be used to divide affinity techniques into various subcategories, for example lectin, immunoaffinity,[4] dye ligand, and immobilised metal ion affinity chromatography.

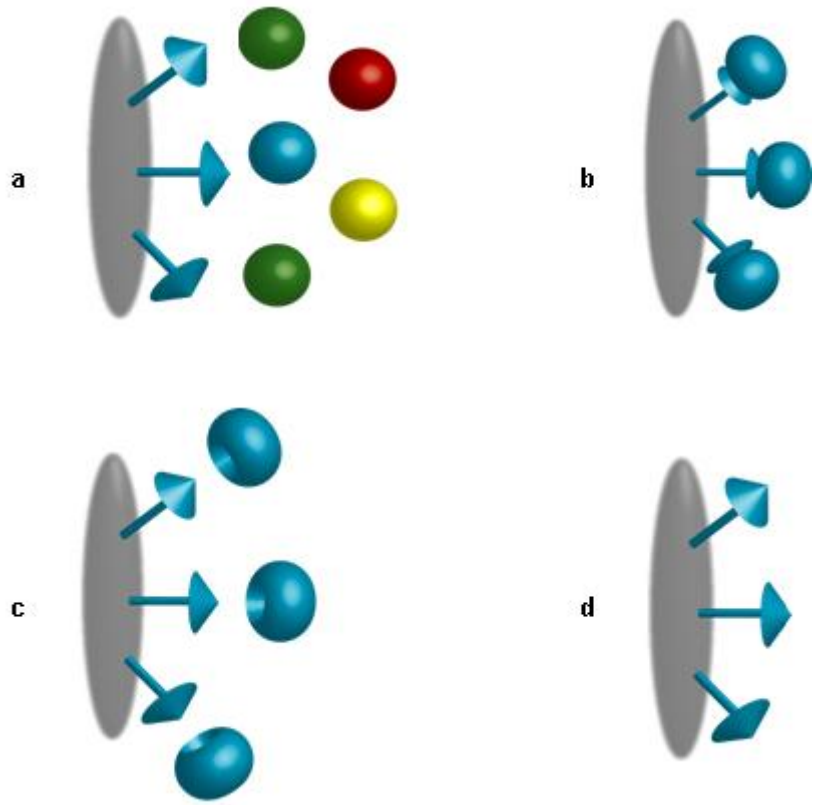


**Figure 1**: A classical affinity chromatography separation. (a) Sample is applied under conditions that favour specific binding of the target biomolecule(s). (b) Target substances bind specifically, but reversibly, to the ligand while unbound material washes through the column. (c) Target protein is recovered by changing conditions to favour elution of the bound molecules. Elution is performed specifically, using a competitive ligand, or non-specifically, by changing the pH, ionic strength or polarity. Target protein is collected in a purified, concentrated form. (d) The affinity medium is re-equilibrated with the binding buffer.

## 1.2 Biomolecular interactions and affinity chromatography

The chemistry of biological interactions involves a variety of mostly non-convalent interactions between reactive groups in the receptor and the ligand. The sum total of the energy contribution of the various forces to the overall stability of the complex receptor-ligand determines the dissociation constant ($K_d$), or affinity of the binding. The dissociation constant is defined by the following equation:[5]

$$K_d = \frac{[A]\,[B]}{[AB]}$$

In which $K_d$ is the dissociation constant and A is for instance an antibody, B an antigen and AB the complex formed between them. Binding affinity is also influenced by solid support characteristics as well as the activity and functional availability of the solid phase-bound protein such that the $K_d$ values for affinity chromatography varies between $10^{-3}$ and $10^{-7}$ M.[5] Both the chemical and mechanical properties of the solid phase are important in this regard. Non-specific interactions between the solid phase and the ligand are inconsistent and unpredictable, hence complicating the elution profiles. On the other hand, the physical structure of the solid phase polymer may sterically hinder effective interaction between free proteins and the immobilised ligand even at high $K_d$ values. Both of these problems can be significantly reduced by the prudent use of inert spacer arms.

## 1.3 Components of an affinity medium

An affinity-based separation system typically consists of a matrix (stationary phase), a spacer arm and one of the two members of the interacting pair, the ligand (Fig. **2**).[2]


**Figure 2**: Physical components of an affinity medium. (a) The matrix is designed for ligand attachment. A matrix should be chemically and physically inert. (b) The spacer arm is used to improve the binding between the ligand and the target molecule by overcoming any effects of steric hindrance. (c) The ligand is a molecule that binds reversibly to a specific target molecule (Figure from ref. 2).

### 1.3.1 The matrix

The matrix is an inert support to which a ligand can be directly or indirectly coupled.[2] Since the success of affinity chromatography relies on specific interactions, extremely low non-specific adsorption to the solid support is required. A suitable matrix for affinity chromatography will offer an open pore structure for high capacity binding even for large biomolecules, stability under a range of experimental conditions (*e.g.* pH, detergents) and good flow properties for rapid separation. Sepharose, a cross-linked sugar polymer of agarose, possesses many of these properties (Fig. **3**).[6] Hydroxyl groups on the sugar residues are easily derivatised for covalent attachment of a ligand, providing an ideal platform for the development of affinity media.[2]

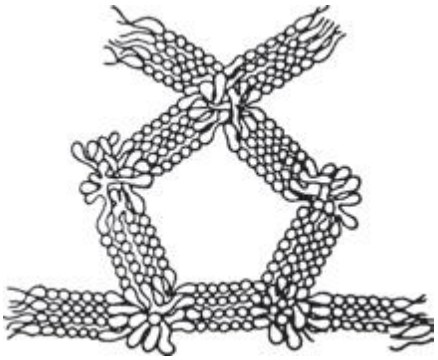

**Figure 3**: Structure of agarose gel (Figure from ref. 2).

In affinity chromatography the particle size and porosity are designed to maximize the surface area available for ligand coupling and binding of the target molecule. A small mean particle size with high porosity increases the surface area. Increasing the degree of cross-linking of the matrix improves its chemical stability. In this way, a more rigid matrix is generated which can tolerate potentially harsh elution and withstand high flow rates.[2]

### 1.3.2 The ligand

The ligand is the molecule that binds reversibly to a specific molecule or group of molecules, enabling purification by affinity chromatography.[2] The selection of the ligand for affinity chromatography is influenced by two factors: the ligand must exhibit specific and reversible binding affinity for the target substance and have chemically modifiable groups that allow attachment to the matrix without destroying the binding activity.[7] It is important to consider the region of the ligand that will be used for attachment to the matrix. For example, many proteins have several equally reactive groups through which coupling can take place resulting in a random orientation of the ligand on the matrix. This phenomenon may result in a reduction of the number of ligand molecules that are available in the correct orientation.

### 1.3.3 Spacer arm

The binding site of a target protein is often located deep within the molecule and an affinity medium prepared by coupling small ligands, such as enzyme cofactors, directly to the matrix may exhibit low binding capacity due to steric interference *i.e.* the ligand is unable to access the binding site of the target molecule (Fig. **4**, a).[2] In order to facilitate an effective binding an inert "spacer arm" is interposed between the matrix and the ligand. Spacer arms must be designed to maximize binding, but to avoid non-specific binding effects. In figure **4** (b) is shown how the spacer arm creates a more effective environment for the interaction.[8]

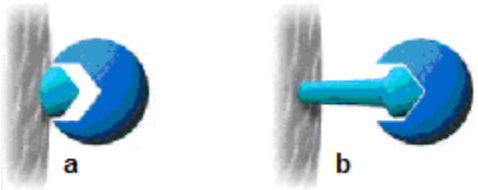


**Figure 4:** The importance of the attachment of the ligand molecule *via* an inert spacer arm (Figure from ref. 2).

The length of the spacer arm is critical. If it is too short, the arm is ineffective and the ligand fails to bind substances in the sample. On the other hand, too long a spacer could favour non specific binding affecting the selectivity of the separation.[2]

## 1.4 Main applications

Over the last 20 years, over 40,000 published articles have described or discussed affinity chromatography techniques. The affinity separation technique has registered an extraordinary development making it no longer only a research tool but also an interesting method from an industrial perspective.[9] From the wide variety of applications of this technique a classical immunoaffinity separation will be briefly described, and some examples of the ever increasing number of applications of affinity chromatography in the field of proteomics and target identification will be given.

### 1.4.1 Immunoaffinity chromatography

Immunoaffinity chromatography adds the selectivity and specificity of an immunological reaction to affinity separation.[4] This specialised form of affinity chromatography uses an immobilised antibody or antigen as the ligand and the selective separation comes about through immunological reactions (Fig. **5**). One of the interacting partners is typically attached to a matrix (*e.g.* polyacrylamide, dextran, rigid plastic beads). Immunoaffinity was first described by Campbell *et al*.,[10] who used diazotised aminobenzyl cellulose to immobilise an antigen for subsequent isolation of specific antibodies. Although most immunoaffinity separations are performed using a low pressure system, the development of suitable support media has allowed the principles of high performance liquid chromatography (HPLC), to be applied to immunoaffinity chromatography. This technique is known as high performance immunoaffinity chromatography (HPIAC).[11]

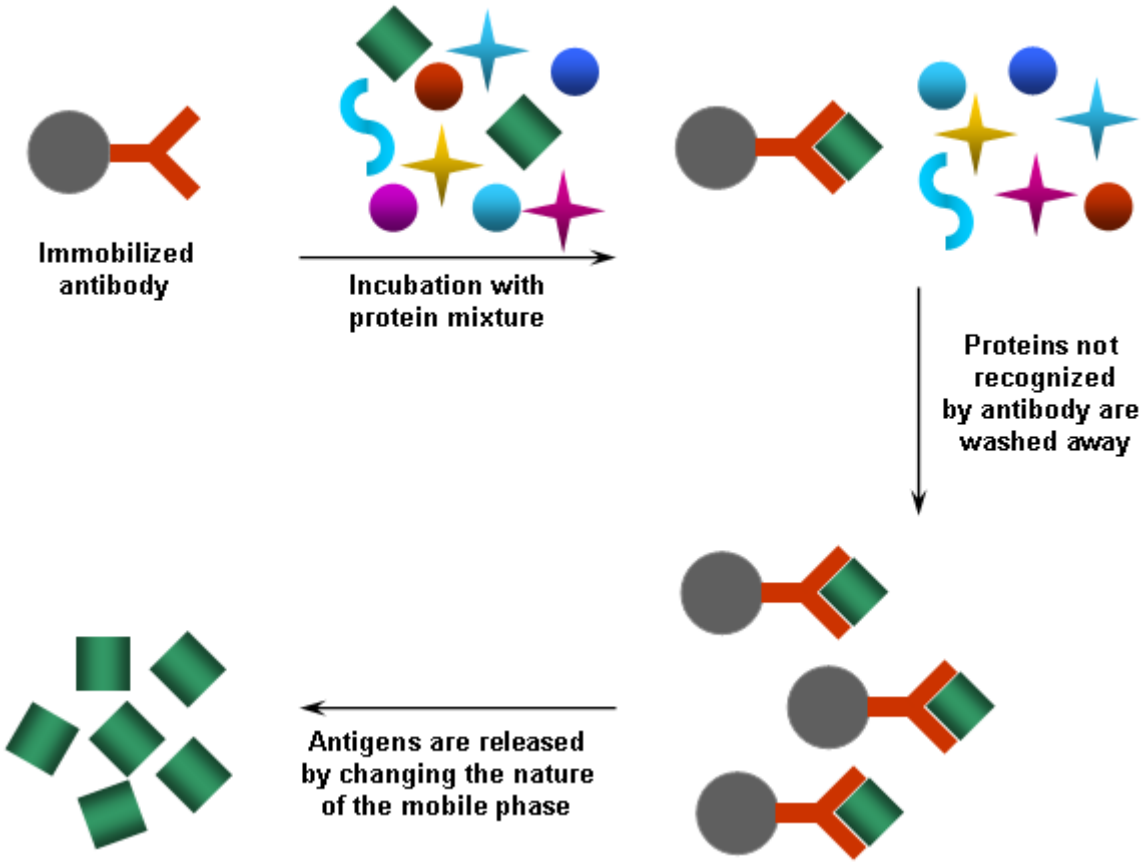


**Figure 5:** An immunoaffinity chromatography separation.

The introduction of monoclonal antibodies has greatly advanced the application of IAC techniques especially in the area of membrane biochemistry.[4] Many monoclonal antibodies have been raised against intact receptors, their subunits, and a wide variety of membrane proteins and glycoproteins. An antibody-coated matrix is packed into a column and a solution containing the specific antigen is passed over the matrix, the antigen is captured and retained while the unreactive material passes through the column in the mobile phase. The antigen is released and recovered by changing the nature of the mobile phase in such a way that dissociation of the immobilised antibody-antigen complex is achieved. Once the complex is fully dissociated, the antigen is released into the mobile phase and passes through the column where it is collected.

### 1.4.2 Proteomics

Since the mid-1990s proteomics (the complete analysis of the protein complement of a cell or an organism, the proteome) has rapidly grown in importance as a discipline in the life sciences.[12] Mass spectrometry (MS), plays a central role in proteomics research, especially since the introduction of techniques such as electrospray ionisation (whose discovery was awarded by the Nobel prize in 2002) and laser desorption/ionisation (LDI). These so called "soft ionisation techniques" have laid the foundations for the modern MS analysis of proteins and peptides.[12] Proteomics has two well recognised branches, namely compound-centric chemical (CCCP) and activity-based probe profiling (ABPP) proteomics (Scheme **1**).[13] CCCP focuses on gaining a better understanding of the molecular mechanism of a biologically active small molecule. Careful choice of the matrix for the preparation of molecular probes for CCCP is required (Scheme **1**). Such a matrix should not interfere with the bioactivity of the target compound in order to successfully investigate the molecular mechanism of action of a certain biomolecule (with a known binding partner). The solid-supported target is then incubated with the appropriate biological extract. Captured proteins are eluted and processed by either SDS-PAGE or by a "gel-free" approach. Following trypsin digestion, the peptides obtained are subjected to MS analysis and identification (bioinformatics). ABPP proteomics is usually focused on the investigation of classes of proteins (enzymes) which are related by their role in a specific condition (*e.g.* a disease). In scheme **1** the two methodologies are directly compared.[13] An ABP typically consists of a reactive warhead, a spacer (linker) and a reporter tag (*e.g.* biotin), which is necessary for the subsequent affinity chromatography step. Upon incubation of this activity-based probe with the cell lysate of interest, targeted proteins are captured on an affinity matrix and digested with trypsin for MS analysis. At this stage, protein database screening and bioinformatics analysis can take place.

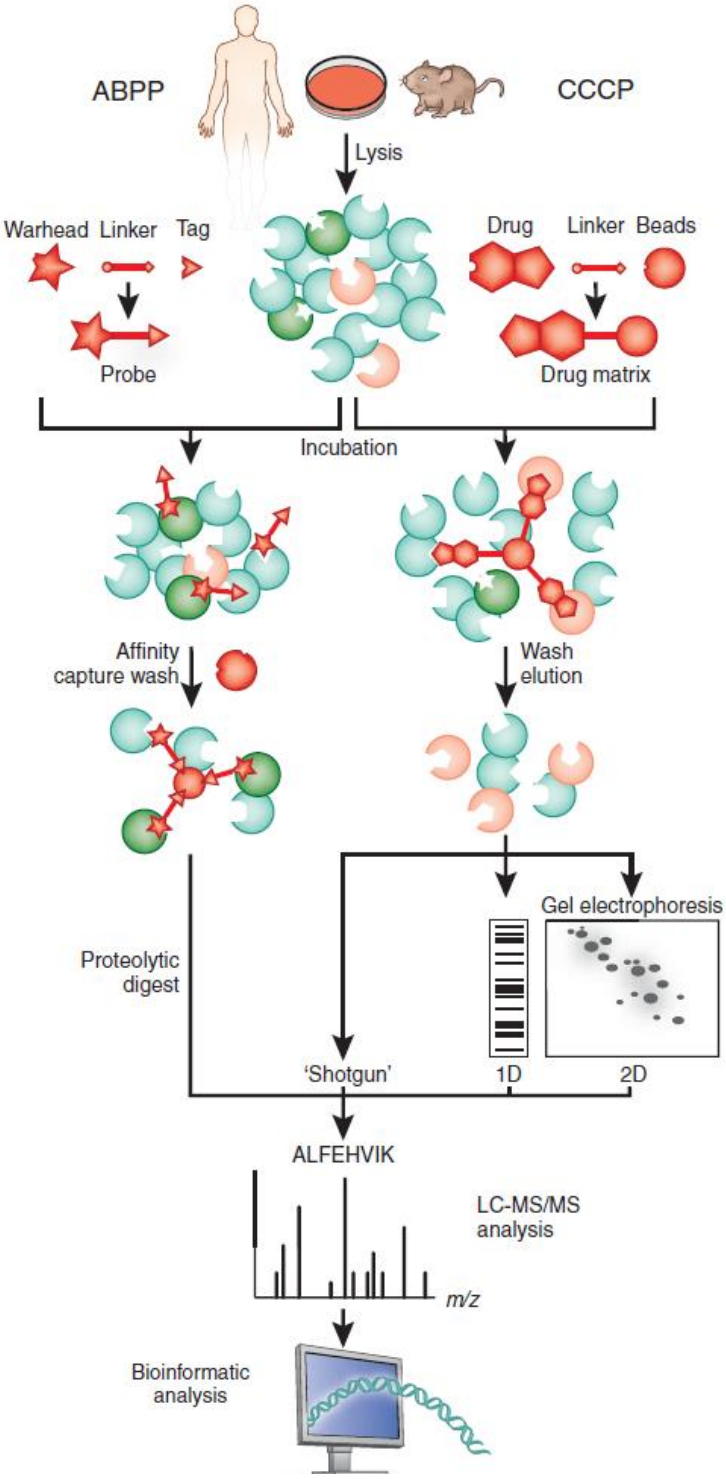


**Scheme 1**: Comparison of activity based probe profiling (ABPP) and compound-centric chemical proteomics (CCCP, scheme from ref. 13).

#### 1.4.2.1 Compound-centric chemical (CCCP) proteomics

Generally, CCCP proteomics makes use of the same principle of the classical drug affinity chromatography techniques, but can benefit from high-resolution mass spectrometry (MS) for analysis and bioinformatics for identification;[13] both forms of analysis have advanced dramatically in recent years.[13] Together with electrospray and nano-electrospray ionisation methods in MS, breakthroughs certainly have included isotope labelling (for quantification) and the ever increasing availability of databases of proteins. In the description of the CCCP approach, it was anticipated that the analysis of the molecules takes place straight after trypsin digestion, which generates a series of peptides. Three pieces of information are required for each peptide: its mass and the list of its fragments (for identification) and the ion intensity (for quantification).[14]

Among several types of mass spectrometers, the most common apparatuses used in proteomics are quadrupole time-of-flight (TOF) and hybrid linear ion trap-orbitrap instruments.[15] In TOF based instruments, separation of the peptide ions occurs depending on their arrival at the detector. In the orbitrap mass analyser, Fourier transformation of the measurement of the frequency of peptide ions oscillating in the trap generates the mass spectrum. For both configurations, MS resolution is fundamental as many peptide ions elute from the chromatographic column at the same time.[15]

A plethora of methodologies is also available for the fragmentation of the peptides. Usually, they are collided with an inert gas, (collision-induced dissociation, CID).[16] In ion trap mass spectrometers peptide ions are excited by an electric field which leads to fragmentation mainly through peptide bond cleavage. In quadrupole TOF instruments, the quadrupole serves as a mass filter allowing through only ions with a specific mass-to-charge (*m/z*) ratio. A TOF spectrum of the ions is obtained straight after fragmentation in the collision chamber.

Isotope labelling has allowed highly accurate quantitative analyses for thousands of proteins as well as post-translational modifications (PTMs), which were previously impossible relying only on MS techniques.[17] To ensure accuracy of the analysis of a proteome, two proteomes of the same type need to be differentially isotopically labelled.

Among the amino acid-specific tagging strategies, the majority are directed towards cysteine residues.[12] Cysteine is widely used because of the presence of a thiol group that can be easily modified and its relatively low abundance (only 1.1%) across several species.[12] In 1999 Aebersold *et al*. reported the first isotope-coded affinity tag (ICAT).[18] The protocol had an enormous impact as this molecule became commercially available soon after its introduction. The tag consisted of a cysteine-reactive iodoacetyl group that allowed the specific attachment of the label to the thiol group of the Cys side chain and a polyether linker (the isotope-coded region, Fig. **6**).

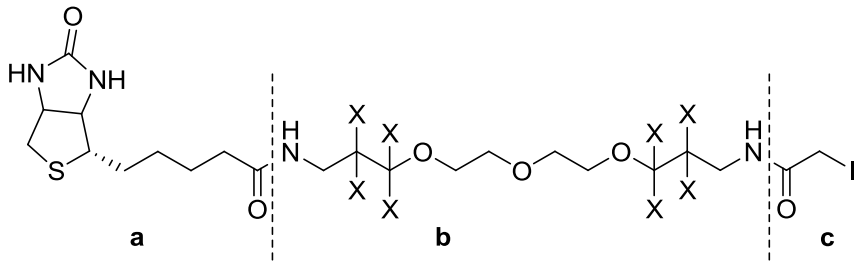


**Figure 6**: Structure of the first ICAT reagent. (a) The biotin moiety which allows enrichment by biotin-avidin affinity chromatography. (b) An isotope-coded linker region, using hydrogen (X = H) or deuterium (X = D). (c) A thiol-reactive iodoacetamide group that allows alkylation of cysteine residues.

The reagent is available in two forms, the light form (normal) containing eight hydrogen atoms and the heavy form (labelled) containing eight deuterium atoms. The polyether linker is directly connected to a biotin moiety, allowing affinity separation.[18]

Stable isotope labelling by amino acids in cell culture (SILAC) is one example of a modern labelling strategy which generally uses Arg and Lys labelled with the stable $^{13}C$ isotope and/or $^{15}N$ isotope.[19] In this type of metabolic labelling the cells incorporate the isotopic label as part of their biosynthesis. The value of the known molecular weight difference between the 'light' (normal) and 'heavy' (labelled) amino acid that is used during the growth of the two cell populations is fundamental for recognising the two proteomes. The ease of use and the accuracy achieved has rendered SILAC the method

of choice in MS-based signalling research and its use has recently been extended to small mammals and human tumour tissues.[20]

The most popular chemical labelling technique uses an isobaric tag for relative and absolute quantification (iTRAQ). In this approach the N-terminus and the Lys residues are enriched with a chemical group (Fig. **7**, a).[21] The chemical differentiation is apparent only in the final spectrum of the fragmented peptide ions (Fig. **7**, b).

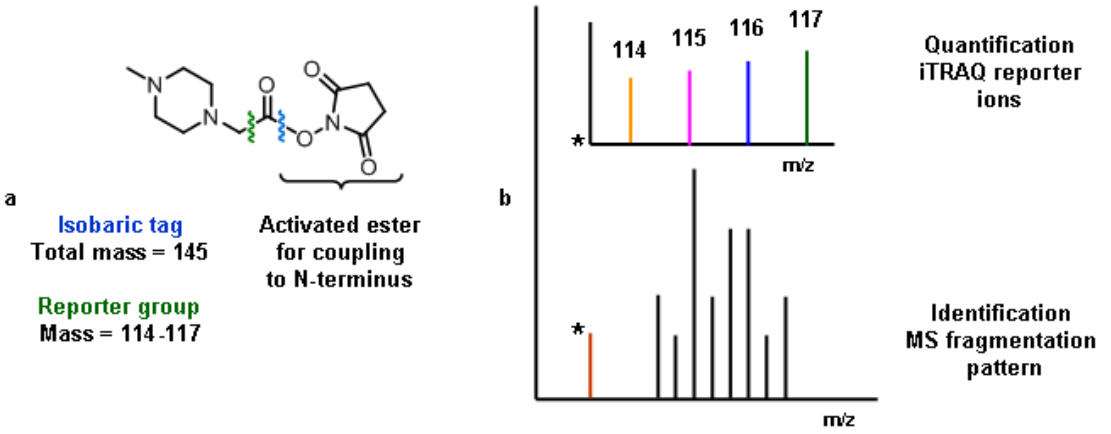


**Figure 7**: Isobaric tag for relative and absolute quantification (iTRAQ). (a) iTRAQ reagent; (b) Identification and quantification of iTRAQ-labelled peptides.

### 1.4.2.2 Applications of CCCP

Among the wide variety of applications of chemical proteomics, two recent examples of successful investigations targeting kinase inhibitors and natural products deserve particular mention.[13] Protein kinases are currently receiving much consideration, as drug targets, because of their role in a wide range of pathologies (*e.g.* oncology, autoimmune disorders).[22,23] Indeed, various kinase inhibitors have entered clinical trials in recent years.[13] Several protocols for the investigation of their activity are currently available (*e.g.* kinase activity assays). All these large-scale approaches provide important information but they need to be completed with parallel proteomics studies. Importantly, chemical proteomics can be performed in disease-relevant cells; hence the underlying

mechanism of action of a particular kinase inhibitor can be more intimately investigated. Recently the complete target profiling of BCR-ABL tyrosine kinase inhibitor imatinib (Gleevec®) and the second-generation drugs nilotinib (Tasigna®), dasatinib (Sprycel®) and bosutinib (SKI-606), which are in clinical use or in late-stage clinical trials for chronic myeloid leukemia, have been reported.[24] In this study, Bantscheff *et al*. made use of a new technology which consisted of using a solid-supported non-specific kinase inhibitor ("kinobeads") together with a specific kinase inhibitor in the solution phase for a crossed investigation of their targets.[24] These investigations led to a greater understanding of the molecular mechanism of these compounds and to the discovery of new targets for these drugs (*e.g.* for imatinib and nilotinib: the receptor tyrosine kinase DDR1 and the oxidoreductase NQO2, which is the first non-kinase target of these compounds).[24,25]

The second application of note is the role of chemical proteomics in the investigation of biologically active natural products. Despite great efforts of the synthetic community, the structural diversity and complexity of natural products is still unmatched by their synthetic counterparts.[13] Furthermore, most newly-isolated natural products are often tested mainly for their potential antibiotic and anticancer activity. Chemical proteomics has remarkably underlined the importance of a greater understanding of the molecular mechanism of such natural products as drugs or as specific tools for the alteration of biological pathways. This concept was nicely illustrated by investigations on the marine natural product, diazonamide A (Fig. **8**).[26]

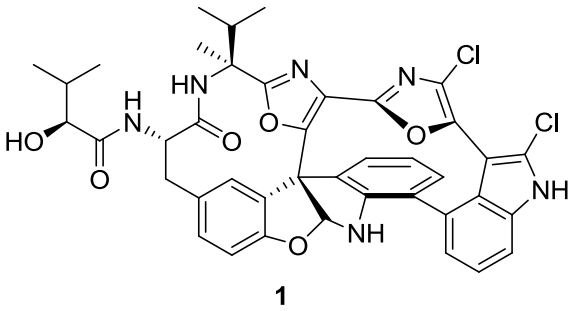


**1**

**Figure 8**: The natural product diazonamide A.

The use of chemical proteomics for the study of this antimitotic compound led to an important discovery about its target, ornithine δ-amino transferase. Interestingly, this enzyme was found to play an important role in mitotic spindle assembly and cell division.[26] The key to the successful target identification was the comparison of the eluate from diazonamide A with the one derived from a close but inactive analogue.[13]

1.4.2.3 Activity-based probe profiling (ABPP) proteomics

ABPP proteomics is a discipline that makes use of small molecules to tag and monitor a specific class of proteins within a complex proteome.[27] At the heart of the activity-based proteomics technologies are the small molecules which are designed to interact with active sites within proteins (usually enzymes).[13] In particular, in the so called mechanism-based ABPs (mainly based on irreversible enzyme inhibitors), the 'warhead' is electrophilic in nature and specifically reacts with catalytic residues in the enzyme active site. An alternative strategy consists of the use of photocross-linkers which can be conjugated to molecules that bind within an active site, resulting in the modification of potentially non-catalytic residues upon irradiation with UV light. In both approaches, the probe binds to the target enzyme in its active form. In the last few years, the strategies for tagging and detection in ABPP have rapidly flourished.[27] Among the tagging methodologies, the use of small molecule fluorophores have seen the greatest advances. The wide variety of commercially available fluorophores and their broad range of absorbance and emission spectra dramatically increased the scope of the application of this field of proteomics.

The most interesting aspect of this technology is, perhaps, the use of fluorescently labelled ABPs for direct imaging of labelled targets (using fluorescence microscopy) and the simplicity of detection in gel based read-outs. A plethora of fluorophores has been used for the preparation of ABPs. The most commonly employed compounds include fluorescein and rhodamine,[28] dansyl,[29] NBD[30] (nitrobenz-2-oxa-1,3-diazole), BODIPY[31] (dipyrromethene boron difluoride) and the cyanine (Cy)-dyes[32] (Fig. **9**). Fluorophores such as fluorescein and rhodamine are relatively cheap, but suffer

from rapid photobleaching (permanent loss of fluorescence), making them less suitable for imaging applications.

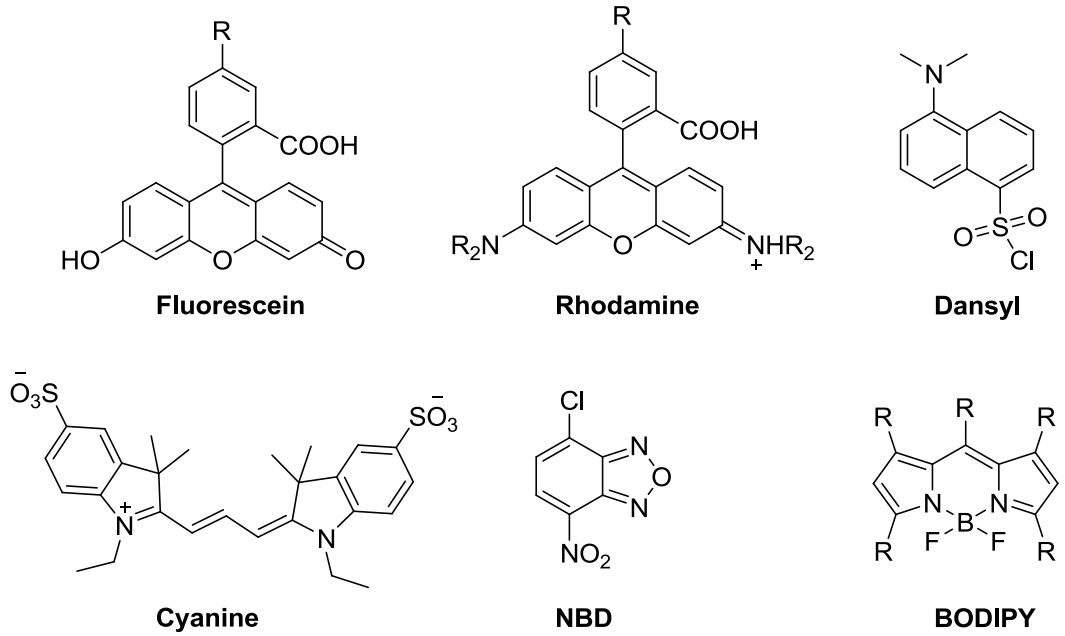


**Figure 9**: Structures of commonly used fluorophores for activity-based proteomics.

BODIPY and Cy-dyes generally guarantee better performances due to their intrinsic properties (*e.g.* high absorption coefficient, narrow absorption peaks) and, being hydrophobic in nature, freely penetrate cell membranes. However, the cost of this class of fluorophores limits their use to small-scale production of ABPs. Molecular probes featuring BODIPY as a fluorophore have been successfully employed for *in vivo* labelling of cysteine cathepsins in whole animals.[31] The encouraging advances of *in vivo* applications of this technology could be translated into new therapeutic imaging agents for use in human patients.[27]

Radio-isotopes have also been shown to be useful in activity-based proteomics. In particular, $^{125}$I has been incorporated into many classes of ABPs as it can be readily introduced following standard iodination methodologies for proteins and peptides.[31] The minimum structural requirement for the preparation of a radio-labelled ABP is the

presence of a phenol moiety (Scheme **2**). One of the most common iodination strategies is the introduction of $^{125}I$ in the *ortho* position in the presence of a radical initiator.

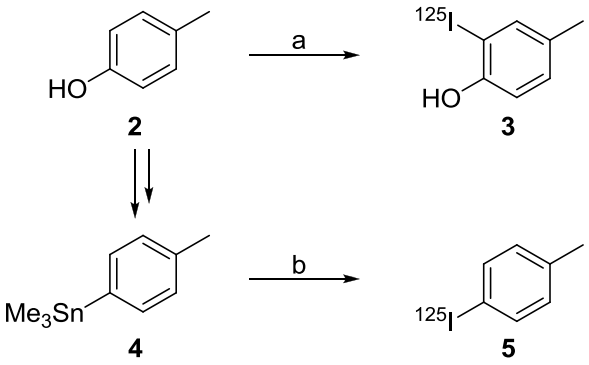


**Scheme 2**: Methods for iodination of phenolic functions facilitated by Iodo-Gen (a), $Na^{125}I$, and chloramine-T, $Na^{125}I$ (b).

Alternatively, the hydroxyl group can be converted into a trimethylstannyl functionality to facilitate the displacement by radioactive iodine in the presence of chloroamine-T (Scheme **2**). Tritium ($^3H$) is also employed, although its use is limited by its overall low specific activity (long exposure times required). The main advantages of this kind of probe are certainly the ease of preparation and detection together with the production of a high ratio of signal to background noise.[31] Furthermore, the size of these probes is quite small (compared to a fluorescent or an affinity tag), resulting in only minimal modification of the lead compound. However, the short half-life of $^{125}I$ does not allow the storage of these probes for long periods and, unlike affinity tags, the radiolabels do not provide a direct means for isolation. The main application of radio-labeled probes is monitoring changes in enzyme activity by analysis of labeled samples by 1D or 2D gel electrophoresis. Examples of *in vitro* applications of radio-labeled probes for profiling changes in activity have been reported for cysteine protease targets, including the cathepsins,[33] the proteasome,[34] and caspases.[33] In addition to radio-isotopes, stable isotopes (although designed for quantitative proteomics applications, *e.g.* ICAT, SILAC) potentially can be used for activity-based proteomics.

Affinity tags have found widespread application as they provide a practical

handle for isolation of the target protein. Biotin is the most common affinity tag due to its exceptional binding affinity with the protein streptavidin. The properties of these biomolecules will be discussed in connection with the preparation of the solid-supported biotin probes in chapter 2. While providing a reliable tool for the purification of isolated targets using a streptavidin-coated matrix, the biotin-labelled probes present a few problems, namely the low cell permeability and the need for harsh conditions for dissociation of the streptavidin/biotin complex. Short peptide sequences (recognised by specific antibodies) can also be employed as affinity tags. The first example of this type of tag was reported for probes that target deubiquitinating (DUB) enzymes.[35]

Important advances have been made in designing new strategies for "tandem labelling".[27] In this approach a chemical handle with orthogonal functionalities is inserted into the ABP. After binding with the target, a second "reporter" tag (*e.g.* a fluorophore tag for visualisation or an affinity tag for isolation) is covalently attached to the probe using highly specific bioorthogonal ligation chemistry. An example of an orthogonal reaction was reported by Bertozzi and colleagues (Scheme **3**).[36]

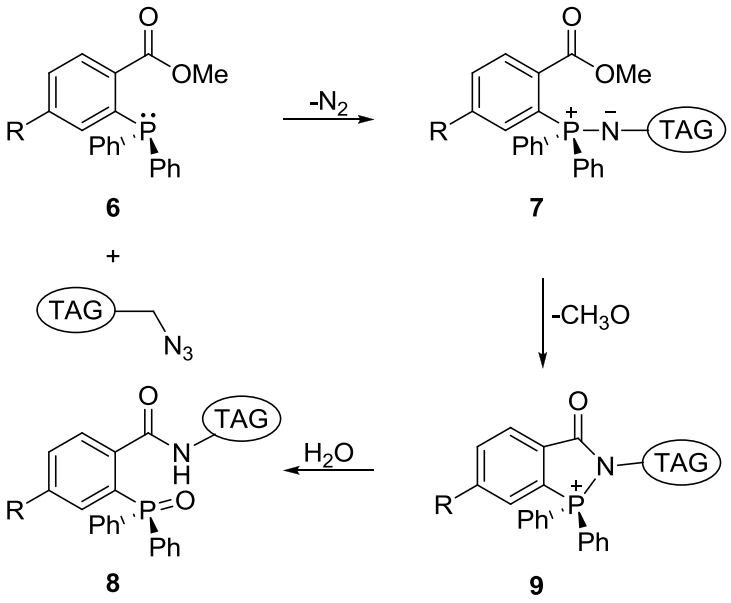


**6** + TAG–$N_3$ → **7** (-$N_2$); **7** → **9** (-$CH_3O$); **9** → **8** ($H_2O$)

**Scheme 3**: A modified Staudinger reaction that produces the stable covalent adduct **8**, in the presence of water as solvent.[36]

A modified Staudinger reaction was employed to tag carbohydrates on the cell surface. In this approach, a probe containing an azide functionality is reduced forming the unstable intermediate aza-ylide **7**. The aza-ylide intermediate rearranges, in aqueous media, to produce an amide linkage and the phosphine oxide (Scheme **3**).A second strategy for bioorthogonal ligation makes use of the most commonly employed reaction in bioconjugated systems, the copper(I)-catalysed Huisgen 1,3-dipolar cycloaddition reaction, also known as the "click" reaction.[37,38] The scope and the advantages of this reaction will be discussed in connection to the synthesis of solid-supported molecular probes in chapter 2.

1.4.2.4 Applications of ABPP

As outlined in section 1.4.2.3, the class of proteins (enzymes) targeted by ABPP proteomics are intimately related by their role in a disease. The most valuable application of this field of proteomics is in cancer research. There are currently ABPs for a multitude of enzyme classes, including many that have central roles in cancer.[39] Besides their use for the discovery of enzymes involved in cancerogenesis, they can be employed to image tumour development in living animals. Integrated with other proteomics methods, ABPs can lead to the mapping of entire proteolitic pathways. A series of fluorophosphonate probes that target the serine hydrolase superfamily have been successfully employed to discover several deregulated enzymes in cancer (Fig. **10**, **10**).[39] Indeed, thanks to these probes two uncharacterised serine hydrolases (KIAA1363[40,41,42] and monoacylglycerol lipase,[43] MAGL) have been found as enzymes highly expressed in aggressive human cancer cells and primary tumours. Using epoxide electrophile probes for cysteine proteases (Fig. **10**, **12**), Joyce and colleagues discovered that cathepsin activity is higher in angiogenic vasculature in carcinomas.[44,45] This finding was also confirmed by the fact that pharmacological inhibition of a wide range of cathepsins limited the tumour growth, vascularity and invasiveness. They also found that cysteine cathepsins are increased in cervical carcinomas induced by human papilloma virus (HPV).[45] ABPs have also been used for imaging enzyme activities

thanks to quenched near-infrared fluorescent activity based probes (qNIRFABPs) which can image cysteine protease activities in tumour xenografts *in vivo* and *ex vivo*.[46] These probes emit the fluorescent signal only after covalently modifying a specific protease target. Caspase-directed ABPs **11** can also be used to monitor small molecule inhibitors of protease targets both biochemically and by direct imaging methods. A variant of probe **11** has been used to detect apoptosis induced by the monoclonal antibody Apomab® in mice bearing xenografted human colorectal tumours.[47]

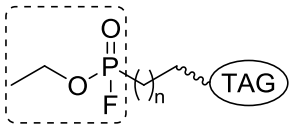


**Serine hydrolases**

**10**

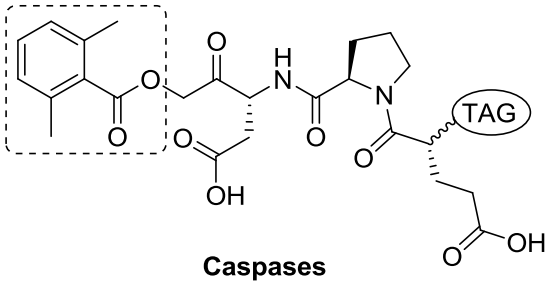


**Caspases**

**11**

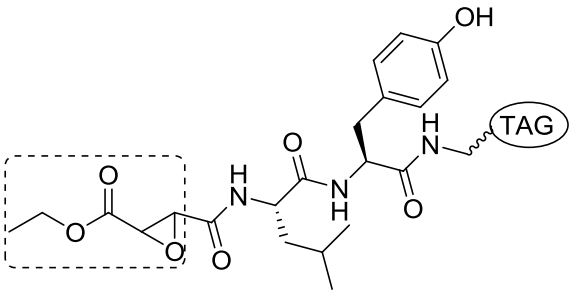


**Cysteine proteases**

**12**

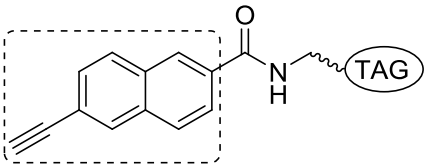


**Cytochrome P450s**

**13**

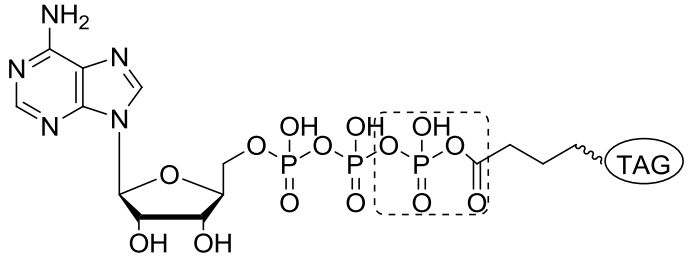


**Kinases**

**14**

**Figure 10**: Representative ABPs and their classes of target enzymes. The regions within the probes which interact with the binding site of the enzymes are highlighted.

The notable advances of ABPP and other proteomics disciplines are providing precious insights into the role of certain classes of enzymes involved in cancer. These enzymes could represent the next generation of cancer therapeutics.

### 1.4.3 Affinity chromatography & target identification

Perhaps one of the most notable early examples of the use of affinity chromatography for the identification of the binding partner of small molecules is furnished by the groundbreaking work of Schreiber *et al*.[48] The target of their investigations was to identify the binding proteins (immunophillins) within the signalling pathway in T lymphocytes, responsible for the biological activity of the immunosuppressant rapamycin and the structurally related macrolide FK506. The synthesis of agarose-based affinity matrices featuring either rapamycin or FK506 was performed and such molecular probes were incubated with an extract from the human T cell line Jurkat. The profiles of the captured proteins from both affinity matrices were remarkably similar, as confirmed by subsequent analyses (*e.g.* densitometry, SDS/PAGE mobility) while certain proteins seemed to belong to a previously unknown family of immunophillins, which included the novel immunophillin FK506 binding protein (FKBP).[48] The main accomplishment of this investigation was to ascertain that the predominant rapamycin binding protein in Jurkat T lymphocytes is FKBP, thus outlining the prominent role of this immunophillin in mediating the biological activity of this drug and the mutual inhibition of the two related compounds. Furthermore, the newly discovered immunophillins were used to gain further insights into the biological actions of these drugs.[48]

More recently, a photoaffinity probe has been successfully employed to investigate the mechanism of the inducible resistance of the glycopeptide antibiotic vancomycin.[49] The mechanism of action of this antibiotic consists of binding the side

chains of the virtually ubiquitous D-Ala D-Ala terminus in bacterial peptidoglycan, thus interfering with cell wall biosynthesis. Since the discovery of vancomycin resistance in 1998, numerous efforts have been made in order to elucidate the resistance mechanism in pathogens.[50] The expression of genes *vanH*, *vanA*, *vanX* is associated with high resistance to the molecule. Inducible expression of these genes is controlled by a two-component regulatory system, which consists of a transmembrane receptor histidine kinase, VanS and a cytoplasmic response regulator, VanR (Fig. **11**).[51]

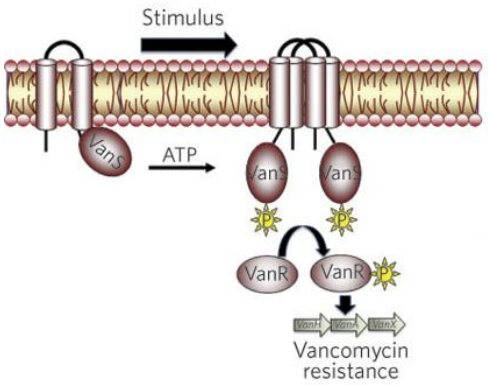


**Figure 11**: The regulatory system VanR and VanS responsible for vancomycin resistance (Figure from ref. 49).

Intriguingly, activation of this regulatory system could be either the result of direct binding of vancomycin to VanS or mediated by cell wall proteins accumulated as a result of antibiotic action. As there was little agreement about the nature of such activation, Wright's team decided to resolve this longstanding controversy by synthesising a vancomycin photoaffinity probe (VPP, Fig. **12**).[49] Molecular probe **15** consists of a benzophenone photoaffinity unit for covalent labelling of protein-probe complexes and a biotin tether for subsequent isolation (Fig. **12**). A series of preliminary screening experiments of the activity of VPP were carried out using VanS proteins from the actinomycetes *Streptomyces coelicor* (VanSsC), which are pathogens resistant to vancomycin. These investigations confirmed that the vancomycin derivative has a resistance profile comparable to the lead compound.[49] Incubation of membranes

expressing VanSsC isolated from *E. coli* with VPP, followed by irradiation, labelled a membrane protein whose molecular weight corresponds to the mass of VPP bound to VanSsC, thus confirming the formation of the protein-probe complex.

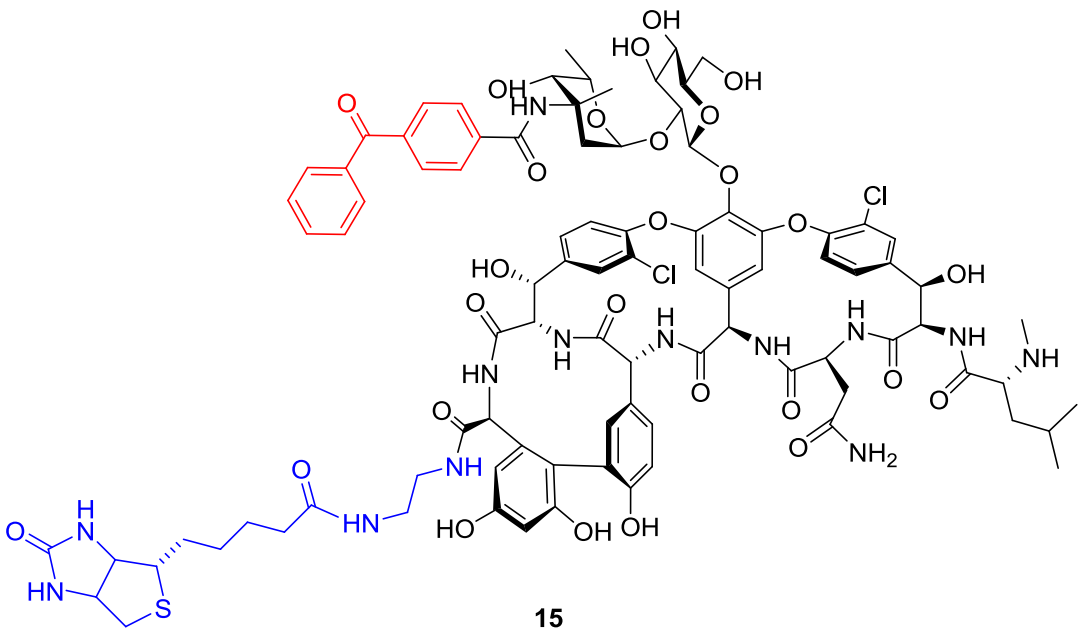

**15**

**Figure 12**: Vancomycin photoaffinity probe (VPP) consists of the vancomycin backbone (black) linked to a benzophenone photoaffinity label (red) and a biotin tether (blue).

### 1.4.4 Other applications

Although it is clear that affinity chromatography can be used in a variety of ways within biological, pharmaceutical and clinical chemistry, there remains plenty of room for further growth and development. Among contemporary applications and recent trends, affinity-based chiral separations, the so-called "metal chelate affinity chromatography" and dye-ligand affinity chromatography will be briefly discussed.

Because of the increasing interest in the pharmaceutical field for methods capable of discriminating between the individual chiral forms of drugs, the ability to quantify the different enantiomers of a drug, or its metabolites, is increasingly required

in therapeutic monitoring.[52] HPLC methods that include chiral stationary phases have been shown to be particularly valuable in the quantification and separation of chiral compounds.[53] As many of the ligands used in affinity chromatography are inherently chiral, these make them ideal stationary phases for these separations.

"Immobilised metal ion affinity chromatography", also known as "metal chelate affinity chromatography", is a widely employed purification methodology. In this purification protocol, the affinity ligand is a metal ion that is complexed with an immobilised chelating agent. Iminodiacetic acid is the most common chelating agent used, but carboxymethylaspartic acid, triscarboxymethylethylenediamine, tris(2-aminoethyl)amine, and dipicolylamine are also used.[52] The metal ions placed within these chelating groups are $Cu^{2+}$, $Zn^{2+}$, $Ni^{2+}$, $Co^{2+}$, or $Fe^{3+}$. This method separates proteins and peptides on the basis of interactions between certain amino acid residues (*e.g.* histidine, tryptophan, and cysteine) and the metal ions within the immobilised metal chelate (Fig. **13**). Since its discovery, several peptides, proteins, and amino acids have been purified by this method.[54,55,56]

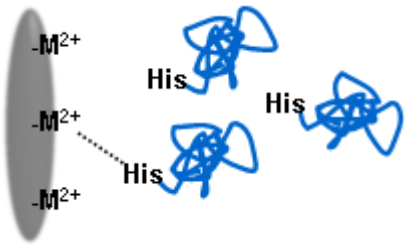


**Figure 13**: Schematic representation of the IMAC system. The affinity ligand (a metal ion complexed with an immobilised chelating agent) interacts with histidine residues within a protein in its native form.

"Dye-ligand affinity chromatography" makes use of synthetic dyes as ligands. Specific ligands used in this method include Cibacron Blue F3G-A, Procion Blue MX-3G or MX-R, Procion Red HE-3B, and Thymol Blue or Phenol Red.[3] Although these compounds are all synthetic in nature, they are still classified as affinity ligands because they interact with the active sites of many proteins and enzymes by mimicking the

structure of the substrates, cofactors, or binding agents for these biomolecules. For example, Cibacron Blue F3G-A (Fig. **14**, **16**) consists of a chlorotriazine ring that has several side groups attached; one of them is an anthraquinone moiety that specifically interacts with enzymes that have a binding site for $NAD^+$, $NADP^+$ or ATP. Some advantages of these dye ligands include their selectivity, the reproducibility of the separations and their ready availability.

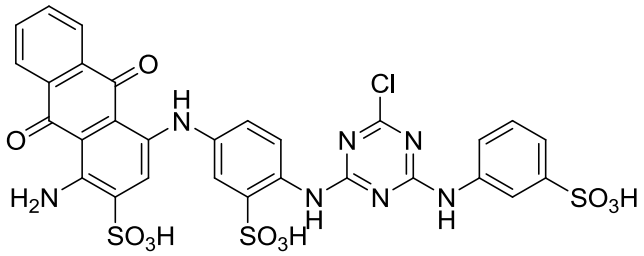


**16**

**Figure 14**: A common dye employed in affinity-based separation, Cibacron Blue F3G-A.

## 1.5 A linker-based approach to enhance elution conditions

Since the introduction of affinity chromatography as a practical laboratory tool in the 1960s, chromatographers have been faced with the question of how to retrieve the bound protein in maximum yield and (usually) in an active form. The subsequent years have seen many developments for solid phase matrices and also the introduction of a wide variety of elution buffers.[5]

### 1.5.1 An overview of potential elution buffers

The role of the elution buffer is to disrupt the interactions between receptors and ligands pushing the ligand back into the mobile phase in order to be collected. In selecting an elution strategy it is important to take into account the chemical effects of different

solutions. Buffers of extreme pH, such us glycine-HCl (pH 2.8) or high pH buffers, employing amines or ethanolamine for instance, disrupt ionic bonds.[57] With these solutions it is often recommended the use of a neutralizing buffer to prevent excessive denaturation of the proteins (Fig. **15**).


**Figure 15**: The use of harsh condition for the elution steps can cause denaturation of the isolated proteins.

Changes in ionic strength induced by high salt solutions also disrupt ionic bonds but can favour hydrophobic interactions.[5] Solutions of NaCl, $MgCl_2$, or LiCl (3-5 M, also saturated) are effective non-denaturing eluants that allow easy column regeneration with lower concentration salt.

Chaotropic ions (ions that favour interactions of non-polar groups with water) both disrupt the stability of the ligand in water and interfere with hydrophobic interactions (*e.g.* potassium isocyanate in a neutral buffer).[5] Denaturing agents and detergents such as urea, and guanidine-HCl dissociate hydrogen bonds.[5] Sodium dodecyl sulphate contains both hydrophobic and strong ionogenic groups. This compound binds to hydrophobic regions of a protein results in a layering of negative charges on the protein's surface, hence causing irreversible unfolding of the structure. The denaturing effect of these solutions limits their suitability to the most stable proteins. Other applications are the removal of "sticky" proteins during column regeneration or when functional eluate is not required. Ideally, an elution buffer should aim to disrupt the various bonds that make up protein-protein interactions. The elution strategy is usually the result of a compromise between convenience, target yield and functionality.

### 1.5.2 Competitive elution

The isolated proteins can be alternatively eluted by washing the column with an excess of the ligand; this process is referred as competitive elution (Fig. **16**).

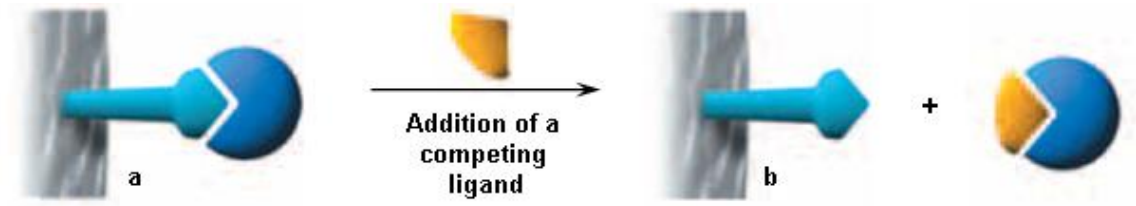


**Figure 16**: The addition of a competitive ligand in solution causes the release of the bound molecule (Figure from ref. 2).

This strategy has several advantages including the retention of column-binding capacity due to the mild elution conditions and the specificity of elution, especially when there is suspicion of non-specific binding of mobile phase components on the solid matrix.[5] However, it may not always be possible to work with a large excess of ligand for practical or economical reasons.

## 1.6 "Affinity-independent" elution of isolated biomolecules

Despite the great advancements in elution techniques in affinity chromatography, the prediction of their efficiency remains complex.[58] Therefore, general elution methods that are independent of the bioaffinity interaction would be desirable. A few examples of affinity-independent retrieval of the separated biological material are discussed below.

A protocol set up by Santala *et al*. describes a novel elution method for the efficient recovery of antibody-displaying phages (viruses able to infect only bacteria) that have been captured with a biotinylated antigen on streptavidin-coated magnetic particles.[58] Using paramagnetic streptavidin beads featuring a nuclease-cleavable DNA linker between streptavidin and the bead surface, a high total recovery and a very low non-

specific background have been achieved (Fig. **17**). It has been shown that this system is suitable for any pre-existing phage display library with no need to adjust the vector construct.[58] The universal (same conditions for all binders) affinity-independent elution should enable the automation of this method for high throughput isolation of binders in large-scale antibody screening programs.[58]

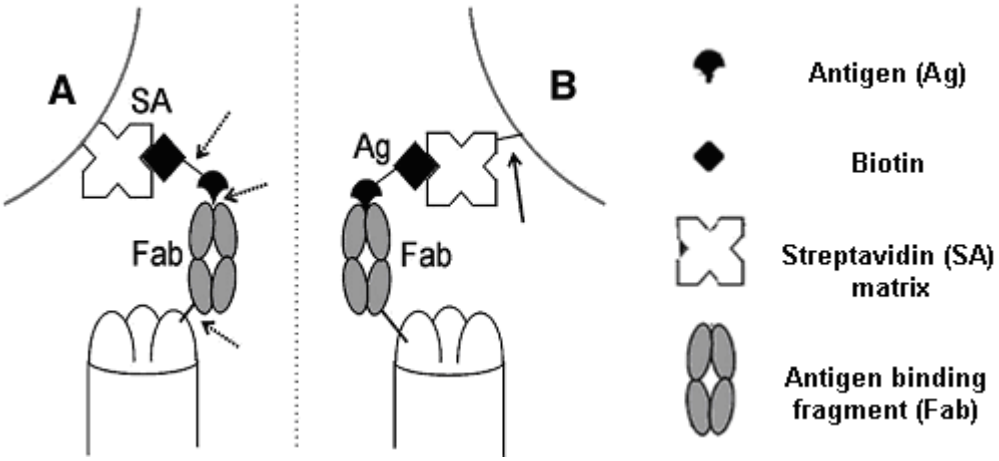


**Figure 17:** Schematic illustration of the elution in a phage display. To elute phages after bioaffinity selection from conventionally coated streptavidin (SA) paramagnetic particles (A), the detachment can be achieved by (dotted arrows): breaking the biotin-antigen bond (Ag) or cleaving the specific linker between Fab (the region of the antibody that binds the antigen) and phage coat protein. Using streptavidin beads containing a DNA linker (B), affinity-independent elution can be achieved by cleaving the DNA linker (solid arrow, figure from ref. 58).

Another elegant example of an affinity-independent elution strategy has been described by Cho *et al*. in their study of the hepatitis C virus (HCV) RNA polymerase protein.[59] A microbead-based affinity chromatography chip (μ-BACC) was developed to separate and purify these proteins by immobilisation of an RNA aptamer (nucleic acid species that have been engineered to bind various molecular targets) on beads (Scheme **5**). A photocleavable linker was conjugated between the beads and the aptamer to allow the elution of the bound RNA polymerase from the RNA aptamer in one step by UV irradiation (Scheme **4**).[59] This linker showed a cleavage activity over 70% upon UV irradiation at 1050 mW $cm^{-2}$ for more than 5 min.

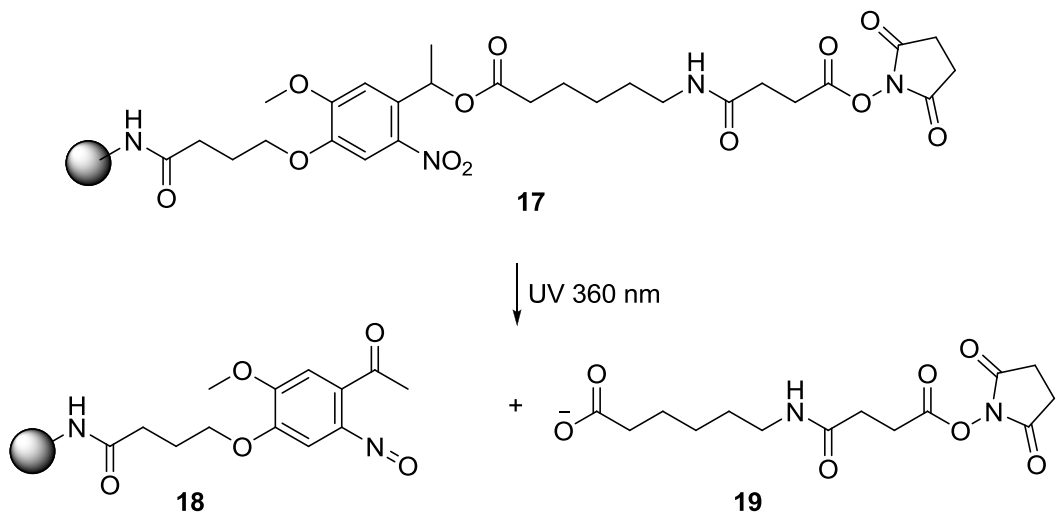


**Scheme 4**: Photocleavable linker used for photoelution of captured proteins. The end of the spacer features a reactive *N*-hydroxysuccinimide ester for covalent binding of aptamer having an amine group in position 3.[54]

In the approach reported by Cho *et al*., an *o*-nitrobenzyl photocleavable linker with an activated ester moiety was connected to PEG-modified beads, and was used for the immobilisation of aminated RNA (Scheme **5**).[59] The recovery of the eluted target, upon exposure to near-UV light, was shown to be possible without protein denaturation. The eluted biomolecules were subsequently subjected to tryptic digestion and the peptide ions analysed using matrix assisted laser desorption/ionisation-time of flight (MALDI-TOF, Scheme **5**).[59] Cleavage conditions depend only on the U.V. wavelength and irradiation time, not on the affinity between ligands and captured molecules, thus providing a significant advantage in the effective elution of a wide range of target biomolecule(s).

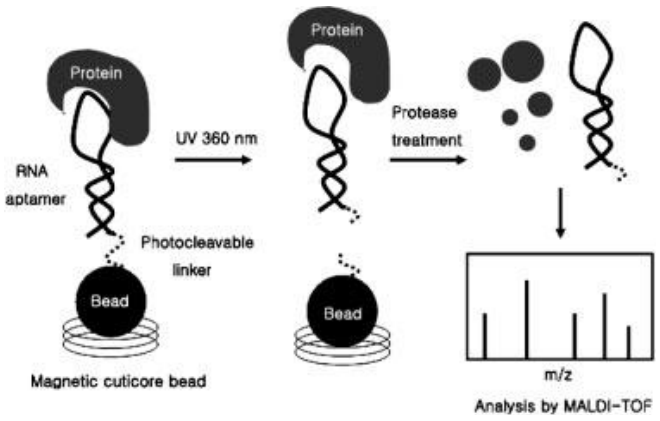


**Scheme 5:** Schematic diagram of protein analysis by the μ-BACC process. Magnetic beads were immobilised in the center of the bead chamber by a permanent magnet. Target protein was captured by the aptamer immobilised on these beads by covalent bonding. Captured proteins eluted following UV irradiation were analysed by MALDI-TOF after tryptic digestion (Scheme from ref. 59).

More recently, Leitner *et al*. synthesised a molecular probe featuring a cleavable unit represented by a malondialdehyde-indole derivative aimed at the investigation of the tyrosine kinase inhibitor bosutinib (Scheme **6**, **24**).[60,61] The indole linker **20** was designed with orthogonal functionalities; a free aldehyde for condensation to the solid support bearing a hydrazine moiety and a carboxylic acid group for coupling to an amino group of the ligand of interest. Incubation with 50 mM pyrrolidine solution causes release of the affinity probe from the solid support. Bosutinib is an ATP-competitive third generation kinase inhibitor which is currently in phase III clinical trials for the treatment of chronic myeloid leukemia (CML).[62,63] An amino functionalised sample of bosutinib was employed for the preparation of molecular probe **24** for pull-down experiments with K562 cell lysate followed by elution of the isolated protein by incubation with pyrrolidine.[61] Immunoblot analysis confirmed the presence of BTK (a known binding partner of the drug of interest) and revealed the presence of new binding partners. LC/MS allowed the identification of 32 binding partners; known binding partners of bosutinib including SRC, ABL, BTK or TEC, together with newly isolated targets such as CAMK2G.[64] However, a high degree of non-specific interactions was also found.

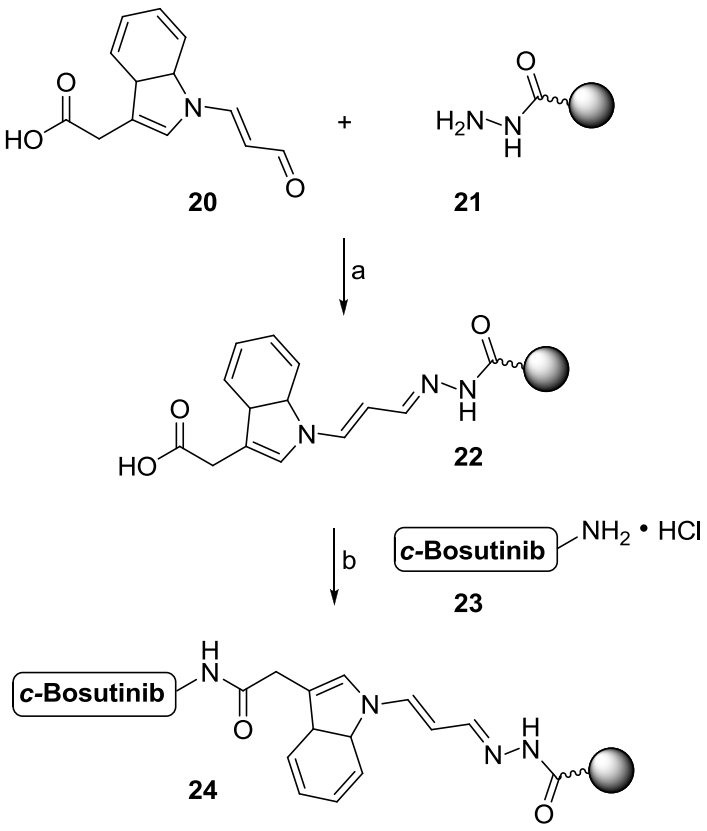


**Scheme 6**: Preparation of *c*-Bosutinib molecular probe **24**; (a) MeCN/$C_2H_7NO_{2(aq)}$, 1/1, pH 4.5, 10 mM aniline, 2 h; (b) DMT-MM, *c*-bosutinib, MeOH, 3 h, RT.

The work discussed in this section presents three different elution strategies in which the recovery of the isolated biomolecules does not rely on reversing the interaction between the ligand and the target molecule. The successful design and applications of molecular probes featuring a cleavable unit has been shown in affinity-based separations.

## 1.7 Hulme group strategy

The initial aim of this project was to gain further insight into the biological activity of the natural product anisomycin using a novel affinity probe. This molecular probe has been designed to capture anisomycin binding partner(s) and release the isolated

biomolecule(s) following an affinity-independent elution protocol. For this reason, it was planned to insert a cleavable azobenzene unit (linker) between the solid matrix and the active compound, thus simplifying the elution procedure and avoiding all the bottlenecks examined in section 1.5.1.

### 1.7.1 Anisomycin

The pyrrolidine antibiotic anisomycin **25** was first isolated from *Streptomyces roseochromogenes* and *S. griseolus* in 1954.[65]

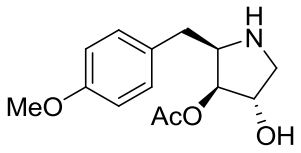


**25**

**Figure 18:** The natural product anisomycin.

Over subsequent years anisomycin has been found to display many interesting biological responses including anti-fungal activity,[65] protein synthesis inhibition[66] and anti-tumour activity in the nanomolar region.[67] The most interesting activity[68] is perhaps its role in the stress activated protein kinase (SAPK) pathways. The SAPK pathways are distinct signalling branches within the mitogen activated protein kinase (MAPK) superfamily and play a vital role in the intracellular signalling triggered by a range of stressors (*e.g.* UV radiation, heat, oxidative stress and chemical stimulants).[69]

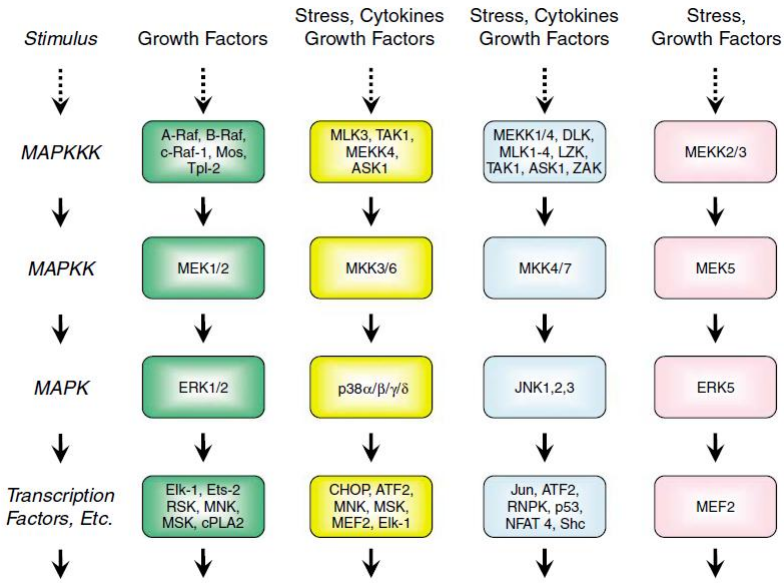


**Scheme 7**: General scheme of the mitogen-activated protein kinase (MAPK) pathways; the SAPK pathways (yellow, light blue and pink) incorporate the target of the natural product anisomycin (Scheme from ref. 70).

Mammalian cells possess four well-characterised MAPK pathways (Scheme **7**).[70] The core unit of these MAPK pathways is a three-membered protein kinase cascade whose components are highly conserved in structure and organisation. In this cascade, the MAPK pathways are phosphorylated and activated by a MAPK kinase (MAPKK/MKK). The MAPKK are "dual-specific" kinases that catalyze the phosphorylation of MAPKs at Thr and Tyr sites, specifically targeting a Thr-X-Tyr motif on MAPK (where X is proline and glycine for the JNK/SAPK1 and p38/SAPK2 modules, respectively).[71] Regulation of these pathways results in controlled activation of downstream kinases and transcription factors including c-Jun, ATF-2, and MAPKAP-K2. This downstream effect is thought to play a role in a range of pathological conditions such as ischemic brain injury resulting from stroke episodes,[72] cancer,[73] and Alzheimer's disease.[74] Although the downstream effects on the SAPK pathway have been well documented, the cellular target of anisomycin and its precise mode of activation of these signalling pathways have yet to be elucidated.

### 1.7.2 Previous work carried out in the Hulme group

Selective biotinylation is one of the most common practises in affinity-based separations.[75] Biotinylated binders such as membranes, nucleic acids, antibodies and other proteins can be detected once an appropriate streptavidin-conjugated probe is available.[75] Biotinylation may be readily achieved through the copper(I) catalysed Huisgen 1,3-dipolar cycloaddition reaction. The high purity and high yields of conjugation that are possible using "click" methodology, together with mild coupling conditions, and excellent regioselectivity render it the method of choice in conjugative routes to biotinylated molecular probes. In the Hulme group, propargyl derivatives of anisomycin **26** and **27** have been prepared and tested for SAPK activity.[76] Gratifyingly, derivative **27** (Fig. **19**) retained the biological activity of the lead compound and has been successfully used in order to synthesize biotinylated analogues of this potent SAPK activator.[76]

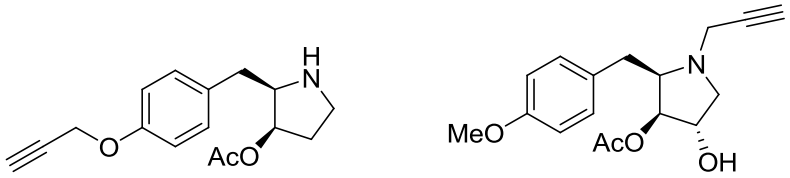


**26** **27**

**Figure 19:** Two representatives of the propargyl derivatives prepared in the Hulme group from the phenol and pyrrolidine series.

Biotinylated anisomycin (Fig. **20**, **28**) was screened using an immunoblot assay for phosphorylation of JNK1/2 in HEK 293 cells and showed a phenotypic SAPK response.[76]

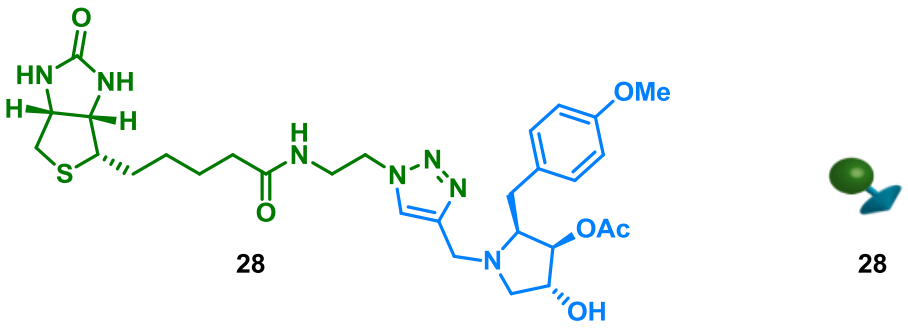


**Figure 20**: Biotinylated probe **28** (and its cartoon representation) synthesised in the Hulme group for affinity capture of the binding partner of anisomycin within SAPK pathways.

The newly synthesised molecular probe was incubated with a HEK 293 cell extract for affinity capture of anisomycin's binding partner (Scheme **8**). The mixture was next immobilised onto a streptavidin-coated matrix. The excess lysate was removed by extensive washing and the matrix treated with SDS at high temperature to remove the isolated biomolecules from the streptavidin-coated matrix. The isolated proteins were separated by gel electrophoresis.[77] Upon screening of different conditions for the pull-down experiments (*e.g.* different incubation time, staining etc.) only a large background response was obtained.[77] When a smaller number of proteins were isolated by SDS-PAGE, they were identified (after MS analysis) as proteins present in the cell extract that have been pulled down in a non-specific manner.[77]

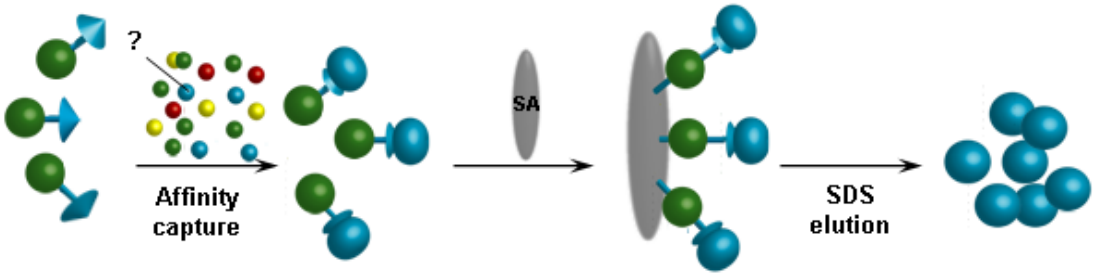


Scheme **8**: Pull-down experiment with molecular probe **28**.

Having successfully synthesised a series of biotin derived molecular probes based on

coupling anisomycin through its pyrrolidine nitrogen; the synthesis of a solid-supported anisomycin was envisaged. Compound **29** was readily achieved from commercially available Affi-gel. The molecular probes synthesised have been used for pull-down experiments in collaboration with the MRC Protein Phosphorylation Unit in Dundee.[77]

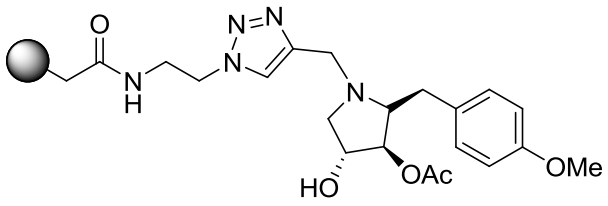


**29**

**Figure 21:** Solid-supported anisomycin.

### 1.7.3 A smart cleavable linker for affinity-based separations

In order to use affinity-based separation for the elucidation of the mechanism of action of anisomycin, an alternative approach to biotinylation and the use of standard biotin/streptavidin affinity interactions was envisaged. As discussed in section 1.6, affinity-independent elution methods present considerable advantages for the retrieval of the separated biomolecules. In the Hulme group, the introduction of a "click"-functionalised linker (Fig. **22**, **30**) between the solid matrix and the active compound was envisaged.[78]

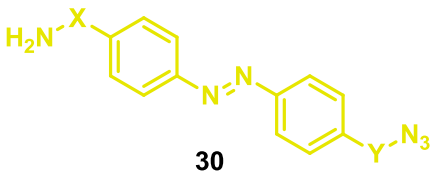


**30**


**30**

**Figure 22:** Hypothetical azobenzene chemically cleavable linker (and its cartoon representation).[78]

It was hypothesised that this molecular probe would be able to capture anisomycin binding partner(s) from within a cell extract. Once the biological material was separated, the linker would be readily cleaved, minimising risk of contamination, protein denaturation and loss of material (Scheme **9**).

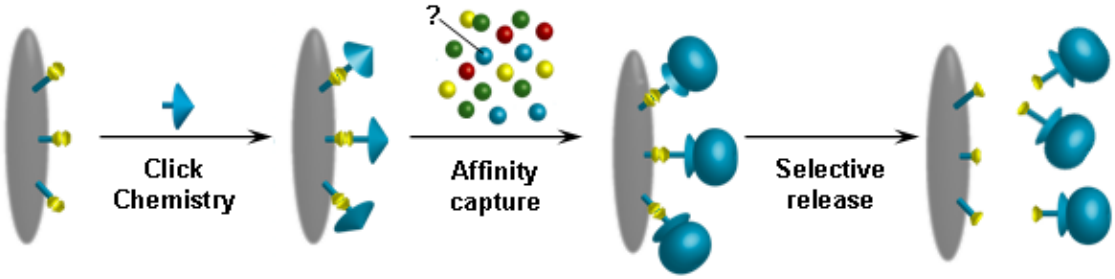


**Scheme 9**: Pull-down experiment with the proposed novel affinity probe.

Azobenzenes were chosen for the linker strategy as they can be cleaved under mild reducing conditions by using sodium dithionite ($Na_2S_2O_4$).[79] Importantly, the cleavage reaction conditions are compatible with biochemical systems, as exemplified by the use of azobenzenes as cleavable cross-linking reagents for proteins[80] and in the functionalisation of a tyrosine residue on the surface of viral capsids.[81] The primary amino group present on the linker would be available for coupling to a solid support. The matrix of choice was commercially available Affi-gel 10 **31** (Bio-Rad), an agarose based affinity media that contains a neutral 10-atom spacer arm and a reactive *N*-hydroxysuccinimide ester (Fig. **23**).

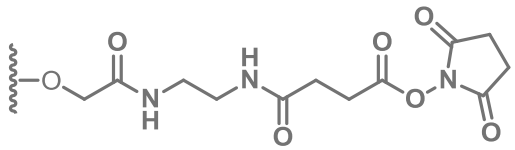

**31**

**Figure 23:** Affi-gel-10.

This solid support is designed to couple selectively to primary amino groups in both aqueous and non-aqueous systems. The azide functionality in the linker **30** would be subsequently coupled to the propargyl derivative **27** of anisomycin using a classical click coupling. The presence of an azide group for click coupling makes this protocol compatible with the extensive range of propargyl functionalised "click" ligands[82,83] that have emerged in recent years.[84,85]

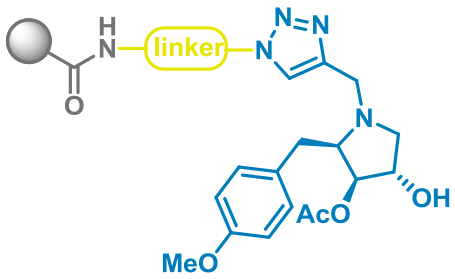


**32**

**Figure 24:** The novel molecular probe **32** featuring the chemically cleavable linker.

The syntheses of the azobenzene chemically cleavable unit and the solid-supported molecular probes will be described in chapter 2. The characterisation of the newly synthesised matrices using solid-state nuclear magnetic resonance spectroscopy (NMR) techniques will be also discussed.

# 2 Results and discussion

The different routes investigated for the synthesis of the novel chemoselective cleavable azobenzene unit **30** are discussed in section 2.1 (Fig. **25**). The design and the preparation of a solution phase analogue mimicking the last portion of the agarose matrix **33** are described in section 2.2.1. The coupling reactions of analogue **34** to anisomycin and biotin are described in section 2.2.2 and 2.2.3. Finally, the syntheses of solid-supported biotin and anisomycin are discussed in sections 2.2.4 and 2.2.5.

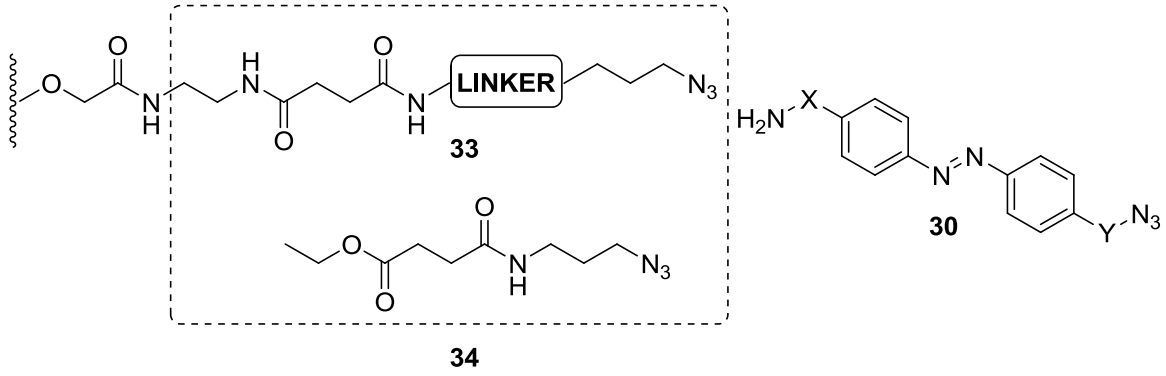


**Figure 25**: Derivatised agarose matrix **33**, solution phase analogue **34** and the hypothetical chemoselective cleavable linker **30** with orthogonal functionalities.

## 2.1 Linker Synthesis

### 2.1.1 Route A

For the synthesis of the chemoselective cleavable unit azobenzene derivative **38** was chosen as it can be readily cleaved under reducing conditions using sodium dithionite (Scheme **10**).[79] In the approach recently reported by Verhelst *et al*., reaction of 4-amino-

benzoic acid **35** with sodium nitrite under acidic conditions gave rise to 4-carboxybenzendiazonium chloride **36** (Scheme **10**).[79]

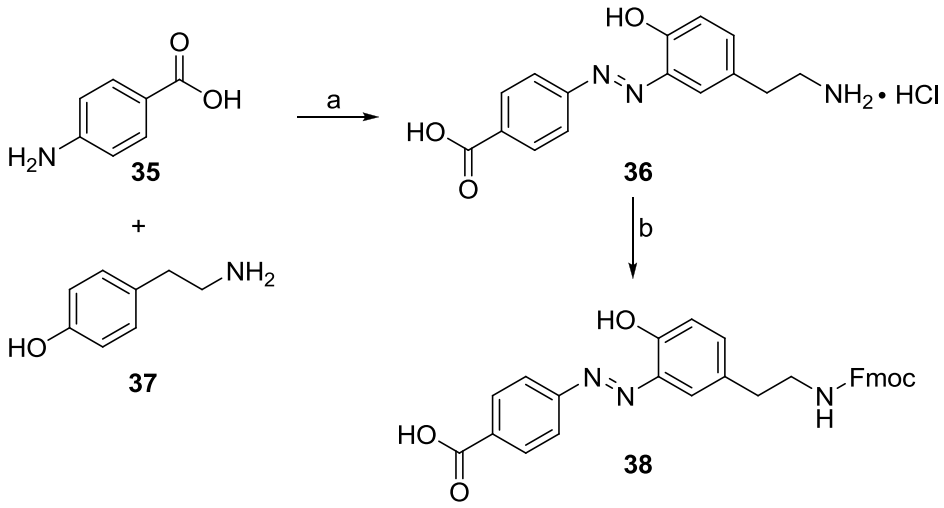


**Scheme 10**: Synthesis of the chemoselective cleavable linker. (a) i. $NaNO_2$,.$HCl_{(aq)}$, 0 °C to RT, ii. **37**, $NaHCO_{3(aq)}$, ~18 h; (b) FmocCl, 1 h, (59% over two steps).

The diazonium salt was then coupled with tyramine **37** (a tyrosine derivative), followed by Fmoc protection of the primary amino group (59%, over two steps).[79] The azobenzene species **38** was appealing because of the presence of both a carboxylic acid and a Fmoc-protected primary amino group.

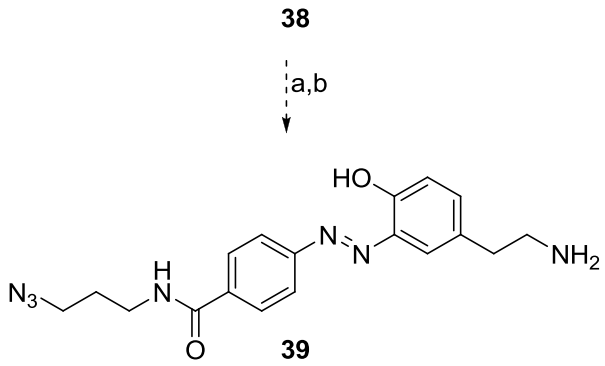


**Scheme 11**: Proposed functionalisation of the linker for affinity chromatography. (a) Coupling with 3-azidopropan-1-amine; (b) Fmoc cleavage in the presence of piperidine.

The carboxylic function could react with an amine bearing an azide functionality to give a stable amide (Scheme **11**, **39**). Following Fmoc deprotection, the newly revealed amine could be selectively attached to the agarose matrix **31**, the affinity media of choice. The presence of an azide functionality in compound **39** would allow coupling to a propargyl derivative of the molecule of interest (*e.g.* propargyl anisomycin **27**) using a copper(I) catalysed Huisgen 1,3-dipolar cycloaddition.

Although TLC analysis suggested complete consumption of amine **36**, it was not possible to isolate compound **38**. In the belief that the use of a different protecting group could favour the protected amine entering the organic phase to be isolated, CbzCl was also employed. However, no better results were achieved. At this point, the use of phenol instead of tyramine **37** for the diazocoupling was proposed, following standard conditions.[86] Azobenzene **40** could be readily prepared in 90% yield in multigram scale.

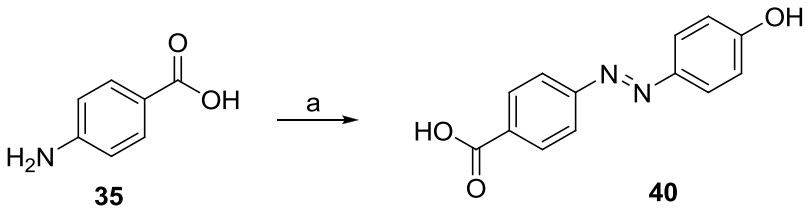


**Scheme 12**: Diazonium salt formation and coupling with phenol. (a) i. $NaNO_2$, HCl, 0 °C, 20 min; ii. PhOH, NaOH, $K_2CO_3$, 0 °C to RT, 3 h, (90%).

### 2.1.2 Route B

With compound **40** in hand, a new route for the extension of the phenol terminus to give a primary amine was planned. Azobenzene **40** was reacted with the hydrochloride salt 2-chloro-ethylamine **41** in the presence of a base (Scheme **13**). Unfortunately the proposed nucleophilic substitution by the phenol of compound **40** proved to be problematic probably because of the presence of the free amino group of compound **41**.

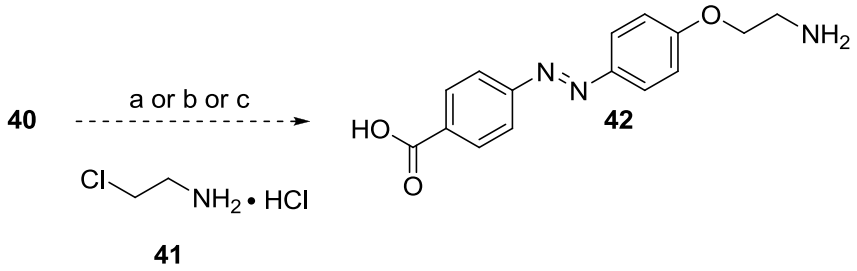


**Scheme 13**: Unsuccessful reactions with unprotected amine **41**. (a) NaH, DMF, RT; (b) $Cs_2CO_3$, DMF, RT; (c) KOH, EtOH, reflux.

For this reason, protection of the amino group was carried out before proceeding with the reaction with azobenzene **40** (Scheme **14**).

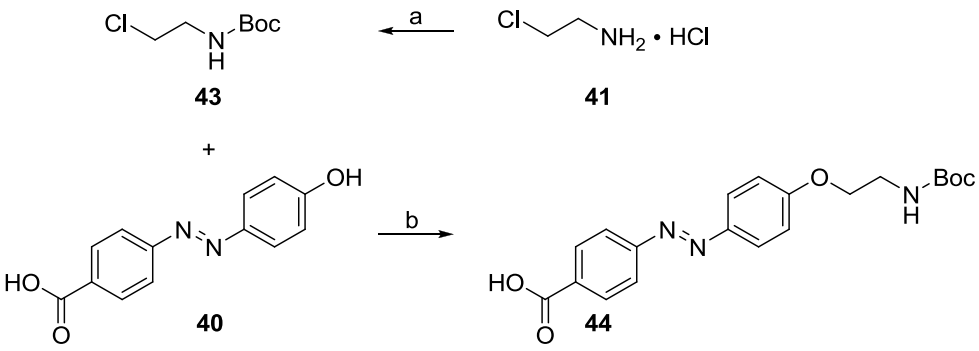


**Scheme 14**: Boc-protected route for the synthesis of compound **44**. (a) $Et_3N$, $(Boc)_2O$, DCM, (60%); (b) **43**, $Cs_2CO_3$, DMF, 80 °C, (23%).

Protection of 2-chloro-ethylamine hydrochloride **41** was readily achieved as described in the literature.[87] Compound **40** was reacted with the Boc-protected amine **43** in the presence of caesium carbonate to give the desired acid **44** in poor yield (23%). The reaction gave rise to a number of side products that were not isolated. Given the low yield of this last step, a new route for the synthesis of the azobenzene unit was envisaged.

### 2.1.3 Route C

Alkylation of azobenzene **40** has been reported in literature using 1,10-dibromodecane[88] (42% yield) and 1,4-dibromobutane[89] (15% yield). Although the yields reported in literature were not excellent the reaction was investigated using 1,3-dibromopropane. In this new synthetic route the azide functionality would be inserted on the OH terminus (Scheme **15**). Once the alkyl bromide **45** was formed, nucleophilic displacement of the bromine to give the azide functionality could take place. The primary amine could be coupled on the carboxylic extremity using a mono-Boc-protected diamine

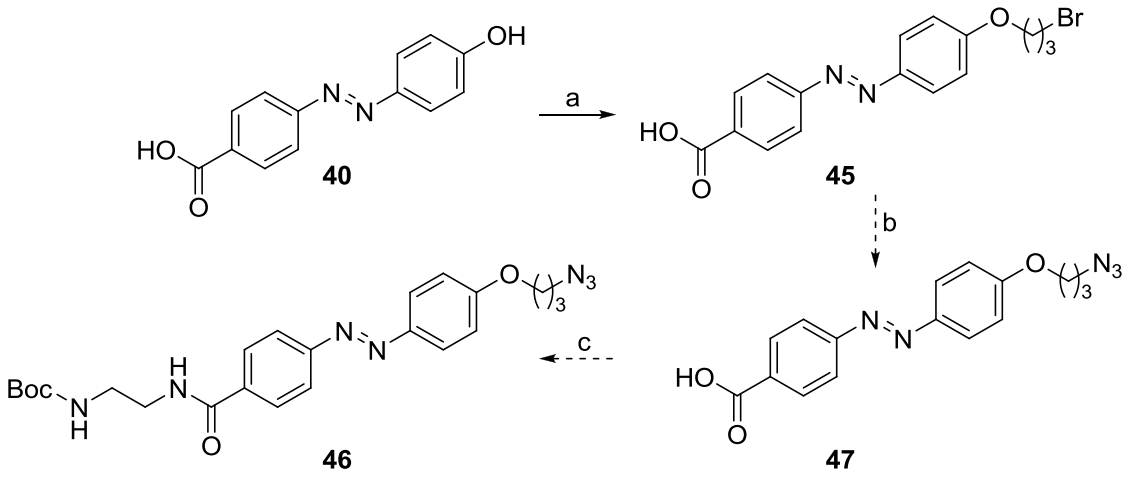


**Scheme 15**: Route C. (a) 1,3-dibromopropane **48**, KOH, EtOH, reflux, (trace); (b) $NaN_3$, DMF; (c) Coupling with $BocNHCH_2CH_2NH_2$.

Unfortunately, alkylation of **40** with the 1,3-dibromopropane **48** gave only a trace of the desired product **47**, and numerous side products which it was not possible to isolate. The results were in agreement with the literature.[88,89] For these reasons, it was decided to first derivatise the carboxylic functionality before proceeding with the alkylation of the phenol.

### 2.1.4 Route D

In order to establish the most convenient route to prepare the azobenzene linker, both the esterification[77] of compound **40** and its coupling with the protected amine[90] **50** were investigated (Scheme **16**). The conversion of the acid **40** into the ester **49** procedeed smoothly. For the coupling of the mono-Boc-protected diamine **50** with compound **40**[91] a range of standard reaction conditions were investigated. The best results were obtained using a water-soluble carbodiimide derivative (EDC) as the coupling agent.

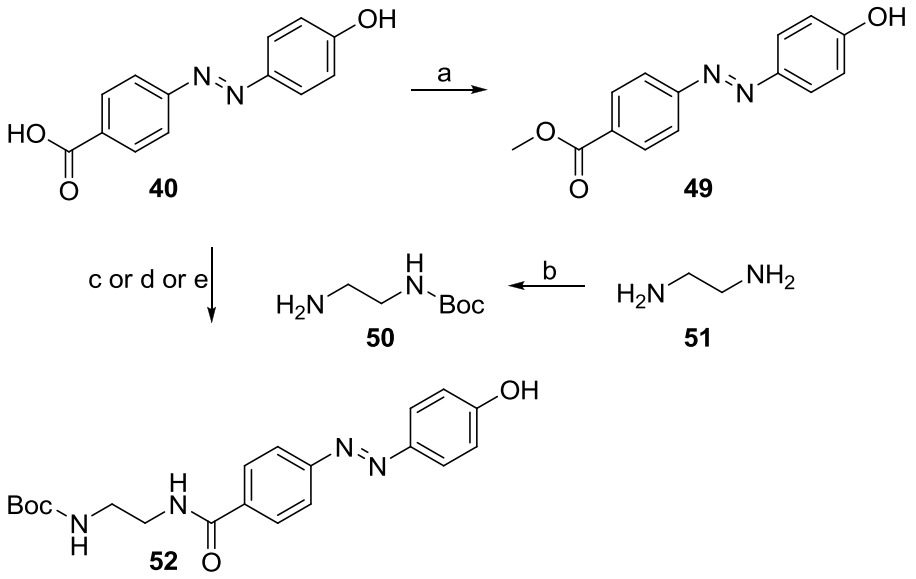


**Scheme 16**: Derivatisation of the carboxylic acid of azobenzene **40**. (a) Acetyl chloride, MeOH, 0 °C to RT, (78%); (b) $(Boc)_2O$, dry DCM, (99%); (c) $Et_3N$, DSC, MeCN, 60 °C to RT (no reaction); (d) $Et_3N$, DIC, DMF, RT (no reaction); (e) EDC, HOBt, DMF, RT (60%).

Carbodiimides catalyse the formation of amide bonds from carboxylic acids and amines by activating the carboxylate to form an *O*-acylurea (Scheme **17**). This intermediate can be attacked by an amine directly to form an amide. The driving force of this reaction is the formation of the urea by-product. The major advantage of the EDC coupling agent with comparison to DIC is the production of a water soluble urea derivative **57** as side product.[92] This species can be easily removed by washing the organic phase with dilute acid or water. In carbodiimide-mediated amide formation, racemisation and acetyl transfer forming the unreactive *N*-acylurea are often observed (Scheme **17**).[93] The

addition of selected nucleophiles (*e.g.* HOBt) that react faster than the competing acyl transfer generates an intermediate which is still active enough to couple with the amine.[93]

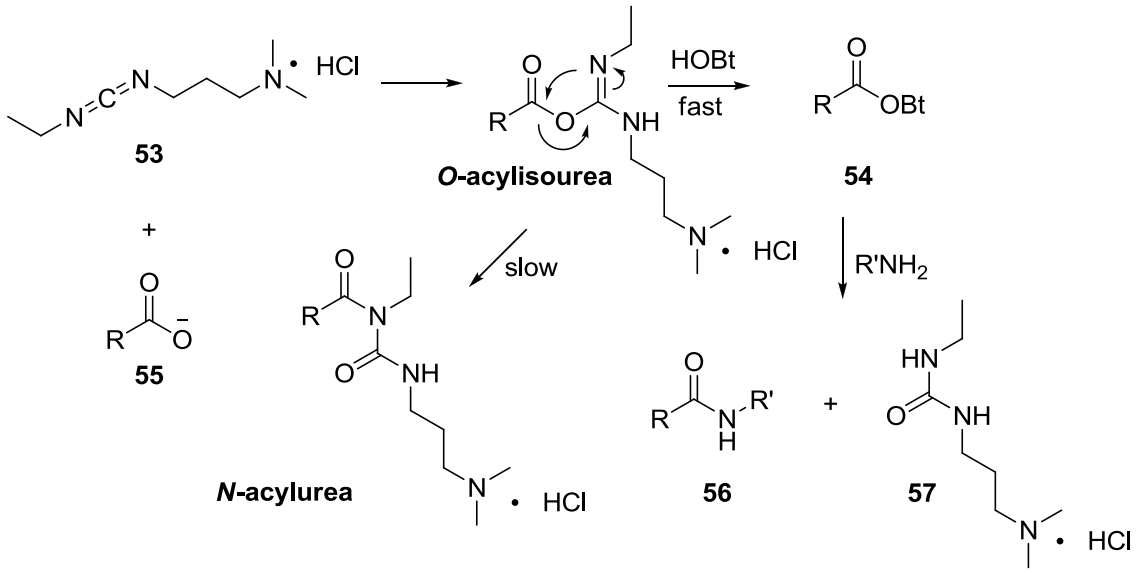


**Scheme 17**: EDC-mediated amine/carboxylic acid coupling in the presence of HOBt as a nucleophile.

Despite the fact that the esterification proceeded smoothly in better yield with respect to the amide bond formation, a new synthetic route starting from the amide **52** was planned. Coupling the carboxylic acid of compound **40** with mono-Boc-protected diamine **50** allowed investigation of the alkylation of phenol **40** without interference from the free acid. Furthermore, in the same step a Boc-protected primary amino group was introduced for subsequent linkage to the agarose matrix **31**. Indeed, once the formation of the amide bond was achieved, the alkylation of the phenol was carried out successfully (Scheme **18**). The use of different solvents for the akylation of phenol **40** such as butan-2-one[85] did not give an enhanced yield (67% for MeCN, 65% for butan-2-one). Nucleophilic displacement of alkyl bromide **58** gave rise to the desired azide functionality on compound **59** in excellent yield. Monitoring the reaction by TLC was found to be difficult due to the almost identical $R_f$ values of the starting material and the

azide **59**. Thus, the completion of this reaction was monitored by MS (ESI+) checking for the disappearance of the bromine-containing molecular ion of the starting material **58**. Boc cleavage of the aminoazide product **60** under acidic conditions readily gave the free amino group as confirmed by NMR (disappearance of the singlet at $\delta_H$ = 1.44 ppm corresponding to the Bu$^t$ group), allowing isolation of the salt of azobenzene linker **60**.[78]

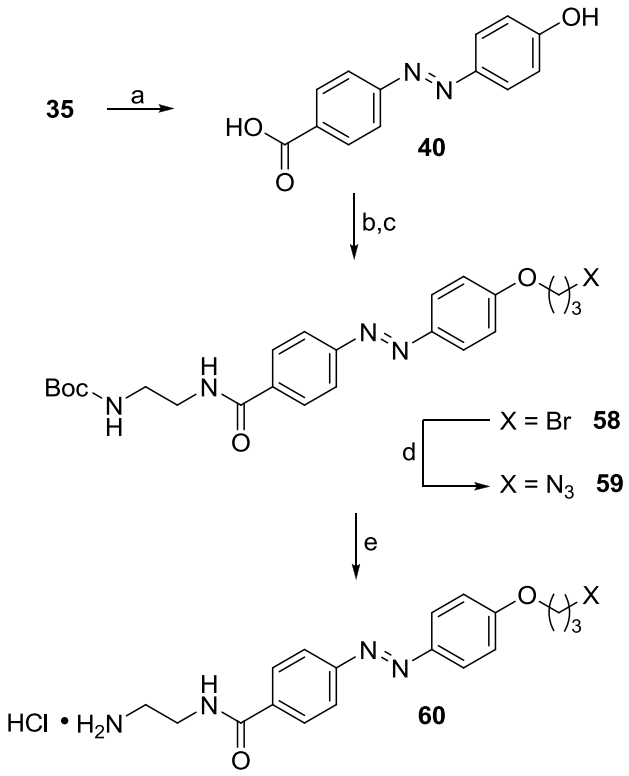


**Scheme 18**: Linker synthesis.[78] (a) i. $NaNO_2$, HCl, 0 °C, 20 min; ii. PhOH, NaOH, $K_2CO_3$, 0 °C to RT, 3 h, (90%); (b) $BocNHCH_2CH_2NH_2$, EDC, HOBt, DMF, 18 h, (60%); (c) 1,3-dibromopropane **48**, $K_2CO_3$, MeCN, reflux, 5 h, (67%); (d) $NaN_3$, DMF, 18 h, (90%); (e) MeOH, $CH_3COCl$, 0 °C to RT, $Et_2O$, 1 h, (90%).

## 2.2 Solution phase mimic and solid-supported molecular probes

Previous investigations carried out in the Hulme group of the click reaction onto solid matrices have proven to be problematic (section 1.7.2).[77] Optimisation of the coupling

conditions as well as the characterisation of the synthesised compounds in the presence of a solid support can be quite complex. For these reasons, the synthesis of a solution phase analogue mimicking the last portion of the agarose matrix was envisaged. This molecule, coupled to ligands of interest, would provide data for the development of optimum coupling conditions and NMR data interpretation.

### 2.2.1 Synthesis of the solution phase analogue

Ethyl 4-(3-azido-1-propylamino)-4-oxobutanoate, compound **34** seemed to be a suitable solution phase mimic. This azidoester features similar functionalities of the final portion of the derivatised solid support: an amide bond, a short hydrocarbon chain and an ester (Fig. **26**).

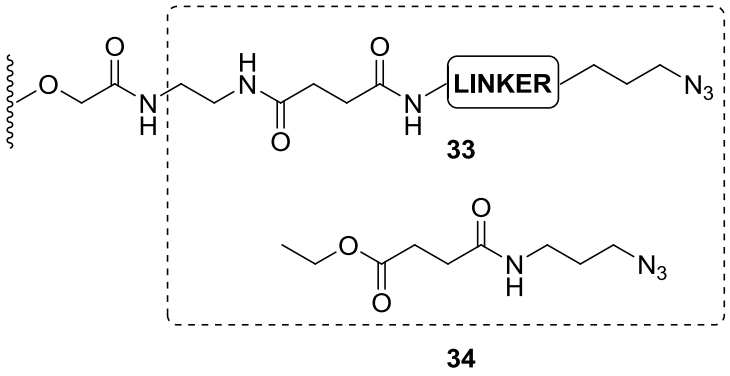


**Figure 26**: Comparison between the final portion of the derivatised matrix and the solution phase analogue.

The conditions for the preparation of compound **34** were optimised using the acid chloride **61** with the hydrochloride salt of compound **62** since aminoazide **64** is highly volatile and tricky to handle (Scheme **19**). Aminoazide **64** is readily achieved from the salt **62** as reported in the literature.[92] The best results were obtained using pyridine as base/solvent which yielded compound **63** in a satisfactory yield (71%). When a lower amount of pyridine was used (up to 5 equivalents) the reaction proved sluggish.

Carrying out the same reaction with aminoazide **64** allowed the preparation of the desired azidoester **34** in 60% yields. Product formation was confirmed by NMR and IR (azide stretch at 2098 $cm^{-1}$).

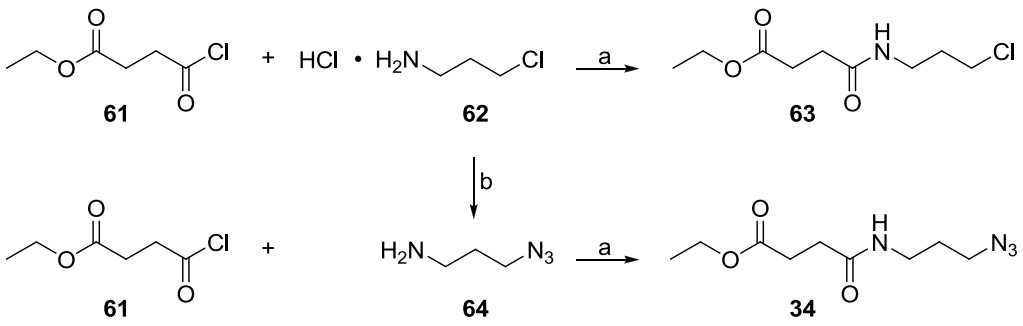


**Scheme 19**: Synthesis of the solution phase analogue. (a) Pyridine, 0 °C to RT, 2 h, (71% for **63** and 60% for **34**); (b) $NaN_3$, $H_2O$, 80 °C, ~18 h, (99%).

## 2.2.2 Coupling of the solution phase analogue to anisomycin

After the successful preparation of the solution phase analogue **34**, the coupling of this compound to the ligand of interest, anisomycin, was investigated. A propargyl derivative of this natural product (with comparable biological activity) is readily accessible as previously reported in the Hulme group (Scheme **20**).[76]

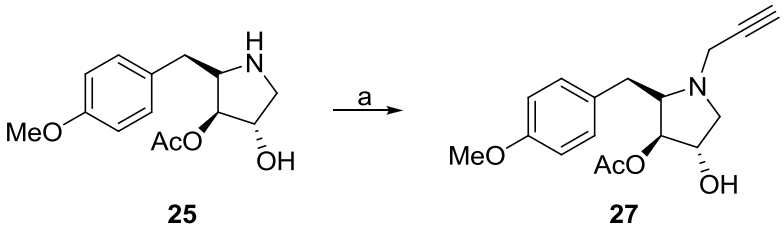


**Scheme 20**: Propargylation of the natural product anisomycin **25**. (a) Propargyl bromide, $K_2CO_3$, DMF, RT, ~18 h, (95%).

The biological properties of this potent activator of the SAPK pathway have been discussed in section 1.7.1. The conjugation method for the coupling of the compound of interest to the solution phase analogue is the copper-catalysed azide-alkyne cycloaddition (CuAAC). The ease with which azides and alkynes[85] are introduced into organic compounds, their biorthogonal properties and tolerance to a wide range of solvents (including water) and pH make them ideal for bioconjugation purposes.[94] The fact that the azide functionality is absent in all known natural compounds, allows selective ligation with a limited number of reaction partners.[94] Click coupling conditions were initially optimised on a simple alkyne, propargyl alcohol, before moving to the anisomycin derivative due to the cost of the natural product. Alkyne-azide coupling is catalysed by copper (I) which is generally obtained *in situ* by reduction of a salt such as copper sulphate.[95] The most accredited mechanism features the formation of an unusual six-membered copper(III) metallacycle (Scheme **21**).

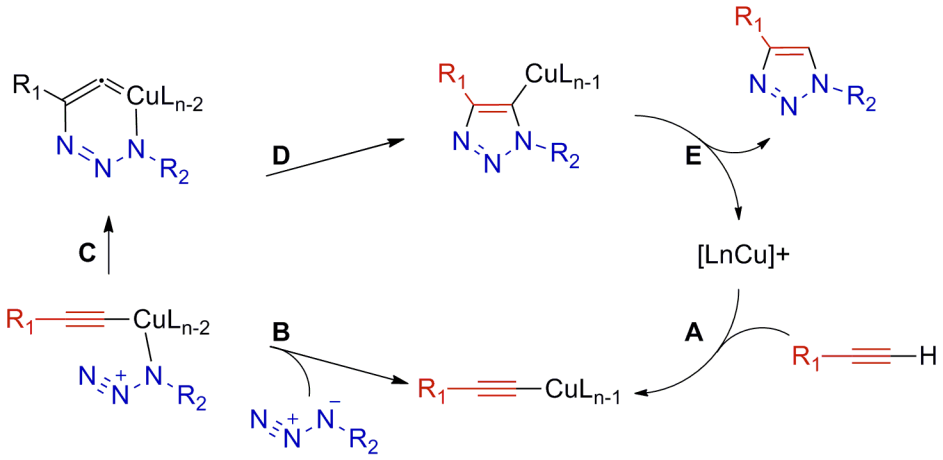


**Scheme 21**: Proposed reaction mechanism for the copper-catalysed azide-alkyne cycloaddition (CuAAC).

Initially, classical coupling conditions were followed with $CuSO_4$ as the source of copper (I), sodium ascorbate as the reducing agent in *t*-BuOH/water. Since no product formation was observed under these reaction conditions, different sources of copper(I) such as copper wire or copper powder, were considered. It has been reported that

formation of the copper (I) catalyst by the oxidation of Cu metal affords the formation of triazole in good yield.[96] However, reaction with Cu metal requires longer reaction times and more copper than other protocols. Coupling with both copper powder and copper wire was attempted. Disappointingly, only traces of the triazole formation were obtained as confirmed by MS (ESI+ showed a small peak at *m/z* = 285). At this point, the possibility of a ligand-assisted click coupling was investigated. Acceleration of the CuAAC click reaction by the amine triazole **65** (TBTA, Fig. **27**) has been described in the literature as a useful tool for all substrates that seem to be unreactive under classical click coupling conditions.[97] TBTA dramatically reduces the minimum catalyst loading (as much as tenfold) without requiring longer reaction times. Ligands such as **65** probably accelerate the reaction by shielding the Cu(I) ion from oxidative degradation.[97]

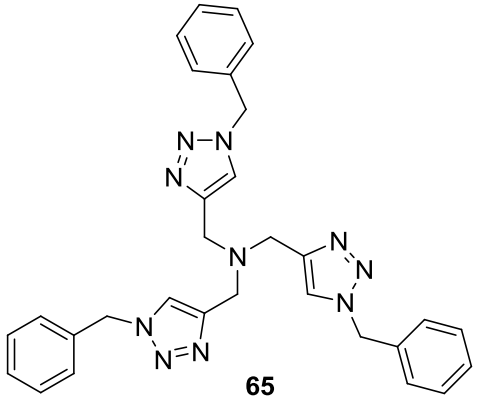


**65**

**Figure 27**: Structure of the trisbenzyltriazolamine (TBTA).

The reaction carried out in the presence of ligand **65** gave rise to the coupled product with the simple propargyl alcohol substrate as well as with propargyl anisomycin in moderate yields (Scheme **22)**.

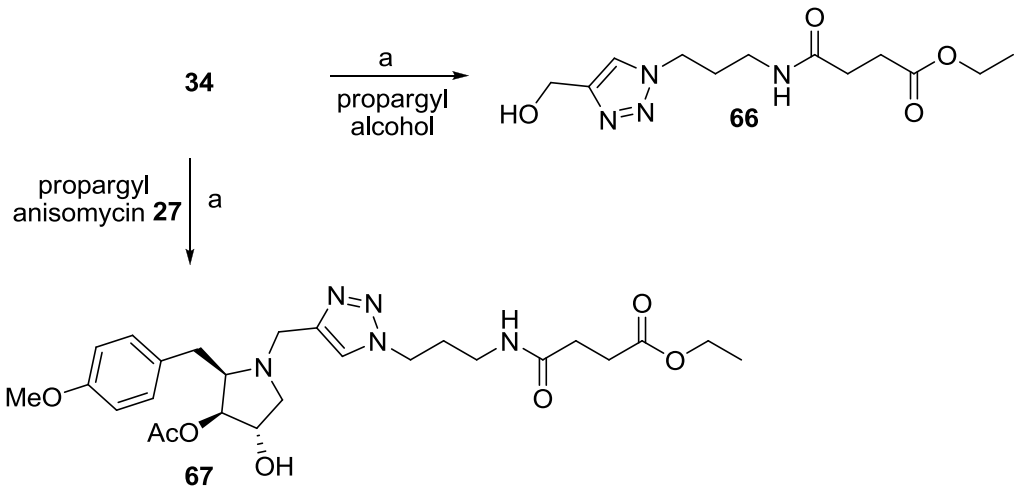


**Scheme 22**: Ligand assisted Cu(I)-catalysed alkyne-azide cycloaddition. (a) Sodium ascorbate, TBTA, $CuSO_4 \cdot 5H_2O$, $H_2O$/*t*-BuOH, RT, ~18 h, (44% for **66** and 62% for **67**).

Both the reactions were monitored by TLC and formation of the products was confirmed by NMR. Both the coupling products showed the diagnostic CH peak of the triazole ring ($\delta_H$ = 7.65 ppm for compound **66** and $\delta_H$ = 7.51 ppm for compound **67**).

### 2.2.3 Coupling of the solution phase analogue to biotin

Coupling of the solution phase analogue **34** to biotin was then investigated in order to provide NMR data to facilitate the characterisation of solid-supported biotin. Furthermore, this solid-supported molecular probe would provide useful material for the preliminary affinity studies discussed in chapter 3. D-Biotin can be readily converted into an activated ester at its carboxylic extremity (NHSbiotin). This activated ester can be readily coupled to propargylamine to form an amide bond and to furnish the desired alkyne functionality (Scheme **23**).[97]

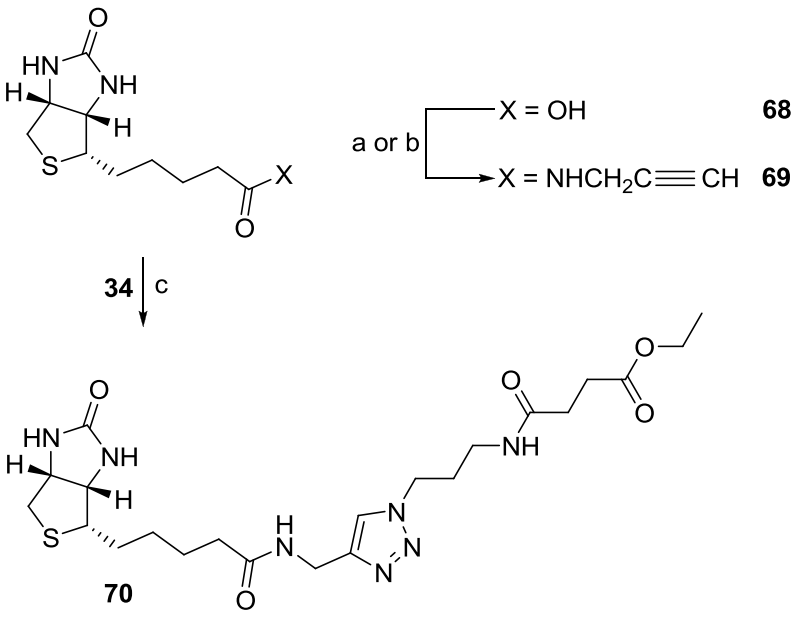


**Scheme 23**: Coupling of the solution phase analogue to biotin. (a) i. *N*-hydroxysuccinimide, EDC, $Et_3N$, 0 °C to RT, ~18 h, (99%); ii. Propargylamine, DCM, RT, 3 h, (77%); (b) Propargylamine, HOBt, DIC, DMF, 60 °C, μwave, 20 min, (88%); (c) Sodium ascorbate, TBTA, $CuSO_4 \cdot 5H_2O$, $H_2O$/*t*-BuOH, RT, ~18 h, (40%).

Alternatively, D-Biotin **68** can be directly submitted to a coupling reaction with propargyl amine under microwave irradiation generating the desired amide derivative **69** in high yield. Under these microwave conditions, conversion of the carboxylic acid **68** into a more reactive *N*-hydroxysuccinimide ester is no longer required, hence shortening the synthesis. The biotin propargyl amide **69** was coupled to the solution phase analogue **34** under the optimised TBTA-assisted CuAAC conditions to give compound **70** (Scheme **23**). Full characterisation of compound **70** was extremely valuable for the subsequent work in solid phase.

### 2.2.4 Coupling of the solid support to biotin

Following the characterisation of solution phase analogue **70**, the syntheses of two solid-supported molecular probes were carried out (Schemes **22** and **23**). Solid-supported

biotin, molecular probes **72** and **74** have been designed to provide a preliminary test of the ability of the new matrix featuring a cleavable unit (azobenzene derivative **60**) to selectively capture the binding partner of a ligand of interest within a biological mixture. Furthermore, the preliminary test using solid-supported biotin featuring a cleavable unit **74** will guarantee that the cleavage of the linker is compatible with biochemical systems. The preliminary affinity studies will be discussed in chapter 3.

Agarose matrix Affi-gel 10 was coupled to azidopropan-1-amine **71** (Scheme **24**). As the conversion to azide is quantitative, the loading of the short chain aminoazide is calculated according to the content of active *N*-hydroxysuccinimide ester (15 μmol $ml^{-1}$). On this premise, 3 equivalents of propargyl amide **69** were employed and the reaction carried out using the previously optimised click coupling conditions (Scheme **24**). The reaction was monitored by IR and stopped once the azide peak at 2100 $cm^{-1}$ disappeared. Similarly, the agarose matrix was reacted with the novel azobenzene derivative **60** and coupled to biotin propargyl amide **69** (Scheme **24**). Successful linkage of the cleavable unit was confirmed by an intense orange colour of the beads which persisted after extensive washings. Even in this case, the click coupling was monitored by IR and the reaction stopped once the azide peak at 2100 $cm^{-1}$ disappeared.

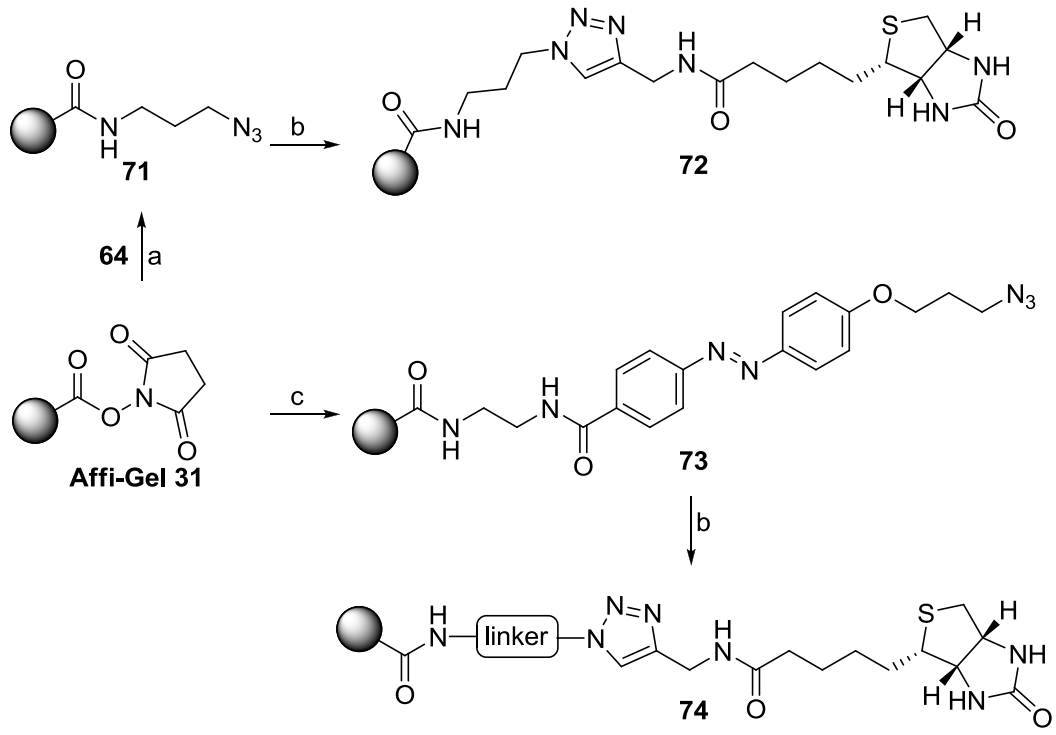


**Scheme 24**: Syntheses of solid-supported biotin, molecular probes **72** and **74**. (a) azidopropan-1-amine **64**, MeOH, ~18 h; (b) Biotin propargyl amide **69** (3 E), $CuSO_4 \cdot 5H_2O$, sodium ascorbate, TBTA, $H_2O$/*t*-BuOH, 2 d (~48 h). (c) linker **60**, $Et_3N$, $H_2O$/MeCN, ~18 h.

Solid-supported azobenzene derivative **73** was also utilised to prepare a simplified molecular probe by coupling to propargyl alcohol under the optimised CuAAC conditions. This simple derivatised matrix **75** was used to test the desired chemoselective reductive cleavage of the azobenzene linker by incubation of the beads with an aqueous solution of sodium dithionite ($Na_2S_2O_4$, scheme **24**).[98,99] The cleavage was attempted at various pH values (from 5 to 7) using different concentrations of sodium dithionite (from 0.05 M to 0.3 M). The best cleavage conditions were found to be the use of a freshly prepared 0.3 M aqueous solution of sodium dithionite at pH 6.5. Following dithionite cleavage of matrix **75**, the corresponding aniline derivative **77** was isolated as confirmed by $^1H$ in good yield (70%, based on the weight of the recovered aniline **78**). This preliminary study demonstrates for the first time that the azo unit is compatible with the reductive conditions of click-based methodologies.[78] The reduction

of the azo group was easily followed since it is accompanied by a dramatic loss of colour of the agarose matrix (Scheme **25**).

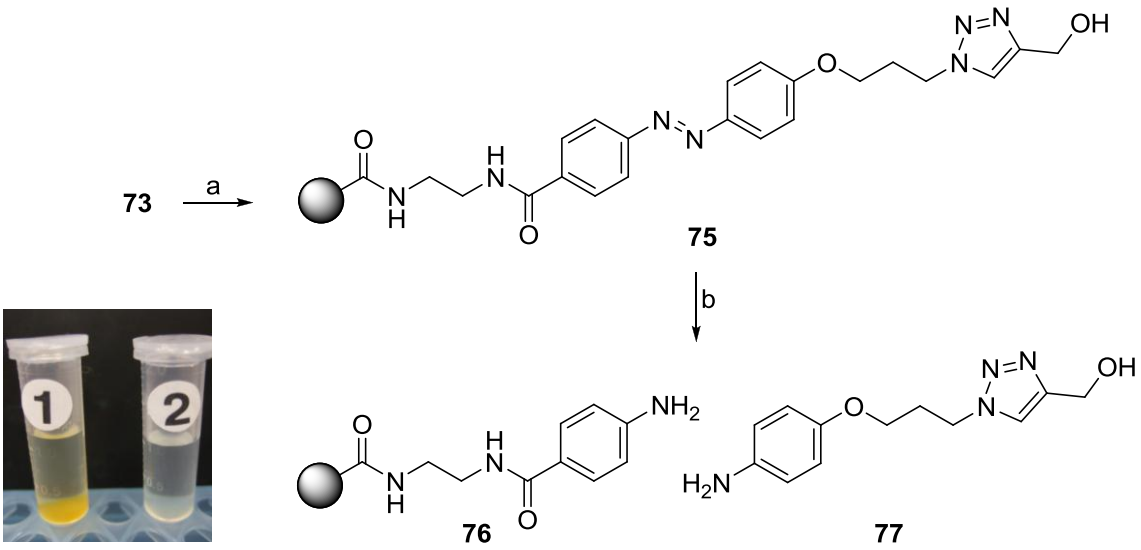


**Scheme 25**: Preparation of a simplified molecular probe and dithionite cleavage. (a) propargyl alcohol (3 E), $CuSO_4 \cdot 5H_2O$, sodium ascorbate, TBTA, $H_2O$/*t*-BuOH, ~18 h; (b) $Na_2S_2O_{4(aq)}$. On the left, two Eppendorf tubes containing simplified molecular probe **75** before (tube 1) and after (tube 2) the cleavage.

### 2.2.5 Coupling of the solid support to anisomycin

After the successful preliminary affinity studies (sections 3.2.2 & 3.2.3) a solid-supported anisomycin, molecular probe **32** was prepared using similar synthetic transformations (Scheme **26**). The reaction was monitored by IR and stopped once the azide peak at 2100 $cm^{-1}$ disappeared. The successful coupling of anisomycin was confirmed by identification of the aniline derivative **78** (MS, ESI+, *m/z* = 496) following dithionite cleavage. This novel molecular probe was employed for pull-down experiments with HEK 293 cells (which express the SAPK pathway) in collaboration with the Cancer Research UK Centre at the Western General Hospital (Edinburgh). These investigations will be described in chapter 3.

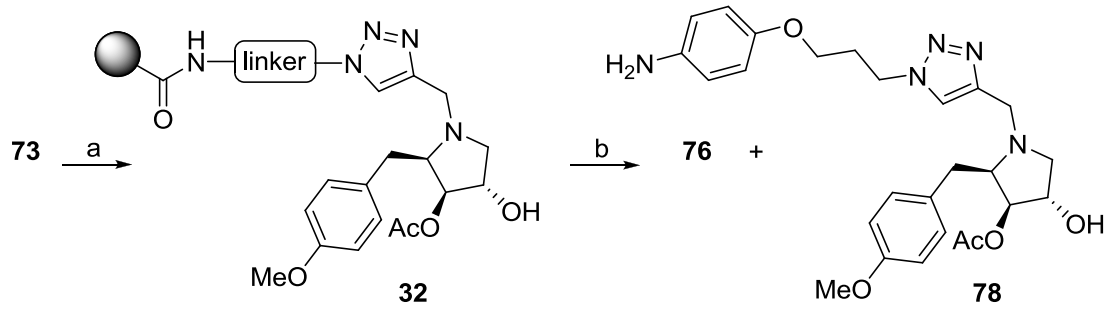


**Scheme 26**: Solid-supported anisomycin coupled through the azobenzene unit to the agarose matrix **32**. (a) propargyl anisomycin, $CuSO_4 \cdot 5H_2O$, sodium ascorbate, TBTA, $H_2O$/*t*-BuOH, ~18 h; (b) $Na_2S_2O_{4(aq)}$.

## 2.3 Conclusion

In conclusion, the synthesis of a novel azobenzene linker for affinity applications was developed (5 steps, 29% overall yield). The central core of compound **60** incorporates an azo group which can be readily cleaved under mild reducing conditions.[79] The amino-terminus can be selectively attached to a functionalised agarose matrix (Affi-gel 10) while the azide functionality can undergo copper(I) catalysed Huisgen 1,3-dipolar cycloaddition with a series of compounds of biological interest (*e.g.* the natural product anisomycin). A series of solid-supported molecular probes have been prepared: solid-supported biotin **72** and **74**, for preliminary affinity studies; a simplified solid-supported triazole **75**, to test the cleavage conditions; and solid-supported anisomycin **79** for pull-down experiments aimed at the isolation of anisomycin's binding partner within the SAPK pathway. In parallel to these syntheses, a solution phase mimic of the Affi-gel 10 agarose matrix has been successfully synthesised and coupled under the optimised TBTA-assisted CuAAC conditions to the propargyl derivatives of biotin and anisomycin. These compounds furnished valuable NMR data to aid the characterisation of the solid-supported molecular probes.

# 3 Results and discussion

## 3.1 Solid state NMR studies

### 3.1.1 Magic angle spinning (MAS) solid state NMR spectroscopy

Magic angle spinning (MAS) solid state NMR spectroscopy was independently described by Andrew *et al.*[100] in 1958 and by Lowe[101] in 1959. Thanks to this spectroscopic technique it is possible to obtain NMR spectra from solid materials.[102] In solution NMR, the anisotropic interactions are averaged by the rapid tumbling of molecules.[103] In contrast, in solid-state NMR, anisotropic interactions such as the chemical shift and dipolar coupling play a major role. This phenomenon results in a broadening of the spectral line width of nuclei in solids.[103] In order to overcome this issue, MAS NMR techniques are applied. This procedure consists of rotating the solid sample about an axis inclined at an angle of 57.74º to the direction of the magnetic field of the NMR magnet (Fig. **28**). It has been demonstrated that sufficiently rapid rotation about this particular axis effectively suppresses most broadening interactions, leaving only fine structures of the type found in the NMR spectra of liquids.[102]

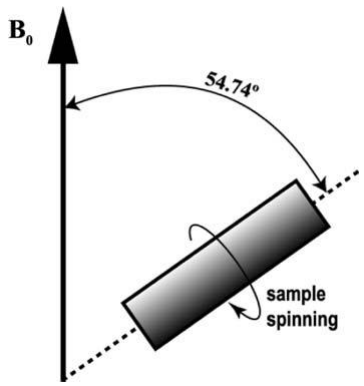


**Figure 28**: Schematic representation of the MAS technique. The spinning axis of the sample is at an angle of 54.74° (magic angle) with respect to the static magnetic field $B_0$ (Figure from ref. 103).

This analytical technique can be applied to all kinds of solid materials: ionic solids, molecular solids, polymers, semiconductors and metals; the solid can be either crystalline or amorphous. The method is also applied for NMR imaging of heterogeneous solid materials.[102]

Among the plethora of applications of this technique in the field of biochemistry, two recent reports will be discussed and an example of the technique for the characterisation of affinity supports will be given. An investigation carried out by Wasner *et al*.[104] in 2009 using solid state NMR spectroscopy allowed the structural characterisation of a specific type of inclusion bodies (IBs) in *E. coli* cells. IBs are expressed proteins which are deposited as insoluble aggregates. A combination of techniques such as; electron microscopy (EM, Fig. **29**), NMR spectroscopy (for H/D exchange experiments), solid-state NMR spectroscopy, and *in vivo* prion infectivity assays have allowed determining that such IBs consisted of fibrillar structures. Indeed, solid-state NMR spectra showed that these IBs adopt virtually the same molecular structure as a particular class of insoluble fibrous protein aggregates, called amyloids. This class of proteins is involved in a range of diseases (*e.g.* Alzheimer's disease, Parkinson's disease), although the relation between the formation of these aggregates and the pathology is yet to be elucidated.[105] The finding that these bacterial IBs displayed a highly ordered and functional amyloid structure supports the emerging concept that amyloid formation is ubiquitous in living organisms.[104]

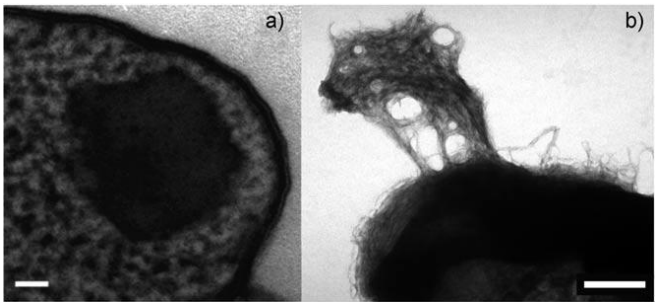


**Figure 29**: a) IBs from *E. coli* observed by cryo-electron microscopy of entire *E. coli* cells. b) Transmission electron micrograph of negatively stained purified IBs (Figure from ref. 104).

More recently, solid state NMR has been employed to study the interaction of proteins and RNA.[106] The structural investigation of large ribonucleoprotein (RNP) complexes can be a difficult task due to the flexibility of RNA and of the protein-RNA interfaces, which often hinders crystallisation. Although solution NMR spectroscopy is an attractive alternative to X-ray crystallography, the large size of typical RNP complexes may limit its applicability. For these reasons, solid-state NMR spectroscopy represents a viable route for such investigations. The complex investigated by Carlomagno *et al*. was the one formed by the protein AF L7Ae and certain RNA nucleotide sequences from the bacterium *Archaeoglobus fulgidis*, as the crystallographic structure of the complex was available for comparison (Fig. **30**).[106]

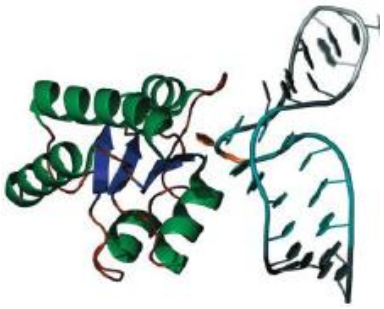

**Figure 30**: The X-ray structure of L7Ae complex with the RNA of *Archaeoglobus fulgidis* showing the K-turn motif of the RNA; the amino acid sequence with secondary structure elements of L7Ae (helix, green; *β*-sheets, blue; loop, red) and the RNA nucleotide sequences interacting with the protein (turquoise and orange, figure from ref. 106).

Using solid state NMR transferred-echo double resonance (TEDOR), the distances between the $^{15}N$ nuclei of the protein backbone and the $^{31}P$ nuclei of the RNA backbone could be measured. In TEDOR experiments the $^{31}P$-$^{15}N$ correlation investigated is highly selective, as proteins do not contain phosphorus, thus ensuring that the observed $^{31}P$-$^{15}N$ cross-peaks are intermolecular. The measured intermolecular distances between $^{15}N$ nuclei of L7Ae and the phosphate backbone of specific nucleotide sequences of RNA were in very good agreement with those expected from the crystallographic structure of the complex (Fig. **30**), hence underlining the potential of this technique for investigation of interactions between biomolecules.[106]

In 1983 characterisation of affinity supports by $^{13}C$ MAS NMR spectroscopy was reported by Bayer *et al*. for the analysis of silica gel derivatives.[107] However, the first report which describes the analysis of an agarose-based affinity support was disclosed by Zumbrink *et al*. in 1994.[108] As discussed in chapter 1, one of the problems in affinity technology is the analysis of the synthesised affinity matrices, as liquid phase methodology can not generally be applied. In this work by Zumbrink *et al.*,[108] the use of $^{13}C$ MAS NMR spectroscopy shed light on the mechanism of the nucleophilic reaction of certain trifluoroethylsulfonyl (tresylate) derivatives of agarose gels in the presence of a base. As highlighted in scheme **27**, tresyl agarose derivative **79** was treated with an aqueous solution of sodium hydroxide generating β-sulfonyl carboxylic acid derivative **80**.

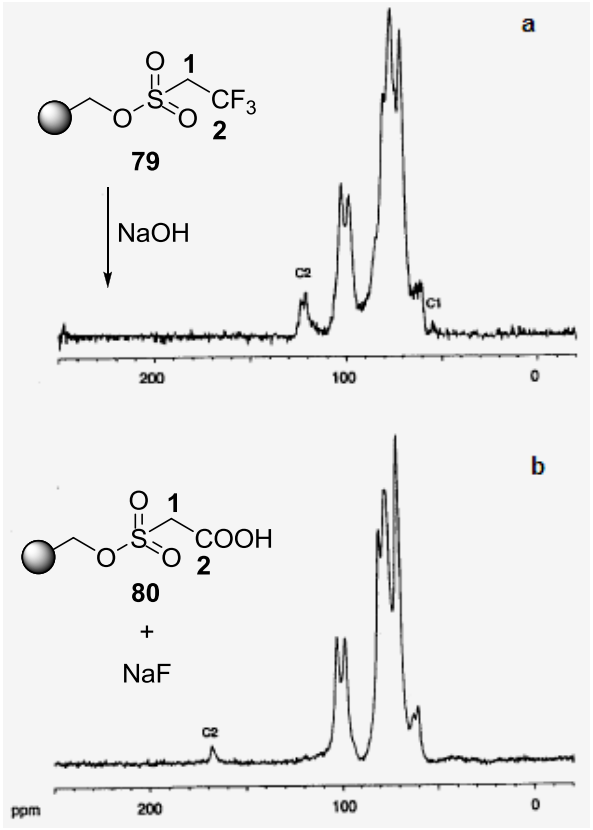


**Scheme 27**: $^{13}C$ MAS NMR spectra of tresyl agarose **79** and its alkaline hydrolysis product **80**.

A new signal at 168.0 ppm corresponding to a carboxylic acid was found, however it was not possible to visualise the α-sulfonyl carbon as the signal had shifted to a higher ppm value, underneath the agarose peaks (Scheme **27**, b). As well as demonstrating the applicability of MAS NMR for characterisation of agarose derivatives, this groundbreaking work allowed $^{13}C$ NMR analysis of nucleophilic reaction products of tresyl agarose (Scheme **27**).[108]

### 3.1.2 Solid-supported biotin molecular probe

Among the solid-supported molecular probes analysed by solid state NMR, molecular probe **72** (Fig. **31**) gave the most significant results. Hence, the full characterisation of its solution phase analogue **70** (Fig. **32**-**34**, $^{1}H$, $^{13}C$, COSY and HSQC spectra), will be reported in this section followed by the $^{1}H$ and HSQC spectra of the solid-supported biotin **72** which were analysed by analogy with the data of the solution phase analogue (Fig. **35** and **36**).

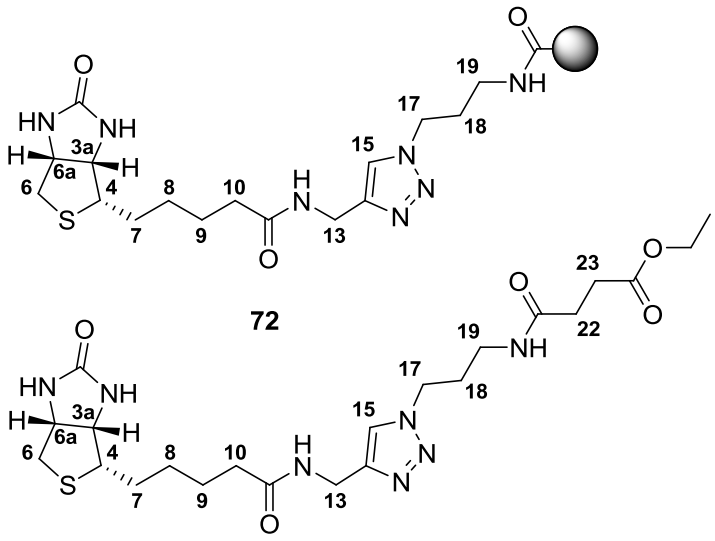


**Figure 31**: Solid-supported biotin **72** versus biotinylated solution phase analogue **70**.

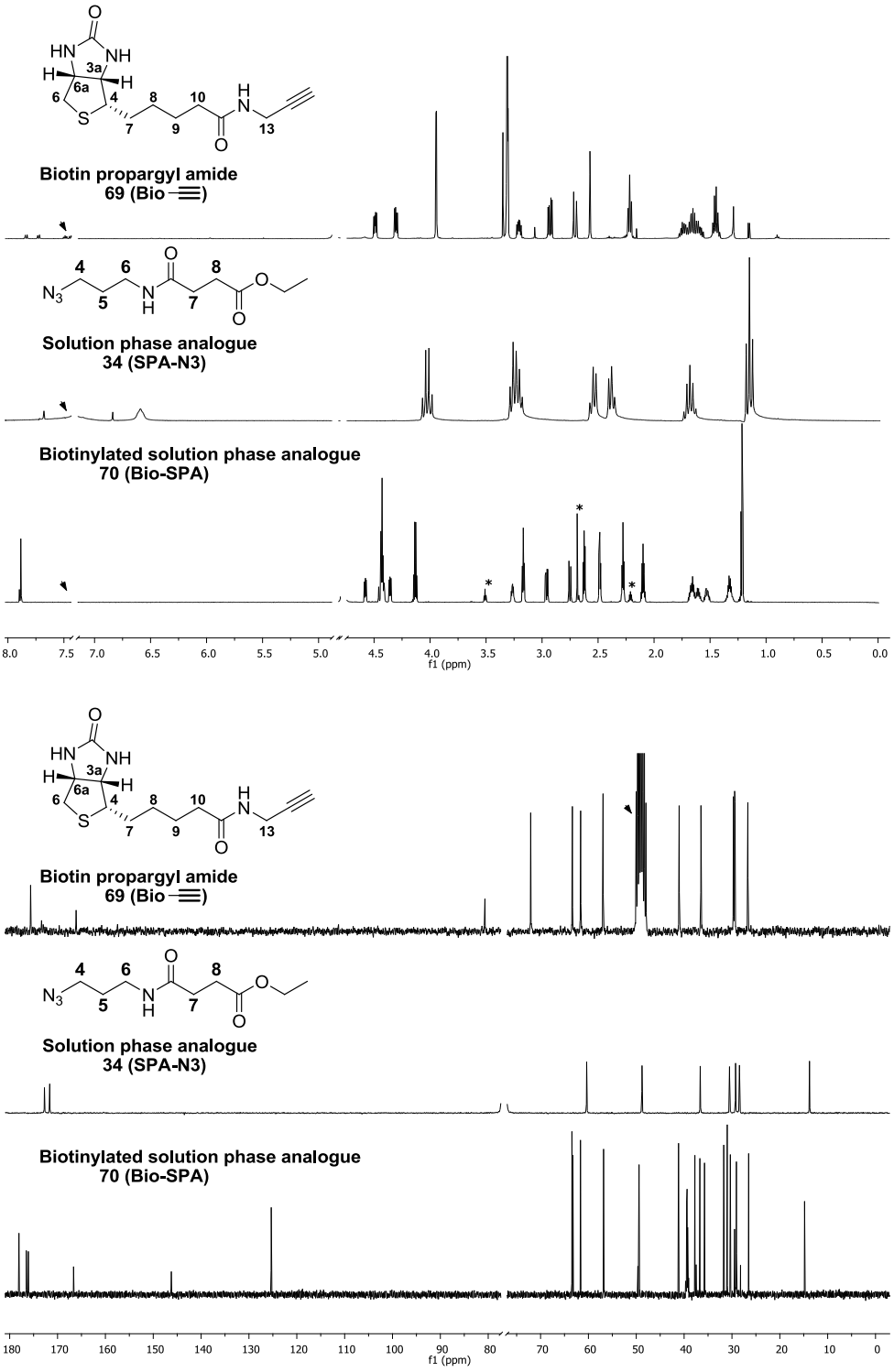


**Figure 32**: $^{1}H$ and $^{13}C$ NMR spectra of solution phase analogue **70** (800 MHz, $D_2O$) and its starting materials, biotin propargyl amide **69** (250 MHz, $CD_3OD$) and azidoester **34** (250 MHz, $CDCl_3$). Solvent residual peaks were omitted for clarity (arrows).

| **$^{1}$H NMR** | **Bio−≡ 69**<br>250 MHz, $CD_3OD$ | **SPA−$N_3$ 34**<br>250 MHz, $CDCl_3$ | **Bio-SPA 70**<br>800 MHz, $D_2O$ |
|---|---|---|---|
| $C_{3a}H$ | 4.30 **dd**, 7.8, 4.3 | | 4.35 **dd**, 7.9, 4.5 |
| $C_4H$ | 3.24-3.16 **m** | | 3.27-3.25 **m** |
| $C_{6a}H$ | 4.49 **dd**, 7.8, 4.9 | | 4.57 **dd**, 7.9, 4.5 |
| $C_6H_aH_b$ | 2.93 **dd**, 12.7,4.9 | | 2.96 **dd**, 13.0, 5.0 |
| $C_6H_aH_b$ | 2.70 **d**, 12.7 | | 2.75 **d**, 13. |
| $C_7H_cH_d$ | 1.81-1.37 **m** | | 1.62-1.58 **m** |
| $C_7H_cH_d$ | 1.81-1.37 **m** | | 1.54-1.50 **m** |
| $C_8H_2$ | 1.81-1.37 **m** | | 1.34-1.30 **m** |
| $C_9H_2$ | 1.81-1.37 **m** | | 1.68-1.63 **m** |
| $C_{10}H_2$ | 2.21 **t**, 7.3 | | 2.28 **t**, 7.1 |
| $C_{13}H_2$ | 3.94 **d**, 2.5 | | 4.42-4.40 **m** |
| $C_{15}H$ | 2.58 **t**, 2.5 | | 7.88 **s** |
| $C_{17}H_2$ | | 3.28-3.17 **m** | 4.43 **t**, 6.7 |
| $C_{18}H_2$ | | 1.62 **qn**, 6.7 | 2.08 **qn**, 6.7 |
| $C_{19}H_2$ | | 3.28-3.17 **m** | 3.16 **t**, 6.7 |
| $C_{22}H_2$ | | 2.51 **t**, 6.7 | 2.62 **t**, 6.7 |
| $C_{23}H_2$ | | 2.35 **t**, 6.7 | 2.48 **t**, 6,7 |
| $C_{26}H_2$ | | 3.98 **q**, 7.2 | 4.13 **q**, 7.1 |
| $C_{27}H_3$ | | 1.12 **t**, 7.2 | 1.21 **t**, 7.1 |
| **$^{13}$C NMR** | **Bio−≡ 69**<br>250 MHz, $CD_3OD$ | **SPA−$N_3$ 34**<br>250 MHz, $CDCl_3$ | **Bio-SPA 70**<br>800 MHz, $D_2O$ |
| $C_1$ | 166.15 | | 166.70 |
| $C_{3a}H$ | 63.39 | | 63.30 |
| $C_4H$ | 56.99 | | 56.84 |
| $C_{6a}H$ | 61.67 | | 61.71 |
| $C_6H_2$ | 41.08 | | 41.23 |
| $C_7H_2$ | 29.49 | | 29.12 |
| $C_8H_2$ | 29.75 | | 29.25 |
| $C_9H_2$ | 26.73 | | 26.56 |
| $C_{10}H_2$ | 36.53 | | 36.76 |
| $C_{11}$ | 175.66 | | 176.58 |
| $C_{13}H_2$ | 29.41 | | 49.46 |
| $C_{14}$ | 72.10 | | 146.27 |
| $C_{15}H$ | 80.73 | | 125.35 |
| $C_{17}H_2$ | | 48.80 | 35.80 |
| $C_{18}H_2$ | | 30.51 | 30.39 |
| $C_{19}H_2$ | | 36.63 | 37.80 |
| $C_{21}$ | | 172.74 | 178.12 |
| $C_{22}H_2$ | | 28.43 | 31.04 |
| $C_{23}H_2$ | | 29.25 | 31.77 |
| $C_{24}$ | | 171.63 | 176.15 |
| $C_{26}H_2$ | | 60.63 | 63.50 |
| $C_{27}H_3$ | | 13.80 | 14.88 |

**Table 1**: Chemical shift values of solution phase analogue **70** (**SPA**) and its starting materials.

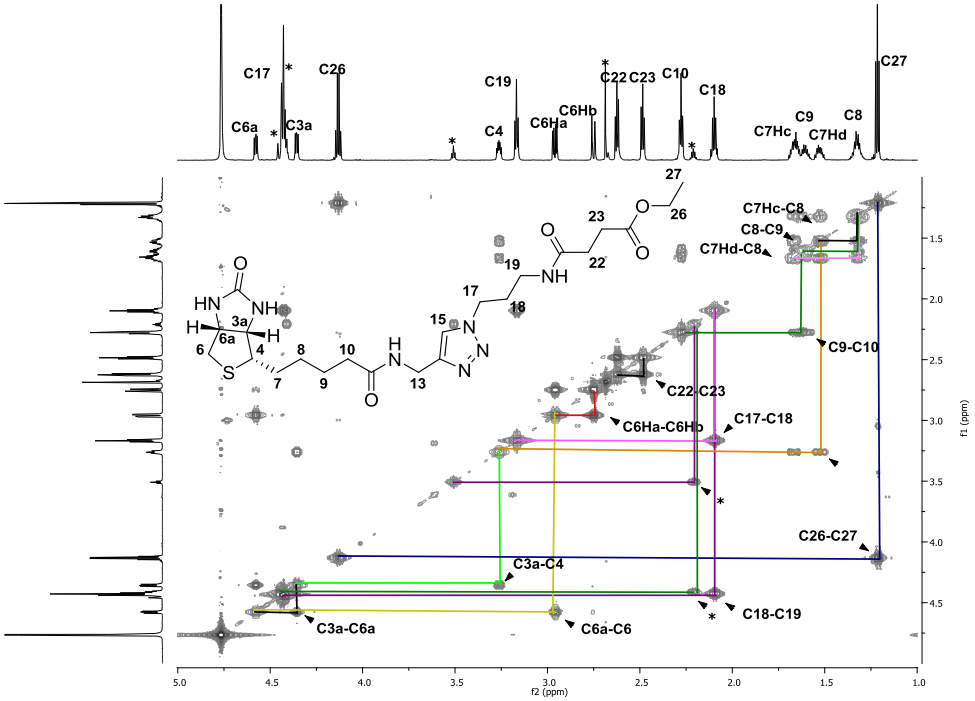


**Figure 33**: COSY spectrum of solution phase analogue **70** (800 MHz, $D_2O$).

Analysis of the $^{1}H$ and $^{13}C$ NMR spectra unequivocally confirmed the formation of the desired triazole with characteristic singlet at 7.88 ppm (Table **1**). The signals relating to the short hydrocarbon chain ($C_{17}$ to $C_{19}$) in azido ester **34** are slightly shifted downfield in the product and in particular the $^{13}C$ NMR spectrum shows a huge difference of chemical shift for $C_{17}$ (Table **1**, from 48.80 to 35.80 ppm). The $^{1}H$ NMR data shows that chemical shift values and multiplicities of the heterocyclic core of biotin propargyl amide **69** are fairly consistent with those found in the spectrum of the product ($C_{3a}$ to $C_6H_aH_b$, particularly when allowing for differences in acquisition solvent). Analysis of the COSY spectrum of compound **70** allowed confident assignment of the overlapped peaks of the hydrocarbon chain of biotin (Fig. **33**). The identity of the carbons of compound **70** was established by HSQC analysis (Fig. **34**). A series of extra peaks were found in the $^{1}H$ NMR at 7.90, 4.46-4.40, 3.51, 2.69 and 2.21 ppm. The singlet peak at 7.90 ppm suggested the presence of a different triazole species; analysis of the COSY spectrum confirmed that this series of peaks did belong to the same molecule. The most

interesting signal was the singlet peak at 2.69, which is a diagnostic peak for the two methylenes of a succinimide ring.[109,110] These observations suggested that perhaps cyclisation of the amide nitrogen in the last portion of the molecule onto carbonyl $C_{24}$ could have generated succinimide **81** as a side product during the click coupling (Scheme **27**). The chemical shift values and multiplicities of signals at 3.51 ppm (**t**, $J$ = 6.7) and at 2.21 (**qn**, $J$ = 6.7) were consistent with the formation of such a succinimide derivative. This cyclisation reaction is not unprecedented; although the formation of succinimide derivatives occurs through cyclisation onto methyl or ethyl esters in high yield (up to 90%) under basic conditions, isolation of this species as a minor side product has been also reported during different type of synthetic transformations.[111,112,113] Indeed, intramolecular cyclisation of a derivatised nucleoside in the presence of triethylamine has been employed by Matsumoto *et al*. for the preparation of a class of pro-drug molecules as potential anti-HIV agents.[112] In 2002, Molina Pinilla *et al*.[111] reported the formation of the succinimide ring in connection to their studies on the hydrolytic degradation of certain poly(ester amide) polymers. Isolation of a succinimide derivative as a minor side product (3% yields) was also reported by Masanori *et al*. when carrying out the methylation of a indole derivative in the presence of diazomethane.[113] The $^{1}H$ and $^{13}C$ NMR signals relating the last portion of side product succinimide derivative **81** are highlighted in the HSQC spectrum of biotinylated solution phase analogue **70** (Fig. **34**, $*C_{13}$ to $*C_{23}$).

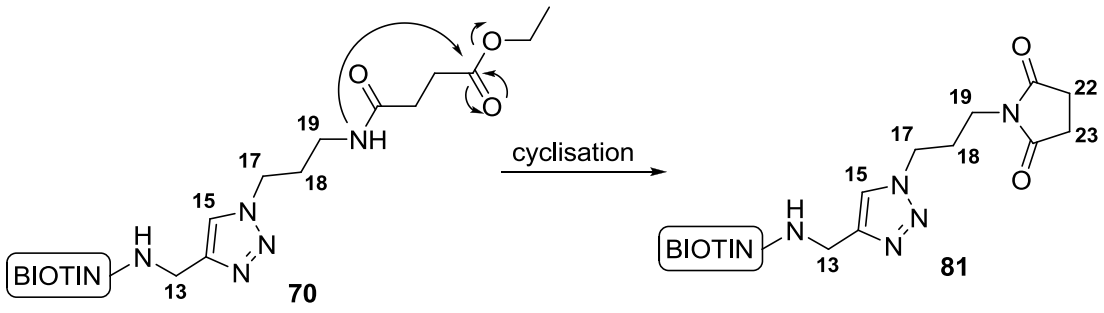


**Scheme 27**: Cyclisation reaction resulting in the formation of succinimide derivative **81** as a side product of the click reaction.

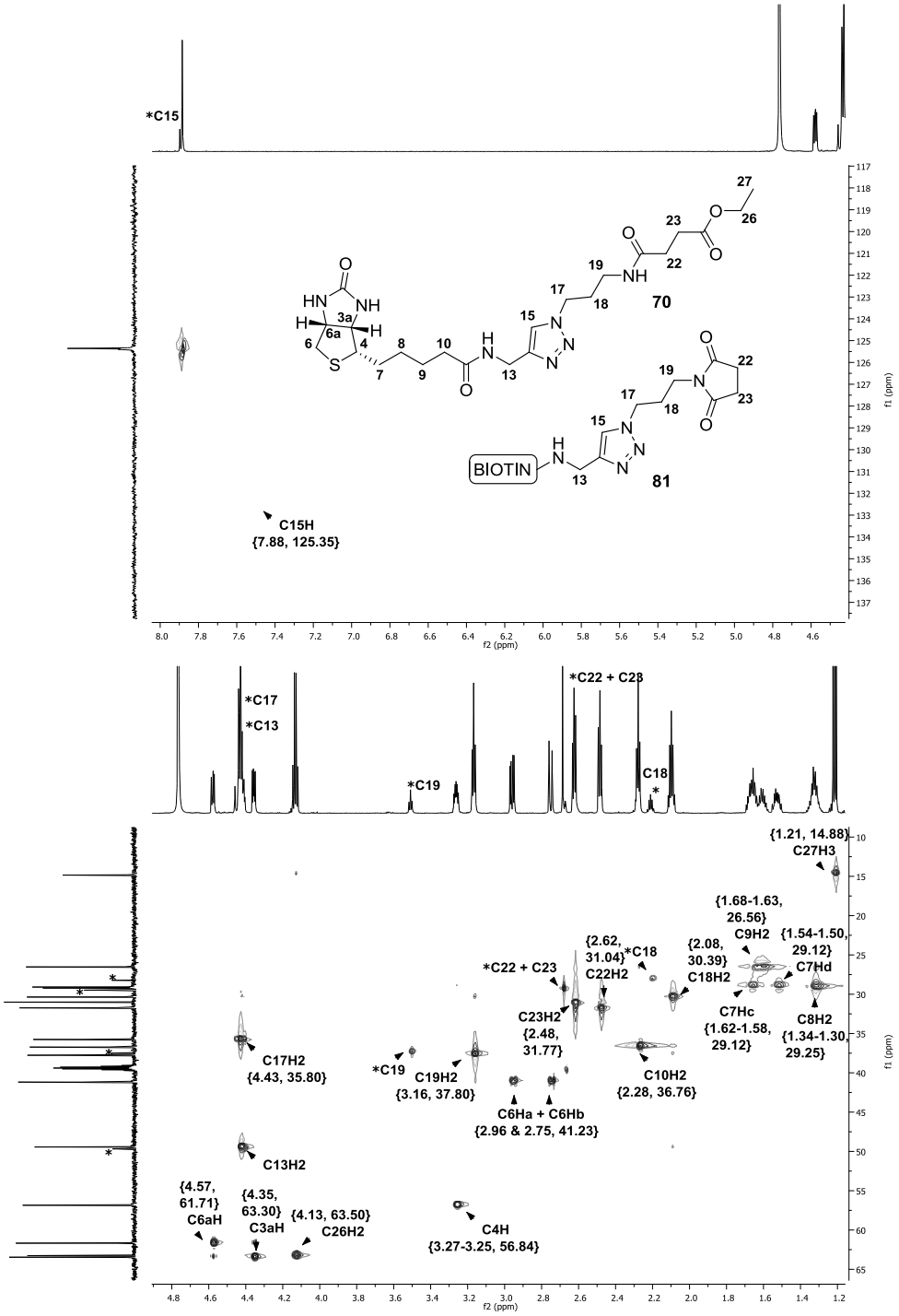


**Figure 34**: HSQC spectrum of solution phase analogue **70** (800 MHz, $D_2O$).

The best results for the solid state NMR of solid-supported biotin **72** were obtained for $^{1}H$ and HSQC NMR spectra (Fig **35** and **36**) which could be analysed by analogy with solution phase analogue **70**.

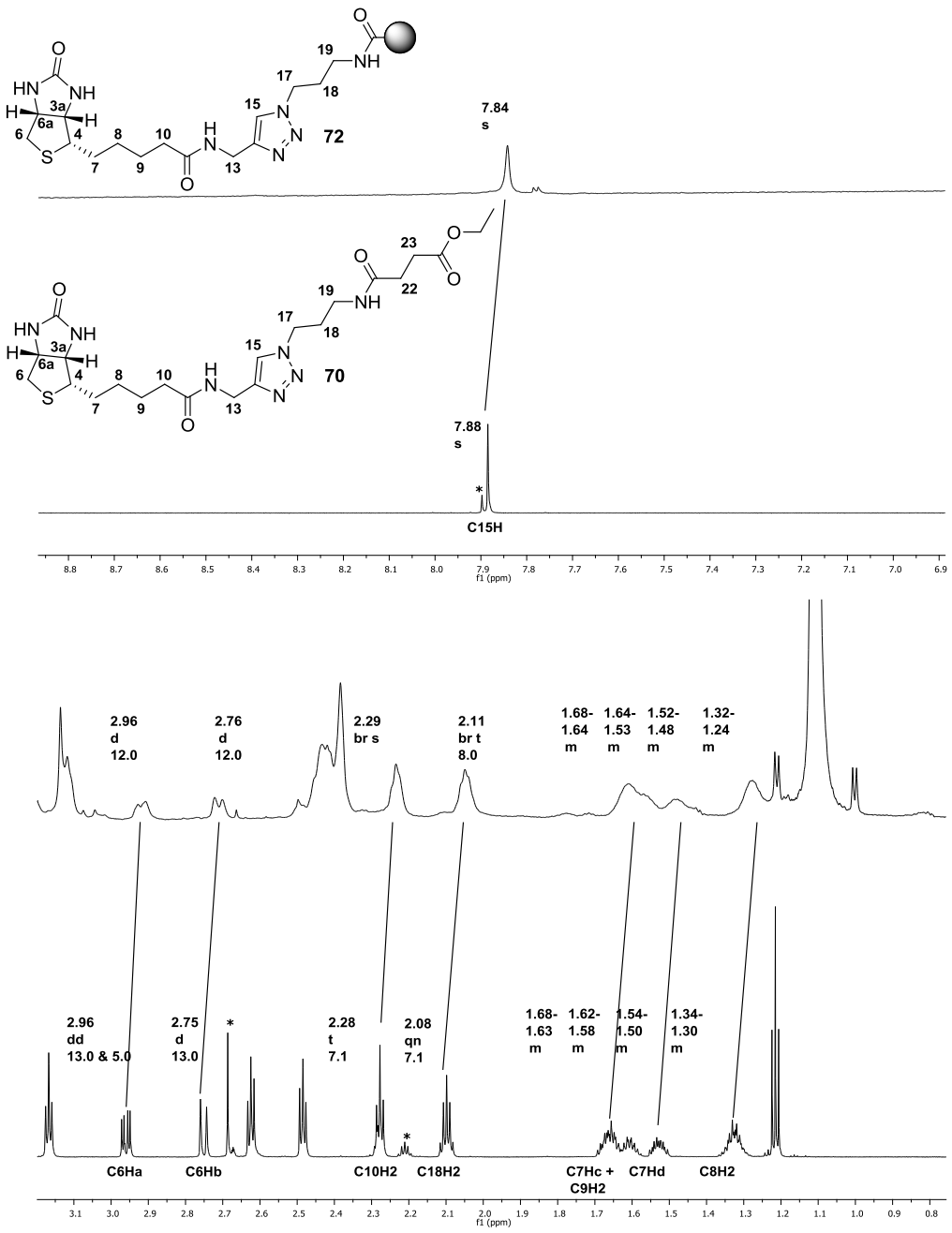


**Figure 35**: Stacked $^{1}H$ spectra of the solid-supported biotin **72** (800 MHz, $D_2O$) and the solution phase analogue **70** (800 MHz, $D_2O$).

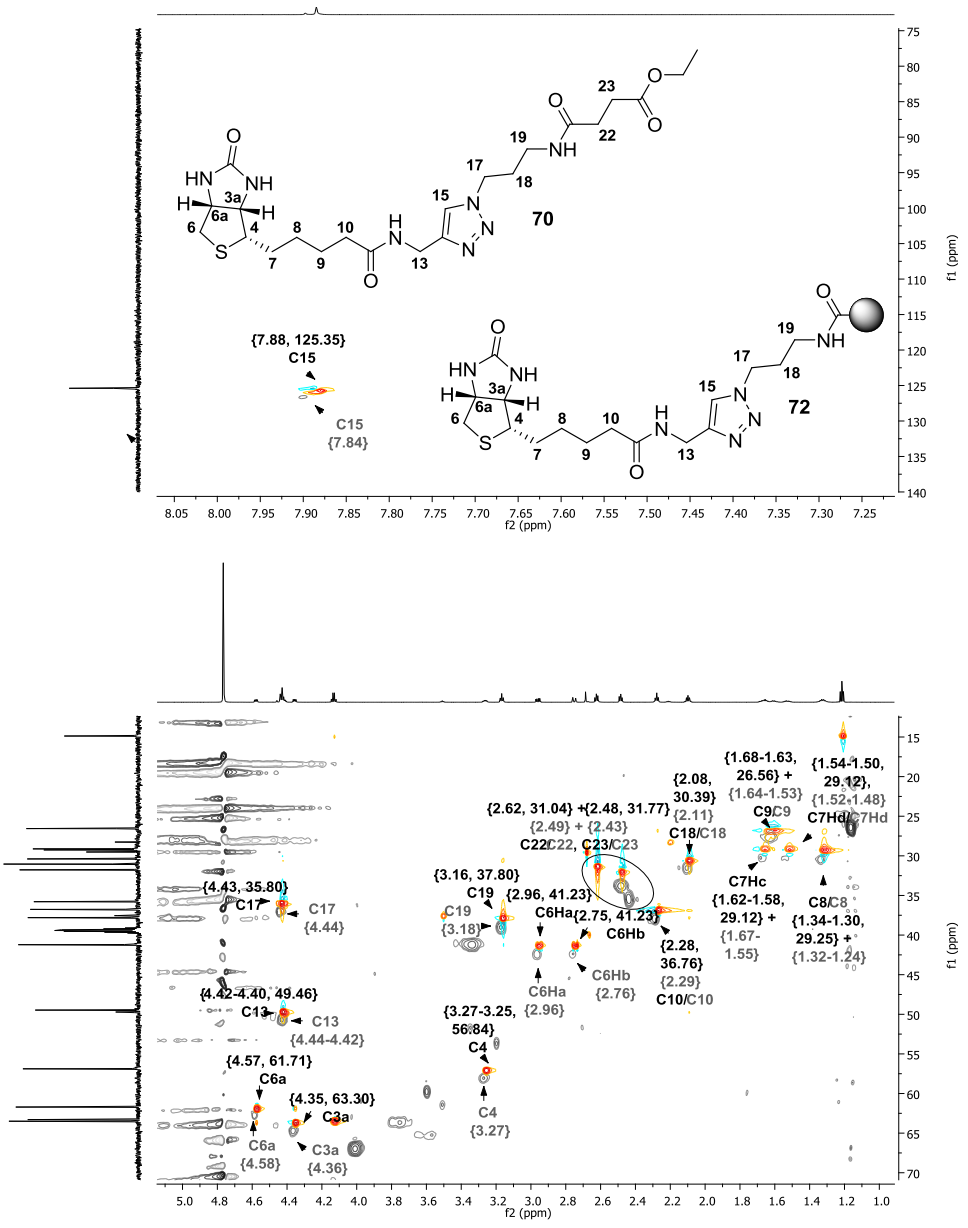


**Figure 36**: Stacked HSQC spectra of the solid-supported biotin **72** (800 MHz, $D_2O$, gray peaks) and the solution phase analogue **70** (800 MHz, $D_2O$, red/light blue peaks).

Gratifyingly, the $^1H$ spectrum of the solid-supported biotin **72** showed the characteristic singlet of the triazole moiety at 7.84 ppm (Fig. **35**) confirming that the click coupling of

biotin propargyl amide to the agarose matrix had occurred. Although the spectral lines are quite broad, it is also possible to recognise by analogy with the solution phase analogue **70** some of the protons of the heterocyclic core of biotin (*e.g.* $C_6H_aH_b$ + $C_6H_aH_b$, Fig. **35**). Furthermore, the chemical shift values of the protons of the hydrocarbon chain of biotin (*e.g.* $C_7H_2$ to $C_9H_2$, from 1.68 to 1.24 ppm) are in good agreement with those of the solution phase analogue. The overlapped HSQC spectra show a distinctive peak for $C_{15}H$ (triazole) for both the compounds (Fig. **36**). Most of the signals of the heterocyclic core and the hydrocarbon chain of the solid-supported biotin were fairly consistent with those of the solution phase analogue. Despite the presence of side product succinimide **81** in the NMR sample of biotinylated solution phase analogue **70**, such compound was a valid reference for the characterisation of solid-supported biotin **72**. This approach for the characterisation of the affinity support proved successful, although time consuming. For the other molecular probes synthesised featuring the chemoselective cleavable azobenzene unit (*e.g.* simplified molecular probe **75**, Scheme **28**), preliminary cleavage and identification of the aniline derivative by either MS or $^1$H NMR was used to ascertain the presence of the ligand on the affinity matrix.

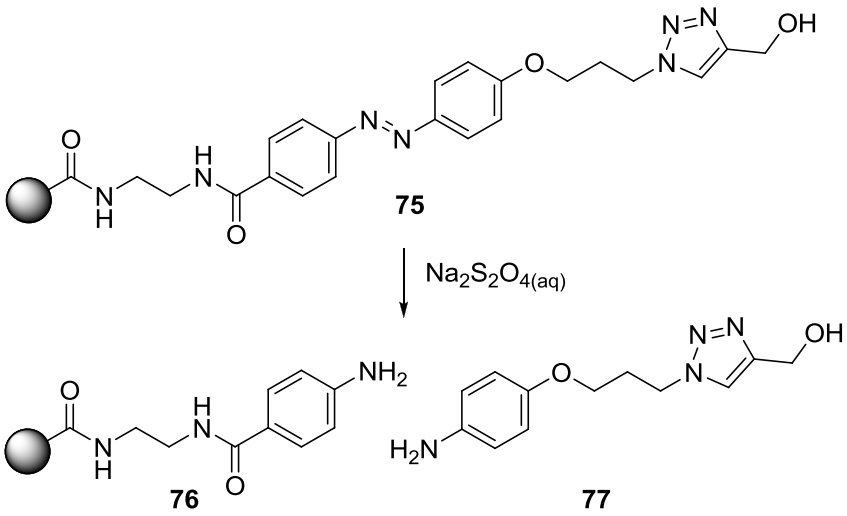


**Scheme 28**: Cleavage of the simplified molecular probe **76** and isolation of aniline **77**.

## 3.2 Affinity investigations

The preliminary affinity studies using solid-supported biotin, molecular probes **72** and **74** (Fig. **37**) will be discussed in sections 3.2.2 and 3.2.3 while the pull-down experiments using anisomycin molecular probe **32** will be reported in section 3.3.

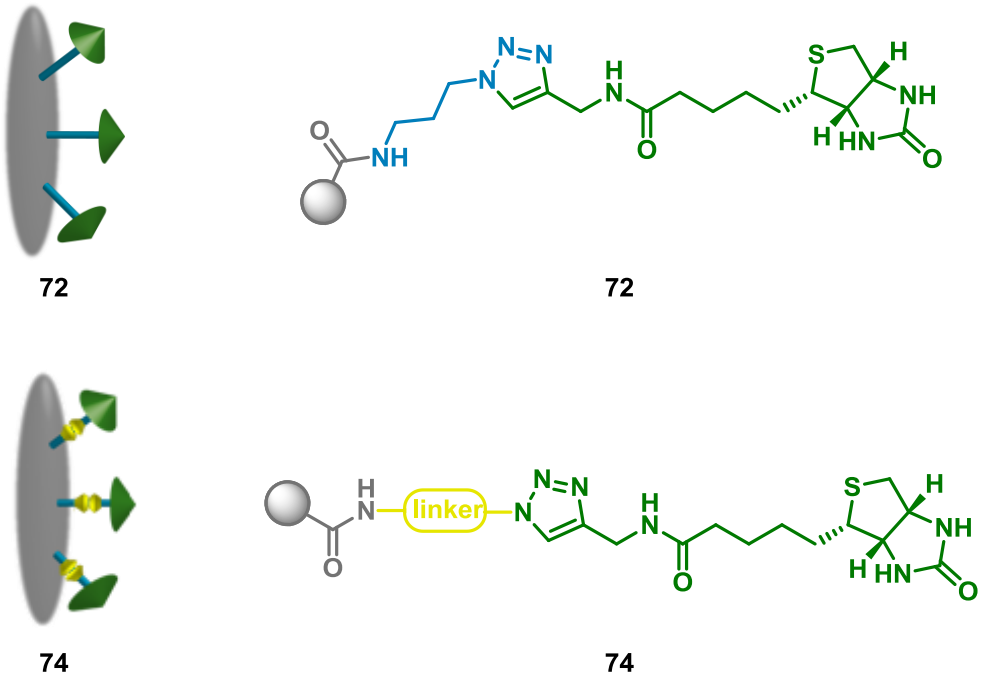


**Figure 37**: The molecular probes employed in the preliminary affinity studies. In the description of the experiments in sections 3.2.2 and 3.2.3 the cartoon representations will be employed.

### 3.2.1 Biotin/streptavidin affinity chromatography

In order to test how robust the affinity independent elution protocol based on the use of the novel azobenzene derivative linker would be, the biotin/streptavidin affinity pair was selected. Biotin and its affinity partner streptavidin have one of the strongest non-covalent interactions known.[75] This exceptional binding affinity ($K_d \sim 10^{-15}$ M) and the slow dissociation rate are fundamentally due to a series of hydrogen bonds between

streptavidin and the heterocyclic core of biotin (Fig. **38**). Because of this peculiar characteristic the streptavidin/biotin system has been employed in countless affinity-based purification protocols in the last 30 years. Chicken avidin (originally isolated from egg white) as well as streptavidin (secreted by *Streptomyces* bacteria) are functionally and structurally analogous proteins (Fig. **38**, respectively mono- and tetrameric proteins).[114]

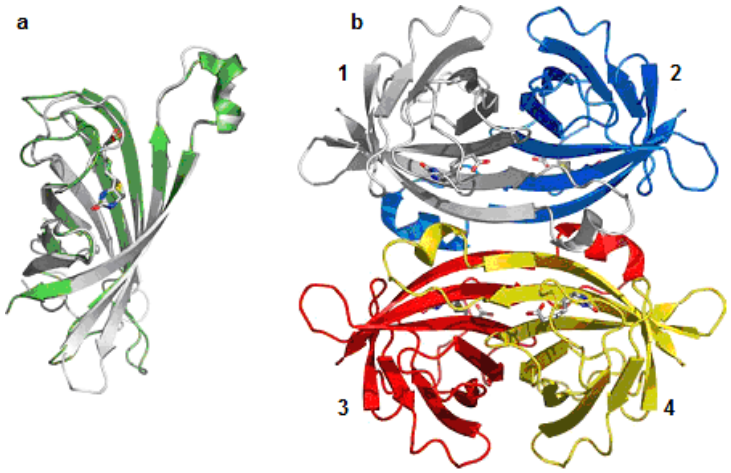


**Figure 38**: (a) Superimposed structure of avidin (gray) and streptavidin (green); the secondary structures are determined by X-ray crystallography. The secondary structural elements are indicated as a cartoon representation and the bound ligand, D-biotin, is shown in stick format. (b) Avidin tetramers. The secondary structural elements are indicated as a cartoon representation and bound ligands, four biotin molecules, are shown in stick format (Figure from ref. 114).

Among the countless applications of this affinity pair in biochemistry, a recent report investigating new reactivities for biotin will be discussed. A novel approach to the biotinylation of electron-rich reporter molecules such as redox-active ferrocene and ruthenocene and luminescent pyrene, based on their Friedel-Crafts acylation using D-biotin, was proposed (Scheme **28**) by Plażuk *et al.*[115] Although Friedel-Crafts products **82-84** lacked an amide bond, they retained their affinity for avidin, as confirmed by their ability to displace 2-(4-hydroxyphenylazo)-benzoic acid (HABA) in its complex with avidin. Formation of the avidin-**84** complex was also evidenced by quenching of the fluorescence from the protein tryptophan residues (342 nm) and appearance of the

emission band of the avidin-bound **84** at 430 nm as a result of a Forster resonance energy transfer (FRET) phenomenon. This report introduced a new approach to the synthesis of biotin derivatives without an amide bond. Interestingly, these compounds should be resistant to the endogenous enzyme biotinidase, which cleaves CO-NH bonds in biotin conjugates, hence remarkably limiting *in vivo* applications of biotin amides.[116]

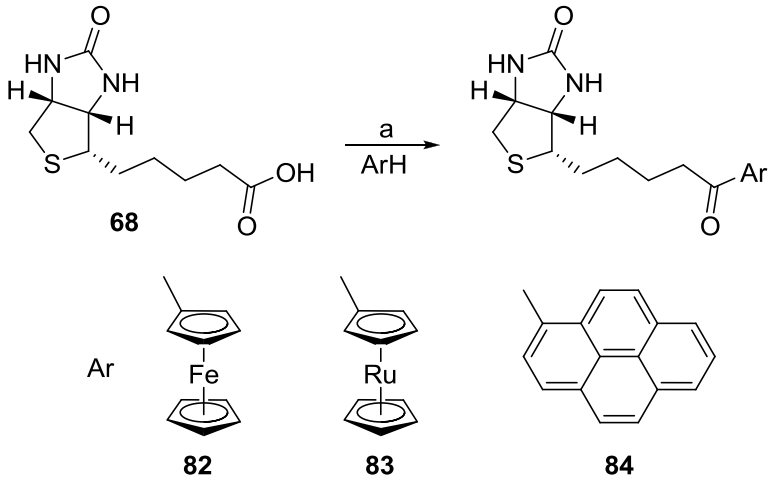


**Scheme 29:** Friedel-Crafts biotinylation of ferrocene, ruthenocene and pyrene. (a) TFAA/TfOH, (55% for **82**, 53% for **83** and 47% for **84**).

### 3.2.2 Competitive capture and release of avidin

The first set of affinity experiments were designed to ascertain that the solid-supported biotin, molecular probes **72** and **74** retained the capability to capture avidin (monomeric) despite the presence of the matrix and the linker. This capture must be selective (*i.e.* without any competing non-specific interactions),[117] hence both the matrices were incubated with both avidin and albumin (negative control, Scheme **30**). Albumin is known as a "sticky" protein that acts as a transporter for blood components such as hormones and lipoproteins.[118] This characteristic makes this protein ideal to ascertain the absence of non-specific interactions of the molecular probes **72** and **74** in a pull-down experiment. For the release of the captured proteins a classical protocol (SDS

elution) was followed for matrix **72**, while dithionite elution[79] was performed for matrix **74** (Scheme **30**, a and b).

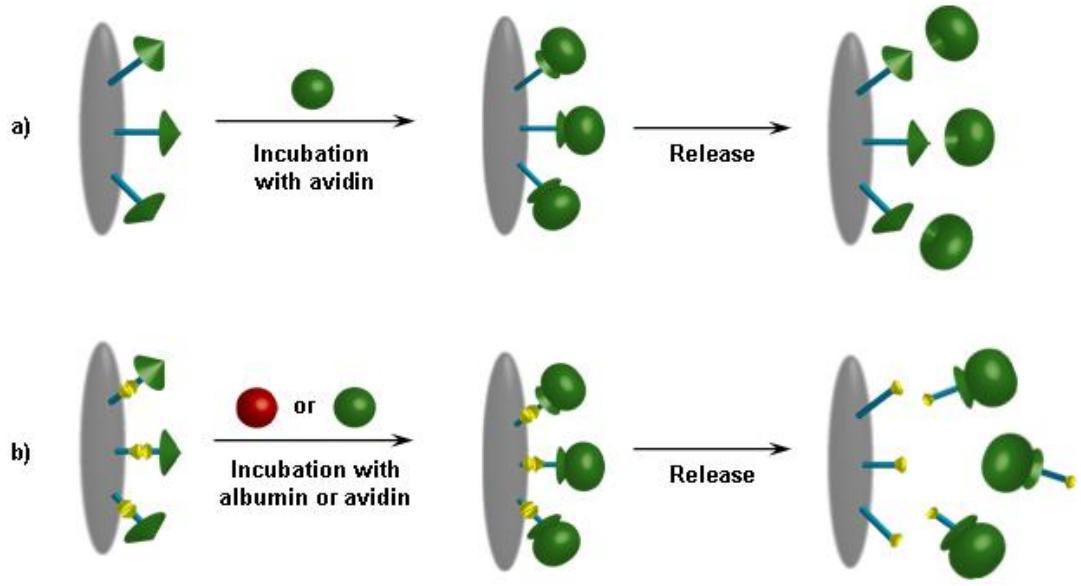


**Scheme 30**: Competitive capture and release of avidin. Albumin = red ligand; avidin = green ligand. (a) A solution of avidin (1 ml, 1 mg $ml^{-1}$) was added to matrix **72** (1 ml, 15 µmol $ml^{-1}$). After extensive washings, the matrix was divided into two aliquots and SDS elution or dithionite cleavage were performed to collect the isolated proteins. (b) A solution of avidin (1 ml, 1 mg $ml^{-1}$) or albumin (1 ml, 1 mg $ml^{-1}$) was added to matrix **74** (1ml, 15 µmol $ml^{-1}$). After extensive washings, the matrix was divided into three aliquots and SDS elution or dithionite cleavage were performed to collect the isolated proteins.

The isolated proteins were analysed by SDS-PAGE and the results are shown in figure **39**. The absence of a clear band for avidin (15 kDa) in the supernatant following incubation shows that both matrices bound avidin (Fig. **39**, lanes A, B, D & E). Quantitative elution of albumin (band at 66 kDa, Fig. **39**, lane C) and the absence of its band following SDS cleavage (Fig. **39**, lane G) also demonstrated that matrix **74** did not exhibit any non-specific interactions for albumin. The efficiency of a classical SDS elution procedure (for matrix **73**) and chemoselective cleavage with sodium dithionite (for matrix **74**) were then compared. Gratifyingly, both elution procedures showed the expected bands for avidin (Fig. **39**, lanes F & $J_{1-3}$). In order to identify the optimal cleavage conditions, the dithionite cleavage was performed at a range of pH values (Fig.

**39**, lanes $J_{1-3}$).[79] The best results were obtained by incubating with a phosphate buffer solution at pH 6.5 and using a large excess of sodium dithionite (Fig. **39**, lane $J_1$). These mild cleavage conditions were shown not to release avidin from matrix **39** in the absence of the azo linker (Fig. **39**, lanes $I_{1-3}$) demonstrating the chemoselectivity of this protocol. On the other hand, the presence of the linker does not interfere with a classical SDS elution protocol, as confirmed by the fact that avidin is released from matrix **74** under these conditions (Fig. **39**, lane H).

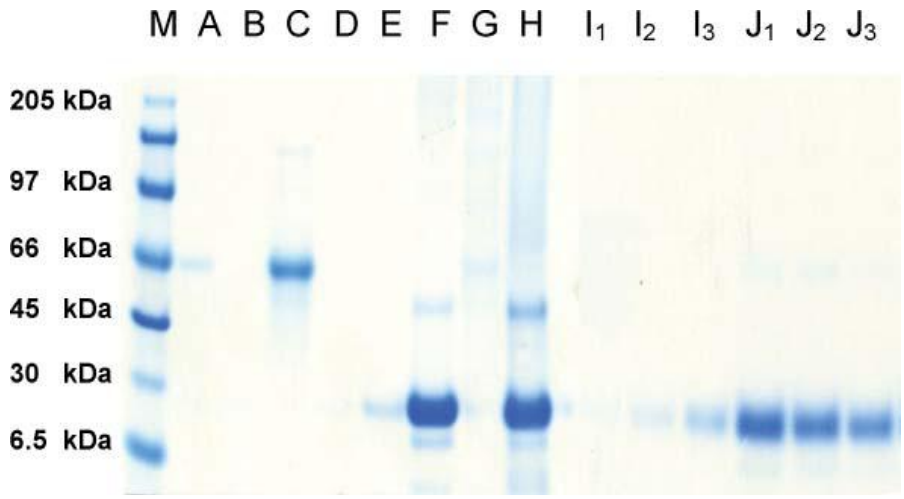


**Figure 39**: SDS-PAGE for experiments with avidin and albumin: lanes **A-E** supernatants after incubation; lanes **F-H** supernatants following SDS elution; lanes $\mathbf{I_1}$-$\mathbf{J_3}$ supernatants following dithionite cleavage. **M**=marker lane; **A** & **B** = supernatant from incubation of matrix **72** with avidin; **C** = supernatant from incubation of matrix **74** with albumin; **D** & **E** = supernatant from incubation of matrix **74** with avidin; **F** = supernatant after SDS elution of matrix **72** incubated with avidin (Lane **A**); **G** = supernatant after SDS elution of matrix **74** incubated with albumin (Lane **C**); **H** = supernatant after SDS elution of matrix **74** incubated with avidin (Lane **D**); $\mathbf{I_1}$-$\mathbf{I_3}$ = supernatant after dithionite cleavage of matrix **72** incubated with avidin (Lane **B**) at pH 6.5, 7.5 & 8.5; $\mathbf{J_1}$-$\mathbf{J_3}$ = supernatant after dithionite cleavage of matrix **74** incubated with avidin (Lane **E**) at pH 6.5, 7.5 & 8.5.

The chemical cleavage proved effective only when using freshly prepared aqueous solution of sodium dithionite. Increasing the incubation time of the reducing agent with the matrix (up to 30 min) did not improve the efficiency of the cleavage. This observation was in agreement with the literature.[119]

### 3.2.3 Capture and release of avidin from a protein mixture

The second set of experiments was aimed to determine whether the solid-supported biotin featuring a cleavable unit, molecular probe **74** could selectively capture its binding partner avidin from a complex mixture of proteins (Fig. **40**, a and b). For these reasons both matrices **72** and **74** were incubated with an avidin enriched fetal bovine serum (FBS) solution (the complexity of this mixture is represented in figure **40**, c, in lane A).

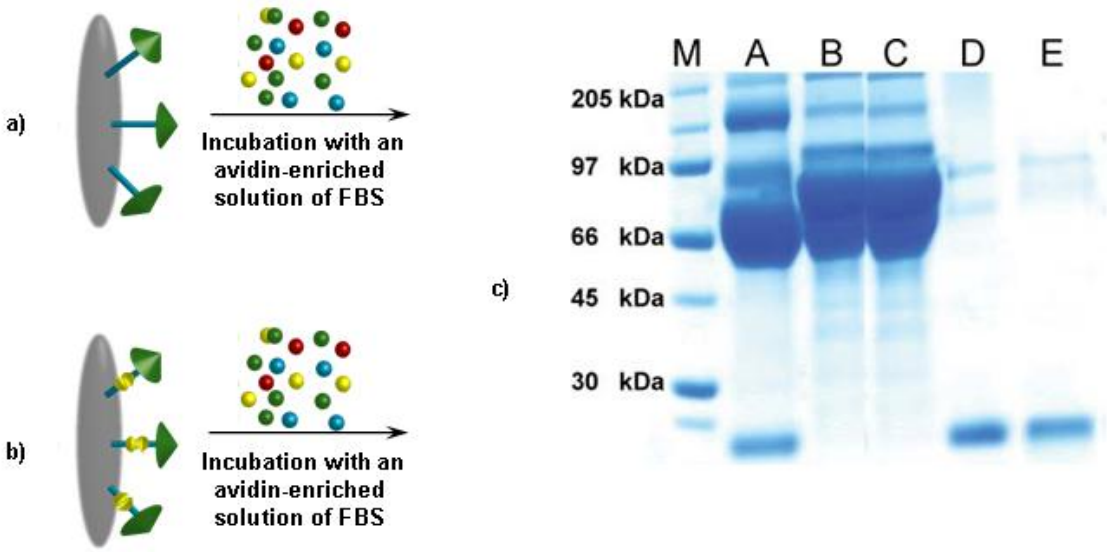


**Figure 40**: Capture and release of avidin from a protein mixture. (a) A solution of avidin-enriched (1 ml, 100 µg $ml^{-1}$) 10 % FBS in PBS was added to matrix **72** (1 ml, 15 µmol $ml^{-1}$). After extensive washings, SDS elution was performed to collect the isolated proteins. (b) A solution of avidin-enriched (1 ml, 100 µg $ml^{-1}$) 10 % FBS in PBS was added to matrix **74** (1 ml, 15 µmol $ml^{-1}$). After extensive washings, dithionite cleavage was performed to collect the isolated proteins. (c) SDS-PAGE for experiments with FBS: **M** = marker lane; **A** = FBS + avidin (control lane); **B** = supernatant after incubation of matrix **72** with FBS + avidin; **C** = supernatant after incubation of matrix **74** with FBS + avidin; **D** = supernatant after SDS elution of matrix **72** incubated with FBS + avidin (Lane B); **E** = supernatant after dithionite cleavage of matrix **74** incubated with FBS + avidin (Lane C).

Because of the abundance and variety of proteins contained, FBS is a standard medium for cell cultures.[120] In these preliminary studies FBS mimics the complexity of a protein

mixture resulting from a cell lysate. The use of 10% FBS in buffer PBS proved to be the ideal concentration (control lane A); when higher concentrations were used (25 and 25% FBS in PBS) it was not possible to distinguish the protein bands. Following incubation with the above described mixture of proteins, the experiments were carried out as before (Fig. **40**, a and b). All the matrices were extensively washed with 4×PBS buffer; the use of PBS in smaller concentrations (2× or 3×) or a different buffer (*e.g.* HEPES) proved less effective for the removal of the unbound proteins. All the isolated proteins were analysed by SDS-PAGE and the results are shown in figure **40**, c. Gratifyingly, both matrices were shown to selectively capture avidin (Fig. **40**, lanes B & C). Furthermore, the release of the bound material could be performed using the optimal cleavage conditions for each matrix: boiling with SDS for matrix **72** (Fig. **40**, lane D); and dithionite cleavage at pH 6.5 for matrix **74** (Fig. 3, lane E). The efficiency of the chemical cleavage was only marginally reduced with comparison to the SDS protocol (difference in intensity between avidin bands in lanes D & E).

## 3.3 Pull-down experiments with anisomycin molecular probe

Once the preliminary studies with matrices **72** and **74** were completed, investigations on the natural product anisomycin were attempted. The synthesis of a solid-supported anisomycin, molecular probe **32** (Fig. **41**) was readily achieved as described in section 2.2.5. Biotinylated anisomycin **28** (Fig. **41**) was also prepared following a protocol previously developed in the Hulme group.[76] This molecular probe was employed in the pull-down experiments together with the novel molecular probe **32** to be able to directly compare these data with the ones previously obtained in the Hulme group with compound **28** (as described in section 1.7.2). Both molecular probes were incubated with a human embryonic kidney (HEK) 293 cell lysate as this cellular line expresses the SAPK pathway with which anisomycin is known to interact. A modified protocol for pull-down experiments using biotinylated peptides optimised in the Ball research group

at the Cancer Research UK Centre at the Western General Hospital (Edinburgh) was followed.[121]

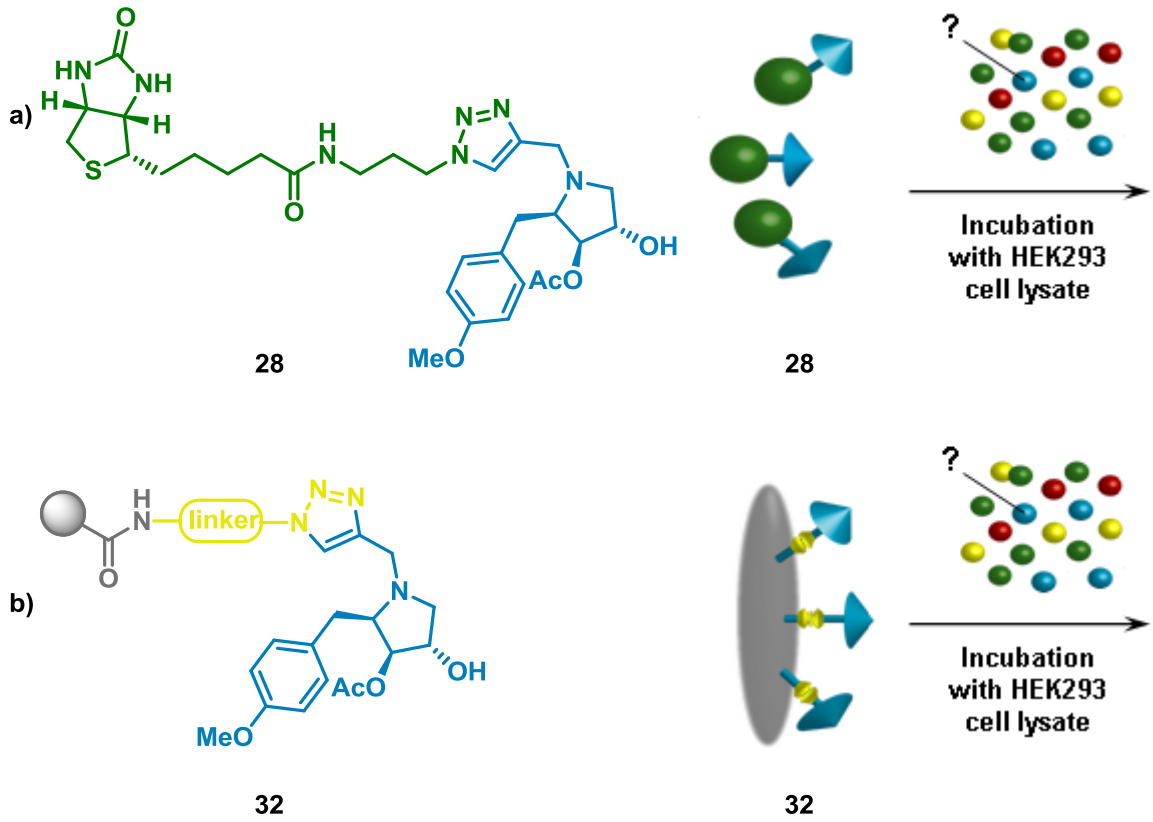


**Figure 41**: Pull-down experiments with HEK 293 cells. (−) = negative control; (+) = positive control; (a) Three solutions of: biotinylated anisomycin **28** (+, 1 µl, 50 mmol ml$^{-1}$), propargyl amide biotin **69** (−, 1 µl, 50 mmol ml$^{-1}$) and a biotinylated peptide (−, 1 µl, 50 mmol ml$^{-1}$) were added to three Eppendorf tubes containing a streptavidin-coated agarose matrix (40 µl, of a 50/50 mixture beads) and gently shaken for 1 h. After extensive washings, a cleared whole lysate of HEK 293 cells (49 µl) was added to all the matrices together with buffer W (151 µl). The matrices were incubated with the cell lysate for 1 h with gentle shaking. After extensive washings, SDS elution was performed to collect the isolated proteins. (b) Two samples of solid-supported anisomycin **32** at different concentrations (+, 40 µl, 5 mmol ml$^{-1}$ and 40 µl, 50 mmol ml$^{-1}$) and two samples of solid-supported azobenzene unit **73** at different concentrations (−, 40 µl, 5 mmol ml$^{-1}$ and 40 µl, 50 mmol ml$^{-1}$) were transferred to four Eppendorf tubes. After extensive washings, a cleared whole lysate of HEK 293 cells (49 µl) was added to all the matrices together with buffer W (151 µl). The matrices were incubated with the cell lysate for 1 h with gentle shaking. After extensive washings, dithionite cleavage was performed to collect the isolated proteins.

Along with the anisomycin molecular probes three negative controls (a biotinylated peptide, biotin propargyl amide **69** and solid-supported cleavable unit **73**) were incubated with the cell lysate. After incubation with the cell lysate, biotinylated samples were immobilised onto a streptavidin-coated matrix. The isolated proteins were analysed by SDS-PAGE (Fig. **42**). At the same time the mixture resulting from incubation of molecular probe **32** and HEK 293 cell lysate was submitted to dithionite cleavage. The isolated proteins were analysed by SDS-PAGE (Fig. **42**). Disappointingly, it was not possible to interpret the results obtained from the gel electrophoresis. The experiments were repeated using different staining solutions (*e.g.* Coomassie blue, ponceau S) with no significant improvement in the visualisation of bands on the gel (data not shown). Similarly, increasing the concentration of the molecular probes (from 5 mmol $ml^{-1}$ to 50 mmol $ml^{-1}$) did not positively affect the results of the experiments (lanes G & H).

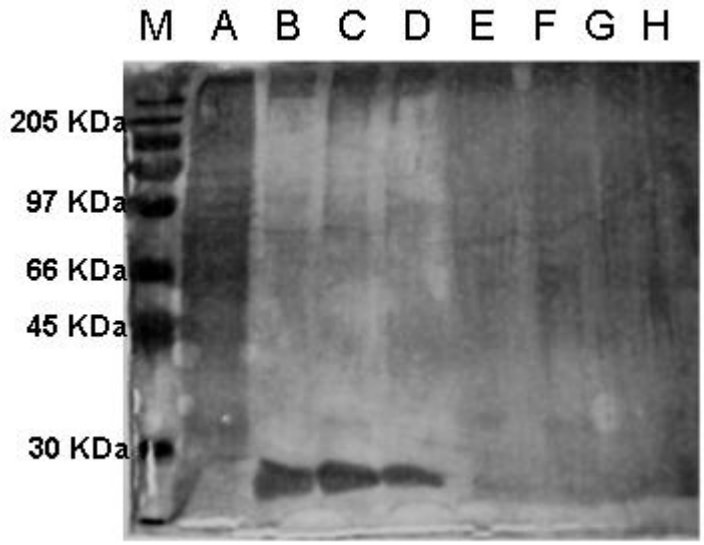


**Figure 42**: SDS-PAGE for pull-down experiments with HEK 293 cells. (−) = negative control; (+) = positive control; **M** = marker lane; **A** = cell lysate (control lane); **B** = supernatant after SDS elution of experiment with propargyl amide biotin **69** (−); **C** = supernatant after SDS elution of experiment with a biotinylated peptide (−); **D** = supernatant after SDS elution of experiment with biotinylated anisomycin **28** (+); **E** = supernatant after dithionite cleavage of experiment with matrix **73** (−, 5 mmol $ml^{-1}$); **F** = supernatant after dithionite cleavage of experiment with matrix **73** (−, 50 mmol $ml^{-1}$); **G** = supernatant after dithionite cleavage of experiment with matrix **32** (+, 5 mmol $ml^{-1}$); **H** = supernatant after dithionite cleavage of experiment with matrix **32** (+, 50 mmol $ml^{-1}$).

## 3.3 Future work

Although the pull-down experiments with HEK 293 needed extensive optimisation to obtain a set of more significant data, it was envisaged that the novel azobenzene could be employed as means of coupling biotin to the ligand. As the binding partner of anisomycin is unknown, there is no data about the dissociation constant ($K_d$) of the complex they form. Hence, a more classical manifold relying on the use of the biotin/streptavidin affinity pair for the immobilisation onto a column and a cleavable unit for the release of the isolated biomolecules seemed more appealing.

Interestingly, this strategy has been recently exemplified by Budin *et al.*[119] who reported a model study using the bacterial type II topoisomerase, DNA gyrase, as the target protein and its inhibitor, the aminocoumarin novobiocin, as the molecular hook. In this study, a new molecular probe featuring a chemoselective cleavable azobenzene derivative, a biotin affinity tag for enrichment on one side and an alkyne moiety and on the other side, is described (Fig. **43**).[119] The use of this cleavable linker allowed the capture and release of native protein complexes as confirmed by functional assays. This work represents an elegant example of the application of this strategy on a complex substrate (a 320 kDa tetrameric multidomain enzyme) and furnishes further data on the cleavage conditions.[119]

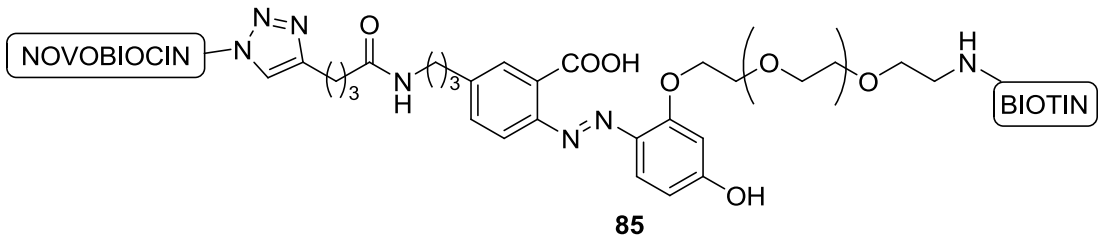


**85**

**Figure 43**: Novobiocin molecular probe **85** used for the capture and release of the target, DNA gyrase (bacterial type II topoisomerase).

Hence, an affinity-independent version of the more classical approach for target identification based upon immobilisation on a streptavidin-coated matrix will be next

attempted. The strategy described below will be applied to anisomycin and to bisebromoamide, a recently isolated natural product with interesting biological activity (Scheme **31**).[122] The biological properties of this novel cytotoxic peptide and the contribution to its synthesis will be discussed in chapters 4 to 6. Completion of the total synthesis of natural product bisebromoamide will provide another ligand to test the reliability of the protocol described in scheme **31**.

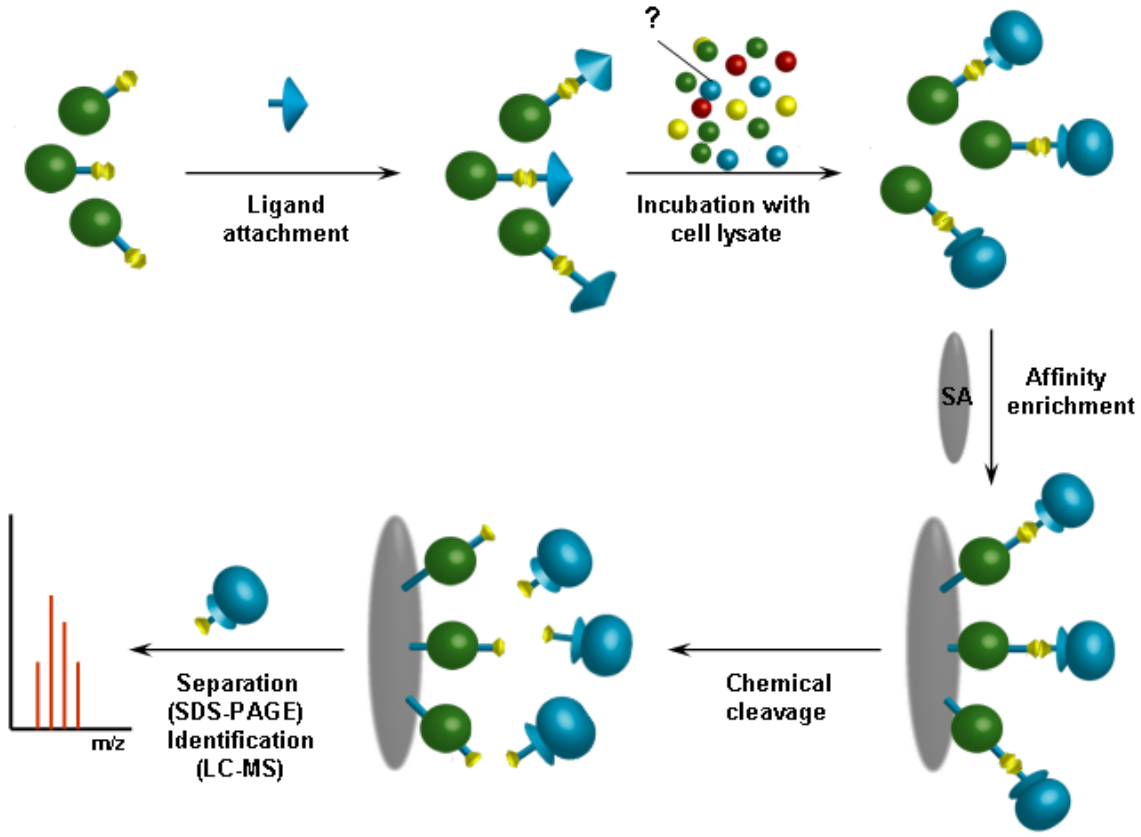


**Scheme 31**: Capture of an "unknown" affinity target for a small-molecule ligand by attachment of biotin to the ligand through a cleavable linker. Capture of the affinity target in solution, immobilisation of the biotinylated ligand complex on a streptavidin-coated matrix, elution under affinity-independent, non-denaturing conditions and analysis of the isolated proteins.

## 3.4 Summary and conclusion

As summarised in section 2.3, a new azobenzene-based linker (compound **60**) for affinity chromatography applications has been designed and synthesised. The molecule may be readily cleaved under mild non-denaturing conditions (elution with $Na_2S_2O_4$) making it suitable for affinity-independent elution protocols. In this protocol, every compound of interest (whose propargyl derivative retains the biological activity of the lead compound) can be coupled to the terminal azide of the linker using the copper(I)-catalysed Huisgen 1,3-dipolar cycloaddition reaction (or "click" reaction) generating a molecular probe for affinity studies. The model studies described in section 3.2.2 and 3.2.3 using matrix **74** displaying a ligand (*e.g.* biotin) coupled to the new linker showed that the affinity capture of the binding partner (*e.g.* avidin) was both efficient and selective even from a complex protein mixture. The chemical cleavage ($Na_2S_2O_4$) was directly compared to the classical elution protocol consisting in SDS boiling indicating similar efficiency. Indeed, the two processes are both compatible with the presence of the new linker.

# 4 Bisebromoamide: a new affinity target

## 4.1 Isolation and biological activity

The novel cytotoxic peptide bisebromoamide was isolated in 2009, from the marine cyanobacterium *Lyngbya* sp. by the Suenaga group.[122] The absolute stereochemistry was recently revised by the Ye group who also carried out the first total synthesis of the natural product.[123] Bisebromoamide **86** contains typical features of cyanobacteria metabolites such as *N*-methylated amino acids and residues of nonribosomal origin (Fig. **44**).[124] The interest in this molecule is connected to its potent antiproliferative activity.[125] Intriguingly, bisebromoamide presents a brominated tyrosine residue which provides a reactive site for the insertion of a propargyl handle. Using a protocol for the preparation of tyrosine derivatives optimised in the Hulme group,[126] bisebromoamide will be then employed for the affinity investigations discussed in section 3.3.

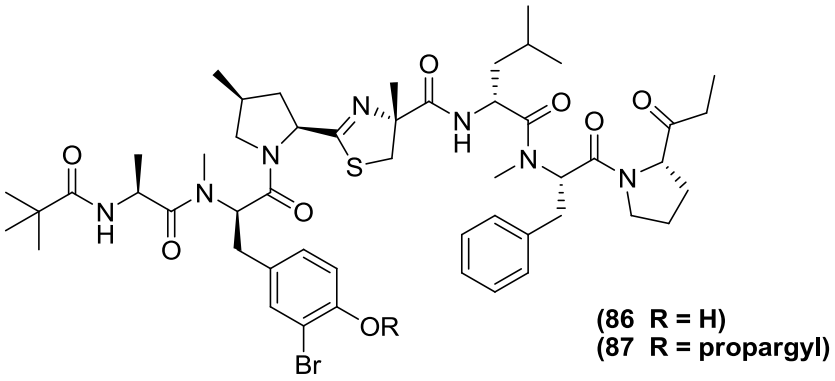


**Figure 44**: The natural product bisebromoamide **86** (revised structure) and its propargyl derivative **87**.

The average 50% growth inhibition ($GI_{50}$) was evaluated against a panel of 39 human cancer cell lines (termed JFCR39) at the Japanese Foundation for Cancer Research and found to be 40 nM. Bisebromoamide **86** exhibited cytotoxicity against HeLa S3 cells with an $IC_{50}$ value of 0.04 μg/ml. Perhaps, the most intriguing activity is the selective

inhibition of the phosphorylation of the extracellular signal regulated protein kinase (ERK) in NRK cells by platelet-derived growth factor (PDGF) stimulation at a concentration of 10 to 0.1 μM. Such inhibition was not found for AKT, PKD, PLCγ1, or S6 ribosomal protein for the same concentration range.[122] This preliminary data suggested that bisebromoamide had potential anticancer activity as a tubulin modulator. Such belief was not confirmed by subsequent specific tests for this class of anti-tumour compounds. Tubulin acetylation is one of the markers to assess the stability of microtubules which is affected after treatment with some tubulin modulators. After treatment with bisebromoamide, the levels of acetylation were unchanged. This data suggested that the anticancer activity of compound **86** is mainly related to the inhibiton of ERK phosphorylation.[122] Aberration of the Raf/MEK/ERK mitogen activated protein kinase cascade is associated with various cancers.[125] Hence, the development of new molecules that could selectively target components of this pathway has attracted increasing attention in the anticancer community.[125] Recently small molecules targeting individual components of the above mentioned pathway have entered clinical trials.[122]

### 4.1.1 The Raf/MEK/ERK cascade: target-based anticancer drug discovery

Historically, oncology drug discovery has relied on assessing the maximum tolerated dose (MTD), safety profile and efficacy.[125] The complete understanding of the mode of action of even common chemotherapeutic agents has not been achieved to date. As scientists have collected more information about the biology of tumours, many more target-based or mechanism-based therapies have made their appearance on the market.[125] As discussed in section 1.7.1, in connection to the biological activity of the natural product anisomycin **25**, mitogen-activated protein kinase (MAPK) cascades play a crucial role in the regulation of cell proliferation, survival and differentiation.[70] These cascades are comprised of three protein kinases which act as a signalling relay, mainly controlled by phosphorylation: a MAPK kinase kinase (MAPKKK), a MAPK kinase (MAPKK) and a MAPK (Scheme **32**).[70] The terminal serine/threonine kinases (MAPKs)

are the ERK1/2, the c-Jun amino-terminal kinases (JNK1/2/3; also called SAPKs), p38 kinases (p38a/b/g/d) and ERK5. Generally, the ERK pathway is activated by growth factor-stimulated cell surface receptors, whereas the JNK, p38 and ERK5 pathways are activated by stress and growth factors. The downstream function of cell surface receptors and other proteins in the cytoplasm towards such cascades is strongly deregulated in cancer and other diseases.

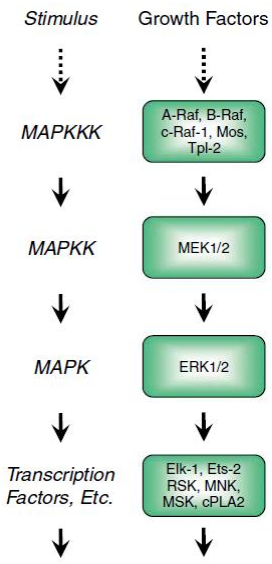


**Scheme 32**: General scheme of the mitogen-activated protein kinase (MAPK) pathways; the Raf/MEK/ERK cascade (green) incorporates the target of the natural product bisebromoamide (Figure from ref. 70).

All the individual components of the Raf/MEK/ERK cascade have been considered as targets of new anticancer therapeutics. Rafs (MAPKKK) are Thr/Ser kinases which activate and phosphorylate MEK1 and 2 (MAPKK), dual specificity kinases.[127,128] MEK1/2 trigger phosphorylation of ERK1/2 (MAPK) and the activation of these kinases regulates the activity of a wide range of proteins.[129] Most ERK substrates are nuclear proteins while a small portion is found in the cytoplasm and other organelles. At the nuclear level, they are responsible for the regulation of transcription factors such as the Ets family (*e.g.* Elk-1) resulting in gene expression.[130,131] The identification of Raf as a

potent retrovirus oncogene defined the importance of this pathway in oncogenesis.[128] According to genetic and pharmacological studies, the role of MEK and ERK is vital for the activation of Ras and other oncogenes.[125] To date, the inhibition of the kinase function of Raf and MEK represents the most investigated approach towards blocking the ERK signalling. Among the Raf inhibitors, it is noteworthy to mention sorafenib (Fig. **45**, **88**, tosylate salt of BAY 43-9006, Nexavar®), which received FDA approval in 2005 for use in advanced renal cell carcinoma (RCC). Crystallographic analyses of this bi-aryl urea derivative complexed with the kinase domain of B-Raf showed that sorafenib bound to the ATP-binding pocket and prevented kinase activation.[132] Among the MEK inhibitors, PD0325901 (compound **89**) showed anti-tumour activity for a variety of tumour xenografts and the molecule is in phase I/II clinical trials.

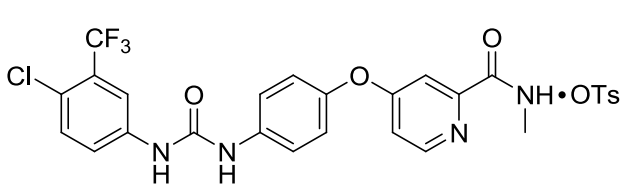


**88**

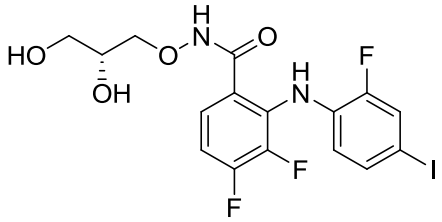


**89**

**Figure 45**: Sorafenib **88** and PD0325901 **89**, respectively Raf and MEK kinase inhibitors.

The number of reports found in the literature suggests that the investigation of molecules like bisebromoamide **86**, an inhibitor of the Raf/MEK/ERK cascade, is of great interest. Hence, it was decided to pursue the total synthesis of compound **86** and its analogues for subsequent affinity-based investigations. Before describing the synthetic approach developed in the Hulme group (section 4.4), two previous total syntheses of the natural product bisebromoamide will also be described (sections 4.2 and 4.3).

## 4.2 The first total synthesis of bisebromoamide

Recently, the Ye group completed the first total synthesis of the natural product bisebromoamide which led to the reassignment of its absolute stereochemistry.[123] The synthetic campaign was based on the assumption that the most challenging part would probably be the formation of the thiazoline heterocycle, due to the possibility of racemisation. Thus, this moiety was assembled from 2-methylcysteine at a late stage in the synthesis. The synthetic strategy consisted of the linkage of four main fragments through the formation of amide bonds and the thiazoline ring.

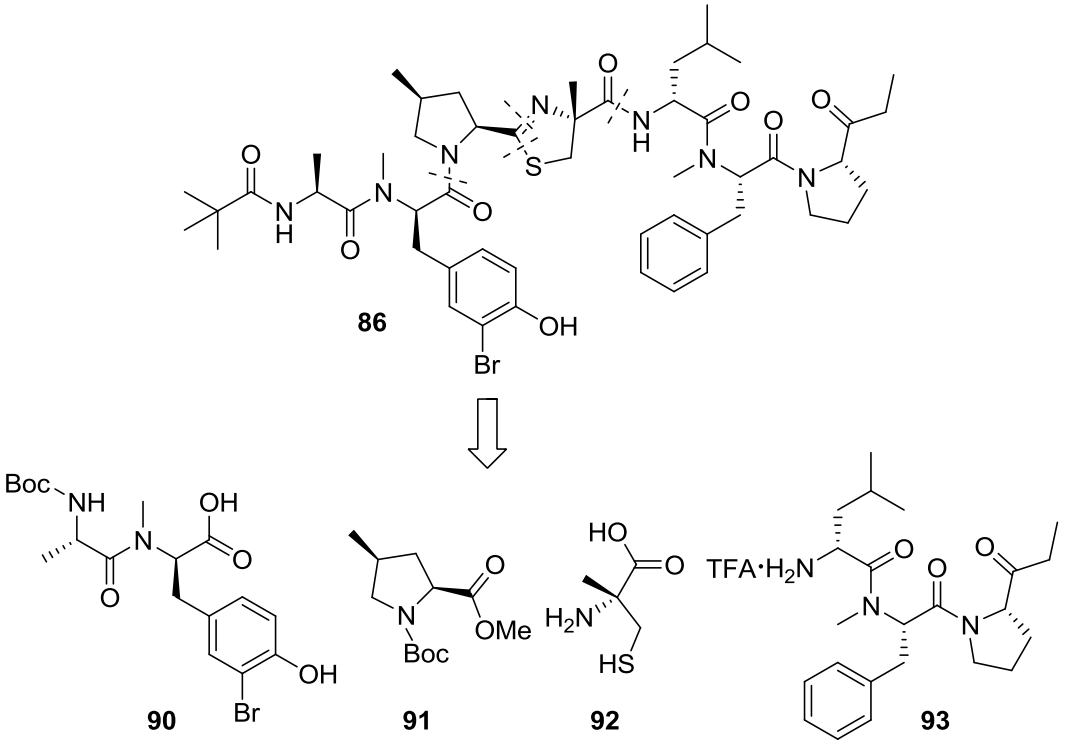


**Scheme 33**: The retrosynthetic analysis of bisebromoamide **86**.

The *N*-Boc-4-methyl proline ester **91** and 2-methylcysteine **92** fragments were prepared following previously published procedures,[133,134] while peptide derivatives **90** and **93** were synthesised *de novo*. Starting from previously reported *N*-methyl D-tyrosine methyl ester **94**,[135] selective monobromination was carried out with *N*-bromosuccinimide and *p*-toluenesulfonic acid in MeCN in satisfactory yield (Scheme **34**). The use of coupling

agent 3-(diethoxyphosphoryloxy)-1,2,3-benzotriazin-4(3H)-one (DEPBT) allowed the formation of dipeptide **95** with Boc-L-Ala-OH. Finally, saponification of **95** gave the corresponding acid **90** in high yield.

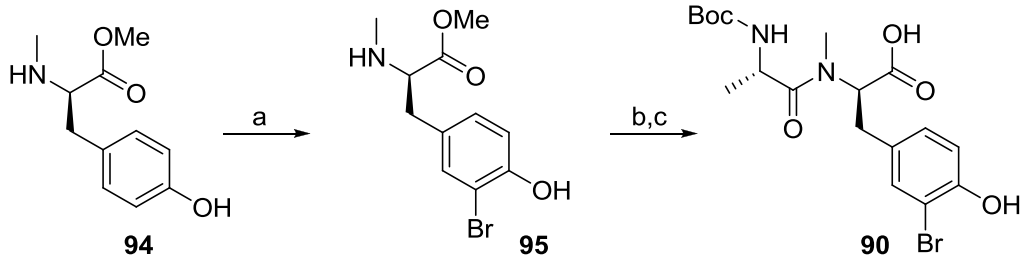


**94** **95** **90**

**Scheme 34**: Synthesis of dipetide **90**. (a) NBS, PTSA, MeCN, RT, (87%); (b) DEPBT, Boc-L-Ala-OH, NMM, THF, (77%); (c) LiOH, THF/MeOH/$H_2O$, (95%).

Bis(2-oxo-3-oxazolidinyl)phosphinic chloride (BOP-Cl) was employed for the condensation of ester **96** with Boc-D-leucine to give dipeptide **97** in high yield (Scheme **35**).[136]

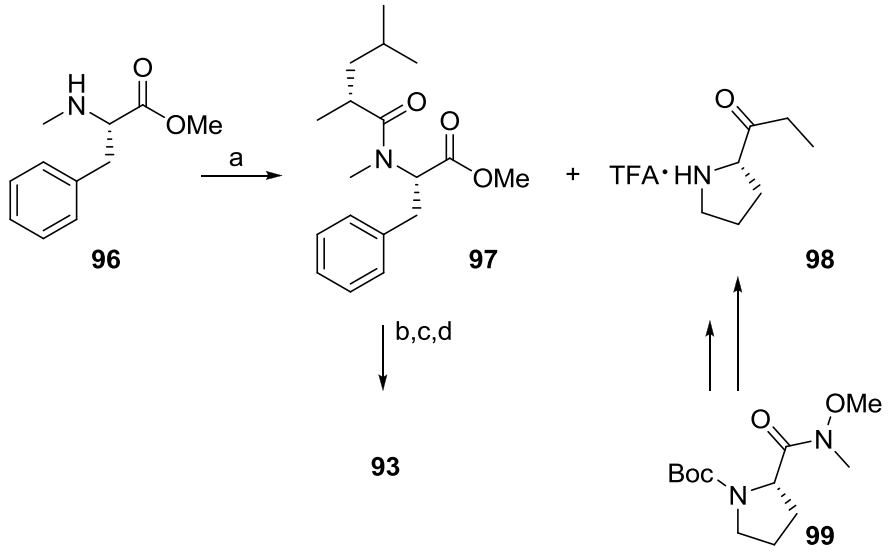


**96** **97** **98** **93** **99**

**Scheme 35**: Synthesis of fragment **93**. (a) BOPCl, Boc-D-Leu, $Et_3N$, DCM, (86%); (b) LiOH, THF/MeOH/$H_2O$; (c) DEPBT, **98**, DIPEA, THF; (d) TFA, DCM, (74% over three steps).

After saponification of the ester moiety, dipetide **97** was submitted to a DEPBT-mediated condensation with amine **98** (prepared by addition of ethylmagnesium bromide to Boc-protected proline-derived Weinreb amide **99**)[137] yielding the corresponding tripeptide. The ammonium trifluoroacetate salt **93** was obtained by cleavage of the Boc group (Scheme **35**). The initial efforts of the Ye group to couple the fragments and form the thiazoline ring focused on the cyclodehydration of a β-hydroxy thioamide and proved unsuccessful, probably due to the sterically demanding substrates involved in the condensation.[123] The final strategy commenced with the preliminary transformation of *N*-Boc-4-methyl proline ester into a nitrile derivative to avoid epimerisation (Scheme **36**).[138] Removal of the Boc group, followed by HATU-mediated condensation, provided the corresponding peptide which was re-subjected to acidic cleavage of the Boc group and the newly revealed amine coupled to pivaloyl chloride to furnish nitrile **101**.[139]

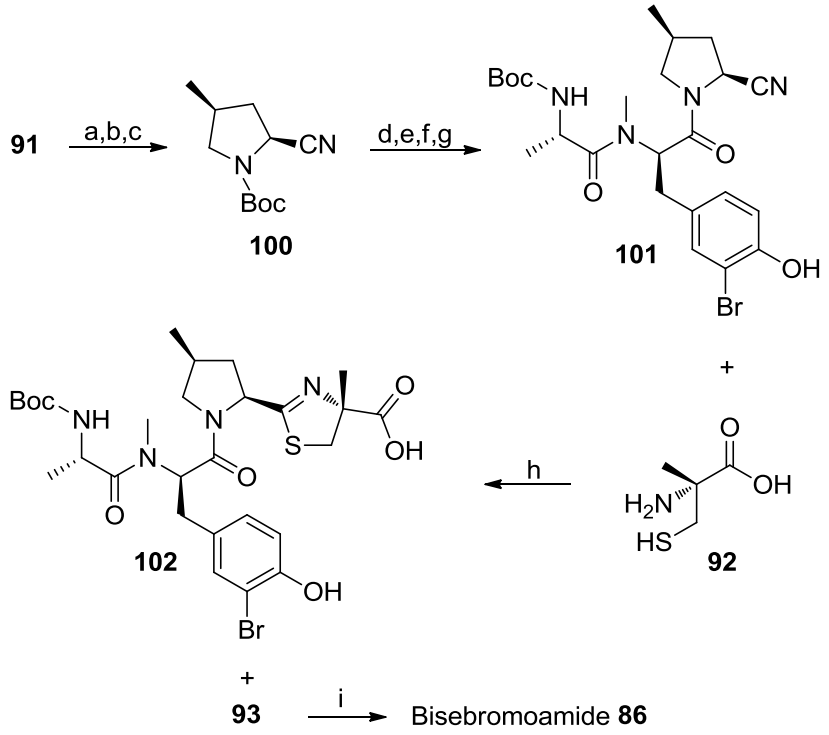


**Scheme 36**: Fragment coupling. (a) LiOH, MeOH/$H_2O$; (b) *i*BuOCOCl, NMM, THF, then $NH_3$; (c) TFAA, Py, THF, (64% over three steps); (d) TFA/DCM; (e) HATU/HOAt, DCM/DMF; (f) TFA/DCM; (g) $^t$BuOCOCl, NMM, DCM, (35% over four steps); (h) DIPEA, EtOH (48%); (i) HATU/HOAt, collidine, DMF, (51%).

The key step of this approach was the cyclocondensation of nitrile **101** with compound **92**. This transformation was carried out in a sealed tube at 90 °C giving the important intermediate **102** in moderate yield as a single isomer. Finally, HATU/HOAt collidine mediated coupling yielded the natural product bisebromoamide **86** (Scheme **36**). The Ye group performed cytotoxicity evaluations on both compounds **86** and its epimer (*S*-configuration of the stereogenic center at the thiazoline ring) which showed that the two compounds have a comparable activity profile.[123,139]

## 4.4 The second total synthesis of bisebromoamide

More recently a new approach to the total synthesis of bisebromoamide has been disclosed from the Ma research group,[139] which confirmed the structural revision proposed by the Ye group and gave interesting insights into the structure-activity relationship (SAR) of the natural product (Scheme **37**).[123] The Ma group synthesised the first proposed structure of bisebromoamide as reported by Teruya *et al*.[122] according to the described retrosynthetic scheme: an initial disconnection at the thiazoline core generates two main fragments; cyanide **103** and protected aminothiol **104**, subsequent disconnections at the amide bonds lead to *N*-methylated amino acids **106** and **107**, dipetide **105** and tripeptide **108** (Scheme **37**).[139] As the stability of the thiazoline ring was a major concern, this moiety was generated at a late stage in the synthesis as in the previously reported approach by the Ye group.[123] Tyrosine derivative **108** was prepared with a sequence of transformations analogous to the one reported by the Ye group[123] and coupled to pyrrolidine derivative **106**. Treatment of **109** with methyltriflate in the presence of LiHMDS, generated lactam **110** in high yield and with a good degree of selectivity (*syn* configuration).[140,141] Treatment with $LiBEt_3H$ followed by $Et_3SiH$ furnished the reduced product **111** in very good yield.[142] The final transformation to cyanide **106** was accomplished in a very similar manner to the previous report. Peptide coupling proceeded smoothly in the presence of HATU and HOAt to give fragment **103**.

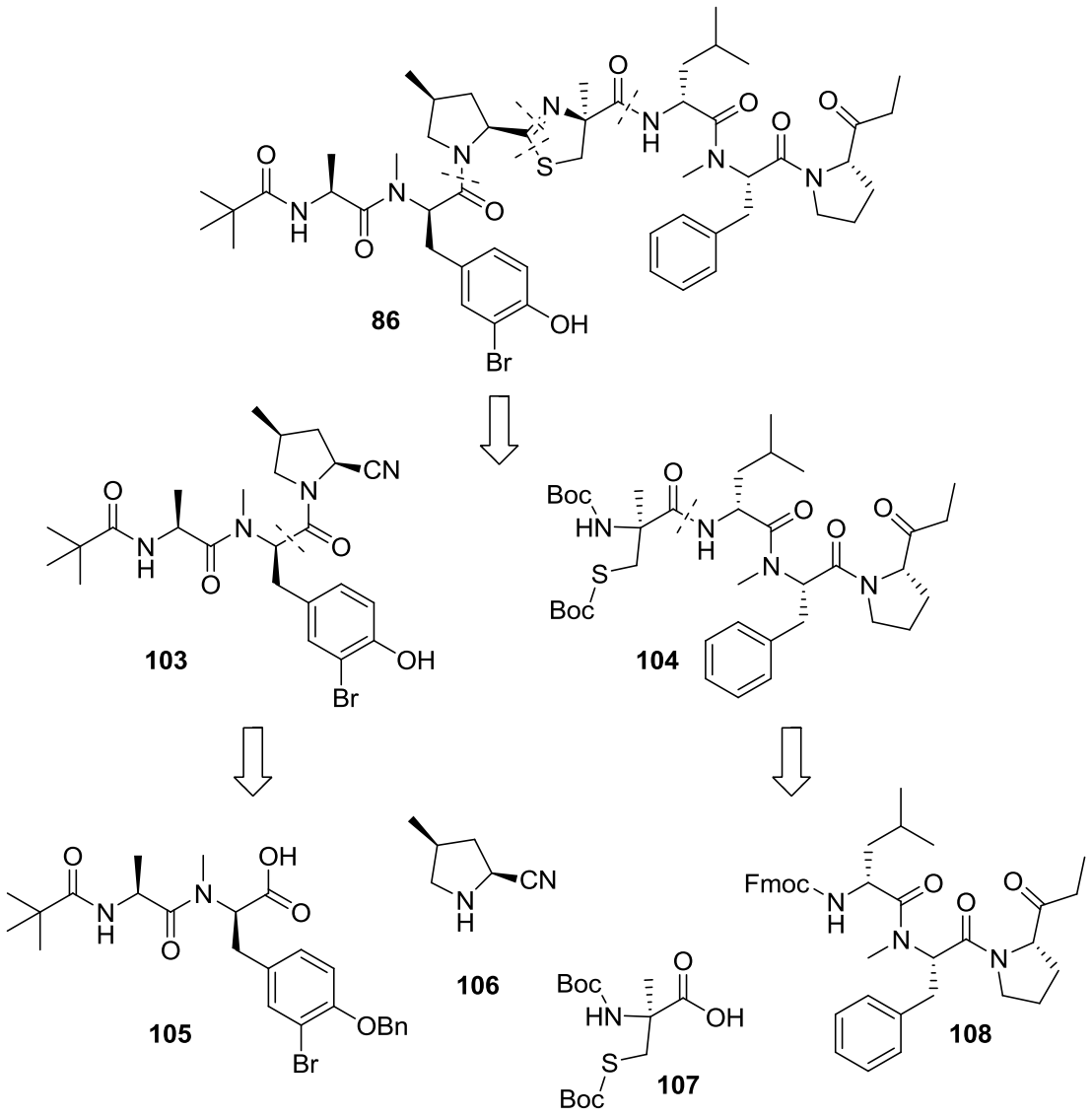


**Scheme 37**: The retrosynthetic analysis of bisebromoamide **86**.

The synthesis of the remaining aminothiol fragment **104** is illustrated in scheme **39**. Removal of the Fmoc protecting group from compound **112** under basic conditions, followed by coupling with D-Fmoc-Leu-OH amino acid in the presence of HATU coupling agent furnished the substrate for the deallylation step. Pd chemistry was used to displace the allyl group, and the newly revealed carboxylic acid functionality was readily coupled to amino alcohol **114** in satisfactory yield.[143]

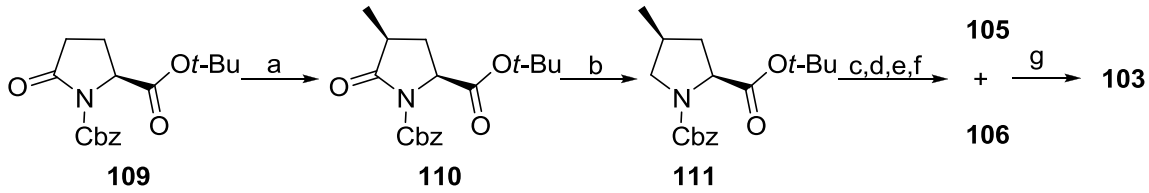


**Scheme 38**: (a) LiHMDS, then MeOTf, toluene, (60%); (b) $LiBEt_3H$, then $Et_3SiH$, $BF_3{\bullet}Et_2O$, (87%); (c) TFA/DCM; (d) $NH_4OH$, HOBt, EDC, DMF; (e) TFAA, $Et_3N$ (99% over three steps); (f) Pd/C, $H_2$, THF, (99%); (g) HATU, HOAt, DIPEA, (82%).

The final transformations to generate bisebromoamide **86** are described in scheme **39.**

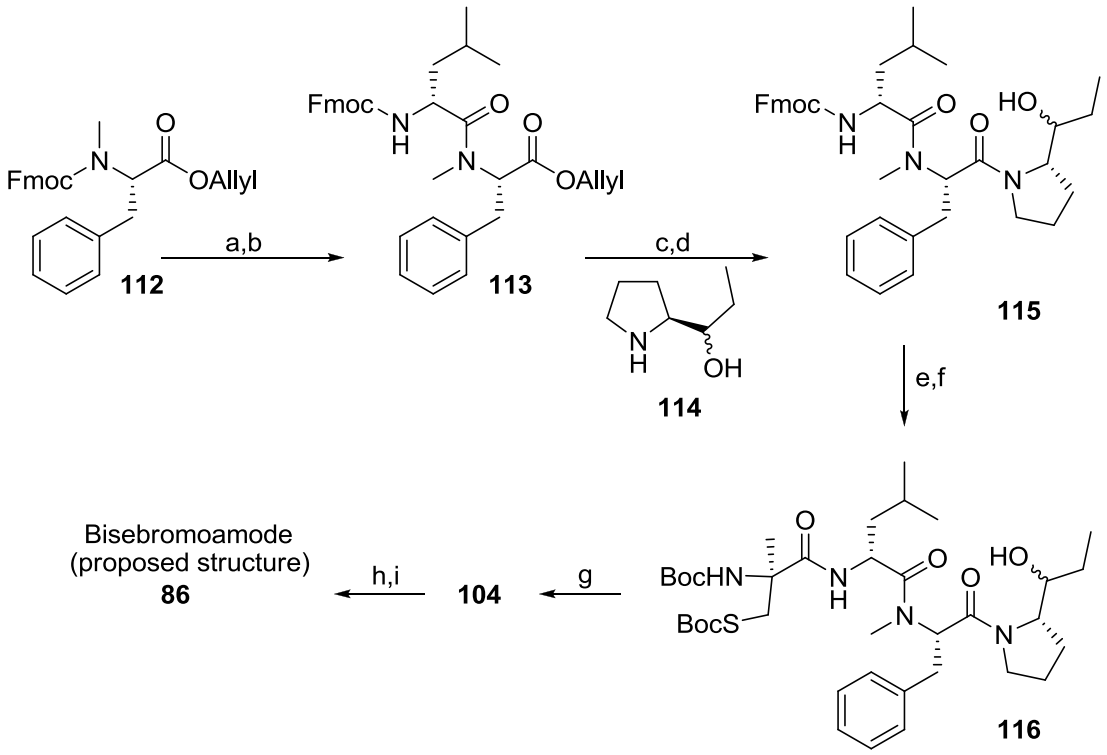


**Scheme 39:** (a) $Et_2NH$, MeCN; (b) D-Fmoc-Leu-OH, HATU, DIPEA, DCM (95% over two steps); (c) $Pd(PPh_3)_4$, NMA, THF; (d) **114**, HATU, HOAt, DIPEA, DCM (94% over two steps); (e) $Et_2NH$, MeCN; (f) **107**, HATU, HOAt, DIPEA, DCM (76% over two steps); (g) DMP, $NaHCO_3$ (100%); (h) TFA, DCM; (i) **103**, $NaHCO_3$, MeOH, pH 6 buffer, 70 °C, (61% over two steps).

The coupling strategy optimised for the synthesis of fragment **105** was applied to the successful preparation of tetrapeptide **116** which was then submitted to Dess-Martin oxidation to give important intermediate **104** in quantitative yield.[139] Following TFA-mediated double deprotection of amino thiol **107**, the target molecule was finally prepared, through coupling of **103** to cyanide **104** in the presence of $NaHCO_3$ in a mixture of methanol and buffer.[144] However, the spectroscopic data of a natural sample of bisebromoamide did not match that of the prepared molecule. The structure proposed by the Ye group (*R*-configuration of the stereogenic center at the thiazoline ring, compound **117**) was then prepared and absolute matching with a natural sample was found.

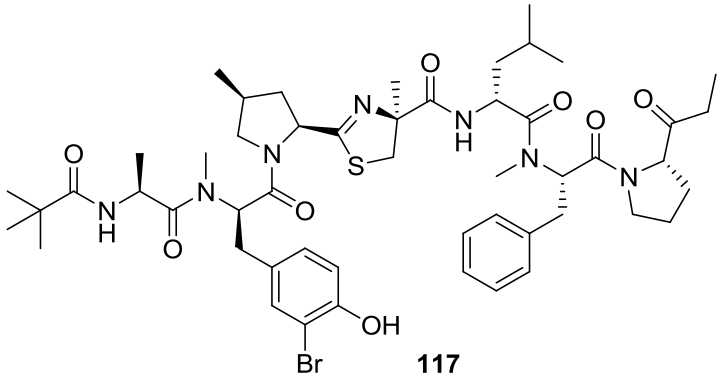


**117**

**Figure 46**: The structure of the natural product bisebromoamide proposed by the Suenaga group.[122]

This second report confirmed that the absolute stereochemistry of this natural product is the one proposed by the Ye group (despite the preliminary assignment following isolation). In addition to the syntheses of **86** and **117**, simplified analogues of the natural product were prepared.[139] The most intriguing results were obtained with a simplified analogue of **86** featuring a proline amino acid instead of 4-Me-Pro. This compound proved as potent as the natural product making it an ideal candidate for further structure activity-relationship (SAR) investigations.

## 4.5 Hulme group strategy

The proposed synthetic strategy is based on the assembly of seven fragments of which three; pivalic acid, and the amino acids alanine and isoleucine, are commercially available (Scheme **40**).

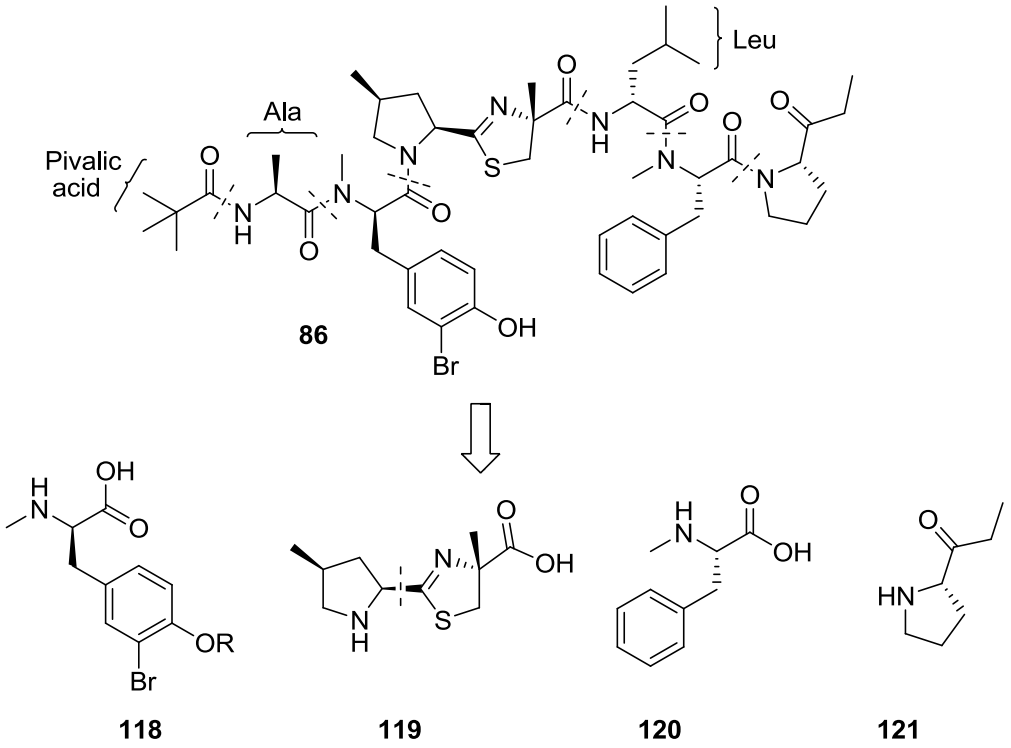


**Scheme 40**: The retrosynthetic analysis of bisebromoamide proposed in the Hulme group.

Fragments **120** and **121** will be prepared according to published procedures.[145,146] The synthesis of tyrosine derivative **118** will be carried out according to a methodology previously developed in the Hulme group.[126] Fragment **119** will result from the coupling of the thiazoline ring, prepared as reported previously[147] and *N*-Me-Proline. The synthetic efforts towards the synthesis of this unusual amino acid will be reported in this manuscript.

## 4.6 Occurrence of 4-methyl proline in natural products

While discussing the isolation of bisebromoamide, it was noted that the most intriguing structural feature of this natural product is the 4-methylproline-derived thiazole, which was unprecedented until the isolation of the dysideaproline series from the marine sponge *Dysidea* sp.[148] Conversely, the occurrence of the 4-methyl proline amino acid is well documented in natural products of biological importance.[149,150,151] Recent examples are; the nospeptides A and B, potent elastase and chymotrypsin inhibitors from cyanobacterium *Nostoc minutum,*[149] the glycosidic compound suomilide from *Nodularia spumigena*[150] and the pteratide series, cytotoxic cyclodepsipeptides from Malaysian *Basidiomycete Pterula* sp.[151] Proline and its derivatives are often responsible for secondary structural motifs in proteins, such as kinks in α-helices and reverse turns.[152] The understanding that the presence of proline amino acids could influence the conformation of the peptide backbone[153] has increased the interest in the synthesis of substituted analogues. Proline-induced turns in close proximity to pharmacophores are often fundamental for biological recognition.[154] As a consequence of these properties, desired functionalities can be projected into specific regions of space within proteins. Furthermore, the incorporation of proline derivatives into peptides and peptidomimetics remains a valuable tool for structure-activity relationship (SAR) elucidation.[155] Gmeiner *et al*. utilised this concept elegantly in the development of new 2-methoxybenzamide derivatives,[156,157] a class of compounds used for treatment of psychotic disorders including schizophrenia.[158] The mechanism of action of these compounds is mediated by the binding to dopamine and serotonin receptors (D1 to D5 and 5-HT1 5-HT4 respectively). Unfortunately, their remarkable binding affinity for the dopamine receptors D2 is associated with a series of side effects.[159] The aim of this study was to synthesise new 2-methoxybenzamide analogues featuring prolinol derivatives which could potentially result in a reduced affinity for these specific dopamine receptors. Starting from natural 4-hydroxyproline, all the 2-aminoalkyl pyrrolidine stereoisomers were prepared and coupled to benzoic acid derivatives (bearing the pharmacophore for antipsychotic activity) leading to the preparation of a series of analogues. Dopamine and

serotonin receptor binding studies were performed to gain insight into the SAR of all different stereoisomers prepared. Binding studies involving the subtypes D1, $D2_{long}$, $D2_{short}$, D3 and D4 as well as 5-$HT1_A$ and 5-HT2, displayed different SARs, especially with respect to the absolute and relative configuration of the test compounds (Fig. **47**). The aminomethyl pyrrolidine derivative **122** and the aminobutyl pyrrolidine derivative **123** showed remarkable affinity and preference for the dopamine D3 and D4 receptor subtypes rather than the D2 type.

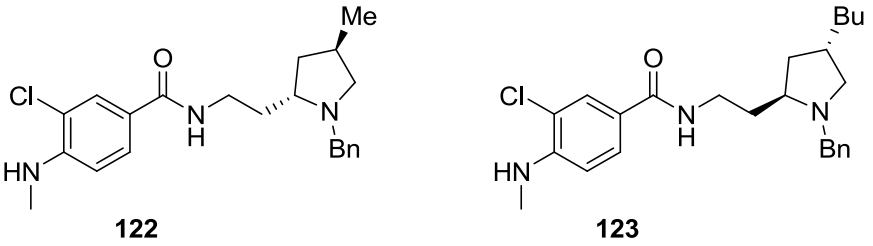


**122** **123**

**Figure 47**: Potential antipsychotic candidates **122** and **123**.

## 4.7 Previous approaches to the synthesis of 4-methyl proline

Two methodologies for the synthesis of 4-methyl proline, from the Goodman[160] and the Munro[133] research groups will be discussed before describing the approach proposed in the Hulme group.

### 4.7.1 Del Valle and Goodman synthesis of 4-methylproline

As part of a peptidomimetic research program aimed to the development of novel pyrrolidine-based building blocks,[160] the Goodman group envisaged a new route for the synthesis of novel 4-arylalkylprolinols and prolines. Starting from *trans*-4-hydroxyproline **124**, compound **125** was readily prepared using modified literature procedures (Scheme **41**).[161,162] Carrying out the synthesis of **125** on the Boc-protected

amino acid and performing the reduction step on a mixed anhydride formed *in situ* was found to be convenient especially for the scalability of the process (Scheme **41**). Compound **125** was submitted to TEMPO-mediated oxidation[163] yielding pyrrolidinone **126** which was subjected to Wittig olefination with various triphenylphosphoranes to generate olefins **127a** to **127f** in satisfactory yields.

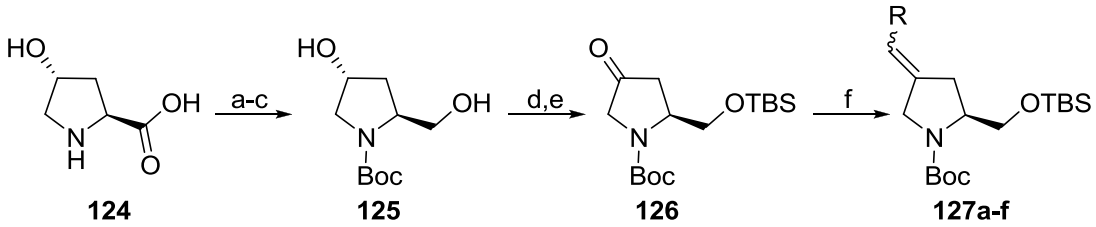


| | 127a | 127b | 127c | 127d | 127e | 127f |
|---|---|---|---|---|---|---|
| R | H | Et | Ph | $C_6H_4$(4-OEt) | $CO_2Me$ | (Boc)Indole |

**Scheme 41:** (a) $Boc_2O$, 10% aq $Na_2CO_3$,/dioxane; (b) isobutyl chloroformate, NMM, DME; (c) $NaBH_4$ in $H_2O$, (76%, over three steps); (d) TBDMSCl, $Et_3N$, DMAP (cat.), DCM, (78%); (e) trichloroisocyanuric acid, TEMPO (cat.), DCM, (88%); (f) ylide, THF, (64-85%).

At this point, two different synthetic paths were envisaged for the hydrogenation step required to generate the proline derivatives. Previous studies on the asymmetric hydrogenation carried out by the Goodman research group,[164] led to the conclusion that the presence of the protecting group on the hydroxymethyl substituent of substrate **127** had a dramatic effect for the facial selectivity of the hydrogenation (Scheme **42**). When the reaction was carried out with silyl-protected pyrrolidine **129**, delivery of hydrogen from the less hindered face of the molecule provided primarily the *cis*-substituted pyrrolidine.

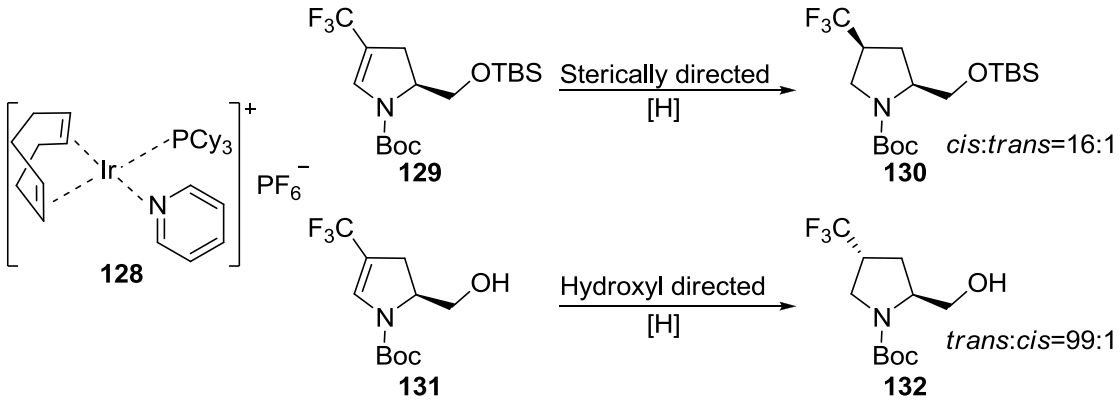


**Scheme 42**: The Crabtree catalyst **128** and the hydrogenation studies in the Goodman group.

Hydrogenation in the presence of Crabtree catalyst **128** with pyrrolidine **131** gave rise to *trans*-substituted pyrrolidine **132**.[165] The exceptional diastereoselectivity is due to the coordination of the catalyst to the directing hydroxyl group. Based on this premise, silyl-protected pyrrolidine **127** was subjected directly to hydrogenation to achieve *cis*-selectivity (Scheme **43**).

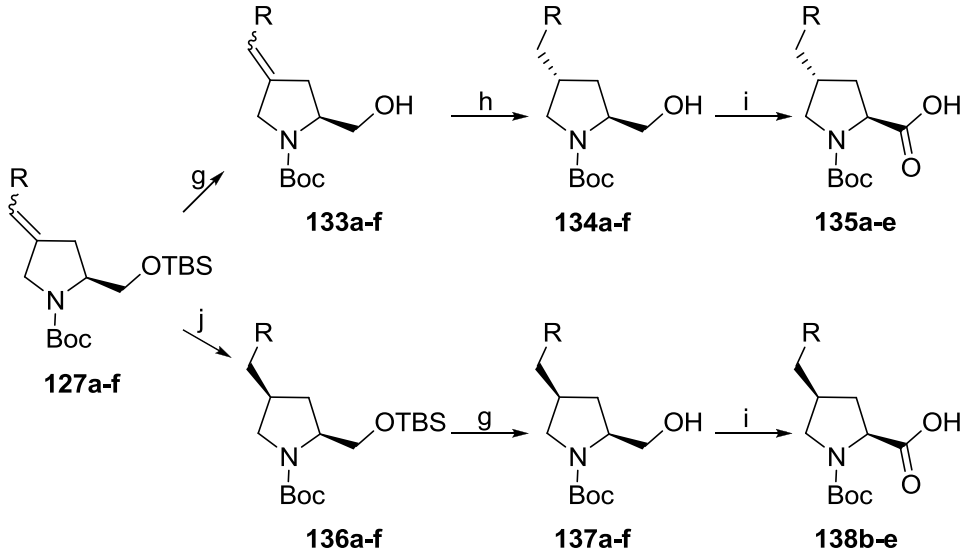


**Scheme 43**: (g) 0.5 M TBAF in THF, (80-95%); (h) $Ir(COD)PyPCy_3PF_6$, (3 mol%), $H_2$, DCM, (78-94%); (i) $NaClO_2$, NaClO (cat.), TEMPO, pH 6.7 phosphate buffer (0.67 M $NaH_2PO_4$)/MeCN, (80-89%); (j) Raney-Ni, MeOH, (77-85%).

The best results were obtained when Raney-nickel was used as the hydrogenation catalyst, with stereoselectivity for the *cis* isomer up to 16:1. Hydrogenation with iridium catalyst **128**, performed on pyrrolidine **133** carrying the newly revealed hydroxyl group, proceeded with *trans*-selectivity as expected, with a greater degree of selectivity. The *trans*-series could be prepared with >40:1 selectivity for most of the substrates investigated. The synthesis of alkylproline derivatives **135a** to **135e** was readily completed with a TEMPO-mediated oxidation at the primary alcohol to give the required carboxylic acid.[166] The same oxidation conditions proved sluggish on indolylprolinol derivatives **134f** and **137f** giving rise to an inseparable mixtures of side products. The authors did not specify why it was not possible to obtain oxidised proline derivative **138a**.[160,164]

### 4.7.2 Munro's modification

More recently, the strategy proposed by Del Valle and Goodman was slightly modified to give a more convergent approach to the synthesis of all four diastereoisomers of 4-methylproline.[133] The key transformation in the former synthesis was the asymmetric hydrogenation which relied on the directing effect of the hydroxyl substituent on the Crabtree catalyst (for the *trans*-series).[164] Based on the assumption that an ester functionality should similarly influence the stereochemical outcome of this reaction,[167] a more succinct route was proposed.[133] Starting from the least expensive of the four diasteroisomers of 4-hydroxyproline, *trans*-4-hydroxy-L-proline and *cis*-4-hydroxy-D-proline, esterification and Cbz-protection proceeded smoothly (Scheme **44**). The oxidation step, carried out with chromium oxide, achieved **140**/ent-**140** in good yield. Olefination on **140**/ent-**140** was attempted using a modified Wittig olefination.[168] However, these conditions led to epimerisation of the α-center. When the milder Petasis reagent was employed instead, the reaction proceeded in modest yield.[169]

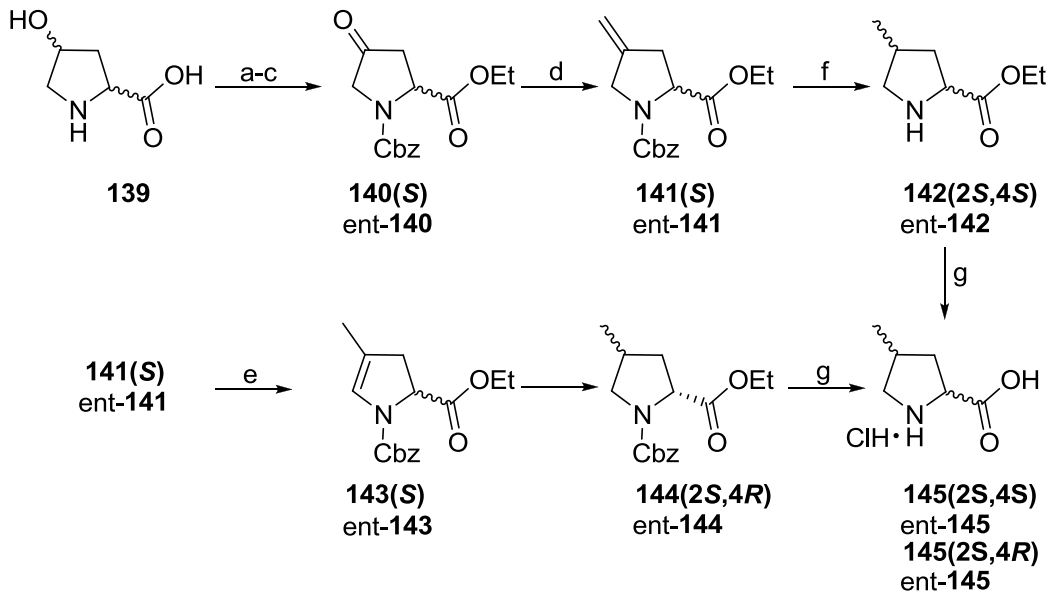


**Scheme 44**: (a) $SOCl_2$, EtOH, reflux, 4 h; (b) CbzCl, $Et_3N$, MeOH, RT, 16 h; (c) $CrO_3$, Py, DCM, RT, 16 h (80% for **140** and 67% for ent-**140** over three steps; (d) dimethyltitanocene, toluene, 90 °C, 3 h (56% for **141** and 42% for ent-**141**); (e) Crabtree's catalyst, $CHCl_3$, $H_2$, 5 d, (84% for **144** and 80% for ent-**144**); (f) Pd/C, DCM, $H_2$, 16 h, (67% for **142** and 100% for ent-**142**); (g) $HCl_{(aq)}$ 6 M, 70 °C, 6 h, (100% for **145** and 87% for ent-**145**).

Hydrogenation on substrate **141** using Pd/C catalyst with concomitant Cbz-removal readily achieved *cis*-substituted compound **142**. Munro and colleagues performed Marfey's derivatisation[170] of each of the diastereoismer of the 4-methyl proline which allowed determination of the optical purity by HPLC analysis.[133] The *cis*-series showed an improved diastereoselectivity (7:1) with comparison to the Goodman approach (3:1).[160] Homogeneous hydrogenation conditions with the Crabtree catalyst on the same substrate yielded only the isomerisation product enamine **143**/ent-**143** after 16 h. Alkene migration under Crabtree catalyst mediated hydrogenation is reported in the literature.[171] Nevertheless, a longer reaction time (5 d) achieved the desired *trans* 4-methyl proline derivative. The selectivity was remarkably reduced for the *trans*-series (15:1) compared to the Goodman approach (>40:1).[160]

# 5 Introduction

Munro's protocol for the synthesis of 4-Me-Pro was one of the most attractive found in the literature.[133] Although the synthetic sequence is quite concise, the limited *cis*-selectivity for the hydrogenation step and the use of chromium oxide for the oxidation reaction suggested that the investigation of a new route was needed. Furthermore, the abundance of this unusual amino acid in natural products of biological importance underlined the utility of a novel synthetic approach. The proposed strategy for the synthesis of 4-Me-Pro started from Schiff bases prepared from glycine esters. Asymmetric alkylation in the presence of a chiral phase transfer catalyst (PTC) would provide the required absolute stereochemistry. After transformation of the conjugated imine into an enamide, ring closing metathesis (RCM) would yield the desired 5-membered ring. Stereoselective hydrogenation would complete the synthesis of 4-Me-Pro.

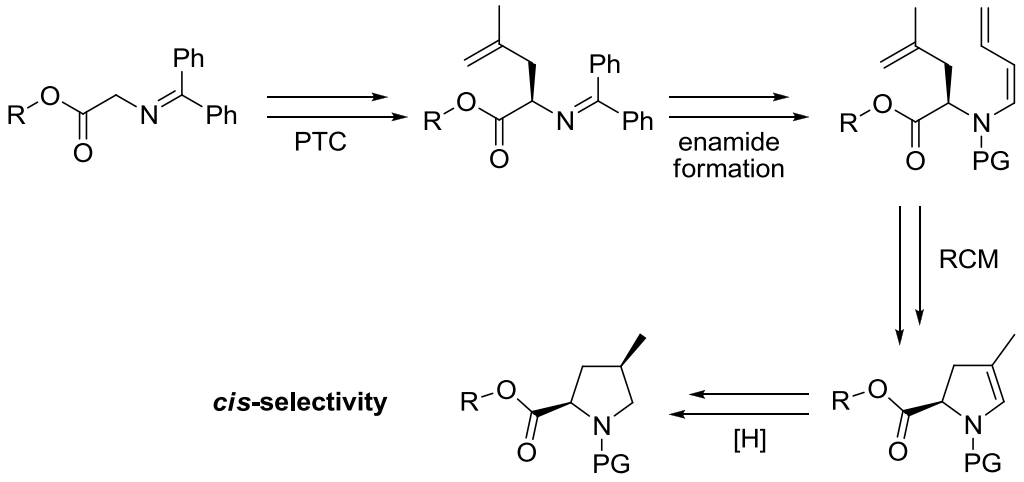


**Scheme 45**: Key transformations of the novel synthetic approach to 4-Me-Pro.

This succinct synthetic sequence (6 steps) would then allow a more efficient approach to this key amino acid required for the total synthesis of bisebromoamide.

## 5.1 Asymmetric alkylation of glycine Schiff bases

The great interest of the synthetic community in phase-transfer catalysis is well documented in the literature by countless reports over the last two decades.[172,173] Mild reaction conditions, the ease of experimental procedures and readily available and inexpensive starting materials account for the attention from both academic and industrial synthetic groups. The first report of an asymmetric reaction employing cinchona alkaloids was disclosed at the end of the 1970s by the Sharpless group[174] describing the use of a cinchona derivative as a co-ligand for $OsO_4$ in dihydroxylation reactions. In 1984, in a series of pioneering experiments, Dolling and co-workers at the Merck laboratories successfully carried out the asymmetric methylation of indanone derivatives using cinchona catalyst **146**, thus introducing this new class of catalysts (Fig. **48**, first generation).[175] The development and the successful application of such catalysts over the last two decades, for asymmetric alkylation of amino acids will be briefly discussed. In this regard, it is noteworthy to mention the outstanding research of Maruoka and collaborators[173] for design of naphtyl-modified phase transfer catalysts (Fig. **48**, **147**) for asymmetric alkylation of amino acids. Although the work of Maruoka and collaborators gave an important contribution to this area of synthetic methodology,[176] this section will focus on cinchona catalysts.

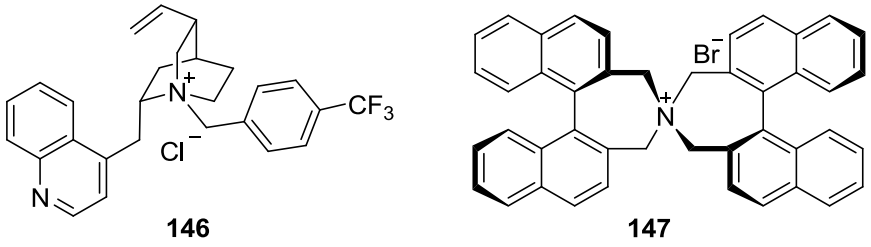


**146** **147**

**Figure 48**: Cinchona-derived PTC **146** (first generation) and synthetic PTC **147** (Maruoka type).

### 5.1.1 Cinchona-based phase-transfer catalysts (PTC)

Despite the wide variety of applications of this remarkable class of catalysts, the precise mechanism of action is not fully understood and is often simplified as in figure **49**. The quaternary ammonium cation ($N^+X^-$) is involved in the formation of a nucleophilic ionic complex with an anion of the nucleophile (*e.g.* an active methylene compound) generated by deprotonation by an inorganic base at the interface of the organic and aqueous layer. Once the nucleophilic complex ($N^{+\cdots}Nu^-$) is formed, it reacts with an electrophile (*e.g.* an alkyl halide, unsaturated enone, Schiff base, aldehyde or ketone) yielding the product (Nu-E). The liberated quaternary ammonium salt returns to the original position at the interface between the two layers, thus regenerating the catalyst.

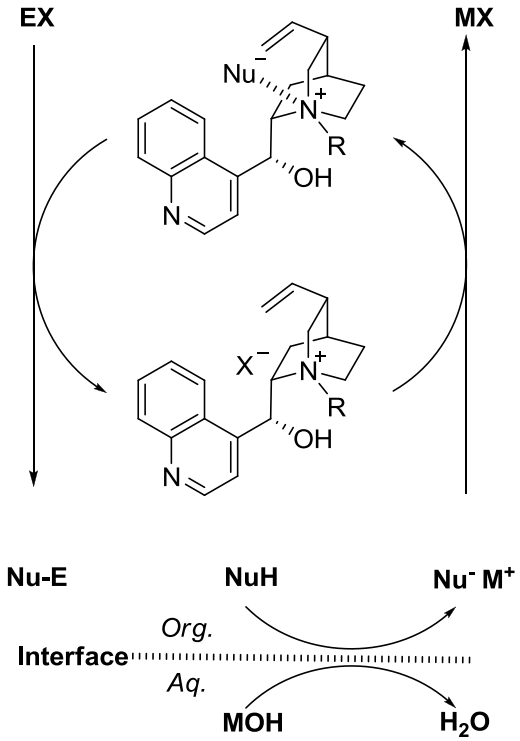


**Figure 49:** Proposed interface mechanism in the presence of a cinchonidine-derived quaternary ammonium salt.

It is during the formation of the above described complex $N^{+\cdots}Nu^-$ that the transfer of the chiral information takes place; the least sterically hindered face is approached by the electrophile to furnish the desired chiral product.

### 5.1.1.1 *N*-9-anthracenylmethyl-*cinchona* PTCs (second generation)

Following the investigations of Dolling at the Merck laboratories,[175] O'Donnell and co-workers developed a similar PTC for the asymmetric benzylation of *N*-(diphenylmethylene)glycine *tert*-butyl ester **148** obtaining alkylated product **149** with a good degree of selectivity (up to 66% ee, scheme **46**).[177] This product could be hydrolysed to afford α-amino acid phenylalanine in high yield. However, the attention of the synthetic community towards this research area only flourished significantly after the introduction of catalysts **151** and **152** by the Lygo[178] and the Corey[179] groups.

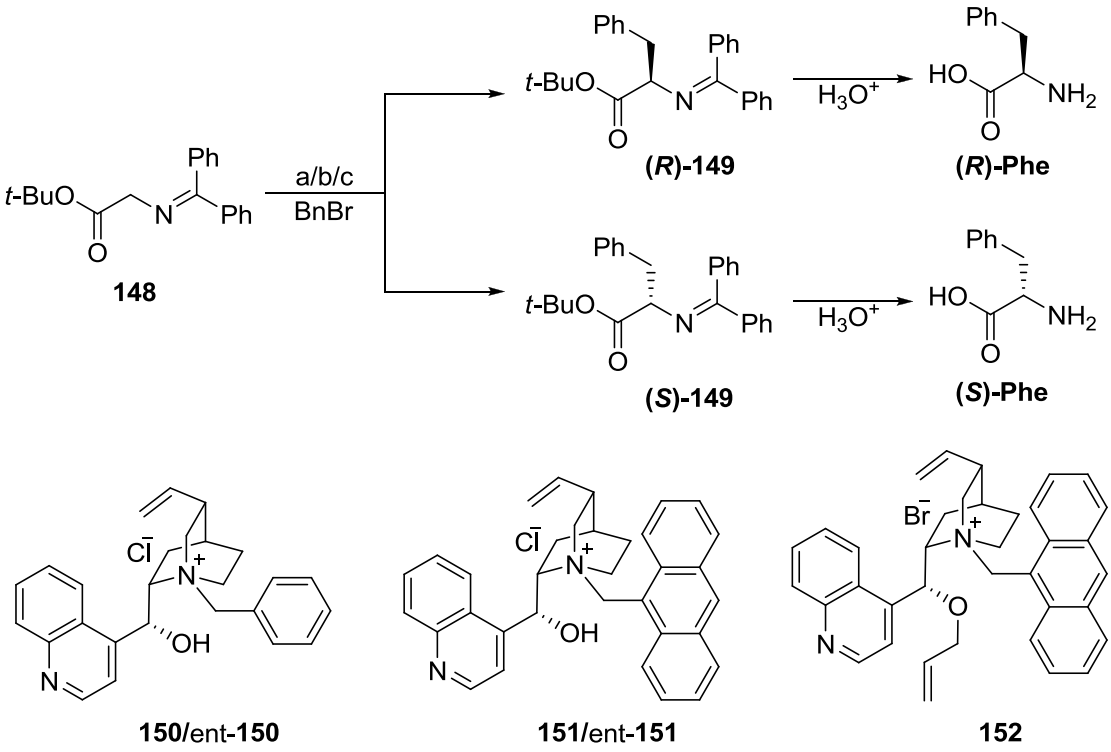


**Scheme 46**: Asymmetric benzylation of *N*-(diphenylmethylene)glycine tert-butyl ester **148** and the PTCs from O'Donnell (**150**, ent-**150**), Lygo (**151**, ent-**151**) and Corey (**152**) research groups. (a) PTC **150** or ent-**150** (10 mol%), 50% $NaOH_{(aq)}$, DCM, RT, 9 h, (75%, 66% ee for **149** and 85%, 64% ee for ent-**149**); (b) PTC **151** or ent-**151** (10 mol%) 50% $KOH_{(aq)}$, toluene, RT, 18 h, (63%, 88% ee for **149** and 69%, 91% ee for ent-**149**); (c) PTC **152** (10 mol%), $CsOH{\cdot}H_2O$, DCM, −78 °C, 23 h, (84%, 94% ee).

These groups independently developed a new class of cinchona PTC featuring a *N*-9-anthracenylmethyl group (Scheme **46**, second generation). This aromatic unit is bulkier than the benzyl group present on the first generation PTCs, probably allowing the catalysts to perform much better in the same asymmetric transformations (Scheme **45**). In 2004, the scope of this reaction was expanded to oxazoline systems in order to prepare α-alkylserine.[180]

### 5.1.1.2 Polymeric PTCs (third generation)

Investigations by Sharpless *et al*. aimed at improving the enantioselectivity and expanding the substrate scope of the Sharpless asymmetric dihydroxylation, led to the introduction of cinchona PTCs with two independent alkaloid units (Scheme **47**).[181]

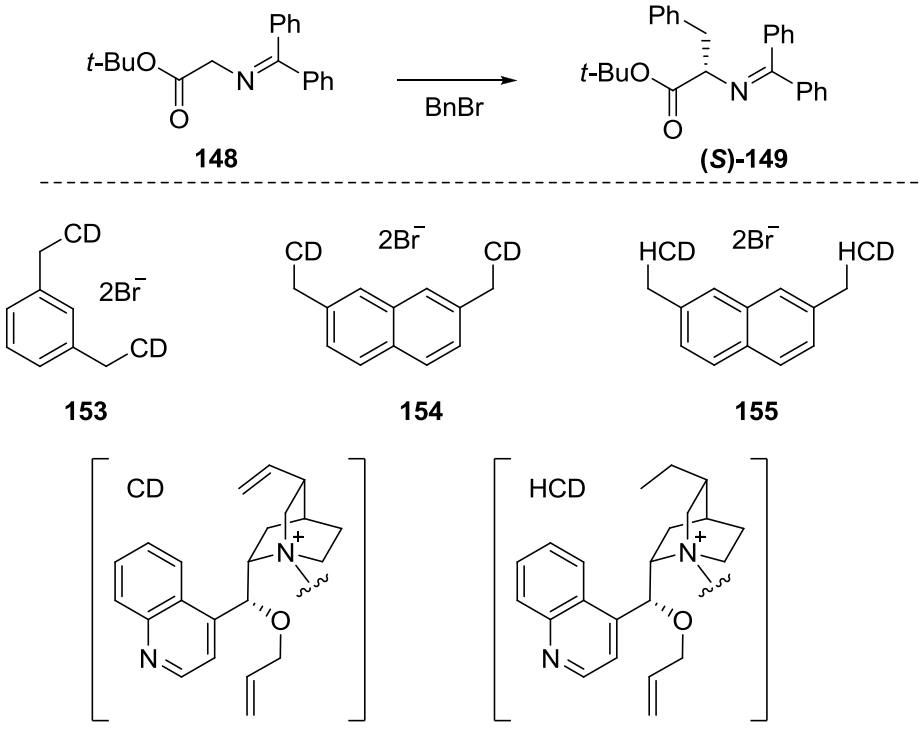


**Scheme 47**: Asymmetric benzylation. PTC (5 mol%), 50% KOH, toluene/$CHCl_3$, 7/3, -20 °C, (*meta*, 94%, 95% ee; *ortho* 88%, 35% ee; *para* 92%, 86% ee).

The same concept was subsequently applied to cinchona PTCs for the asymmetric alkylation of amino acids. In 2001, the Park-Jew team designed the first dimeric[182] and trimeric[183] cinchona PTCs (polymeric PTCs, third generation) di- and tri-substituted in the *meta*, *ortho* and *para* positions, using a phenyl spacer. These catalysts were evaluated for asymmetric benzylation (Scheme **47**). The *meta*-dimers performed remarkably better than the others (*meta* 94% yield, 95% ee; *ortho* 88% yield, 35% ee; *para* 92% yield, 86% ee) – the authors speculated this was due to steric factors.[182] One year later, the same team developed an improved series of *meta*-dimeric cinchona PTCs featuring a naphthalene unit as spacer.[184] The naphthalene spacer in compound **155** (2.4 Å longer than the phenyl spacer in **153**) allows a more favourable conformation which decreases the steric hindrance between the two alkaloid units. PTC **155** bearing a hydrocinchonidine unit showed better solubility than the unsaturated counterpart allowing a lowering of the catalyst loading. The applicability of the 2,7-naphthyl dimeric PTC **155** was demonstrated by the Park-Jew team in the first enantioselective total synthesis of (+)-hygrine, a precursor of tropane alkaloids (Scheme **48**).[185]

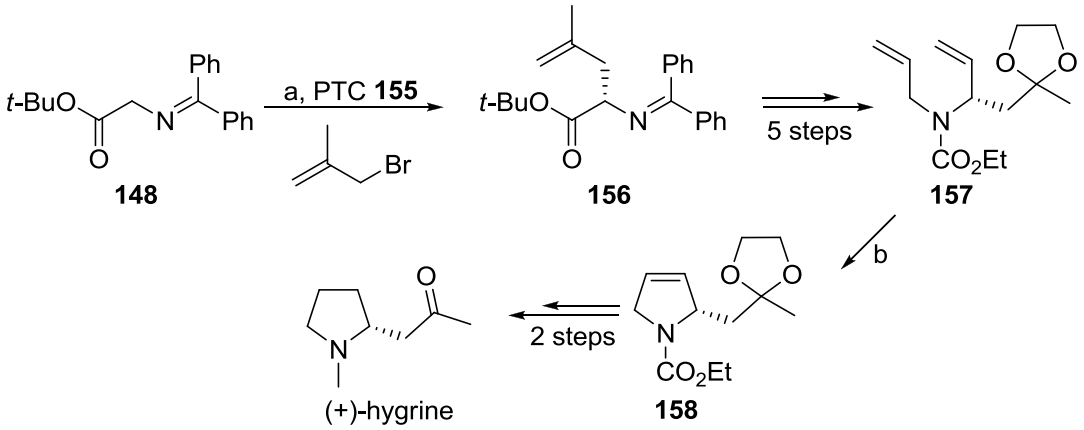


**Scheme 48**: First enantioselective synthesis of (+)-hygrine. (a) PTC **155** (10 mol%), toluene/$CHCl_3$, 0 °C, 7 h, (95%, 97% ee); (b) Grubbs II catalyst, DCM, RT, 3 h, (99%).

Key steps in the synthesis were asymmetric alkylation of Schiff base **148** with methallyl bromide and ring closing metathesis (RCM) for the construction of the pyrrolidine ring. Interestingly, epimerisation of the chiral center was not reported after the metathesis

reaction. Alkylated product **156** could be converted to (+)-hygrine in a further ten steps with 29% overall yield.[185]

### 5.1.1.3 Electronic factor-based *cinchona* PTC (fourth generation)

The cinchona PTCs of the first three generations were designed mainly taking into account steric factors while the electronic properties were not systematically considered.[186] The ion pair of the cinchona quaternary ammonium cation and the anionic substrate plays a dramatic role in the transfer of the chiral information, thus, the electronic effects of the substituent may influence the enantioselectivity. On this assumption the Park-Jew team started to explore the effect of electron withdrawing functional groups.[186] The most representative compound is probably the fluorine derivative PTC **159** (X = F) which gave the best performance in the asymmetric benzylation reaction.[186] This result was rationalised by the formation of a network of hydrogen bonds among molecules of water, the oxygen of the ether functionality and the fluorine atom. The role of the fluorine atom at position 2 was fundamental for the enantioselectivity on the model reaction. Although comparable degrees of selectivity were obtained with other electron withdrawing groups (*e.g.* nitrile and nitrogen oxide) at position 2, only the fluorine substituent (Fig. **50**) afforded ee of up to 96% (Scheme **48**).

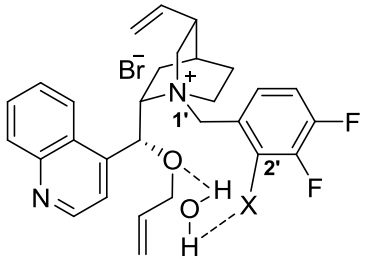


**159**

**Figure 50:** Coordination with molecules of water *via* hydrogen bonding results in a more rigid conformation of the catalyst.

An example of the successful application of the fourth generation PTC was the asymmetric dialkylation of the aldimine system (Scheme **49**).[187] After optimisation of the reaction conditions and substrate, a series of α-alkylalanines (**161a-h**) were prepared with up to 96% enantioselectivity.

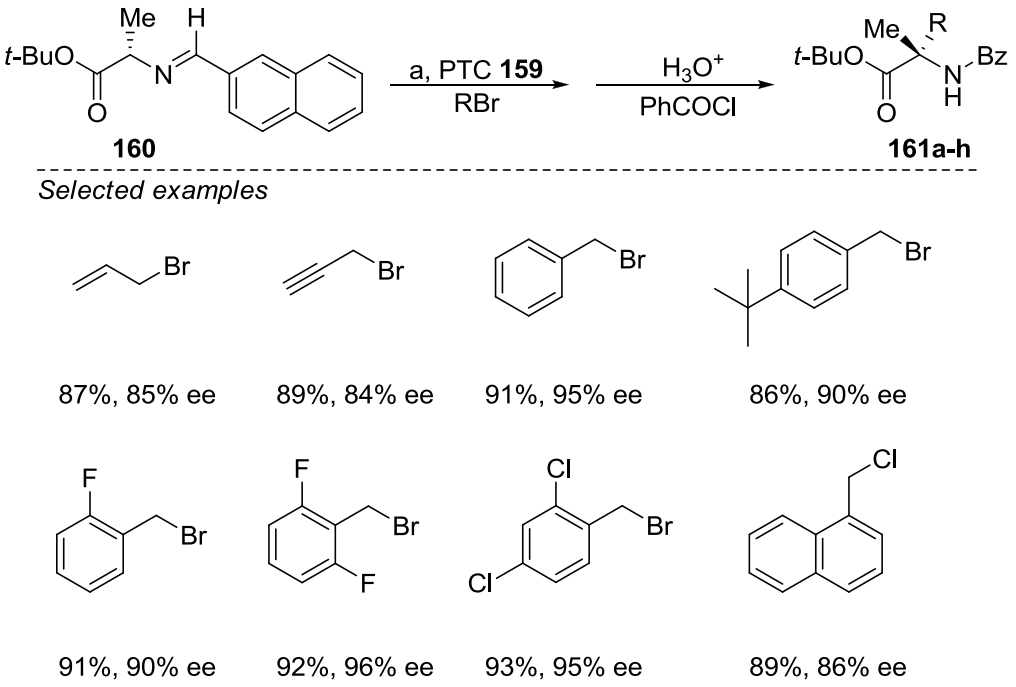


**Scheme 49**: Enantioselective phase-transfer catalytic alkylation for α-alkylalanines. (a) RbOH, toluene, -35 °C.

It is worth noting that solid-supported and supramolecular cinchona PTCs, have also been employed in the enantioselective synthesis of α-amino acids.[188,189] Despite many reports and groups working in this research area, the number of organocatalytic reactions using cinchona PTCs remains limited. Greater structural diversity and the investigation of new reactions and substrates are still needed.[172]

## 5.2 Synthesis of dienamides from imine precursors

Due to their variety, their occurrence in biologically relevant compounds (*e.g.* antibiotic bacillaene) and their synthetic utility, dienamides are attractive chemical intermediates.[190,191] The most widespread synthetic application is as the diene in the Diels-Alder reaction.[192] More recently, dienamides have been employed in asymmetric cycloadditions.[193] In 2008, an intramolecular Diels-Alder reaction featuring dienamides for the synthesis of hexahydroindole carboxylic acids was reported.[194] Hexahydroindole carboxylic acids were targeted by the research group as building blocks for the synthesis of the natural product rostratin C. Starting from readily prepared amino ester hydrochloride **162**, condensation with crotonadehyde proceeded smoothly to yield an unstable imine derivative.[194] This imine was isolated by filtration and immediately treated with tertiary amine diethylaniline in the presence of a series of acid chlorides. With these protected enamides in hand, the group managed to prepare four hexahydroindole derivatives in modest yield and excellent stereoselectivity (Scheme **50**).[194]

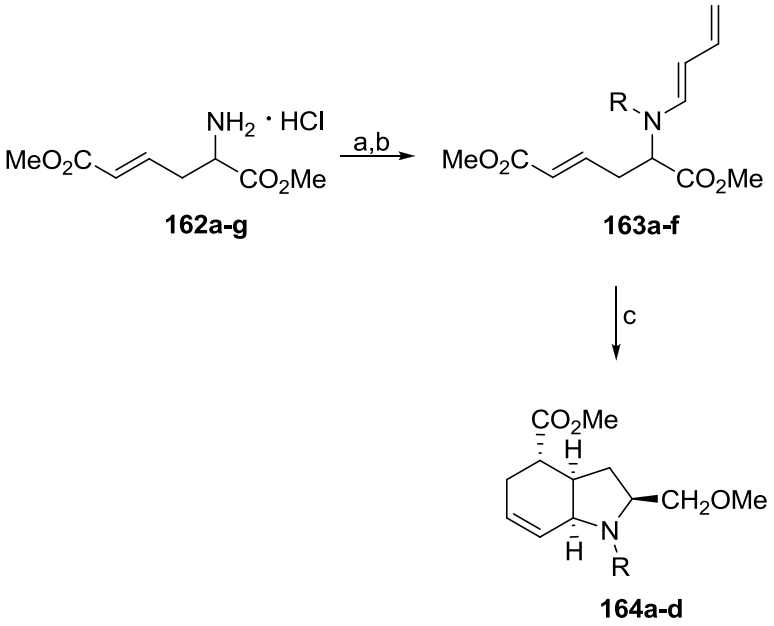


**162a-g** **163a-f** **164a-d**

| | R |
|---|---|
| **162a** | Cbz |
| **162b** | p-$BrC_6H_4CO$ |
| **162c** | $CO_2Me$ |
| **162d** | $COCH_2Cl$ |
| **162e** | $COCHCl_2$ |
| **162f** | CO*i*-Pr |
| **162g** | Alloc |

**Scheme 50**: Preparation of hexahydroindoles derivatives. (a) crotonaldehyde, $Et_3N$, RT, 15 h, (94%); (b) RCl, $PhNEt_2$, toluene, 0 °C to RT, 12 h, (45-96%); (c) *N*,*O*-bistrimethylsilylacetamide (BSA), toluene, (pressure vessel), 130 to 210 °C (51-62%).

The methodology for the preparation of the dienamide precursors was developed in 1975 by the Oppolzer group.[195] Following previous studies on the use of dienamides as substrates for Diels-Alder reactions,[196,197] the preparation of a series of new dienamides from crotonaldehyde was achieved (Scheme **51**).

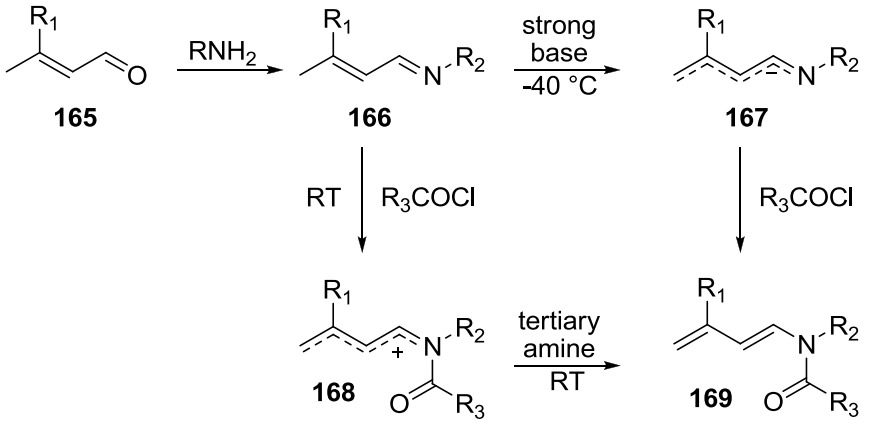


**Scheme 51**: Mechanism of enamide formation in the presence of a strong base at low temperature *vs* simplified method using milder conditions.

Dienamide **169** was initially prepared using strong bases (*e.g.* NaHMDS) at low temperatures[198] according to the mechanism proposed in scheme **51**: deprotonation of **166** to give intermediate **167**, followed by *N*-acylation of anion **167**. Alternatively, prior acylation of the imine **166** by an acid chloride provides delocalised cation **168**, which then needs only a mild base to give the desired dienamide **169**. This methodology has been applied in the proposed strategy for the synthesis of 4-Me-Pro discussed in chapter 6. Asymmetric cycloadditon using dienamides was reported by Rawal *et al.*[193] in connection to their research on the chemistry of 1-amino-3-siloxy-1,3-butadienes. These substrates undergo Diels-Alder reaction in the presence of α-substituted acroleins with excellent regio- and *endo*-selectivity. However, it is not possible to discriminate between the two enatiomeric *endo* adducts obtained. The group envisaged that the use of a chiral Lewis acid, such as Jacobsen's Cr(III)-salen could selectively provide the desired Diels-Alder adduct. The screening of several counterions of catalyst **172** and alkyl substituents on substrate **170** provided the best reaction conditions with enantioselectivity up to 97%

(Scheme **52**). The optimised conditions were applied to a series of substituted methacroleins, providing Diels-Alder adducts with comparable degrees of selectivity.

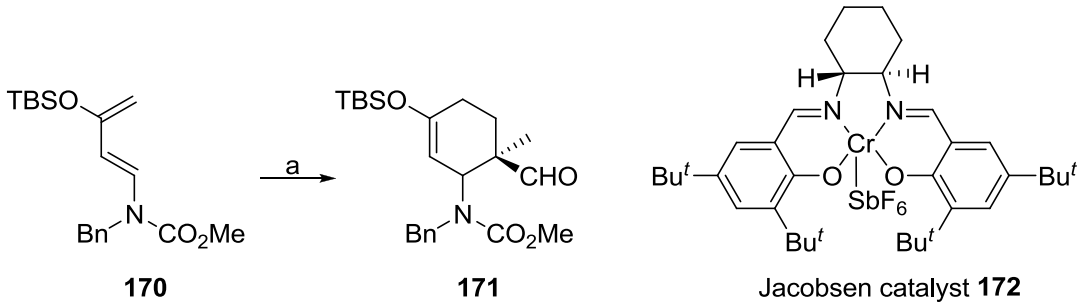


**170** **171** Jacobsen catalyst **172**

**Scheme 52**: Asymmetric Diels-Alder reaction. (a) methacrolein, catalyst **172** (5 mol%), DCM, -40 °C, 2 d (~48 h), (93%, 97% ee).

## 5.3 Enamide-Olefin Ring-closing metathesis (RCM)

### 5.3.1 Ring closing metathesis (RCM) and importance in total synthesis

Since Grubbs and his group developed ruthenium catalyst **173** in 1992 and showed the synthetic utility of this methodology,[199] ring closing-metathesis (RCM) has become one of the most attractive tools for carbon-carbon bond formation in industrial and academic laboratories.[200] Common RCM catalysts are: first and second generation Grubbs catalysts (Fig. **51**, Grubbs I and II, **173** and **175**),[201,202] the molybdenum-based reagent (Shrock reagent, **177**),[203] first and second generation Hoveyda-Grubbs catalysts (**178** and **179**).[204,205] The introduction of Grubbs II catalyst allowed for ring closure of unsaturated carbonyl compounds.[202] Although the molybdenum-based catalysts are more active and offer better selectivity in asymmetric RCM,[206] the ease of handling, air stability and functional group tolerance of the ruthenium-based catalysts make them the most commonly employed catalyst in RCM reactions.[207] Complex drug molecules,[208] supramolecular assemblies[209] and small-molecule libraries[210] have been prepared using RCM-based methodology.

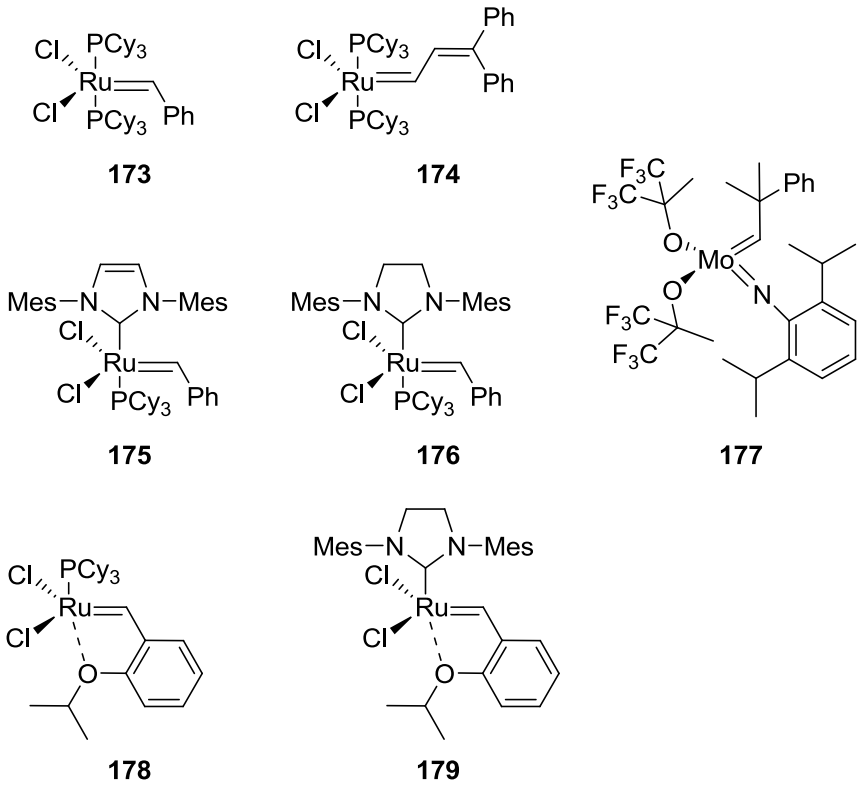


**Figure 51**: Structures of the most common RCM catalysts. Mes = 2,4,6-trimethylphenyl.

A recent report of the total synthesis of alkaloid (−)-nakadomarin A combines organocatalysis and a RCM-based methodology.[211] This marine alkaloid has displayed cytotoxic activity and it is not accessible in significant amount through extraction.[212] The synthetic plan for nakadomarin A was based on multiple carbon-carbon bond forming steps and cascade sequences which allowed a more concise synthesis. The retrosynthesis highlights the main transformations involved: a highly *Z*-selective olefin metathesis, a diastereoselective multicomponent nitro-Mannich/lactamisation and asymmetric Michael addition using cinchona catalyst **186** (Scheme **54**). Fragment **185** was prepared in six steps from the tosylate of pyroglutamol. In this synthetic sequence the first example of intramolecular *Z*-selective Julia-Kocienski olefination was reported.[213] Fragment **185** was constructed in four steps from inexpensive materials to yield furanyl nitro olefin **184**. At this point, cinchona derivative **186**, known for its remarkable selectivity in Michael addition reactions, was successfully employed

allowing for the preparation of nitro ester **183** as 10:1 mixture of diastereoisomers. Subjecting **183** to a three component nitro-Mannich lactamisation according to a previously reported protocol by the same research group allowed for the construction of **182**.[214]

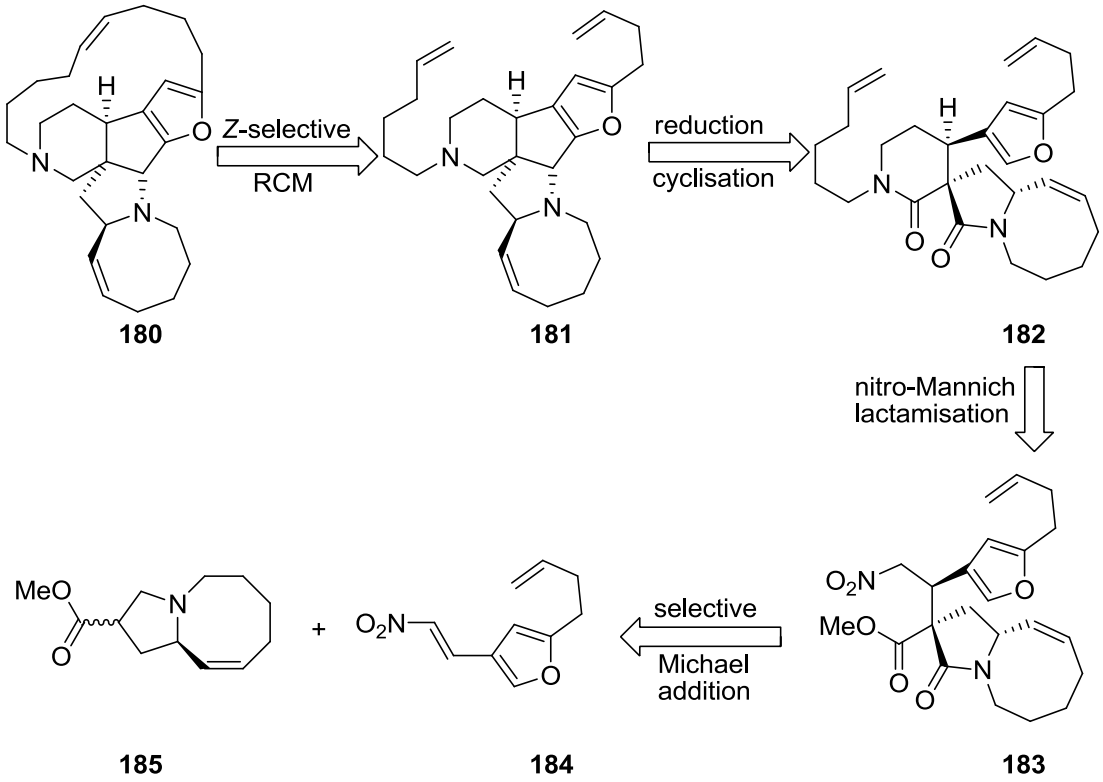


**Scheme 53**: Retrosynthetic analysis of (−)-nakadomarin A.

Gratifyingly, the reduction step proceeded in a regioselective manner on the six-membered lactam, in the presence of $LiAlH_4$ at low temperature to give the 5-membered lactam **188** in high yield (Scheme **54**). After extensive optimisation, hydride delivery was achieved with DIBAL in toluene at -20 °C; to the resulting mixture was added a chilled aqueous solution of hydrochloric acid and heated for 24 h. This reduction/iminium ion formation/diastereoselective carbon-carbon bond-forming cyclisation was unprecedented. The last step of this synthetic sequence, highlighted in 2010 in a report by Martin and Vanderwal,[215] features a *Z*-selective ring-closing

metathesis using Grubbs I in the presence of an excess of either (+)- or (−)-camphorsulfonic acid (CSA). Due to the stereoselectivity and convergence of the route, it was possible to prepare 101 mg of the alkaloid (−)-nakadomarin A.

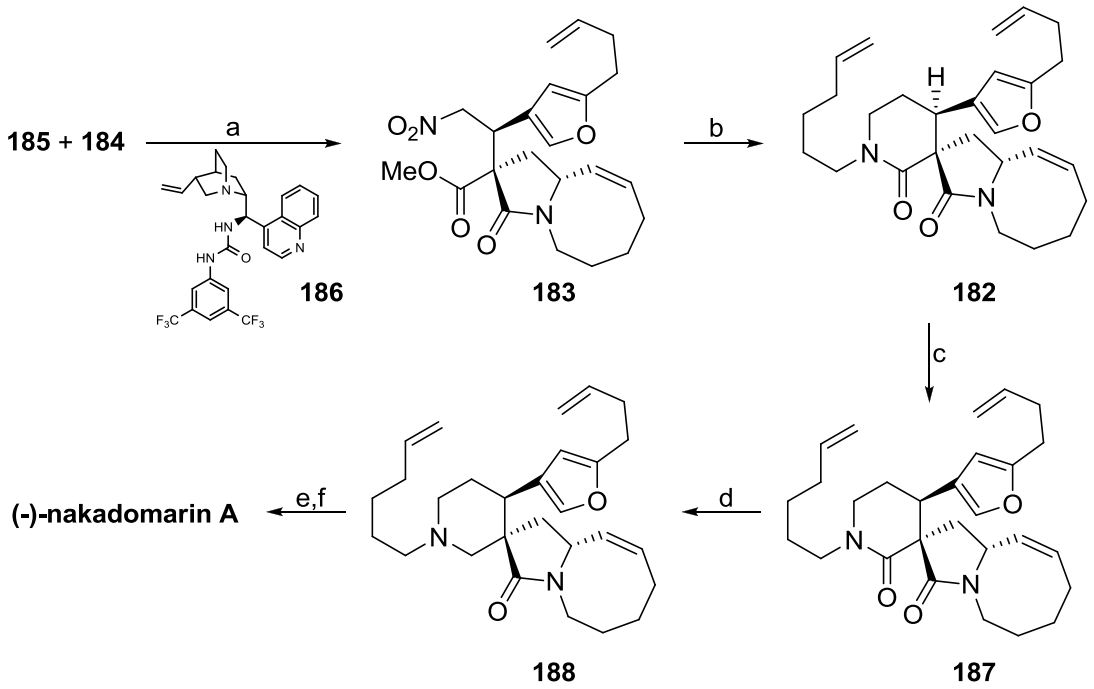


**Scheme 54**:The total synthesis of (−)-nakadomarin. (a) PTC **186** (15 mol%), toluene, 30 °C, 8 d, (57%, 91:9 dr); (b) hex-5-enamine, $CH_2$=O, MeOH, reflux, 3 h, (68%); (c) AIBN, $Bu_3SnH$, toluene, reflux, 4 h, (70%); (d) $LiAlH_4$, toluene, -20 °C, 1 h, then HCOOH, RT, 14 h, (86%); (e) DIBAL, toluene, -20 °C, 1 h, then HCl, 90 °C, 24 h, (41%); (f) Grubbs I, (+)-CSA, DCM, reflux, 3.5 h, (62%, 63/37 = Z/E).

### 5.3.2 Ene-enamide Ring Closing Metathesis

Despite the plethora of successful applications of RCM, the reports of sulphur, phosphorus, and nitrogen-containing heterocycles obtained through olefin metathesis are not abundant. In particular, RCM of olefinic enamides was unprecedented until 2001, when Rutjes and co-workers reported the preparation of five and six-membered cyclic enamides.[216] The Rutjes group investigated the reactivity of a series of protected

enamides towards olefin metathesis in the presence of Grubbs I at temperatures between 20 and 40 ºC.[216] The first results were not very encouraging. Indeed, RCM on substrates **189a-d**, with a methyl substituent at position 1, proved sluggish. However, the use of more stable Grubbs II at higher temperatures readily yielded product **190** (Table **2**). Partial degradation of starting material and product was reported for substrates with a benzoyl or ethoxycarbonyl protecting group, when increasing the temperature. Comparable yields were obtained with six-membered rings (data not shown).

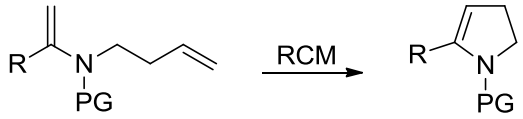


**189a-d** **190a-d**

| substrate | R | PG | conditions | product | yield (%) |
|---|---|---|---|---|---|
| **189a** | Ts | H | G1, 20 °C, 16 h | 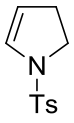 | 84 |
| **189b** | Ts | Me | G1, 40 °C, 2 h<br>G2, 84 °C, 2 h | 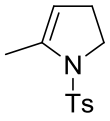 | 59<br>86 |
| **189c** | Bz | Me | G2, 84 °C, 4 h<br>G1, 40 °C, 6 h | 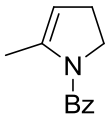 | 63<br>60 |
| **189d** | $CO_2Et$ | Me | G1, 40 °C, 4 h | 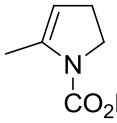 | 62 |

**Table 2**: RCM of olefinic enamides: 17,5 µM substrate concentration; 1-5 mol%. Grubbs I was used in DCM, while Grubbs II was used in dichloroethane.

Since RCM is often employed for the synthesis of pharmaceutically relevant molecules,[217] the question of lowering the catalyst loading has been posed recently.[218] As ruthenium removal can be a cumbersome process, decreasing the loading could minimise the risk of ruthenium contamination. In this regard, the investigation conducted by Pederson *et al*. proved that using more efficient ruthenium-based catalysts

could yield five-, six-, and seven-membered carbamate-protected cyclic amines efficiently while lowering the catalyst loading from 2-5 mol% to 500 ppm.[218]

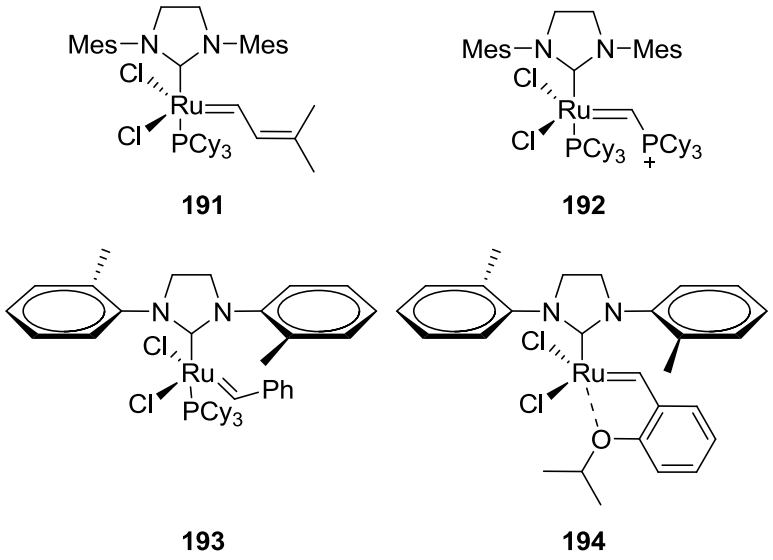


**Figure 52**: Some of the ruthenium-based catalysts involved in the investigation. Mes = 2,4,6-trimethylphenyl.

The screening process was performed by Symyx robotic technology to test a large number of RCM reactions using ppm catalyst loading and establish the efficiency of the catalyst considering both reaction conditions and substrate design (Table **3**). Catalysts **193** and **194** were the most efficient in this RCM reaction. The reaction could be carried out neat for five-membered rings while more dilute substrate concentrations were needed for larger rings. The screening of several ruthenium-based catalysts for trisubsituted heterocyclic olefins proved that NHC-bearing catalysts were more efficient at low catalyst loadings. Satisfactory results were also obtained for tetra-subsituted alkenes. In the presence of catalyst **194** and with methyl *tert*-butyl ether (MTBE) as solvent, catalyst loading could be lowered to 1000 ppm, with yields >90%.[218]

| substrate | conc [M] | product | yield (%) |
|---|---|---|---|
| 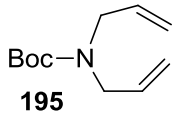 **195** | neat<br>1 M<br>0.2 M | 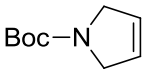 **196** | 87<br>99<br>99 |
| 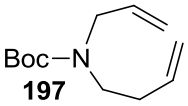 **197** | 1 M<br>0.2 M<br>0.05 M | 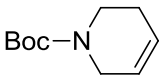 **198** | 96<br>99<br>92 |

**Table 3**: Effects of concentration on the formation of di-substituted five- and six-membered carbamate protected cyclic amines by catalyst complex **194**. All the reactions were carried out at 50 °C.

### 5.3.4 Applications in total synthesis

Finally, the first example of macrocylisation using an ene-enamide RCM for the total synthesis of cyclopeptide alkaloid (−)-paliurine E is worthy of discussion.[219] The retrosynthetic strategy is based on the connection of hydroxyproline-styrene fragment **202** to a series of enamides **201a-d** in order give ene-enamide substrates **200a-d** for the key RCM macrocyclisation step (Scheme **55**). It was envisaged that coupling to the last phenylalanine derivative portion at the pyrrolidine nitrogen would yield the desired natural product. In order to evaluate the reactivity of different substrates towards RCM, different ene-enamides were prepared from *N*-Boc-isoleucine (Scheme **55**).[219] Careful removal of the Boc protecting group using anhydrous zinc bromide, followed by EDC-HOBt mediated coupling with carboxylic acid **202** furnished ene-amides **201a-d** in good overall yields. These compounds were subjected to RCM in the presence of Grubbs II (10 mol% added over 48 h) in 1,2 dichloroethane (reflux) under high dilution conditions (0.005 M).

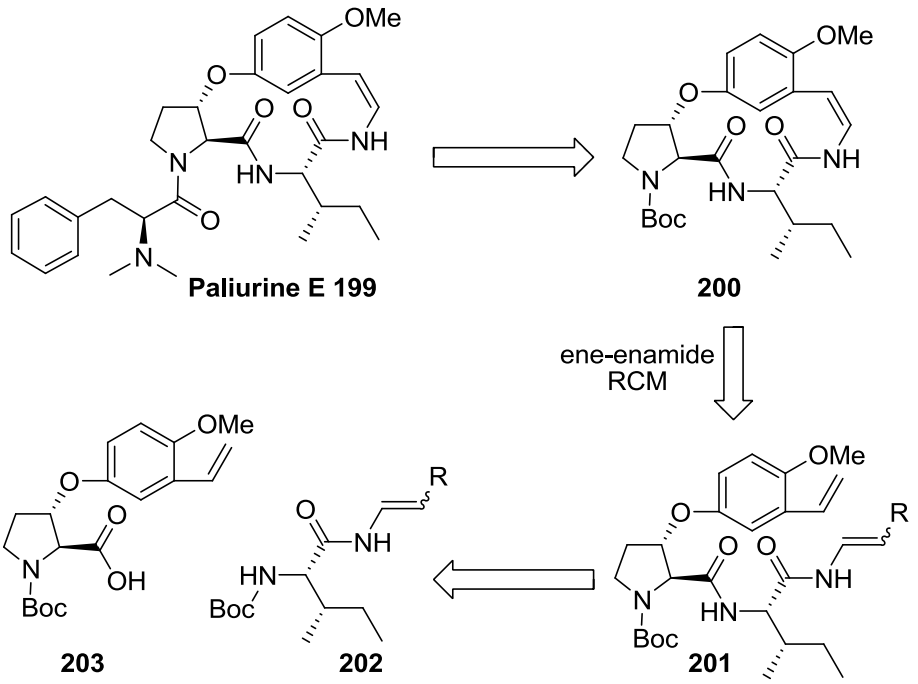


**Scheme 55**: The retrosynthetic analysis of paliurine E.

Reaction on substrate **201a** proved sluggish under the conditions described below, yielding primary amide **203** (Scheme **56**). This amide was formed even in the absence of the catalyst, thus suggesting instability of the starting material. The presence of a methyl group on ene-enamide **200b** probably conferred greater stability to the substrate allowing macrocyclisation in a preparatively useful yield (49%). The uses of additives for this transformation did not lead to significant optimisation.[220] RCM did not take place for substrate **200c**; an alternative relay RCM was then considered for this particular substrate which unfortunately led to an unidentifiable mixture of products.[221] The most stable of the ene-enamides considered, compound **200d** featuring a benzyl group did not react significantly but decomposed to amide derivative **205** which possessed an unusual aldehyde in place of a styrene double bond. The formation of this side product will be discussed in the next chapter, in connection to the results of the investigations of the ene-enamide RCM reaction.

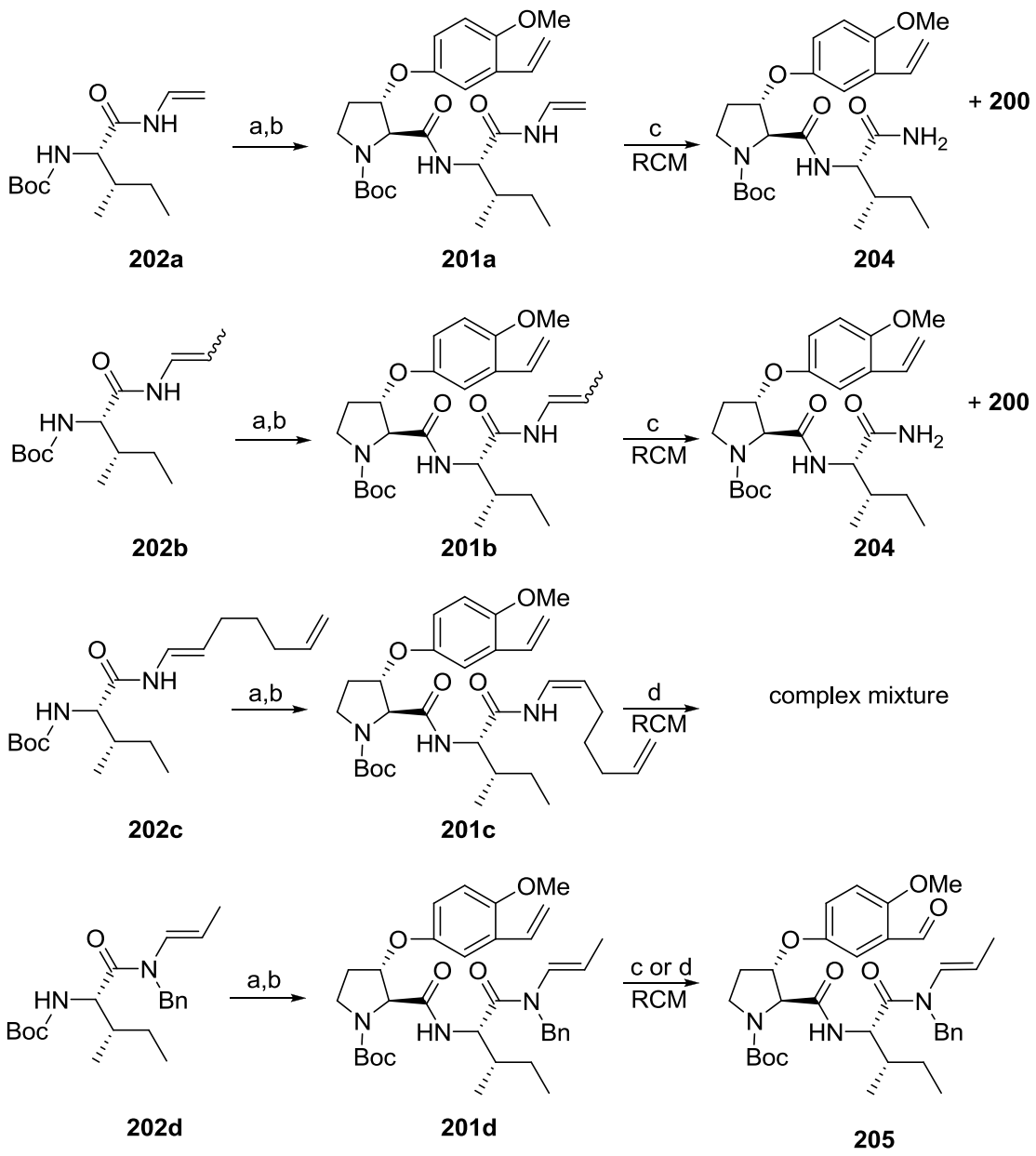


**Scheme 56:** Synthesis of ene-enamide substrates and RCM. (a) $ZnBr_2$, DCM, 0 °C to RT; (b) **203**, EDC, HOBt, NMM, DMF, 0 °C to RT (86% for **202a**, 79% for **202b**, 85% for **202c**, 91% for **202d**) (c) Hoveyda-Grubbs II (2 x 10 mol%), dicholoroethane (0.005 M), reflux, (8% of **200** for **201a**, 49% of **200** for **201b**, no product for **201c**, no product for **201d**); (d) Hoveyda-Grubbs II (1 E), dicholoroethane (0.005 M), reflux, (39% of aldehyde **205**).

In addition to this new methodology, the group found that fragment **200** could be prepared through an intriguing sequence of a ruthenium-catalysed isomerisation

followed by ene-enamide RCM (after removal of the benzyl group on substrate **201d**), thus shortening the synthesis.[222] Natural product (−)-paliurine E was obtained from **200** following deprotection of the pyrrolidine nitrogen and coupling to *N*,*N*-dimethyl-L-phenylalanine. This report outlines the potential of ene-enamide RCM while providing interesting insights into the macroyclisation mediated by this reaction.

## 5.4 Selective hydrogenation of cyclic enamides

The synthesis of 4-Me-Pro by Munro *et al*.[133] (reported in section 4.8.2) described the selective hydrogenation of an exocyclic di-substituted double bond in pyrrolidine derivatives with concomitant removal of a Cbz protecting group. This reaction was performed with a good degree of *cis*-selectivity using Pd/C. Pyrrolidine substrate **206** features an endocyclic tri-substituted double bond, hence it is not possible to predict the stereochemical outcome of the reaction for this isomer directly. Several homogeneous and heterogeneous stereoselective hydrogenation protocols have been developed in the last few decades,[223] hence the screening of different conditions will be necessary.

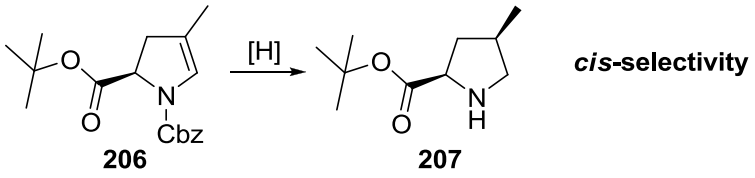


**Scheme 57**: Selective hydrogenation of cyclic enamide and Cbz removal.

Stereoselective hydrogenation of tri-substituted double bonds of enamides has been reported by Baldwin *et al*. in connection to their studies towards the synthesis of the kainoids (a family of non-proteinogenic aminoacids). Their substrates featured a substituent at position 3 rather than at position 2 (Table **4**).[224]

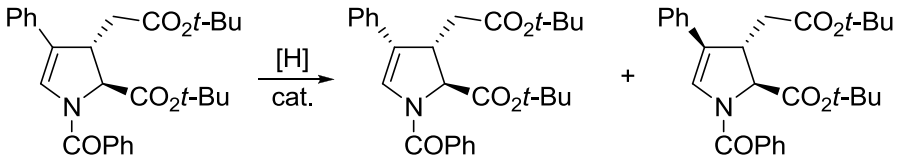


**208** **209** **210**

| cat. | solvent | reaction time | ratio 209:210 |
|---|---|---|---|
| 10% Pd/C | EtOAc | 20 h | 12:1 |
| Pd black | EtOAc | 6 h | 1:0 |
| Raney Ni | EtOH | 6 h | a |
| $PtO_2$ | EtOH | 6 h | a |
| $PtO_2$ | EtOH | 1 h | 6:1 |
| $Pd(OH)_2$-C | EtOH | 6 h | 8:1 |
| Rh/C | EtOAc | 3 d | b |

**Table 4**: Investigations into the catalytic reduction of cyclic enamide **208**. (a) Reduction of the phenyl groups occurred; (b) no reaction.

After investigation of a series of reaction conditions, the use of palladium black as a catalyst gave the best results in terms of yield and selectivity (81% of diastereoisomer **209**). The use of homogeneous catalysts such as Wilkinson's and Crabtree's catalysts over a range of temperatures and pressures failed to reduce enamide **208**, probably because of the steric hindrance imposed by the tri-substituted double bond.[224] In order to investigate the role of the substituents, methyl analogues at position 2 and 3 were prepared. In agreement with a previous report, the substituent in position 2 had a dramatic effect on the stereoselectivity of the reduction step.In a recent report platinum dioxide has been utilised for efficient hydrogenation of pyrrolidine derivative**s** in good yields and selectivity.[225,226]

In this chapter a general overview of the synthetic methodologies investigated for the novel approach towards the synthesis of 4-Me-Pro has been given. The results of these investigations and the future application of this work will be discussed in chapter 6.

# 6 Results and discussion

The synthetic efforts (Scheme **58**) towards the synthesis of racemic 4-Me-Pro will be discussed in section 6.1 (route A) and 6.2 (route B).

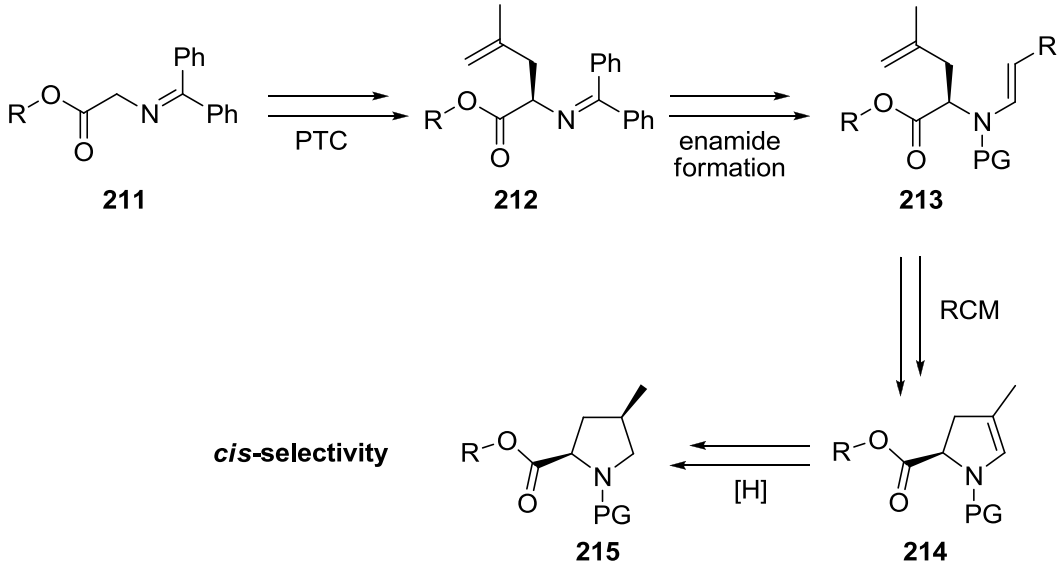


**Scheme 58**: Key transformations of the novel synthetic approach to 4-Me-Pro.

The methodologies investigated to install the stereochemistry at the α-position (compound **212**), Pd-catalysed allylation (section 6.3.1) and PTC-catalysed asymmetric alkylation (section 6.3.2), will be also discussed.

## 6.1 Racemic route A

The first racemic route started with the preparation of Schiff base **218** from the inexpensive starting material methyl glycine ester hydrochloride[227] and allyl carbonate **217** from the alcohol precursor.[228] These species, which could be readily synthesised in

multigram quantities, were subjected to Pd-catalysed allylation in the presence of $Pd(PPh_3)_4$ (Scheme **59**).[229,230]

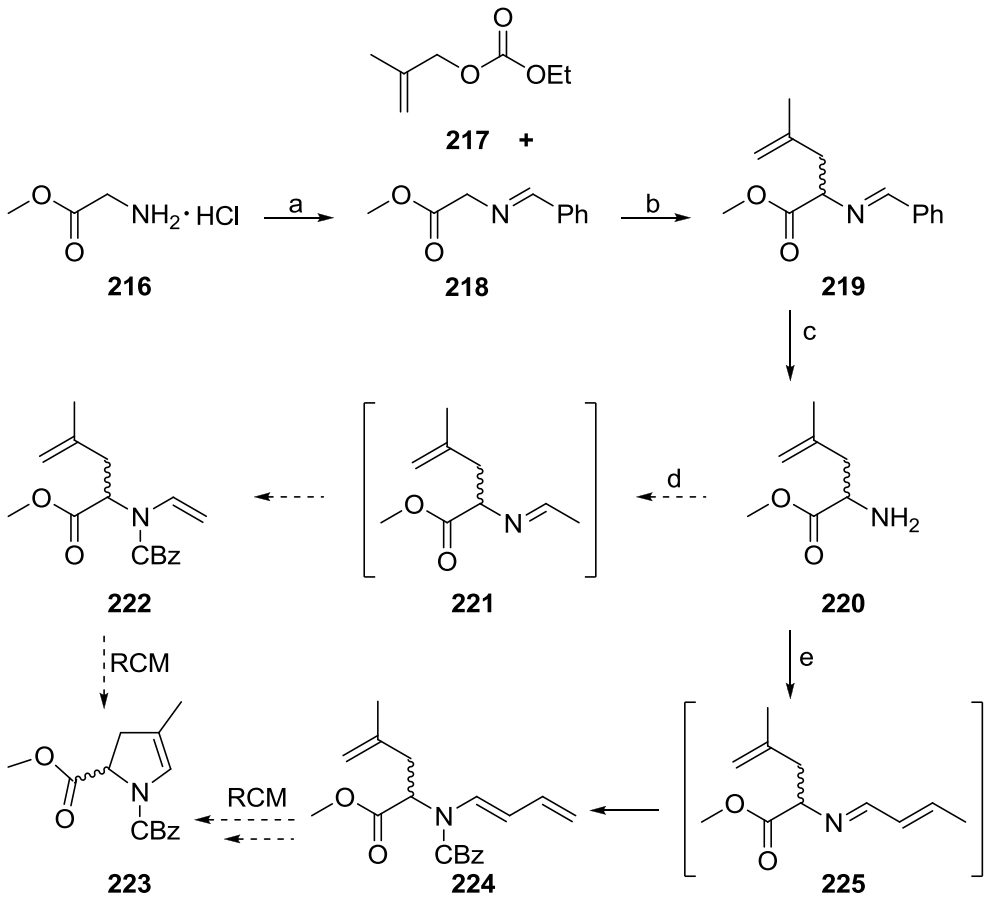


**Scheme 59**: Racemic route A. (a) $Et_3N$, DCM, $MgSO_4$; then PhCHO, ~18 h, (99%); (b) dry THF, $Pd(PPh_3)_4$, 5-7 h, RT, (72%); (c) 1.5 M $HCl_{(aq)}$,2 h, RT, (85%); (d) acetaldehyde, DCM, molecular sieves, 0 °C to RT,~18 h, (traces); (e) i. crotonaldehyde, DCM, molecular sieves, RT, ~18 h; ii. benzyl chloroformate, toluene, *N*,*N*-Diethylaniline, 0 °C to RT, ~18 h, (49%).

The reaction proceeded smoothly to give monoallylated Schiff base **219** in 5-7 h in the presence of 1.5 equivalents of allyl carbonate **217**. Longer reaction times and the use of a higher number of equivalents of allyl carbonate resulted in a mixture of mono- and di-allylated products as confirmed by analysis of crude NMR (data not shown). Although purification of the allylated product by flash chromatography has been reported,[229] this

process resulted in partial hydrolysis of the imine group yielding benzaldehyde and the primary amine. This problem was clearly connected to the acid-sensitive nature of the imino-group, thus different purification protocols were investigated. Silica deactivation by adding 0.1% triethylamine to the eluent before sample loading did not improve the overall yield. The use of activated alumina (neutral and basic, Brockmann I) limited the decomposition but resulted in low recovery of product **219**. Finally, the crude product was filtered through a short plug of either basic alumina or Celite in order to remove the palladium residues and the material was used without further purification. Hydrolysis of the imino group was readily achieved under acidic conditions yielding primary amine **220** and benzaldehyde as a side product.[229] At this point, the possibility of using either acetaldehyde or crotonaldehyde for imine condensation with **220** was investigated. Although the difficulties of handling acetaldehyde (bp ~20 °C) and the possible instability of the product **221** were obvious, this route was more appealing because of the formation of a more reactive substrate, (following conversion to the corresponding enamide, *i.e.* compound **222**) towards RCM. Encouragingly, in 1994 the use of acetaldehyde in imine condensation reactions was reported for the preparation of *N*-phosphonoalkyl dipeptide inhibitors of human collagenase (Scheme **60**).[231]

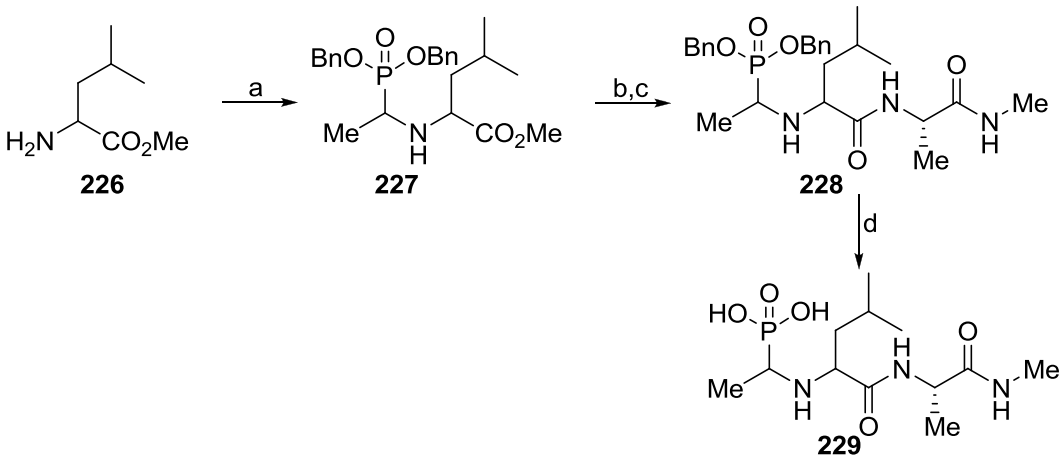


**Scheme 60**: Synthesis of *N*-phosphonoalkyl dipeptide inibhitor **229**. (a) Acetaldehyde; then dibenzyltrimethylsilyl phosphate, DCM, 0 °C; (b) NaOH, MeOH, $H_2O$; (c) $H_2NCH(Me)CONHMe$, EDC, HOBt, DCM; (d) EtOH, 10% Pd/C, $H_2$.

In addition, the belief that the use of acetaldehyde could generate the desired intermediate **222** was supported by other reports.[232,233] In order to prepare iminoester **221**, a solution of amine **220** in DCM was cooled to 0 °C in the presence of molecular sieves. Acetaldehyde was added and the stirring was continued at RT overnight (~18 h). Although formation of the product was confirmed by LCMS, crude $^1$H NMR showed an unidentifiable mixture of products. The use of shorter reaction times or different drying agents (*e.g.* $MgSO_4$) did not improve the results. Imine condensation carried out with crotonaldehyde instead,[194] yielded the desired iminoester **225** as confirmed by LCMS and crude $^1$H NMR. This product could not be stored for any significant length of time and was used without further purification for the next step. Following the protocol described in chapter 5 for the preparation of dienamides from imine precursors, a solution of iminoester **225** was reacted with benzyl chloroformate in the presence of *N*,*N*-diethylaniline (Scheme **61**).[194] NMR analysis of the isolated material, purified by flash chromatography, revealed that half of the starting material was converted to the Cbz-protected amine **230** and the desired enamide **224** was obtained only in poor yield.

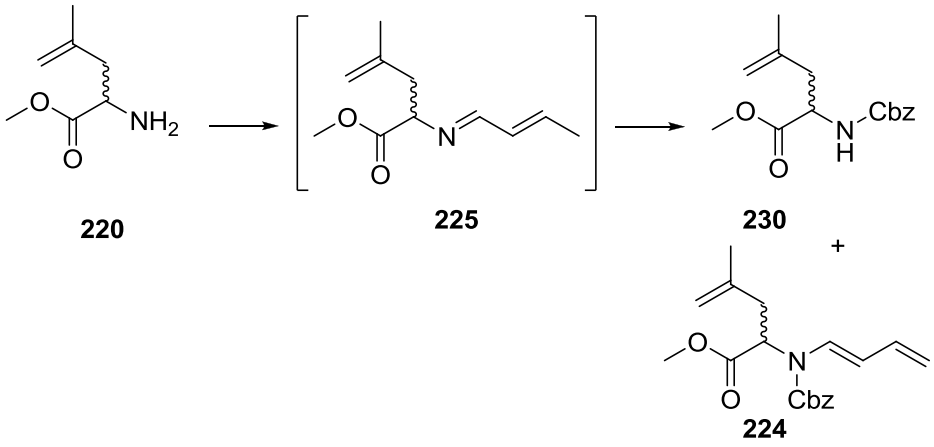


**Scheme 61**: The synthesis of dienamide **224**.

Reducing the amount of the acid chloride[197] (from 1.5 equivalents to 1) did not result in any significant decrease of the formation of side product amide **230**. More forcing reaction conditions (NaHMDS in toluene at -40 °C) led to decomposition of starting

material **220**.[198,196] Thus, a new route starting from *tert*-butyl ester glycine hydrochloride was envisaged, in the hope that this substrate would provide greater stability for the subsequent formation of the desired dienamide.

## 6.2 Racemic route B

In the second racemic route Schiff base **148** was prepared by condensation of *tert*-butyl ester glycine hydrochloride and dibenzophenone imine.[234] The product could be readily recrystallised from hexane yielding the desired Schiff base **148** in high yield and purity. This substrate underwent Pd-catalysed allylation smoothly as in the previous approach (**148** to **232**, Scheme **62**).[229,230] Gratifyingly, no purification issue arose from the acid-sensitive imine group in this case, as the presence of a second aromatic moiety conferred greater stability to the compound. Careful flash chromatography, carried out with basic silica as recommended in the literature[235] yielded alkylated Schiff base **232** in excellent yield and purity. However, a later study on the use of regular silica showed only a marginal reduction of the yield. Acidic hydrolysis[236] of **232** furnished primary amine **233**, which could be purified by flash chromatography, in high yield. At this point, imine condensation was carried out as before in the presence of crotonaldehyde. Upon confirmation of the formation of the iminoester **234** by LCMS and $^{1}$H NMR, the product was treated with benzyl chloroformate and *N*,*N*-diethylaniline to obtain Cbz-protected dienamide **235** in moderate yield.[194,195] The use of acetaldehyde instead of crotonaldehyde yielded the same dienamide **235** in poor yield (data not shown); despite the $^{1}$H NMR of the crude iminoester intermediate showing the desired structure **236**. This is probably due to partial hydrolysis of the imino group in intermediate **236** (less stable than **234**); the liberated molecules of acetaldehyde can then react to give dienamide **235**. Even dienamide **235** was shown to be not particularly stable.

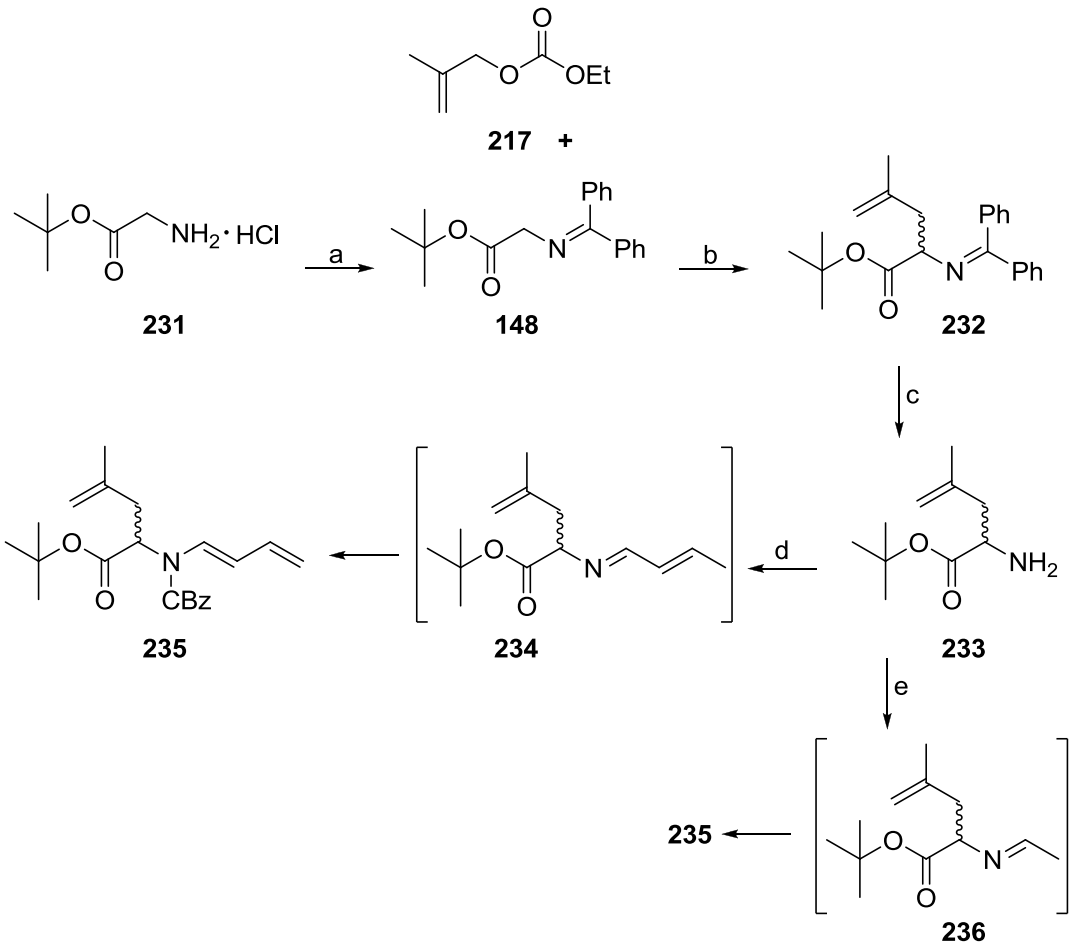


**Scheme 62**: Racemic route B. (a) dibenzophenone imine, DCM, RT, ~18 h, (91%); (b) dry THF, $Pd(PPh_3)_4$, 5-7 h, RT, (92%); (c) 1 M $HCl_{(aq)}$, THF, 2-3 h, RT, (93%); (d) i. crotonaldehyde, DCM, molecular sieves, RT, ~18 h; ii. benzyl chloroformate, toluene, *N*,*N*-diethylaniline, 0 °C to RT, ~18 h, (67%); (e) i. acetaldehyde, DCM, molecular sieves, RT, ~18 h; ii. benzyl chloroformate, toluene, *N*,*N*-diethylaniline, 0 °C to RT, ~18 h.

Indeed, upon storage on the bench for a few days, the compound decomposed to crotonaldehyde and Cbz-protected amine **237** (Scheme **63**). Storage at -20 °C was shown to be possible for up to 2 weeks. High temperature (323 K) NMR experiments also showed that this was the most common decomposition pathway (Scheme **63**). Crotonaldehyde peaks at δ 6.93-6.84 and 6.22-6.15 (Scheme **63**, b) and diagnostic aldehyde peak at δ 9.50 (data not shown) confirmed the formation of such compound. Comparison between $^1$H NMR of isolated Cbz-protected amine **237** and the one of the

dienamide **235** heated at 323 K overnight (~18 h) revealed the presence of the **237** in the sample (dd at δ 2.51 and 2.37 for C-3 protons, Scheme **63**, e & f).

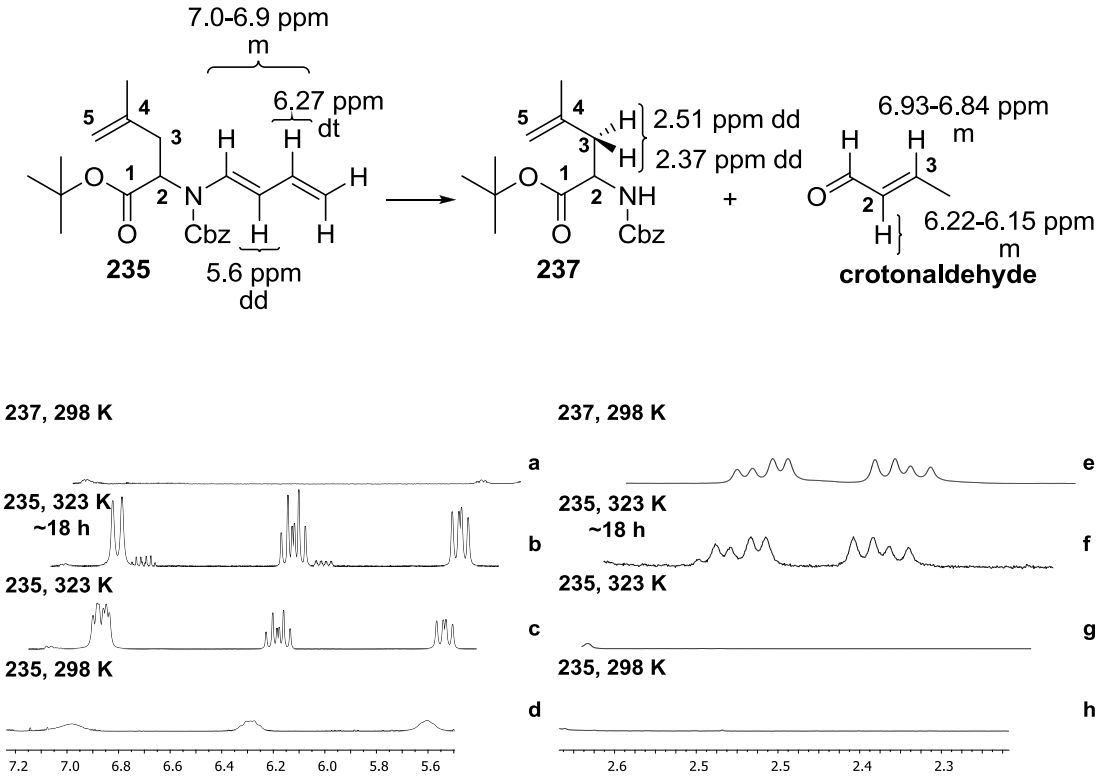


**Scheme 63**: Decomposition of dienenamide **235** to Cbz-protected amine **237** and crotonaldehyde and chemical shifts of diagnostic peaks (top). High temperature $^{1}$H NMR experiments with dienamide **235** and comparison with $^{1}$H NMR of Cbz-protected amine **237** at RT (bottom).

Although further optimisation was needed for the imine/enamide conversion, efforts were focussed on the ene-enamide metathesis step to ascertain the feasibility of this synthetic sequence. The first series of ene-amide RCM on **235** was carried out using Grubbs II and Hoveyda-Grubbs II catalysts (Table **5**, entries 1-5), as these catalysts are known to have a wider substrate scope compared to the first generation catalysts.[202] Besides this consideration, Grubbs II catalyst has been employed before on dieneamide substrates showing selectivity for the internal double bond.[237] Furthermore, ring closure on the internal double bond was reported to be favoured for 5-membered rings.[238] DCM

and toluene were used as solvents at a range of different temperatures. After 2-3 hours a new species was visualised on the TLC plate for all the reactions with $R_f$ = 0.27 which was believed to be the desired RCM product as eventual dimers were more likely to be at $R_f$ values higher than the starting material ($R_f$ = 0.40). Therefore, the reactions were allowed to run overnight (~18 h) in the hope of a total conversion of the starting material. Disappointingly, the isolated compound at $R_f$ = 0.27 appeared to be aldehyde **238**. Increasing the catalyst loading (up to 25 mol% in three portions) as suggested in the literature[239] and employing a longer reaction time resulted in higher conversion of the starting material to the aldehyde side product (Table **5**).

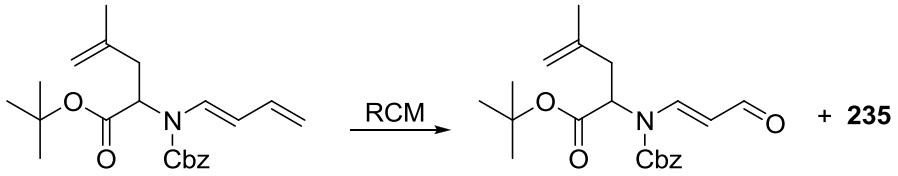


**235** **238**

| entry | cat. | mol% | solvent | running time | T | 235 % | 238 % | unknown % |
|---|---|---|---|---|---|---|---|---|
| 1 | G2 | 8% | DCM | ~18 h | 40 °C | 50 | 20 | 20 |
| 2 | HG2 | 8% | DCM | ~18 h | 40 °C | 50 | ~40 | - |
| 3 | G2 | 8% | tol. | ~18 h | 50 °C | 80 | 20 | - |
| 4 | HG2 | 8% | tol. | ~18 h | 50 °C | 70 | 20 | - |
| 5 | G2 | 8% | DCM | ~18 h | RT | 50 | 10 | 30 |
| 6 | G2 | 8% | tol. | ~18 h | RT | 50 | ~30 | ~10 |
| 7 | G1 | 8% | tol. | ~48 h | RT | 80 | ~20 | - |
| 8 | G1 | 8% | tol. | ~48 h | ~90 °C | 50 | 20 | 20 |
| 9 | G1 | 8% | DCM | ~48 h | RT | 60 | 20 | ~10 |
| 10 | G1 | 8% | DCM | ~48 h | 40 °C | 60 | 20 | ~10 |
| 11 | G2 | 25% | tol. | ~48 h | ~90 °C | ~10 | ~50 | 30 |

**Table 5**: Summary of investigation of ene-enamide ring-closing metathesis on dienamide **235**. The relative percentages refer to the conversion as judged by TLC.

Similarly, the use of Grubbs I catalyst gave no better results (Table **5**, entries 7-10). A third species appeared on the TLC plate in some cases, as summarised in the table (this species was never observed when Hoveyda-Grubbs II catalyst was employed). Unfortunately, it was not possible to isolate this compound ($R_f$ = 0.37).

The formation of this atypical aldehyde is not unprecedented; a similar result has been observed by Toumi *et al*. in the synthesis of (−)-paliurine E.[219]

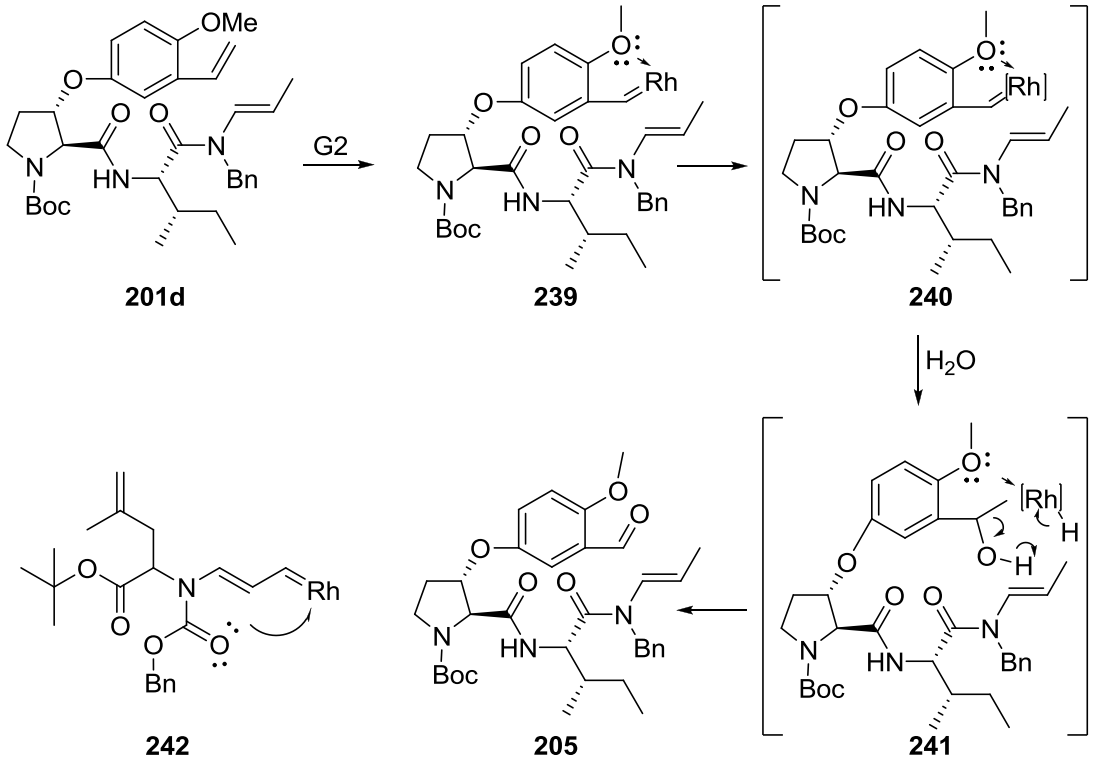


**Scheme 64**: Possible intermediate for the formation of aldehyde **205** and analogy with the dienamide substrate used in the investigation of the ene-enamide RCM reaction.

The authors speculated that the *ortho* methoxy group in the styrene substrate may contribute to the formation of a relatively stable alkylidene complex (Scheme **64**).[240] At this point, a change in conformation of the enamide, probably due to the presence of the benzyl group, or simply steric hindrance prevents the desired [2 + 2] cycloaddition from occurring. It is likely that the alkylidene complex **240** reacts with a molecule of water instead of the enamide substrate, and a subsequent rearrangement furnishes aldehyde

**205**. Perhaps the carbonyl functional group in the enamide substrate **242** triggers a similar phenomenon (Scheme **64**).

## 6.3 Installing the stereochemistry at the α-position

### 6.3.1 Pd-catalysed allylation

Allylic alkylation is a well established transformation for carbon-carbon bond formation which may be catalysed by transition metal complexes.[241] Although metals such as molybdenum,[242] rhodium,[243] iridium,[244] or tungsten[245] have been used recently for this reaction, palladium remains the most widely employed metal.[241]

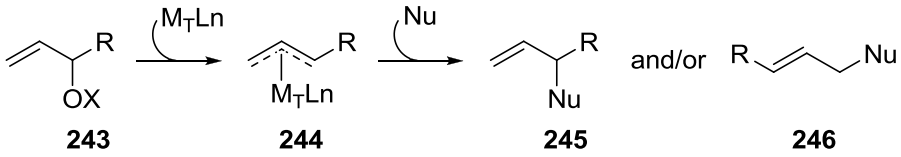


**Scheme 65**: General mechanism of transition metal-catalysed allylic alkylation.

This variety of metals has been introduced in order to achieve selective transformations by modulating the reactivity of allylic complex **244**, generated *in situ* by oxidative addition to an allylic substrate **243** (*e.g.* ethers, alcohols, esters, carbonates etc.). In 1987, Genet *et al*. reported the first example of transition metal-catalysed allylic alkylation, using Schiff bases derived from α-amino acid esters as prochiral nucleophiles and allylic carbonates under neutral conditions.[246]

More recently, the asymmetric Pd-catalysed allylic alkylation of glycine imino ester with a series of allyl acetates in the presence of an inorganic base was reported by the Takemoto group.[247] The investigation was carried out using an achiral metal complex $[Pd(\pi\text{-allyl})Cl)]_2$ with different ligands and a chiral cocatalyst, phase-transfer

catalyst (PTC) derived from cinchona alkaloids. The results obtained using allyl acetate are summarised in table **6**. The use of second generation cinchona PTC (chloride version)[247] yielded allylated product **247** in high yield but with poor enantioselectivity (entry 1); *O*-alkylated PTCs performed marginally better with regard to the selectivity (entries 2 & 3). The screening of different ligands showed that the use of $(PhO)_3P$ and $(EtO)_3P$ could improve the selectivity at the expense of the chemical yield (entries 4-8).

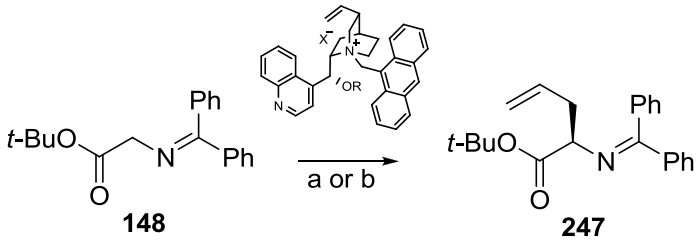


| entry | R | X | ligand mol% | base | yield % | ee % |
|---|---|---|---|---|---|---|
| 1 | H | Cl | DPPE (8) | KOH | 83 | 3 |
| 2 | allyl | Br | DPPE (8) | KOH | 71 | 12 |
| 3 | Bn | Br | DPPE (8) | KOH | 91 | 9 |
| 4 | Me | I | DPPE (8) | KOH | 74 | 24 |
| 5 | Me | I | *n*-$Bu_3P$ (16) | KOH | 69 | 4 |
| 6 | Me | I | $Ph_3P$ (16) | KOH | 32 | 59 |
| 7 | Me | I | $(EtO)_3P$ (16) | KOH | 25 | 50 |
| 8 | Me | I | $(PhO)_3P$ (16) | KOH | 19 | 82 |
| 9 | Me | I | $(PhO)_3P$ (16) | 50% KOH | 82 | 94 |
| 10 | Me | I | DPPE(0) (10) | 50% KOH | 83 | 93 |

**Table 6**: Asymmetric alkylation of **148** with allyl acetate in the presence of chiral PTCs; (a) toluene, solid KOH, $[PdCl(\pi\text{-}C_3H_5)]_2$ RT; (b) toluene, 50% $KOH_{(aq)}$, $[PdCl(\pi\text{-}C_3H_5)]_2$, 0° C.

The best results in terms of chemical yield and enantioselectivity were obtained using *O*-methylated PTC (iodide version) with either $(PhO)_3P$ or 1,2-bis(diphenylphosphine)ethane monoxide [DPPE(O)] (entries 9 & 10). These last two sets of conditions were of particular interest and were employed to investigate the

reactivity of substrate **248a-c** towards allylic substitution with ethyl 2-methylallyl carbonate. Three different prochiral nucleophiles (derived from different esters of glycine), were used to investigate the role that the substituent could have on the selectivity. All the substrates could be easily prepared in high yield and purity as before.[234] Although allylic alkylation on substrate **248c** with $(PhO)_3P$ has been reported, in our hands this transformation led only to isolation of the starting material (entry 3, Table **7**). Similar results were obtained when methyl- and ethyl-derivatives **248a** and **248b** were employed (entries 1 & 2). Next, the use ligand [DPPE(O)] was considered, and the reaction repeated with the *tert*-buyl derivative **248c** used in the literature with two different PTCs (chloride and iodide version, entries 4-7). The use of PTC (chloride) yielded the desired product in high yield essentially as a racemic mixture (entry 4). The use of PTC (iodide) at room temperature gave rise to the desired product in good yield with some enantioselectivity (5%). Decreasing the temperature (0 °C and -20 °C) improved the selectivity of the transformation at the expense of the chemical yield. Moreover, the product obtained was actually ent-**248c** so the reaction yielded allylated Schiff base with opposite stereochemistry (Table **7**).

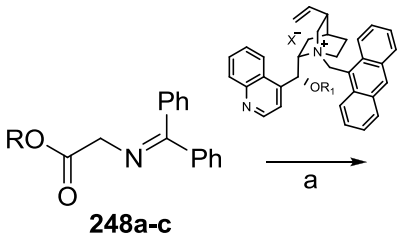


**248a-c** **249a-c**

| | R |
|---|---|
| **a** | Me |
| **b** | Et |
| **c** | *t*-Bu |

| entry | R | X | $R_1$ | T | running time | ligand mol% | yield % | ee % |
|---|---|---|---|---|---|---|---|---|
| 1 | Me | I | Me | 0 °C to RT | ~18 h | $(PhO)_3P$ (16) | - | - |
| 2 | Et | I | Me | 0 °C to RT | ~18 h | $(PhO)_3P$ (16) | - | - |
| 3 | $^t$Bu | I | Me | 0 °C to RT | ~18 h | $(PhO)_3P$ (16) | - | - |
| 4 | $^t$Bu | Cl | H | RT | 7 h | DPPE(0) (10) | 85 | - |
| 5 | $^t$Bu | I | Me | RT | 7 h | DPPE(0) (10) | 84* | 5 |
| 6 | $^t$Bu | I | Me | 0 °C | 7 h | DPPE(0) (10) | 80* | 10 |
| 7 | $^t$Bu | I | Me | -20 °C | ~18 h | DPPE(0) (10) | 75* | 15 |

**Table 7**: Asymmetric alkylation of **248a-c** with ethyl-methylallyl carbonate in the presence of chiral PTCs. (a) toluene, 50% $KOH_{(aq)}$. *The product obtained in the last three entries is ent-**249c**.

The increased steric hindrance of ethyl 2-methylallyl carbonate compared to the allyl acetate used in the literature[247] probably accounts for the differences of stereoselectivity observed in these reactions.

### 6.3.2 Phase-transfer-catalysed asymmetric alkylation

The next investigation centred on the preparation of the alkylated Schiff base **250** by PTC-catalysed asymmetric alkylation using allyl bromide derivative **251** as shown in scheme **66**.

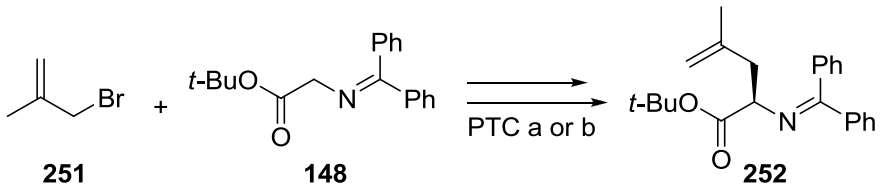


**Scheme 66**: Enantioselective alkylation of glycine Schiff base **148**. (a) Cinchona derivative PTC; (b) Maruoka type.

As presented in chapter 5, a plethora of methods for the alkylation of glycine derived Schiff bases have been devised over the years.[172,173] Both cinchona derivatives and Maruoka type catalysts (Fig. **48**, **146** and **147**) have been successfully employed for this transformation. However, the ease of preparation of cinchona derivatives makes them ideal for preparation on large-scale often needed in total synthesis. The reported example of enantioselective alkylation of glycine Schiff base **148** for the total synthesis of natural product (+)-hygrine in section 5.1.1.2 was particularly appealing due to its close parallel with the intermediate **235** (Scheme **66**).[185] Hence, cinchona PTC **258** was prepared according to published procedures.[184,185] The synthesis of the desired cinchona

PTC started with the Pd-catalysed hydrogenation of (+)-cinchonidine. This transformation readily achieved (+)-hydrocinchonidine,[184] but careful removal of the palladium was required to guarantee the purity of the product.[248] In order to prepare dibromominated naphthalene derivative **256**, a radical bromination was carried out with *N*-bromosuccinimide in the presence of radical initiator AIBN, as reported (Scheme **67**).[184]

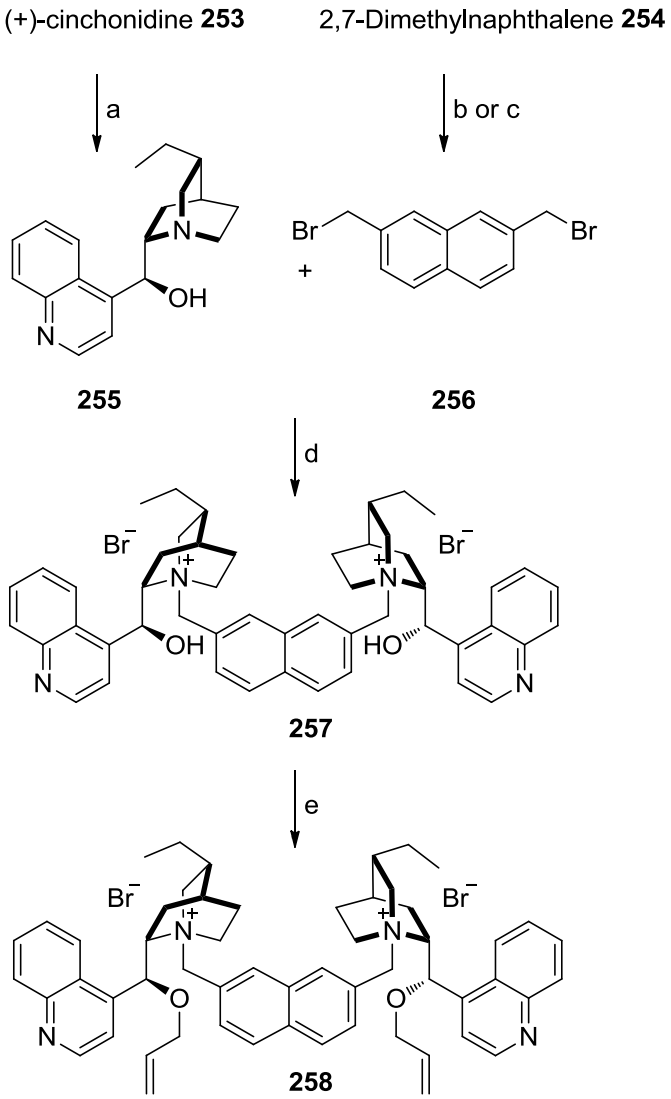


**Scheme 67**: Preparation of cinchona PTC **258**. (a) $H_2$, 10% Pd/C, MeOH, RT, ~18 h, (80%); (b) NBS, AIBN, $CCl_4$, reflux, 10 min (~20%); (c) NBS, benzoyl peroxide, PhH, reflux, 2 h, (77%); (d) EtOH, DMF, $CHCl_3$, reflux, 2 h, (71%); (e) allyl bromide, 50% $KOH_{(aq)}$, DCM, RT, ~ 5 h, (92%).

In our hands, this reaction proved sluggish giving rise to a mixture of mono- and dibrominated naphthalene derivatives. These brominated compounds could be separated by flash chromatography furnishing dibromominated naphthalene derivative **256** in poor yield (~20%). Using NBS in the presence of the radical initiator benzoyl peroxide, dibrominated naphthalene derivative **256** could be prepared in high yield and purity.[248] Dimeric quaternary ammonium salt **257** was obtained by stirring dibromide **255** and quinoline **256** in a mixture of EtOH, DMF and DCM at high temperature (~ 100 °C). Subsequent *O*-allylation of diol **257** was carried out in the presence of allyl bromide and aqueous potassium hydroxide, furnishing **258** in excellent yield (52% over three steps). Enantioselective alkylation of glycine Schiff base **148** (Scheme **68**) with cinchona PTC **258** proceeded smoothly in high yield and selectivity (92%, 91% ee, calculated by chiral HPLC).

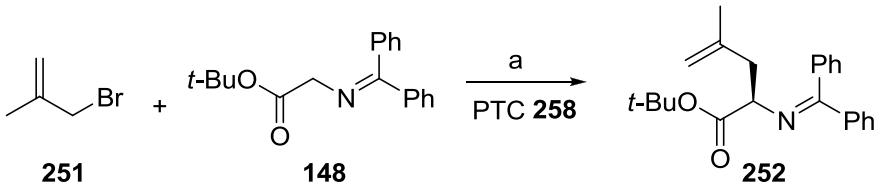


**251** **148** **252**

**Scheme 68**: Enantioselective alkylation of glycine Schiff base **148**. (a) Cinchona derivative PTC, 50% $KOH_{(aq)}$, toluene, $CHCl_3$, 0 °C, ~10 h, (92%, 91% ee).

The reduced degree of selectivity reported compared to the literature[185] (up to 97% ee) can be rationalised by the presence of possible impurities in the catalyst. Further purification of catalyst **258** could have resulted in improved selectivity. Investigation of this enantioselective transformation is ongoing in the Hulme group and will certainly shed light on this issue.

## 6.4 Future work

Following the disappointing results of the investigations of RCM on substrate **235**, new strategies are envisaged for the synthesis of 4-Me-Pro. Primarily, a ring-relay metathesis approach was considered (scheme **69**).[249] This expedient reaction is often used in the presence of comparatively unreactive or hindered alkenes.[250] The rationale behind this strategy is that although initiation of the catalytic cycle of a hindered or unreactive alkene is complicated, the intramolecular reaction of a ruthenium alkylidene onto such an alkene is possible.[250] Such a relay approach is often promoted by the presence of a tether featuring an unencumbered alkene. As the end of the tether gives the least hindered position within the metathesis substrate, this site becomes the most likely point for initiation of the catalytic cycle.

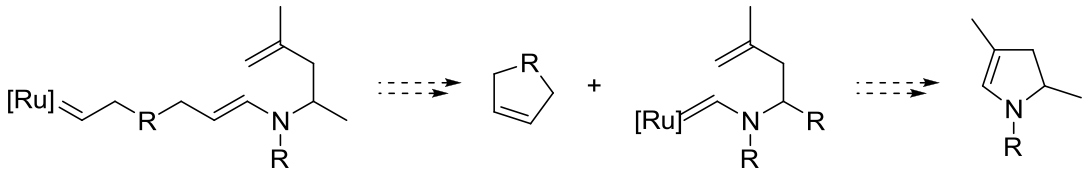


**Scheme 69**: General description of ring-relay metathesis on the proposed substrate.

Both alkyl and ethereal tethers (R = $CH_2$ or O) are commonly employed. Promisingly, the formation of 5-membered rings is reported to be favourable and side products easily separated from the desired olefin. This approach to expedite this transformation is currently under investigation in the Hulme group. Another alternative strategy is a ruthenium catalysed isomerisation followed by RCM as reported by Toumi *et al.* (Scheme **70**).[219] Hydrolysis of the iminogroup and Cbz-protection of the primary amino group in compound **148**, followed by *N*-allylation of the secondary amine, would furnish an ideal substrate for investigation of the feasibility of this transformation on substrate **259**.

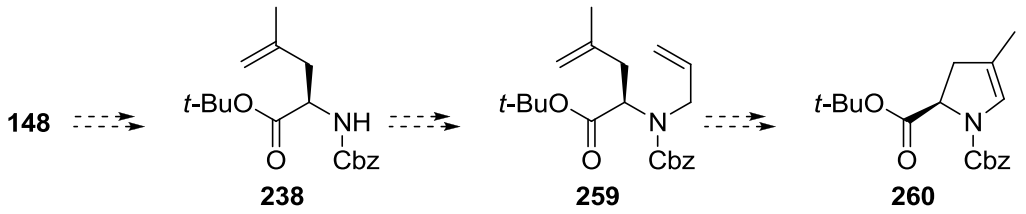


**Scheme 70**: Ruthenium-induced isomerisation/RCM strategy.

As reported in the total synthesis of paliurine E,[219] the isomerisation of the double bond and subsequent RCM would be attempted by treatment with Grubbs II catalyst. A final alternative strategy is based on the Buchwald-Hartwig amination, a Pd or Cu- catalysed cross coupling reaction between primary or secondary amino groups and vinyl or aryl halides, as the key transformation (Scheme **71**).[251]

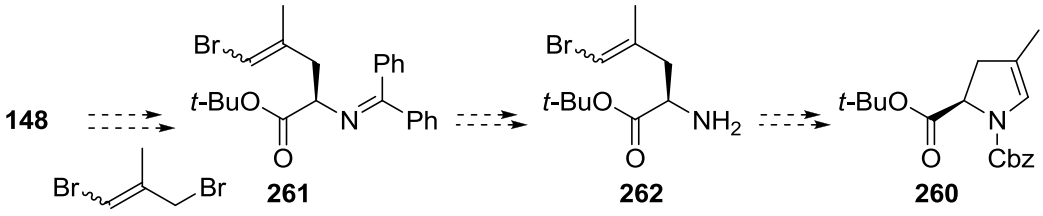


**Scheme 71**: Buchwald-Hartwig cross coupling-based strategy.

Substrate **261** (racemic) would be prepared using a Pd-catalysed alkylation of 1,3-dibromo-1-propene. Next, a PTC-based asymmetric strategy will be attempted to obtain alkylated glycine Schiff base **262** in an enantioselective manner. After hydrolysis of the imino group, the newly revealed primary amino group would undergo an intramolecular Buchwald-Hartwig type coupling with the vinyl bromide within **261**. Successfully carrying out both PTC-catalysed enantioselective alkylation with 1,3-dibromo-1-propene and the Buchwald-Hartwig coupling would expand the substrate scope of these transformations and would make the synthesis of 4-Me-Pro extremely attractive.

## 6.5 Summary and conclusion

To conclude, the synthetic route to functionalised amine **233** (Scheme **72**) has been optimised allowing multigram scale preparation for effective investigation of the alternative routes considered in section 6.4.

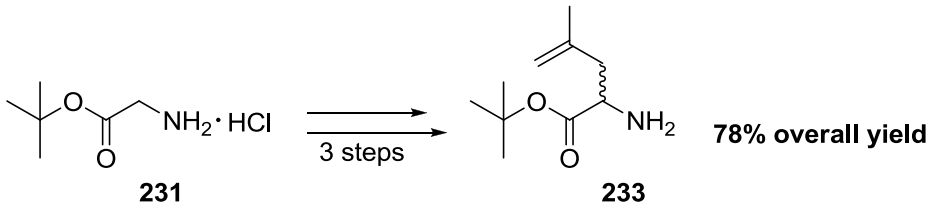


**Scheme 72**: Optimised route to functionalised amine **233**.

For the installation of the stereochemistry at the α-position to the nitrogen in 4-Me-Pro, two different methodologies have been investigated (Scheme **73**): Pd-catalysed allylation in the presence of a cinchona catalyst and PTC-catalysed asymmetric alkylation with cinchona PTC catalyst **258** (Scheme **73**).

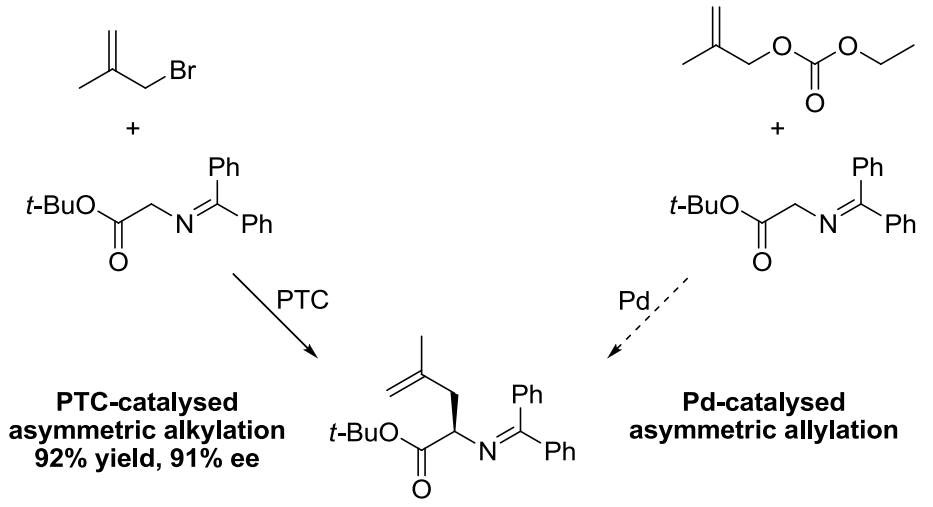


**Scheme 73**: Enantioselective alkylation of glycine Schiff base **148**.

After screening different substrates and reaction conditions for Pd-catalysed allylation, the preparation of alkylated Schiff base in high yield and purity (Scheme **73**) was readily achieved using a PTC-based strategy.

# 7 Experimental procedures

## 7.1 General experimental

All starting materials and reagents were purchased from commercial suppliers and were used as supplied. Anhydrous DCM was distilled from calcium hydride. Unless otherwise indicated, organic extracts were concentrated under reduced pressure using a rotary evaporator.

$^{1}$H nuclear magnetic resonance (NMR) spectra were recorded at room temperature (unless otherwise stated) on Bruker AC250 (250 MHz), Bruker DPX360 (360 MHz) Bruker 400 (400 MHz), Bruker 500 (500 MHz) and Bruker 800 (800 MHz) Fourier Transform instruments. The data is presented as follows; chemical shift (in ppm on the scale relative to $\delta_{tms} = 0$), multiplicity (s = singlet, d = doublet, t = triplet, q = quartet, qn = quintet, m = multiplet), coupling constants and interpretation. $^{13}$C nuclear magnetic resonance (NMR) spectra were recorded at room temperature (unless otherwise stated) on Bruker AC250 (62.9 MHz), Bruker DPX360 (90.6 MHz), Bruker 500 (201.3 MHz). Fourier transform instruments were referenced to the solvent carbon peak. The data is presented as follows: chemical shift (in ppm on the $\delta$ scale), relative intensity and assignment and were confirmed by DEPT90 and DEPT135.

Flash column chromatography was carried out on Merck Kieselger 60 (Merck 9385). Basic silica was used for the purification of acid sensitive compounds. Aminopropyl silica gel (FLUKA 09298) was used for sample loading while the silica gel used for column packing was prepared as follows: 100 g of activated silica were mixed to NaOH (30 ml, 1N aq.) and mechanically stirred until a uniform mixture was obtained. Eluent compositions are quoted as v/v ratios.

Infra-red spectra were recorded on a Perkin Elmer Paragon 100 FT-IR machine using 5 mm sodium chloride plates or potassium bromide discs. The wavelengths of maximum absorbance ($\upsilon_{max}$) are quoted in $cm^{-1}$. Melting points were determined on a Gallenkamp Electrothermal melting point apparatus and are uncorrected.

Electrospray Ionisation (ESI) mass spectra were recorded on a Finnigan 450 or micromass platform instrument at the University of Edinburgh. The parent ion or relevant fragment is quoted, followed by significant figures and their percentages. Chiral HPLC analysis was performed on an Agilent 1100 instrument. Optical rotations were performed on an Optical Activity POLAAR 20 polarimeter. Microwave reactions were performed using a Biotage microwave synthesiser. Thin Layer Chromatography (TLC) was performed on MERCK $60F_{254}$ (0.25 mm) glass silica plates and visualised by ultraviolet (UV) light and potassium permanganate.

## 7.2 Experimental procedures for chapters 2 and 3

**Ethyl 4-(3-chloropropylamino)-4-oxobutanoate 63**

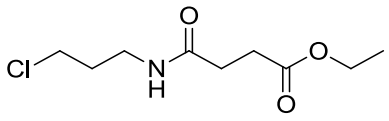

To a stirred solution of 3-chloro-1-propylamine hydrochloride (260 mg, 2.00 mmol) in pyridine (5 ml) was added ethyl 4-chloro-4-oxobutanoate (165 mg, 1.00 mmol) at 0 °C. The reaction was allowed to reach RT and stirred for 2 h. The solvent was removed *in vacuo* to give the crude ester as a pale yellow oil. The crude ester was purified by flash chromatography (25% cyclohexane in EtOAc) to give the desired ester as a colourless oil (290 mg, 71% yield ); $\mathbf{R_f}$ (50% EtOAc in cyclohexane) = 0.61; $\mathbf{\nu_{max}}$ (neat)/$cm^{-1}$ 1729 (CO), 1654 (CO); **$^1$H NMR** $\delta$ (250 MHz, $CDCl_3$) 6.71 (1H, br s, N*H*), 4.28 (2H, q, *J* = 7.1 Hz, C*H*$_2$CH$_3$), 3.73 (2H, t, *J* = 6.5 Hz, C*H*$_2$Cl), 3.53 (2H, q, *J* = 6.5 Hz, C*H*$_2$NH), 2.80 (2H, t, *J* = 7.1 Hz, C*H*$_2$CO), 2.63 (2H, t, *J* = 7.1 Hz, C*H*$_2$CO), 2.13 (2H, qn, *J* = 6.5 Hz, CH$_2$C*H*$_2$CH$_2$), 1.40 (3H, t, *J* = 7.1 Hz, C*H*$_3$); **$^{13}$C NMR** $\delta$ (62.9 MHz, $CDCl_3$) 172.85 (C), 171.72 (C), 60.49 ($CH_2$), 42.26 ($CH_2$), 36.77 ($CH_2$), 31.96 ($CH_2$), 30.70 ($CH_2$), 29.40 ($CH_2$), 14.35 ($CH_3$); ***m/z*** (ESI+) 244 ([$^{35}$ClM+Na]$^+$, 100%), 222 ([M+H]$^+$, 5), 176 (40), 56 (98); **HRMS** (FAB, THIOG) [ClM+Na]$^+$ found 244.0709, $C_9H_{16}O_3{}^{35}ClNa$ requires 244.0711.

**Ethyl 4-(3-azido-1-propylamino)-4-oxobutanoate 34**

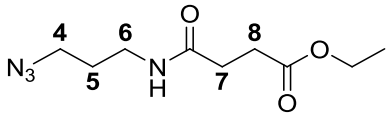

To a stirred solution of the 3-azido-1-propylamine (400 mg, 4.00 mmol) in pyridine (6 ml) was added ethyl 4-chloro-4-oxobutanoate (428 mg, 2.60 mmol) at 0 °C. The

reaction was allowed to reach RT and stirred overnight (~18 h). The solvent was removed *in vacuo* to give the crude ester as a pale yellow oil. Flash chromatography (30% EtOAc in cyclohexane) gave the desired azidoester as a colourless oil (356 mg, 60% yield ); **$R_f$** (50% EtOAc in cyclohexane) = 0.61; **$\nu_{max}$** (neat)/$cm^{-1}$ 2098 ($N_3$), 1733 (CO), 1652 (CO); **$^1$H NMR** δ (250 MHz, $CDCl_3$) 6.56 (1H, br s, NH), 3.98 (2H, q, *J* = 7.2 Hz C*H*$_2$CH$_3$), 3.28-3.17 (4H, m, C*H*$_2$NH+C*H*$_2$N$_3$), 2.51 (2H, t, *J* = 6.3 Hz, C*H*$_2$CO), 2.35 (2H, t, *J* = 6.3 Hz, CH$_2$CO), 1.62 (2H, qn, *J* = 6.7 Hz, CH$_2$C*H*$_2$CH$_2$), 1.12 (3H, t, *J* = 7.2 Hz, C*H*$_3$); **$^{13}$C NMR** δ (62.9 MHz, $CDCl_3$) 172.74 (C), 171.63 (C), 60.63 ($CH_2$), 48.80 ($CH_2$), 36.63 ($CH_2$), 30.51 ($CH_2$), 29.25 ($CH_2$), 28.43 ($CH_2$), 13.80 ($CH_3$); ***m/z*** (FAB, 3-NOBA) 229 ($[M+H]^+$ 100%), 154 (71), 136 (64); **HRMS** (FAB, 3-NOBA) $[M+H]^+$ found 229.1299, $C_9H_{17}O_3N_4$ requires 229.1295.

***N*-[3-(4-Hydroxymethyl-[1,2,3]triazol-1-yl)-propyl]-succinamic acid ethyl ester 66**

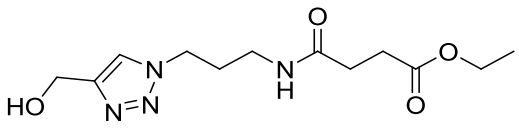


To a solution of ethyl 4-(3-azido-1-propylamino)-4-oxobutanoate (55 mg, 0.20 mmol) in a mixture of $H_2O$/*t*-BuOH (2/1, 3 ml), propargyl alcohol (0.15 µl, 0.20 mmol,), TBTA (~2.0 mg, 2.0 µmol), sodium ascorbate (10.3 mg, 0.05 mmol) and copper sulphate (8.0 mg, 0.020 mmol) were added. The reaction was stirred at RT for 24 h. The organic solvent was removed *in vacuo* while the aqueous layer was extracted with DCM (2 × 5 ml) and EtOAc (2 × 5 ml). The organics were collected and concentrated in *vacuo*. The crude material was purified by flash chromatography (5% MeOH in DCM) to give the desired triazole as a colourless oil (25 mg, 44% yield); **$R_f$** (5% MeOH in DCM) = 0.13; **$\nu_{max}$** (neat)/$cm^{-1}$ 1728 (CO), 1653 (CO); **$^1$H NMR** *δ* (360 MHz, $CDCl_3$) 7.65 (1H, s, Ar*H*), 6.02 (1H, br s, N*H*), 4.79 (2H, s, C*H*$_2$OH), 4.42 (2H, t, *J* = 6.5 Hz, C*H*$_2$NN), 4.13 (2H, q, *J* = 7.1 Hz, C*H*$_2$CH$_3$), 3.27 (2H, q, *J* = 6.5 Hz, C*H*$_2$NH), 2.75 (1H, br s, O*H*), 2.64 (2H, t, *J* = 6.5 Hz, NCOC*H*$_2$) 2.41 (2H, t, *J* = 6.5 Hz, OCOC*H*$_2$), 2.10 (2H, qn, *J* = 6.5 Hz, CH$_2$C*H*$_2$CH$_2$), 1.25 (3H, t, *J* = 7.1 Hz, CH$_2$C*H*$_3$); **$^{13}$C NMR** *δ* (90.6, $CDCl_3$)

173.25 (C), 172.04 (C), 145.30 (C), 105.78 (CH), 60.81 ($CH_2$), 56.43 ($CH_2$), 47.84 ($CH_2$), 36.53 ($CH_2$), 30.80 ($CH_2$), 30.02 ($CH_2$), 29.38 ($CH_2$), 14.14 ($CH_3$); ***m/z*** (ESI+), 307 ($[M+Na]^+$ 100%), 285 ($[M+H]^+$ 7), 105 (52); **HRMS** (ESI+) found $[M+Na]^+$ 307.1379, $C_{12}H_{20}N_4O_4Na$ requires 307.1377.

**(2*R*,3*S*,4*S*)-3-Acetoxy-4-hydroxy-2-(4'-methoxybenzyl)-1-prop-ynyl-pyrrolidine 27**

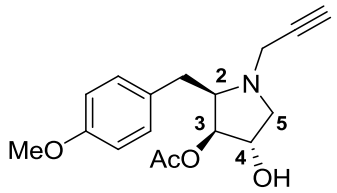


To a stirred solution of anisomycin (50 mg, 0.19 mmol) in DMF (2 ml) potassium carbonate (26 mg, 0.19 mmol) and propargyl bromide (16 µl, 0.19 mmol) were added. The reaction was stirred for 8 h at RT. The solvent was removed *in vacuo* and the crude material purified by flash chromatography (5% MeOH in DCM) to give propargyl anisomycin **27** as a colourless oil (54 mg, 95% yield); $\mathbf{R_f}$ (5% MeOH in DCM = 0.25); $\boldsymbol{\nu_{max}}$ (neat)/$cm^{-1}$ 3374 (OH), 1727 (CO); $^{1}$**H NMR** $\delta$ (250 MHz, $CDCl_3$) 7.09 (2H, d, $J$ = 8.6 Hz, Ar*H*), 6.80 (2H, d, $J$ = 8.6 Hz, Ar*H*), 4.47 (1H, dd, $J$ = 5.7 & 1.6 Hz, $C_3H$), 4.13 (1H, br t, $J$ = 7.0 Hz, $C_4H$), 3.78 (3H, s, OMe), 3.58 (2H, d, $J$ = 2.3 Hz, $HCCCH_2$), 3.34 (1H, dd, $J$ = 9.8 & 7.0 Hz, $C_5H_aH_b$), 3.21 (1H, dt, $J$ = 10.2 & 5.2 Hz, $C_2H$), 2.85 (1H, dd, $J$ = 13.4 & 4.5 Hz, $CH_cH_dAr$), 2.70 (1H, dd, $J$ = 13.4 & 10.2 Hz, $CH_cH_dAr$), 2.61 (1H, dd, $J$ = 9.8 & 7.0 Hz, $C_5H_aH_b$), 2.30 (1H, t, $J$ = 2.3 Hz, $CHCCH_2$), 2.14 (3H, s, OAc); $^{13}$**C NMR** $\delta$ (62.9 MHz, $CDCl_3$) 172.20 (C), 158.53 (C), 130.54 (C), 130.24 (2 × CH), 114.28 (2 × CH), 82.80 (CH), 76.71 (C), 75.60 (CH), 74.24 (CH), 63.47 (CH) 57.86 ($CH_2$), 55.20 ($CH_3$), 39.85 ($CH_2$), 32.00 ($CH_2$), 21.03 ($CH_3$); ***m/z*** (ESI+) 326 ($[M+Na]^+$, 23%), 304 ($[M+H]^+$, 100), 244 (22).

All spectroscopic data were in good agreement with the literature.[76]

***N*-(3-{4-[(2*R*,3*S*,4*S*)-3-Acetoxy-4-hydroxy-2-(4-methoxy-benzyl)-pyrrolidin-1-ylmethyl]-[1,2,3]triazol-1-yl}-propyl)-succinamic acid ethyl ester 67**

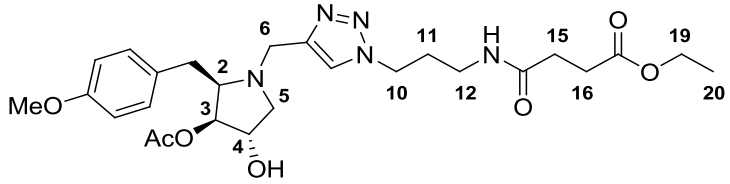


To a stirred solution of propargyl anisomycin **27** (20.0 mg, 0.060 mmol) in $H_2O$/*t*-BuOH (1/1, 2 ml) azidoester **34** (16.4 mg, 0.07 mmol) was added, followed by sodium ascorbate (2.4 mg, 0.010 mmol), TBTA (~1.00 mg, 0.0010 mmol) and copper sulphate (3.5 mg, 0.010 mmol). The mixture was stirred overnight (~18 h) at RT. The organic layer was removed *in vacuo* and the aqueous layer extracted with DCM (3 × 5 ml). The organics were collected and concentrated in *vacuo*. The crude material was purified by flash chromatography (2% MeOH in DCM) to give anisomycin derivative **67** as colourless solid (20 mg, 60% yield); $\mathbf{R_f}$ (2% MeOH in DCM) = 0.25; $\mathbf{\nu_{max}}$ (neat)/$cm^{-1}$ 1727 (CO), 1669 (CO); **$^1$H NMR** $\delta$ (360 MHz, $CDCl_3$) 7.51 (1H, s, Ar*H*), 7.10 (2H, d, *J* = 8.6 Hz, Ar*H*), 6.80 (2H, d, *J* = 8.6 Hz, Ar*H*), 6.04 (1H, br s, N*H*), 4.54 (1H, dd, *J* = 4.7 & 1.2 Hz, $C_3H$), 4.40 (2H, t, *J* = 6.5 Hz, $C_{10}H_2$), 4.13 (2H, q, *J* = 7.1 Hz, $C_{19}H_2$), 4.11-4.07 (1H, m, $C_4H$), 4.06 (1H, d, *J* = 15.0 Hz, $C_6H_aH_b$), 3.96 (1H, d, *J* = 15.0 Hz, $C_6H_aH_b$), 3.77 (3H, s, OMe), 3.45 (1H, dd, *J* = 10.4 & 6.5 Hz, $C_5H_cH_d$), 3.22-3.16 (2H, m, $C_2H$ + $CH_eH_fAr$), 3.15-3.08 (2H, m, $C_{12}H_2$), 2.79 (1H, dd, *J* = 14.5 & 10.8 Hz, $CH_eH_fAr$), 2.66 (2H, t, *J* = 6.5 Hz, $C_{15}H_2$), 2.52 (1H, dd, *J* = 10.4 & 5.5 Hz, $C_5H_cH_d$), 2.44 (2H, t, *J* = 6.5 Hz, $C_{16}H_2$), 2.13 (3H, s, OAc) 2.11 (2H, qn, *J* = 6.5 Hz, $C_{11}H_2$), 1.25 (3H, t, *J* = 7.1 Hz, $C_{20}H_3$); **$^{13}$C NMR** $\delta$ (62.9, $CDCl_3$) 173.06 (C), 172.08 (C), 171.44 (C), 158.02 (C), 142.61 (C), 130.65 (C), 129.91 (2 × CH), 123.38 (CH), 113.80 (2 × CH), 81.80 (CH), 75.07 (CH), 64.52 (CH), 60.78 ($CH_2$), 58.32 ($CH_2$), 55.21 ($CH_3$), 47.40 ($CH_2$), 46.10 ($CH_2$), 36.23 ($CH_2$), 32.43 ($CH_2$), 30.96 ($CH_2$), 30.15 ($CH_2$), 29.44 ($CH_2$), 21.06 ($CH_3$), 14.16 ($CH_3$); ***m/z*** (ESI+) 554 ($[M+Na]^+$, 28%), 532 ($[M+H]^+$, 100), 123 (100); **HRMS** (ESI+) $[M+H]^+$ found, 532.2761, $C_{26}H_{38}N_5O_7$ requires 532.2766.

**Ethyl 3-({3-[4-({5-[(3aS,4*S*,6a*R*)-2-oxo-hexahydro-1H-thieno[3,4-*d*]imidazolidin-4-yl]pentanamido}methyl)-1H-1,2,3-triazol-1-yl]propyl}carbamoyl) propanoate 70**

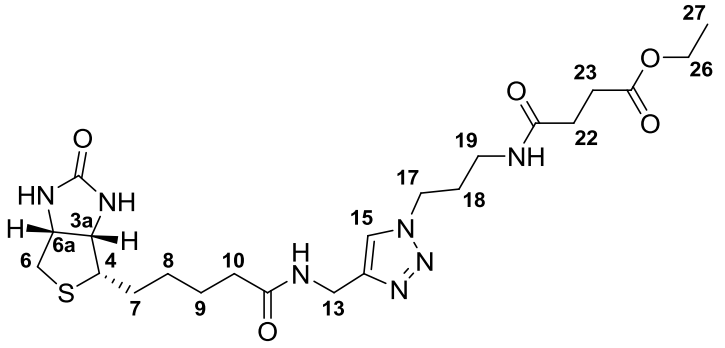


To a solution of ethyl 4-(3-azido-1-propylamino)-4-oxobutanoate (39 mg, 0.17 mmol) in $H_2O$/*t*-BuOH (2/1, 3 ml), propargyl biotin (50 mg, 0.14 mmol), sodium ascorbate (10 mg, 0.050 mmol) and copper sulphate (8.0 mg, 0.020 mmol) were added. The reaction was stirred at RT for 3 h. The organic solvent was removed *in vacuo* and the aqueous layer was extracted with DCM (2 × 5 ml) and with EtOAc (2 × 5 ml). The organics were collected and concentrated in *vacuo*. Flash chromatography (2 to 10% MeOH in DCM) gave the desired triazole as a colourless solid (60 mg, 40% yield); $\mathbf{R_f}$ (10% MeOH in DCM = 0.33); **mp** 174-176 °C $\boldsymbol{\nu_{max}}$ (nujol)/$cm^{-1}$ 2389 (NH), 2251 (NH), 1768 (CO), 1664 (CO); **$^1$H NMR** $\delta$ (800 MHz, $D_2O$) 7.88 (1H, s, $C_{15}H$), 4.57 (1H, dd, $J$ = 7.9 & 4.5 Hz, $C_{6a}H$), 4.43 (2H, m, t, $J$ = 6.7 Hz, $C_{19}H_2$), 4.35 (1H, dd, $J$ = 7.9 & 4.5 Hz, $C_{3a}H$), 4.13 (2H, q, $J$ = 7.1 Hz, $C_{26}H_2$), 3.27-3.25 (1H, m, $C_4H$), 3.16 (2H, t, $J$ = 6.7 Hz, $C_{17}H_2$), 2.96 (1H dd, $J$ = 13.0 & 5.0 Hz, $C_6H_aH_b$), 2.75 (1H d, $J$ = 13.0 Hz, $C_6H_aH_b$), 4.42-4.40 (2H, m, $C_{13}H_2$), 2.62 (2H, t, $J$ = 6.7 Hz, $C_{22}H_2$), 2.48 (2H, t, $J$ = 6.7 Hz, $C_{23}H_2$), 2.28 (2H, t, $J$ = 7.1 Hz, $C_{10}H_2$), 2.08 (2H, qn, $J$ = 6.7 Hz, $C_{18}H_2$), 1.68-1.63 (2H, m, $C_9H_2$), 1.62-1.58 (1H, m, $C_7H_cH_d$) 1.54-1.50 (1H, m, $C_7H_cH_d$) 1.34-1.30 (2H, m, $C_8H_2$) 1.21 (3H, t, $J$ = 7.1 Hz, $C_{27}H_3$); **$^{13}$C NMR** $\delta$ (200 MHz, $D_2O$) 178.12 ($C_{21}$), 176.58 ($C_{11}$), 176.15 ($C_{24}$), 166.70 ($C_1$), 146.27 ($C_{14}$), 125.35 ($C_{15}H$), 63.50 ($C_{26}H_2$), 63.30 ($C_{3a}H$), 61.71 ($C_{6a}H$), 56.88 ($C_4H$), 49.46 ($C_{13}H_2$), 41.23 ($C_6H_2$), 37.80 ($C_{17}H_2$), 36.76 ($C_{10}H_2$), 35.80 ($C_{19}H_2$), 31.77 ($C_{23}H_2$), 31.04 ($C_{22}H_2$), 30.39 ($C_{18}H_2$), 29.25 ($C_8H_2$), 29.12 ($C_7H_2$),

26.56 ($C_9H_2$), 14.88 ($C_{27}H_3$); ***m/z*** (ESI+) 532 ($[M+Na]^+$, 5%), 510 ($[M+H]^+$, 6%), 312 (9); **HRMS** (ESI+) found $[M+H]^+$ 509.2424 $C_{22}H_{35}N_7O_5S$ requires 509.2415.

**2,5-dioxopyrrolidin-1-yl 5-[(3a*S*,4*S*,6a*R*)-2-hexahydro-1H-thieno[3,4-*d*]imidazolidin-4-yl]-pentanoate 263**

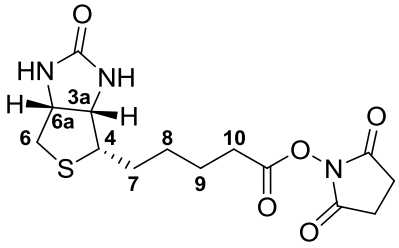


D-Biotin (200 mg, 0.820 mmol) was dissolved in DMF (5ml) and the solution cooled to 0 °C. *N*-hydroxysuccinimide (188 mg, 1.64 mmol), EDC (314 mg, 1.64 mmol) and $Et_3N$ (237 µl, 1.64 mmol) were added and the mixture was stirred overnight (~ 18 h). The solvent was removed *in vacuo* and the resulting residue dissolved in DCM (10 ml). The organic phase was washed with $H_2O$ (2 × 5 ml) and the solvent was removed *in vacuo*. The crude material was purified by flash chromatography (10% MeOH in DCM) to give the NHS ester **263** as a colourless solid (280 mg, 99% yield); $\mathbf{R_f}$ (10% MeOH in DCM) = 0.33; **mp** 170-172 °C; $\mathbf{\nu_{max}}$ (KBr)/$cm^{-1}$ 1820 (CO), 1790 (CO), 1730 (CO), 1703 (CO); **$^1$H NMR** $\delta$ (250 MHz, $(CD_3)_2SO_2$) 6.42 (1H, s, N*H*), 6.36 (1H, s, N*H*), 4.30 (1H, dd, *J* = 7.6 & 4.1 Hz, $C_{3a}H$), 4.14 (1H, ddd, *J* = 7.6 & 4.5 & 1.6 Hz, $C_{6a}H$), 3.14-3.06 (1H, m, $C_4H$), 2.88 (1H, m, $C_6H_a$), 2.80 (4H, s, 2 × $CH_2O$), 2.72 (1H, m, $C_6H_b$), 2.66 (2H, m, $C_{10}H_2$), 1.70-1.56 (6H, m, $C_7H_2$ + $C_8H_2$ + $C_9H_2$); **$^{13}$C NMR** $\delta$ (62.9 MHz, $(CD_3)_2SO_2$), 170.18 (2 × C), 168.85 (C), 162.61 (C), 60.93 (CH), 59.11 (CH), 55.15 (CH), 35.71 ($CH_2$), 29.92 ($CH_2$), 27.76 ($CH_2$), 27.50 ($CH_2$), 25.36 (2 × $CH_2$), 24.22 ($CH_2$); ***m/z*** (ESI+) 342 ($[M+H]^+$, 18%), 227 (18), 146 (44).

All spectroscopic data were in good agreement with the literature.[252]

**5-[(3aS,4*S*,6a*R*)-2-oxo-hexahydro-1H-thieno[3,4-*d*]imidazolidin-4-yl]-N-(prop-2-1-yl)pentanamide 69**

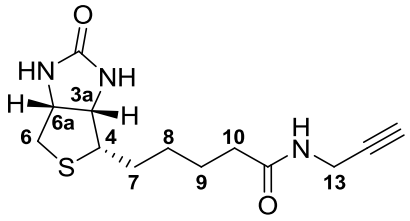


**Method A**

A suspension of biotin NHS ester (280 mg, 0.81 mmol) and propargyl amine (104 µl, 1.62 mmol) in DCM (20 ml) was stirred for 3 h at RT. Completion of the reaction was determined by TLC. The solvent was removed *in vacuo*. The crude product was purified by flash chromatography (10 to 15% MeOH in DCM). Propargyl amide **69** was isolated as a colourless solid (210 mg, 77% yield).

**Method B**

A solution of D-Biotin (200 mg, 0.81 mmol) was dissolved in DMF (20 ml). HOBt (324 mg, 2.4 mmol) and DIC (373 µl, 2.40 mmol) were added and the solution stirred at RT for 10 min. Propargyl amine (167 µl, 2.40 mmol) was added and the reaction mixture was heated to 60 °C by microwave irradiation (20 min). The solvent was removed *in vacuo*. The crude product was purified by flash chromatography (0 to 10% MeOH in DCM). The product was isolated as a colourless solid (200 mg, 88% yield); $\mathbf{R_f}$ (15% MeOH in DCM = 0.45); **mp** 168-170 °C; $\boldsymbol{\nu_{max}}$ (nujol)/cm$^{-1}$ 3288 (NH), 1694 (CO), 1648 (CO); **$^1$H NMR** $\delta$ (250 MHz, $CD_3OD$) 4.49 (1H, ddd, $J$ = 7.8 & 4.9 & 0.8 Hz, $C_{6a}H$), 4.30 (1H, dd, $J$ = 7.8 & 4.3 Hz, $C_{3a}H$), 3.94 (2H, d, $J$ = 2.5 Hz, $C_{13}H_2$), 3.24-3.16 (1H, m, $C_4H$), 2.93 (1H, dd, $J$ = 12.7 & 4.9 Hz, $C_6H_aH_b$), 2.70 (1H, d, $J$ = 12.7 Hz, $C_6H_aH_b$), 2.58 (1H, t, $J$ = 2.5 Hz, C$H$CC), 2.21 (2H, t, $J$ = 7.3 Hz, $C_{10}H_2$), 1.81-1.37 (6H, m, $C_7H_2$ + $C_8H_2$ + $C_9H_2$); **$^{13}$C NMR** $\delta$ (62.9 MHz, $CD_3OD$), 175.66 ($C_{11}$), 166.15 ($C_1$), 80.73 ($C_{15}$), 72.10 ($C_{15}$H), 63.39 ($C_{3a}$H), 61.67 ($C_{6a}$H), 56.99 ($C_4$H), 41.08 ($C_6H_2$), 36.53

($C_{10}H_2$), 29.75 ($C_8H_2$), 29.49 ($C_7H_2$), 29.41 ($C_{13}H_2$), 26.73 ($C_9H_2$); ***m/z*** (ESI+) 585 ($[2M+Na]^+$, 31%) 304 ($[M+Na]^+$, 37), 282 ($[M+H]^+$, 32), 158 (27), 141 (12).

All spectroscopic data were in good agreement with the literature.[253]

**5-[(3aS,4*S*,6a*R*)-2-oxo-hexahydro-1H-thieno[3,4-*d*]imidazolidin-4-yl]-N-(3-azidopropyl)-pentanamide 264**

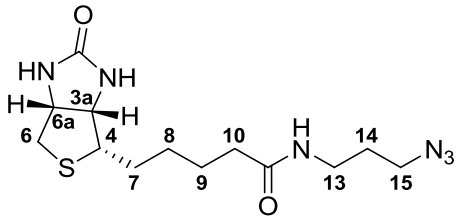


A solution of D-Biotin (100 mg, 0.40 mmol) was dissolved in DMF (10 ml). HOBt (108 mg, 0.80 mmol) and DIC (124 µl, 0.80 mmol) were added and the solution stirred at RT for 10 min. 3-Azido-1-propylamine (120 mg, 1.20 mmol) was added and the reaction mixture was heated to 60° C by microwave irradiation (20 min). The solvent was removed *in vacuo*. Flash chromatography (dry loaded silica column, 0 to 8% MeOH in DCM) gave the product as a colourless solid. (92 mg, 70% yield); $\mathbf{R_f}$ (10% MeOH in DCM = 0.18); **mp** 175-177 °C; $\boldsymbol{\nu_{max}}$ (KBr)/$cm^{-1}$ 2102 ($N_3$), 1696 (CO), 1646 (CO); **$^1$H NMR** $\delta$ (500 MHz, $CD_3OD$) 4.49 (1H, ddd, $J$ = 7.8 & 4.6 Hz, $C_{6a}H$), 4.30 (1H, dd, $J$ = 7.8 & 4.6 Hz, $C_{3a}H$), 3.36 (2H, t, $J$ = 6.7 Hz, $C_{15}H_2$), 3.25 (2H, t, $J$ = 6.7 Hz, $C_{13}H_2$), 3.23-3.19 (1H, m, $C_4H$), 2.93 (1H, dd, $J$ = 12.7 & 5.0 Hz, $C_6H_aH_b$), 2.71 (1H, d, $J$ = 12.7 Hz, $C_6H_aH_b$), 2.21 (2H, t, $J$ = 7.3 Hz, $C_{10}H_2$), 1.75 (2H, qn, $J$ = 6.7 Hz, $C_{14}H_2$), 1.70-1.54 (4H, m, $C_7H_2$ + $C_9H_2$), 1.49-1.38 (2H, m, $C_8H_2$); **$^{13}$C NMR** $\delta$ (126 MHz, $CD_3OD$), 176.31 ($C_{11}$), 166.27 ($C_1$), 63.53 ($C_{3a}H$), 61.77 ($C_{6a}H$), 57.16 ($C_4H$), 50.24 ($C_{15}H_2$), 41.18 ($C_6H_2$), 37.83 ($C_{13}H_2$) 36.92 ($C_{10}H_2$), 29.94 ($C_{14}H_2$), 29.89 ($C_8H_2$), 29.63 ($C_7H_2$), 27.00 ($C_9H_2$); ***m/z*** (ESI+) 675 ($[2M+Na]^+$, 100%) 349 ($[M+Na]^+$, 82), 327 ($[M+H]^+$, 39), 141 (13); **HRMS**, (ESI+) found $[M+H]^+$ 327.1588, $C_{12}H_{23}N_6O_2S$ requires 327.1589.

**(2*R*,3*S*,4*S*)-1-{[1-({5-[(3a*S*,4*S*,6a*R*)-2-oxo-hexahydro-1H-thieno[3,4-*d*]imidazolidin-4-yl]pentanamido}propyl)-1H-1,2,3-triazol-4-yl]methyl}-4-hydroxy-2-[(4-methoxyphenyl)methyl]pyrrolidin-3-yl acetate 28**

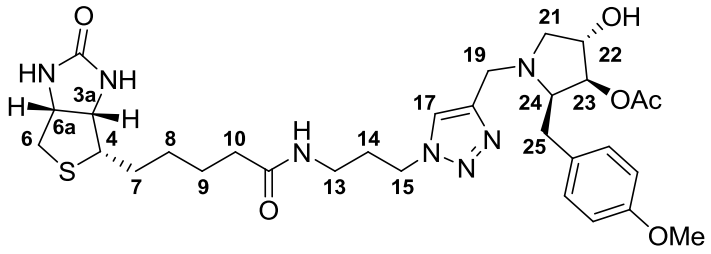


To a solution of biotin azido derivative **264** (78 mg, 0.24 mmol) in $H_2O$/*t*-BuOH (1/2, 3 ml), sodium ascorbate (4.0 mg, 0.020 mmol) and copper sulphate (3.0 mg, 0.010 mmol) were added. The mixture was strirred for 10 min, and then propargyl anisomycin (50 mg, 0.16 mmol) was added. The reaction was stirred at RT overnight (~ 18 h). The organic solvent was removed *in vacuo* and the aqueous layer was extracted with DCM (2 × 5 ml) and EtOAc (2 × 5 ml). The organics were collected and concentrated in *vacuo*. Flash chromatography (2 to 10% MeOH in DCM) gave the desired triazole **28** as a colourless solid (65 mg, 64% yield); $\mathbf{R_f}$ (20% MeOH in DCM = 0.35); **mp** 175-177 °C; $\mathbf{\nu_{max}}$ (KBr)/$cm^{-1}$ 3410 (OH), 1687 (CO), 1646 (CO) **$^1$H NMR** $\delta$ (360 MHz, $CD_3OD$) 7.97 (1H, s, $C_{17}H$), 7.13 (2H, d, $J$ = 8.6 Hz, Ar*H*), 6.84 (2H, d, $J$ = 8.6 Hz, Ar*H*), 4.66 (1H, dd, $J$ = 5.0 & 1.5 Hz, $C_{23}H$), 4.52-4.48 (1H, m, $C_{6a}H$), 4.47 (2H, t, $J$ = 6.7 Hz, $C_{15}H_2$), 4.30 (1H, dd, $J$ = 7.8 & 4.5 Hz, $C_{3a}H$), 4.06 (1H, d, $J$ = 14.2 Hz, $C_{19}H_cH_d$), 4.04-3.99 (1H, m, $C_{22}H$), 3.84 (1H, d, $J$ = 14.2 Hz, $C_{19}H_cH_d$), 3.77 (3H, s, OMe), 3.41-3.35 (1H, m, $C_4H$), 3.23 (2H, t, $J$ = 6.8 Hz, $C_{13}H_2$), 3.21-3.18 (1H, m, $C_{24}H$), 3.16 (1H, dd, $J$ = 9.4 & 4.5 Hz $C_{21}H_eH_f$), 3.05 (1H, dd, $J$ = 13.1 & 5.0 Hz $C_6H_aH_b$), 2.93 (1H, dd, $J$ = 13.1 & 5.0 Hz, $C_6H_aH_b$), 2.74 (1H, dd, $J$ = 13.1 & 5.0 Hz, $C_{25}H_gH_h$ + $C_{25}H_gH_h$), 2.51 (1H, dd, $J$ = 10.7 & 4.2 Hz, $C_{21}H_eH_f$), 2.23 (2H, t, $J$ = 7.3 Hz, $C_{10}H_2$), 2.13 (2H, t, $J$ = 6.7 Hz, $C_{13}H_2$) 2.12 (3H, s, OAc), 1.84-1.55 (4H, m, $C_7H_2$ + $C_9H_2$), 1.49-1.38 (2H, m, $C_8H_2$); **$^{13}$C NMR** $\delta$ (90 MHz, $CD_3OD$), 176.21 ($C_{11}$), 172.02 (C, OAc), 166.05 ($C_1$), 159.67 (C, Ar), 144.16 ($C_{18}$), 131.82 (C, Ar), 130.98 (2 × CH, Ar), 125.54 ($C_{17}H$), 114.92 (2 × CH, Ar), 81.21 ($C_{23}H$), 74.65 ($C_{22}H$), 66.48 ($C_{24}H$), 63.33 ($C_{3a}H$), 61.60

($C_{6a}H$), 60.12 ($C_{21}H_2$), 56.97 ($C_4H$), 55.66 ($CH_3$, OMe), 48.76 ($C_{15}H_2$), 48.30 ($C_{19}H_2$), 41.04 ($C_6H_2$), 37.35 ($C_{13}H_2$), 36.74 ($C_{10}H_2$), 33.58 ($C_{25}H_2$), 31.17 ($C_{14}H_2$), 29.76 ($C_8H_2$), 29.46 ($C_7H_2$), 26.77 ($C_9H_2$), 20.97 ($CH_3$, OAc); ***m/z*** (ESI+) 652 ($[M+Na]^+$, 20%) 630 ($[M+H]^+$, 100), 315 (15); **HRMS**, (ESI+), found $[M+H]^+$ 630.3067, $C_{30}H_{44}O_6N_7S$ requires 630.3068.

**(2-Chloroethyl)-carbamic acid *tert*-butyl ester 43**

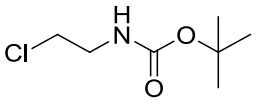

A mixture of triethylamine (3.00 ml, 20.0 mmol), di-*tert*-butylcarbonate (3.94 g, 20.0 mmol), and 2-chloroethylamine hydrochloride (2.32 g, 20.0 mmol) in DCM (30 ml) was stirred for 3 d. Then HCl (20 ml, 0.5 M aq.) was added to the mixture. The organic layer was separated, washed with NaCl (sat. aq.) and worked up to yield the carbonate **43** (1.93 g, 60% yield); $\mathbf{R_f}$ (25% MeOH in DCM) = 0.1; $\mathbf{\nu_{max}}$ (neat)/$cm^{-1}$ 3345 (NH), 1698 (CO); **$^1$H NMR** $\delta$ (250 MHz, $CDCl_3$) 4.95 (1H, br s, N*H*), 3.59 (2H, t, $J$ = 5.4 Hz, C$H_2$Cl), 3.50-3.41 (2H, m, C$H_2$NH), 1.44 (9H, s, 3 × $CH_3$); **$^{13}$C NMR** $\delta$ (62.9 MHz, $CDCl_3$) 155.60 (C), 79.80 (C), 44.30 ($CH_2$), 42.42 ($CH_2$), 28.33 (3 × $CH_3$); ***m/z*** 204 ($[^{37}ClM+Na]^+$, 8), 202 ($[^{35}ClM+Na]^+$, 16), 126 (11), 124 (32), 102 (100).

All spectroscopic data were in good agreement with the literature.[87]

**4-[4-(2-*tert*-Butoxycarbonylamino-ethoxy)-phenylazo]-benzoic acid 44**

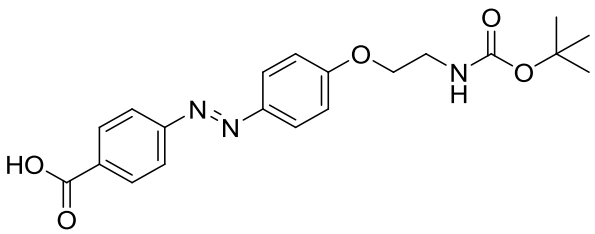

To a stirred solution of 4-(4-hydroxy-phenylazo)-benzoic acid (67.0 mg, 0.300 mmol) in DMF (2 ml) caesium carbonate (228 mg, 0.700 mmol) was added. After 15 min the chlorocarbonate **43** (50.0 mg, 0.300 mmol) was added and the mixture stirred at 80 °C overnight (~18 h). The solvent was removed *in vacuo* and the product purified by flash chromatography (33% EtOAc in cyclohexane). The ether **44** was isolated as an orange solid (25.0 mg, 23 yield%); $\mathbf{R_f}$ (33% EtOAc in cyclohexane) = 0.31; **mp** 133-135 °C; $\boldsymbol{\nu_{max}}$ (neat)/cm$^{-1}$ 1716 (CO), 1698 (CO); **$^1$H NMR** $\delta$ (360 MHz, $CD_3OD$) 8.20 (2H, d, $J$ = 8.9 Hz, Ar*H*), 7.93-7.85 (4H, m, Ar*H*), 6.93 (2H, d, $J$ = 8.9 Hz, Ar*H*), 4.36 (2H, t, $J$ = 5.3 Hz, C$H_2$), 3.41 (2H, t, $J$ = 5.3 Hz, C$H_2$), 1.43 (9H, s, 3 × C$H_3$); ***m/z*** (ESI-) 384 ([M-H]$^-$, 3), 113 (21), 59 (100); **HRMS** (ESI-) $[M+NH_4]^+$ found 403.1979, $C_{20}H_{27}O_5N_4$ requires 403.1976.

**4-(4-Hydroxy-phenylazo)-benzoic acid methyl ester 49**

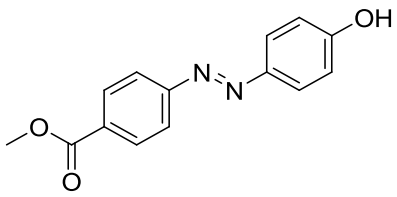


To a solution of MeOH (3 ml) cooled to 0 °C acetyl chloride (42 µl, 0.60 mmol) was added and the mixture was stirred for 30 min 4-(4-hydroxy-phenylazo)-benzoic acid (50 mg, 0.20 mmol) was added portionwise and the mixture heated to reflux for 3 h. The solvent was removed *in vacuo* and the crude material purified by flash chromatography (25% EtOAc in cyclohexane) to achieve the methyl ester **49** (40 mg, 78%); $\mathbf{R_f}$ (33% EtOAc in cyclohexane) = 0.31; **mp**; 214 °C; $\boldsymbol{\nu_{max}}$ (neat)/cm$^{-1}$ 1693 (CO), 1424 (NN); **$^1$H NMR** $\delta$ (250 MHz, $(CD_3)_2CO$) 8.15 (2H, d, $J$ = 9.0 Hz, Ar*H*), 7.89 (2H, d, $J$ = 9.0 Hz, Ar*H*), 7.86 (2H, d, $J$ = 9.0 Hz, Ar*H*), 6.93 (2H, d, $J$ = 9.0 Hz, Ar*H*), 3.94 (1H, s, C$H_3$); **$^{13}$C NMR** $\delta$ (62.9 MHz, $CD_3OD$) 195.75 (C), 163.13 (C) 156.94 (C), 147.54 (C), 132.25 (C), 131.58 (2 × CH), 126.49 (2 × CH), 123.27 (2 × CH), 116.91 (2 × CH), 52.78 ($CH_3$);

***m/z*** (ESI+) 535 ([2M+Na]$^+$, 5%), 257 ([M+H]$^+$, 28), 157 (100); **HRMS** (ESI+) [M+H]$^+$ found 257.0928, $C_{14}H_{13}N_2O_3$ requires 257.0921.

***N*-(2-Amino-ethyl) 4-{-2-[4-(3-azido-propoxy)-phenyl]-vinyl}-benzamide 265**

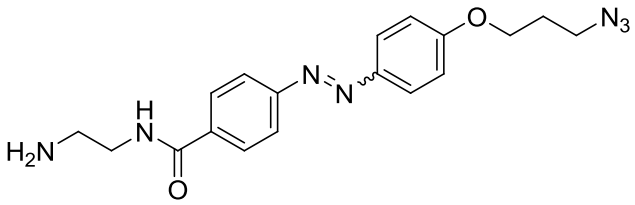

Boc-protected aminoazide **59** (600 mg, 1.28 mmol) was dissolved in a mixture of TFA/DCM (10/1, 11 ml) and the solution was stirred for 1 h. The solvent was removed *in vacuo*. Flash chromatography (5 to 20% MeOH in DCM) gave the desired aminoazide **59** as an orange oil (450 mg, 95%), (85:15, *E*:*Z*); $\mathbf{R_f}$ (10% MeOH in DCM) = 0.51; $\mathbf{\nu_{max}}$ (neat)/cm$^{-1}$ 2071 ($N_3$), 1675 (CO); **$^1$H NMR** $\delta$ (400 MHz, $CD_3OD$); 8.04 (1.70H (*E*), d, *J* = 8.7 Hz, Ar*H*), 7.96 (1.70H (*E*), d, *J* = 8.7 Hz, Ar*H*), 7.95 (1.70H (*E*), d, *J* = 8.7 Hz, Ar*H*), 7.85 (0.30H (*Z*), d, *J* = 8.7 Hz, Ar*H*), 7.12 (1.70H (*E*), d, *J* = 8.8 Hz, Ar*H*), 6.99-6.91 (0.60 H(*Z*), m, Ar*H*), 6.84 (0.30H (*Z*), d, *J* = 9.0 Hz, Ar*H*), 4.20 (1.70H (*E*), t, *J* = 6.0 Hz, C$H_2$), 4.00 (0.30 H (*Z*), t, *J* = 6.0 Hz, C$H_2$), 3.66 (1.70H (*E*), t, *J* = 6.0 Hz, C$H_2$), 3.64-3.59 (0.30 H (*Z*), m, C$H_2$), 3.56 (1.70H (*E*), t, *J* = 6.0 Hz, C$H_2$), 3.49 (0.30H (*Z*), t, *J* = 6.0 Hz, C$H_2$), 3.13 (1.70H (*E*), t, *J* = 6.0 Hz, C$H_2$), 3.08 (0.30H (*Z*), t, *J* = 6.0 Hz, C$H_2$), 2.10 (1.70 H (*E*), qn, *J* = 6.3 Hz, C$H_2$), 2.01 (0.30 H (*Z*), qn, *J* = 6.3 Hz, C$H_2$); **$^{13}$C NMR** $\delta$ (101 MHz, $CD_3OD$), 170.27 (C) (*E*), 169.93 (C) (*Z*), 163.52 (C) (*E*), 160.46 (C) (*Z*), 158.26 (C) (*Z*), 156.03 (C) (*E*), 148.38 (C) (*E*), 147.52 (C) (*Z*), 136.41 (C) (*E*), 133.42 (C) (*Z*), 129.63 (2 × CH) (*Z*), 129.54 (2 × CH) (*E*), 126.16 (2 × CH) (*E*), 125.05 (2 × CH) (*Z*), 123.45 (2 × CH) (*E*), 120.70 (2 × CH) (*Z*), 116.03 (2 × CH) (*E*), 115.46 (2 × CH) (*Z*), 66.42 ($CH_2$) (*E*), 66.23 ($CH_2$) (*Z*), *49.43 ($CH_2$) (*E*), 49.30 ($CH_2$) (*Z*), 41.31 ($CH_2$) (*E*), 41.27 ($CH_2$) (*Z*), 40.19 ($CH_2$) (*E*), 40.13 ($CH_2$) (*Z*), 29.76 ($CH_2$) (*E*), 29.67 ($CH_2$) (*Z*); ***m/z*** (ESI+) 390 ([M+Na]$^+$, 8%), 368 ([M+H]$^+$, 20), 56

(100); **HRMS** (FAB, 3-NOBA) $[M+H]^+$ found 368.1838, $C_{12}H_{22}N_7O_2$, requires 368.1835.

*This $CH_2$ (E & Z) is hidden under the MeOH residual peak.

**4-(4'-Hydroxy-phenylazo)-benzoic acid 40**

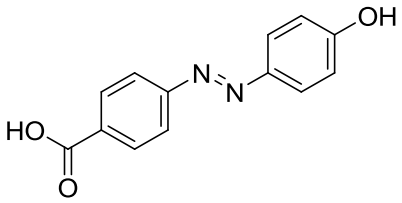


4-aminobenzoic acid (1.23 g, 9.00 mmol), was dissolved in a mixture of hydrochloric acid (1.2 ml, conc.) and $H_2O$ (24 ml) and the suspension obtained was cooled to 0 °C. Sodium nitrite (1.04 g, 15.0 mmol) dissolved in $H_2O$ (5 ml) was added next and the pale yellow solution formed was stirred for 20 min. A second solution of phenol (667 mg, 7.20 mmol), sodium hydroxide (257 mg, 6.42 mmol) and potassium carbonate (1.33 g, 9.60 mmol) dissolved in $H_2O$ (20 ml) was prepared, cooled to 0 °C and added dropwise to the reaction mixture. The reaction was allowed to reach RT and stirred for 3 h. The brown suspension formed was acified with HCl (1 M aq.) and filtered. The filtrate was dissolved in MeOH, silica was added and the mixture dried *in vacuo*. Flash chromatography (dry loaded silica column, 15% MeOH in DCM) gave product **40** as an orange solid (1.57 g, 90% yield); $\mathbf{R_f}$ (5% MeOH in DCM = 0.25); **mp** 275-277 °C; $\boldsymbol{\nu_{max}}$ (neat)/$cm^{-1}$ 3286 (OH), 1642 (CO), 1538 (NN); $^{\mathbf{1}}$**H NMR** $\delta$ (250 MHz, $CD_3OD$) 8.19 (2H, d, $J$ = 8.5 Hz, Ar*H*), 7.92 (2H, d, $J$ = 8.5 Hz, Ar*H*), 7.90 (2H, d, $J$ = 8.8 Hz, Ar*H*), 7.17 (2H, d, $J$ = 8.8 Hz, Ar*H*); $^{\mathbf{13}}$**C NMR** $\delta$ (62.9 MHz, $CD_3OD$) 163.23 (C), 162.88 (C), 156.84 (C), 147.58 (C), 133.00 (C), 131.81 (2 × CH), 126.46 (2 × CH), 123.21 (2 × CH), 116.87 (2 × CH); ***m/z*** (ESI–) 241 ($[M-H]^-$, 48%), 226 (12), 112 (100).

All spectroscopic data were in good agreement with the literature.[254,86]

**(2-Aminoethyl)-carbamic acid *tert*-butyl ester 50**

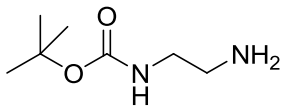

To a stirred solution of ethane-1,2-diamine (9.97 g, 167 mmol) in DCM (100 ml) at RT was added a solution of di-*tert*-butylcarbonate (6.10 g, 28.0 mmol) in DCM (400 ml) over 5 h. The resulting solution was stirred for 24 h at RT and then concentrated *in vacuo* to obtain a colourless oil which was partitioned between $Na_2CO_3$ (20 ml, 2 M aq.) and DCM (20 ml). The aqueous layer was extracted with DCM (2 × 20 ml) and concentrated under reduced pressure to give the Boc-protected amine **50** as a colourless oil (4.45 g, 99% yield); $\mathbf{R_f}$ (10% MeOH in DCM) = 0.1; $\mathbf{\nu_{max}}$ (neat)/$cm^{-1}$ 3446 (NH), 1710 (CO); **$^1$H NMR** $\delta$ (360 MHz, $CD_3OD$) 3.13 (2H, t, $J$ = 6.2 Hz, C$H_2$NHCO), 2.73 (2H, t, $J$ = 6.2 Hz, C$H_2NH_2$), 1.44 (9H, s, 3 × C$H_3$); **$^{13}$C NMR** $\delta$ (90.6 MHz, $CD_3OD$), 158.68 (C), 80.18 (C), 43.26 ($CH_2$), 42.20 ($CH_2$), 28.79 (3 × $CH_3$); ***m/z*** (ESI+) 183 ($[M+Na]^+$, 8%), 161 ($[M+H]^+$, 58).

All spectroscopic data were in good agreement with the literature.[255]

**2-[4'-(4''-Hydroxy-phenylazo)-benzoylamino]-ethyl-carbamic acid *tert*-butyl ester 52**

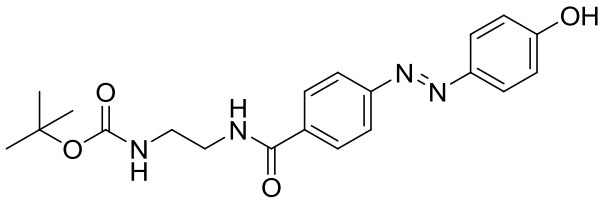

To a solution of benzoic acid **2** (100 mg, 0.413 mmol), in DMF (3 ml), EDC (94.0 mg, 0.500 mmol) and HOBt (27.0 mg, 0.200 mmol) were added. After stirring for 15 min *N*-Boc-ethylenediamine **50** (131 mg, 0.800 mmol) was added and the reaction stirred for 48 h at RT. The solvent was removed *in vacuo*, the crude material was dissolved in DCM (2 ml) and the solution washed with HCl (5 ml, 1 M aq.). The solvent was removed *in vacuo*. The crude product was dissolved in MeOH (2 ml), silica was added and the mixture dried *in vacuo*. Flash chromatography (dry loaded silica column, 2% MeOH in DCM) yielded the desired amide as an orange solid (94 mg, 60% yield); $\mathbf{R_f}$ (5% MeOH in DCM) = 0.31; **mp** 169-171 °C; $\mathbf{\nu_{max}}$ (neat)/cm$^{-1}$ 3361 (NH), 1689 (CO), 1637 (CO), 1535 (NN); **$^1$H NMR** $\delta$ (250 Mz, $(CD_3)_2CO$) 8.06 (2H, d, *J* = 8.6 Hz, Ar*H*), 7.90 (2H, d, *J* = 8.6 Hz, Ar*H*), 7.89 (2H, d, *J* = 8.8 Hz, Ar*H*), 7.04 (2H, d, *J* = 8.8 Ar*H*), 6.47 (1H, br s N*H*), 3.73-3.66 (2H, m, C$H_2$), 3.55-3.48 (2H, m, C$H_2$), 1.58 (9H, s, C$H_3$); **$^{13}$C NMR** $\delta$ (62.9 MHz, $(CD_3)_2CO$) 167.11 (C), 162.20 (C), 161.66 (C), 155.17 (C), 147.27 (C), 137.13 (C), 129.18 (2 × CH), 126.15 (2 × CH), 123.03 (2 × CH), 116.91 (2 × CH), 79.02 (C), 41.63 ($CH_2$), 41.06 ($CH_2$), 28.71 (3 × $CH_3$); ***m/z*** (ESI-) 383 ([M-H]$^-$, 18%), 134 (100), 113 (72); **HRMS** (ESI+) $[M+NH_4]^+$ found 402.2132, $C_{20}H_{28}O_4N_5$ requires 402.2136.

**2-{4'''-[4''-(3'-Bromo-propoxy)-phenylazo]-benzoylamino}-ethyl-carbamic acid *tert*-butyl ester 58**

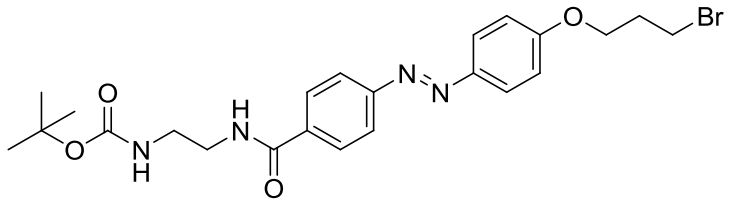


To a stirred solution of phenol **52** (800 mg, 2.08 mmol) in MeCN (30 ml) was added potassium carbonate (430 mg, 16.6 mmol) and the mixture was heated to 70 °C. 1,3-Dibromopropane (1.70 ml, 16.6 mmol) was added and the reaction heated to reflux for 5 h. The solvent was removed *in vacuo* to give the crude bromide. Purification by flash chromatography (5% MeOH in DCM) yielded the desired bromide **58** (710 mg, 67%

yield) as a yellow solid; **$R_f$** (5% MeOH in DCM) = 0.58; **mp** 188-190 °C; **$\nu_{max}$** (neat)/$cm^{-1}$ 1700 (CO), 1659 (CO); **$^1$H NMR** $\delta$ (250 MHz, $CDCl_3$) 7.98-7.88 (6H, m, Ar*H*), 7.44 (1H, br s, N*H*), 7.26-7.21 (2H, m, Ar*H*), 5.12 (1H, br s, N*H*), 4.20 (2H, t, *J* = 6.0 Hz, C$H_2$), 3.64 (2H, t, *J* = 6.4 Hz, C$H_2$), 3.60-3.55 (2H, m, C$H_2$), 3.48-3.40 (2H, m, C$H_2$), 2.37 (2H, qn, *J* = 6.0 Hz, C$H_2$), 1.44 (9H, s, C$H_3$); **$^{13}$C NMR** $\delta$ (62.9 MHz, $CDCl_3$) 175.55 (C), 175.27 (C), 167.57 (C), 162.00 (C), 154.70 (C), 135.24 (C), 128.40 (2 × CH), 125.50 (2 × CH), 122.96 (2 × CH), 115.21 (2 × CH), 80.49 (C), 66.06 ($CH_2$), 42.76 ($CH_2$), 40.28 ($CH_2$), 32.60 ($CH_2$), 30.14 ($CH_2$), 28.75 (3 × $CH_3$); ***m/z*** (ESI+) 529 ([$^{81}$BrM+Na]$^+$, 38%), 527 ([$^{79}$BrM+Na]$^+$, 36), 507 ([$^{81}$BrM+H]$^+$, 2), 505 ([$^{79}$BrM+H]$^+$, 2); **HRMS** (FAB, 3-NOBA) [M+H]$^+$ found 505.1461, $C_{23}H_{30}N_4O_4{}^{79}Br$ requires 505.1450.

**2-{4'''-[4''-(3'-Azido-propoxy)-phenylazo]-benzoylamino}-ethyl-carbamic acid *tert*-butyl ester 59**

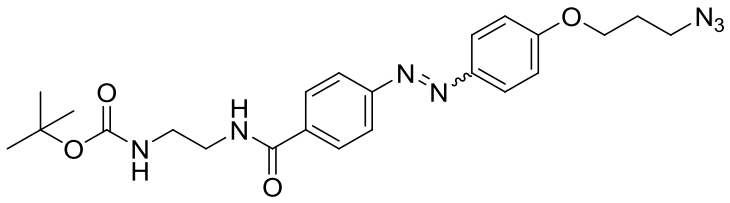

The Boc-protected bromide **58** (710 mg, 1.40 mmol) was dissolved in DMF (15 ml) and sodium azide (273 mg, 4.20 mmol) was added. The solution was stirred overnight (~18 h) at RT. The solvent was removed *in vacuo* and the crude material dissolved in diethyl ether (20 ml), washed with brine (20 ml) and $H_2O$ (20 ml) to give the azide **59** (588 mg, 90% yield) as a pale yellow solid (90:10, *E*:*Z*); **$R_f$** (5% MeOH in DCM) = 0.58; **mp** 173-174 °C; **$\nu_{max}$** (neat)/$cm^{-1}$ 3366 (NH), 3317 (NH), 2100 ($N_3$), 1680 (CO), 1636 (CO); **$^1$H NMR** $\delta$ (250 MHz, $CDCl_3$), 7.96-7.86 (5.40 H (*E*), m, Ar*H*), 7.74 (0.20 H (*Z*), d, *J* = 8.5 Hz Ar*H*), 7.35 (0.90 H (*E*), br s, N*H*), 7.07-6.93 (1.80 H (*E*), m, Ar*H*), 6.87 (0.40 H (*Z*), m, ArH), 6.71 (0.20 H (*Z*), d, *J* = 8.8 Hz, ArH), 5.00 (0.90 H (*E*), br s, N*H*), 4.13 (1.80 H (*E*), t, *J* = 6.0 Hz, C$H_2$), 3.98 (0.20 H (*Z*), t, *J* = 6.0 Hz, C$H_2$), 3.66-3.34 (6H, m, 2 ×

C*H*$_2$NH+C*H*$_2$N$_3$), 2.14-1.94 (2H , m, CH$_2$C*H*$_2$CH$_2$), 1.42 (8.10 H (*E*), s, 3 × CH$_3$) 1.39 (0.90 H (*Z*), s, 3 × CH$_3$); **$^{13}$C NMR** $\delta$ (62.9 MHz, CDCl$_3$) 167.35 (C), 161.79 (C), 157.95 (C), 154.62 (C), 147.34 (C), 135.53 (C), 128.21 (2 × CH), 125.32 (2 × CH), 122.80 (2 × CH), 115.00 (2 × CH), 80.40 (C), 65.09 (CH$_2$), 48.36 (CH$_2$), 42.68 (CH$_2$), 40.09 (CH$_2$), 28.94 (CH$_2$), 28.56 (3 × CH$_3$); ***m/z*** (ESI+) 957 ([2M+Na]$^+$, 27%), 490 ([M+Na]$^+$, 100), 390 (52), 71 (43); **HRMS** (FAB, 3-NOBA) found [M+H]$^+$ 468.2351, $C_{23}H_{30}N_7O_4$ requires 468.2359.

### *N*-(2-Amino-ethyl)-4-{-2-[4-(3-azido-propoxy)-phenyl]-vinyl}-benzamide hydrochloride 60

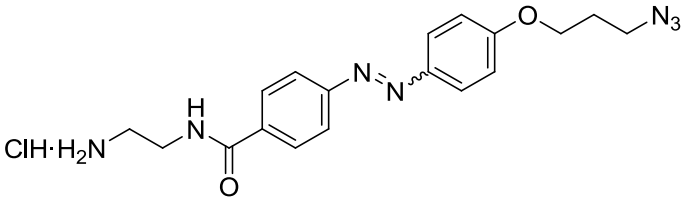


Acetyl chloride (10 ml) was added to dry MeOH (60 ml) at 0 °C and the solution was stirred for 30 min. Boc-protected aminoazide **59** (850 mg, 1.82 mmol) was dissolved in this solution and stirred for 1 h. Completion of the reaction was monitored by TLC. Diethyl ether (20 ml) was added and the amine hydrochloride salt precipitated as a yellow solid. The salt **60** was filtered and used without further purification (720 mg, 95% yield), (80:20, *E*:*Z*); **R$_f$** (20% MeOH in DCM = 0.42); **mp** 250 °C (decomposition); **$\nu_{max}$** (nujol)/cm$^{-1}$ 3413 (NH), 3273 (NH), 2100 (N$_3$), 1639 (CO); **$^1$H NMR** $\delta$ (800 MHz, (CD$_3$)$_2$CO) 8.77 (0.80 H (*E*), br s, N*H*), 8.61 (0.20 H (*Z*), br s, N*H*), 8.06 (1.60 H (*E*), d, *J* = 8.5 Hz, Ar*H*), 7.95-7.93 (3.20 H (*E*), Ar*H*), 7.82 (0.40 H (*Z*), d, *J* = 8.5 Hz, Ar*H*), 7.17 (1.60 H (*E*), d, *J* = 8.8 Hz, Ar*H*), 6.94 (0.40 H (*Z*), d, *J* = 8.5 Hz, Ar*H*), 6.91-6.87 (0.80 H (*Z*), Ar*H*), 4.18 (1.60 H (*E*), t, *J* = 6.1 Hz, C*H*$_2$), 4.00 (0.40 H (*Z*), t, *J* = 6.1 Hz, C*H*$_2$), 3.56-3.52 (3.20 H (*E*), m, 2 × C*H*$_2$), 3.48-3.46 (0.80 H (*Z*), m, 2 × C*H*$_2$ ), 3.03 (1.60 H (*E*) br s, N*H*$_2$), 2.98 (0.40 H (*Z*) br s, N*H*$_2$), 2.03 (1.60 H (*E*), qn, *J* = 6.4 Hz, C*H*$_2$), 1.94 (0.40 H (*Z*), qn, *J* = 6.4 Hz, C*H*$_2$); **$^{13}$C NMR** $\delta$ (200 MHz, (CD$_3$)$_2$CO),

166.21 (C) (*E*), 166.04 (C) (*Z*), 161.60 (C) (*E*), 156.46 (C) (*Z*), 153.55 (C) (*E*), 146.25 (C) (*E*), 146.19 (C) (*Z*), 135.51 (C) (*E*), 131.88 (C) (*Z*), 128.69 (2 × CH) (*E*), 128.40 (2 × CH) (*Z*), 124.87 (2 × CH) (*E*), 123.21 (2 × CH) (*Z*), 121.98 (2 × CH) (*E*), 118.95 (2 × CH) (*Z*), 115.19 (2 × CH) (*E*), 114.36 (2 × CH) (*Z*), 65.27 ($CH_2$) (*E*), 64.91 ($CH_2$) (*Z*), 47.63 ($CH_2$) (*E*), 47.56 ($CH_2$) (*Z*), 38.65 ($CH_2$) (*E*), 37.20 ($CH_2$) (*E*), 37.10 ($CH_2$) (*Z*), 28.01 ($CH_2$) (*E*), 27.96 ($CH_2$) (*Z*); ***m/z*** (ESI+) 368 ($[M+H]^+$, 60%) **HRMS**, (FAB, 3-NOBA), found [M+H+], 368.1844, $C_{18}H_{22}N_7O_2$ requires 368.1835.

**3-Azido-1-propylamine 64**

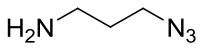


To a stirred solution of 3-chloropropylamine hydrochloride (560 mg, 4.31 mmol), dissolved in $H_2O$ (5 ml) sodium azide was added (840 mg, 12.0 mmol), and the mixture heated to 80 ºC. After 15 h, KOH in pellets was added to basify the solution, followed by extraction with diethyl ether (3 × 5 ml). The combined organic phases were dried over magnesium sulphate and concentrated to give the desired amine as a colourless volatile oil (413 mg, 99% yield); $\mathbf{\nu_{max}}$ (neat)/$cm^{-1}$ 2104 ($N_3$) **$^1$H NMR** $\delta$ (250 MHz, $CDCl_3$) 3.35 (2H, t, *J* = 6.8 Hz, C*H*$_2$NH), 2.90 (2H, t, *J* = 6.8 Hz C*H*$_2$N$_3$) 1.83 (2H, qn, *J* = 6.8 Hz $CH_2CH_2CH_2$) 1.35 (2H, br s, $NH_2$); **$^{13}$C NMR** $\delta$ (62.9 MHz, $CDCl_3$) 49.12 ($CH_2$), 39.30 ($CH_2$), 32.43 ($CH_2$); ***m/z*** (ESI+) 101 ($[M+H]^+$, 68%), 76 (32), 58 (100).

All spectroscopic data were in good agreement with the literature.[92]

**Safety in the Handling of Sodium Azide and other Azides:**[256] Sodium azide is toxic and can be absorbed through the skin. It decomposes explosively upon heating to above 275 °C. Sodium azide reacts vigorously with $CS_2$, bromine, nitric acid, dimethyl sulfate, and a series of heavy metals, including copper and lead. In reaction with $H_2O$ or Brønsted acids the highly toxic and explosive hydrogen azide is released. It has been

reported that sodium azide and polymer-bound azide reagents form explosive di- and triazidomethane with DCM and $CHCl_3$, respectively. Heavy-metal azides that are highly explosive under pressure or shock are formed when solutions of $NaN_3$ or $HN_3$ vapors come into contact with heavy metals or their salts. Heavy-metal azides can accumulate under certain circumstances, for example, in metal pipelines and on the metal components of diverse equipment (rotary evaporators, freeze drying equipment, cooling traps, $H_2O$ baths, waste pipes), and thus lead to violent explosions. Some organic and other covalent azides are classified as toxic and highly explosive, and appropriate safety measures must be taken at all times.

**Affi-Gel supported azide 71**

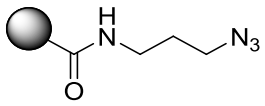

3-Azido-1-propylamine (562 mg, 5.62 mmol), was added to a solution of Affi-Gel 10 in isopropanol (25.0 ml, 0.375 mmol). The suspension was shaken gently for 48 h. The matrix was filtered, washed with MeOH (3 × 5 ml), $H_2O$ (3 × 5 ml), and stored in isopropanol (12.0 ml); $\boldsymbol{\nu_{max}}$ (KBr)/$cm^{-1}$ 2103 ($N_3$), 1656 (CO).

**Affi-Gel supported azide 73**

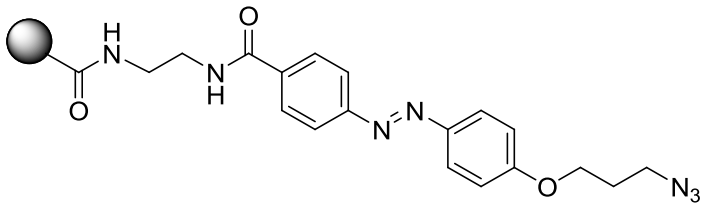

The hydrochloride salt of diazobenzene linker **60** (226 mg, 0.560 mmol) was dissolved in $H_2O$/MeCN (1/1, 4 ml) and $Et_3N$ (81.0 µl, 0.560 mmol) was added. The mixture was added to a solution of Affi-Gel 10 in isopropanol (12.5 ml, 0.187 mmol) and the

suspension was shaken gently for 24 h. The matrix was filtered, washed with MeOH (3 × 5 ml), $H_2O$ (3 × 5 ml) and stored in isopropanol (12.5 ml) $\nu_{max}$ (KBr)/$cm^{-1}$ 2103 ($N_3$), 1660 (CO).

**Affi-Gel supported alcohol 75**

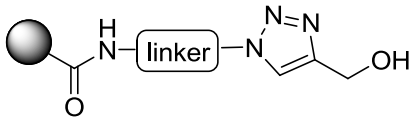


Affi-Gel supported azide **73** in isopropanol (10 ml, 0.15 mmol) was filtered, washed with MeOH (3 × 3 ml), $H_2O$ (3 × 3 ml) and resuspended in $H_2O$/*t*-BuOH (1/1, 10 ml). Sodium ascorbate (6.0 mg, 0.030 mmol) and $CuSO_4$ (4.0 mg, 0.010 mmol) were dissolved in a minimal amount of $H_2O$ and the solution was added to the suspended resin, followed by a solution of TBTA (8.00 mg, 0.010 mmol) dissolved in *t*-BuOH (0.5 ml). After stirring for 10 min propargyl alcohol (26 µl, 0.45 mmol) was added and the mixture was shaken gently for 48 h. The reaction was monitored by IR and stopped once the azide peak at 2100 $cm^{-1}$ disappeared. The matrix was filtered, washed with MeOH (3 × 3 ml), $H_2O$ (3 × 3 ml), EDTA (3 × 3 ml, 0.1 M aq.) and the matrix **75** was stored in isopropanol (12.5 ml); $\nu_{max}$ (KBr), 1626 (CO).

**Affi-Gel supported biotin 72**

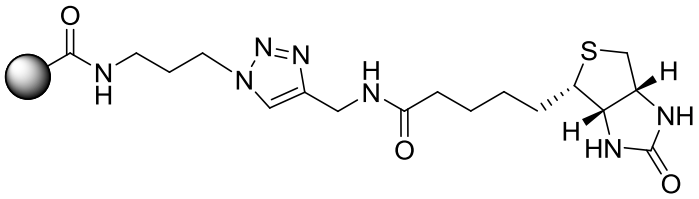


Affi-Gel supported azide **71** in isopropanol (25.0 ml, 0.375 mmol) was filtered, washed with MeOH (3 × 5 ml), $H_2O$ (3 × 5 ml) and resuspended in $H_2O$/*t*-BuOH (2/1, 24.0 ml). Propargyl biotin (316 mg, 1.12 mmol), sodium ascorbate (14.8 mg, 0.0750 mmol) and

$CuSO_4$ (10.0 mg, 0.0370 mmol) were dissolved in $H_2O$ (0.5 ml) and the solution was added to the suspended resin. The suspension was shaken gently for 48 h. The reaction was monitored by IR and stopped once the azide peak at 2100 $cm^{-1}$ disappeared. The matrix was filtered, washed with MeOH (3 × 5 ml), $H_2O$ (3 × 5 ml), EDTA (3 × 5 ml, 0.1 M aq.) and matrix **72** was stored in isopropanol (25.0 ml); $\boldsymbol{\nu_{max}}$ (KBr), 1638 (CO), 1618 (CO).

**Affi-Gel supported biotin 74**

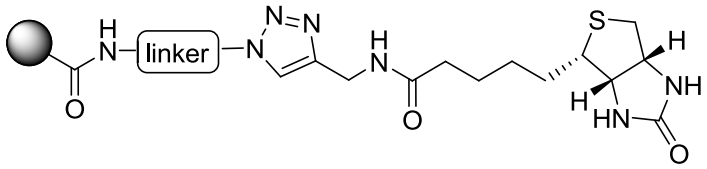


Affi-Gel supported azide **73** in isopropanol (12.5 ml, 0.187 mmol) was filtered, washed with MeOH (3 × 5 ml), $H_2O$ (3 × 5 ml) and resuspended in $H_2O$/*t*-BuOH (2/1, 12 ml). Sodium ascorbate (6.00 mg, 0.0300 mmol) and $CuSO_4$ (4.00 mg, 0.0100 mmol) were dissolved in $H_2O$ (0.5 ml) and the solution was added to the suspended resin, followed by a solution of TBTA (8.00 mg, 0.0100 mmol) dissolved in *t*-BuOH (0.5 ml). After stirring for 10 min propargyl biotin was added (158 mg, 0.562 mmol) and the mixture was shaken gently for 48 h. The reaction was monitored by IR and stopped once the azide peak at 2100 $cm^{-1}$ disappeared. The matrix was filtered, washed with MeOH (3 × 5 ml), $H_2O$ (3 × 5 ml), EDTA (3 × 5 ml, 0.1 M aq.) and matrix **74** was stored in isopropanol (12.5 ml); $\boldsymbol{\nu_{max}}$ (KBr), 1651 (CO).

**Solid-supported anisomycin featuring a cleavable unit 32**

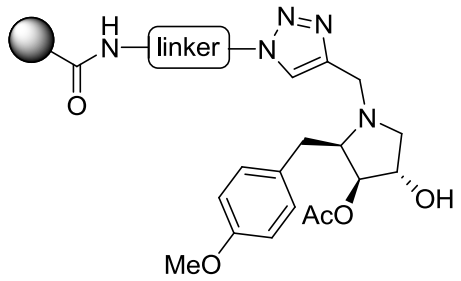


Affi-Gel supported azide **73** in isopropanol (5.0 ml, 0.075 mmol) was filtered, washed with MeOH (3 × 3 ml), $H_2O$ (3 × 3 ml) and resuspended in $H_2O$/*t*-BuOH (1/1, 8 ml). Sodium ascorbate (6.0 mg, 0.030 mmol) copper sulphate (4.0 mg, 0.010 mmol) previously dissolved in a minimal amount of $H_2O$ and TBTA (8.0 mg, 0.010 mmol) dissolved in *t*-BuOH, were added. After strirring for 10 min, propargyl anisomycin (45 mg, 0.15 mmol) was added. The mixture was gently shaken for 48 h. The reaction was monitored by IR and stopped once the azide peak at 2100 $cm^{-1}$ disappeared. The matrix was filtered, washed with MeOH (3 × 3 ml), $H_2O$ (3 × 3 ml), EDTA (3 × 3 ml, 0.1 M aq.) and suspended in isopropanol (12.5 ml).

**{1-[3-(4-Amino-phenoxy)-propyl]-1*H*-1,2,3-triazol-4-yl}-methanol 77**

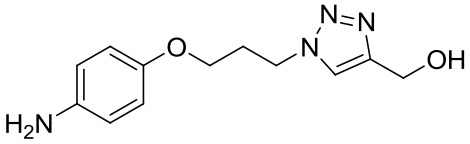


Affi-Gel supported alcohol **75** in isopropanol (0.075 mmol, 5 ml) was filtered and resuspended in a solution of sodium dithionite, (3 ml, 0.3 M aq.) and shaken gently for 10 min. The matrix was filtered and the procedure repeated twice. The cleavage was monitored by the change in colour of the matrix (from bright orange to colourless). The combined washings were extracted with EtOAc (3 × 5 ml) to give the aniline **77** as a colourless oil (13 mg, 70 % yield). **$^1$H NMR** δ (250 MHz, $CDCl_3$) 7.50 (1H, s, Ar*H*), 6.76-6.54 (4H, m, Ar*H*), 4.77 (2H, s, C$H_2$OH), 4.56 (2H, t, *J* = 6.8 Hz, C$H_2$O), 3.87 (2H,

t, $J$ = 6.0 Hz, C$H_2$N), 2.33 (2H, qn, $J$ = 6.5 Hz, C$H_2$), 1.56 (2H, br s, N$H_2$); ***m/z*** (ESI+) 271 ([M+Na]$^+$, 30%), 249 ([M+H]$^+$, 100).

## 7.3 Preliminary affinity studies

### 7.3.1 Material and methods

SDS-PAGE materials and avidin were from Invitrogen; NuPAGE 4-12% Bis-Tris Gels (NP0321) were run according to manufacturers descriptions using 4×SDS loading buffer (NP0007) and 10×reducing agent (NP0004). Molecular weight markers were Precision Plus unstained standards from Bio-Rad (161-0363). Phosphate Buffered Saline (PBS) was prepared by dissolving PBS tablets from Oxoid (BR0014G) in distilled water. Avidin was purchased from Invitrogen. All other reagents were from Sigma Aldrich and were of the highest available purity.

### 7.3.2 Competitive capture and release of avidin

Five affinity experiments were carried out in parallel as follows:

1: Compound **72** + avidin (classical elution method)
2: Compound **72** + avidin (chemical cleavage)
3: Compound **74** + albumin (classical elution method)
4: Compound **74** + avidin (classical elution method)
5: Compound **74** + avidin (chemical cleavage)

Matrix **72** or **74** in isopropanol (0.015 mmol, 1 ml) was transferred to a Falcon tube, pelleted by centrifugation (5 min at 3,000g) and the solvent was decanted. The matrix was washed with water (3 × 5 ml) and HEPES buffer (3 × 5 ml, 50 mM HEPES, pH 7.5, 150 mM NaCl). A solution of avidin (1 ml, 1 mg $ml^{-1}$) was added to matrix **72** (exp 1 & 2) and matrix **74** (exp 4 & 5), and a solution of albumin (1 ml, 1 mg $ml^{-1}$) was added to matrix **74** (exp 3). The matrix was further diluted with HEPES buffer (4 ml) and incubated for 30 min with gentle shaking. The matrix was pelleted and the supernatant

collected and analysed by SDS-PAGE (Fig. **39**, Lanes A-E). The matrix was further washed with HEPES buffer (3 × 5 ml) prior to the elution protocol. The matrix (exp 1, 3 & 4) was suspended in 2×SDS loading buffer (1 ml) and HEPES buffer (1 ml), heated for 10 min at 100 ºC, pelleted by centrifugation (2 min at 10,000g), and the supernatant collected. The supernatants were analysed by SDS-PAGE (Fig. **39**, Lanes F-H). The matrix (exp 2 & 5) was divided into three aliquots which were treated with a freshly prepared solution of sodium dithionite (25 µl, 0.3 M) at three different pHs (6.5, 7.5 & 8.5, 50 mM KPO4). The matrix was gently shaken for 10 min, pelleted by centrifugation (2 min at 10,000g) and the supernatant collected. The cleavage procedure was repeated and the supernatants were pooled, treated with 2×SDS loading buffer and heated for 10 min at 100 ºC. The supernatants were analysed by SDS-PAGE (Fig. **39**, Lanes $I_1$-$J_3$).

### 7.3.3 Capture and release of avidin from a protein mixture

Two affinity experiments were carried out in parallel as follows:

1: Compound **72** + avidin enriched FBS in PBS (classical elution method)
2: Compound **72** + avidin enriched FBS in PBS (chemical cleavage)

Matrix **72** or **74** in isopropanol (0.015 mmol, 1 ml) was transferred to a Eppendorf tube, pelleted by centrifugation (2 min at 10,000g) and the solvent was decanted. The matrix was washed with water (3 × 1.5 ml) and PBS buffer (3 × 1.5 ml). A solution of avidin enriched (100 µg $ml^{-1}$) 10 % FBS in PBS (1 ml) was added. The matrix was incubated with the protein mixture for 30 min with gentle shaking. The matrix was pelleted and the supernatant collected and analysed by SDS-PAGE (Fig. **40**, Lanes B & C). The matrix was washed with 4×PBS buffer (3 × 1.5 ml) prior to the elution protocol. Matrix **72** was resuspended in 4×SDS loading buffer (100 µl) and 10× reducing agent (10 µl) and heated for 10 min at 100 ºC, centrifuged (2 min at 10,000g) and the supernatant collected. The supernatant was analysed by SDS-PAGE (Fig. **40**, Lane D). Matrix **74**

was incubated with a freshly prepared solution of sodium dithionite (25 µl, 0.3 M) at pH 6.5. The matrix was gently shaken for 10 min, pelleted by centrifugation (2 min at 10,000g) and the supernatant collected. The cleavage procedure was repeated and the supernatants were pooled, treated with 4×SDS loading buffer (25 µl) and 10×reducing agent (8 µl) and heated for 10 min at 100 ºC. The supernatants were analysed by SDS-PAGE (Fig. **40**, Lane E).

### 7.3.4 Pull-down experiments with HEK 293 cells

A series of pull-down experiments were carried out using biotinylated anisomycin **28** and solid supported anisomycin featuring a cleavable unit **32**. Along with these two molecular probes (positive controls, +), a series of negative controls (−) at various concentrations were employed and indicated as follows:

1: Biotin propargyl amide **69**, 50 mM (**BP**): (−)
2: A biotinylated peptide, 50 mM (**BPe**): (−)
3: Biotinylated anisomycin **28**, 50 mM (**BA**): (+)
4: Solid-supported cleavable unit **73**, 50 mM (**$SL_{50}$**): (−)
5: Solid-supported cleavable unit **73**, 5 mM (**$SL_5$**): (−)
6: Solid-supported anisomycin featuring a cleavable unit **32**, 50 mM (**$SLA_{50}$**): (+)
7: Solid-supported anisomycin featuring a cleavable unit **32**, 5 mM (**$SLA_5$**): (+)

A streptavidin-coated agarose matrix (40 µl, of a 50/50 mixture beads) was transferred to three Eppendorf tubes. The matrices were washed with Buffer W* (3 × 300 µl), pelleted by centrifugation (2 min at 4,000g) and the solvent was decanted. Biotinylated compounds (**BP**, **BPe** and **BA**, 1 µl, 50 mmol $ml^{-1}$) were added to the matrices together with Buffer W (200 µl). The matrices were incubated with the biotinylated compounds for 1 h with gentle shaking at RT. The matrices were then washed with Buffer W* (3 × 300 µl), pelleted by centrifugation (2 min at 4,000g) and the solvent was decanted.

Solid-supported compounds (**$SL_{50}$**, **$SL_5$**, **$SLA_{50}$** and **$SLA_5$**, 40 µl) were transferred to four Eppendorf tubes. The matrices were washed with Buffer W (3 × 300 µl), pelleted by centrifugation (2 min at 4,000g) and the solvent was decanted. A cleared whole lysate of HEK 293 cells (49 µl) was added to all the matrices together with Buffer W (151 µl). The matrices were incubated with the cell lysate[1] for 1 h with gentle shaking. All the matrices were washed with Buffer W (3 × 300 µl), than PBS + 0.2% Triton (4 × 300 µl) and again Buffer W (1 × 300 µl), pelleted by centrifugation (4 min at 2,000g) and the solvent was decanted. Matrices **BP**, **BPe** and **BA** were resuspended in 2×SB loading buffer (40 µl), heated for 15 min at 95 ºC, pelleted by centrifugation (5 min at 2,000g) and the supernatants collected. The supernatants were analysed by SDS-PAGE. Solid supported compounds **$SL_{50}$**, **$SL_5$**, **$SLA_{50}$** and **$SLA_5$** were incubated with a freshly prepared solution of sodium dithionite (25 µl, 0.3 M) at pH 6.5. The matrix was gently shaken for 10 min, pelleted by centrifugation (2 min at 10,000g) and the supernatant collected. The cleavage procedure was repeated and the supernatants were pooled, treated with 2×SB loading buffer (40 µl), heated for 15 min at 95 ºC and analysed by SDS-PAGE.

(1) HEK 293 cell lysate preparation.

The cells were harvested (7 min, 4 °C, 4,000g), lysed in in 0.1% Triton Lysis buffer** (400ul/plate, 20min) and pelleted by centrifugation (12 min, 4 °C, 13,200g). Cell lysate was treated with avidin (40 µg $ml^{-1}$ of a 2mg/ml stock) for 30 min on ice and and the pellets were discarded. Treated lysate was pre-cleared of endogenous biotinylated proteins using Sepharose-4B (Sigma) beads for 1 h at 4 °C. The supernatant was collected and the protein content was estimated by Bradford assay.

*__Buffer W__: 100 mM Tris pH 8, 150 mM NaCl, 1mM EDTA.

**__0.1% Triton Lysis Buffer__: 50 mM HEPES, 0.1 mM EDTA, 150 mM NaCl, 10 mM NaF, 2 mM DTT, 0.1% Triton×100, 1×PIM.

## 7.4 Experimental procedures for chapters 5 and 6

**{[1-Phenyl-meth-(*E*)-ylidene]-amino}-acetic acid methyl ester 218**

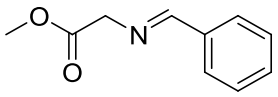

To a suspension of glycine methyl ester hydrochloride (30.0 g, 240 mmol) and $MgSO_4$ (38.1 g, 320 mmol) in DCM (400 ml), $Et_3N$ (40.4 ml, 280 mmol) was added. The mixture was stirred at RT for 1 h, and then benzaldehyde (20.4 ml, 200 mmol) was added. The reaction was stirred overnight (~18 h) at RT. The mixture was filtered and the filtrate was washed with $H_2O$ (500 ml). The aqueous phase was extracted with DCM (2 × 250 ml) and the combined organic layers were washed with NaCl (3 × 400 ml, sat. aq.), dried over $MgSO_4$ and the solvent removed *in vacuo*. The resulting glycine iminoester was isolated as a yellow oil (35.4 g, 99% yield) with minor impurities and used without further purification; $\mathbf{R_f}$ (30% EtOAc in hexane) = 0.41; $\mathbf{\nu_{max}}$ (neat)/$cm^{-1}$ 1743 (CO), 1648 (CN); **$^1$H NMR** $\delta$ (500 MHz, $CDCl_3$) 8.29 (1H, s, C*H*N), 7.84-7.74 (2H, d, *J* = 6.5 Hz, Ar*H*), 7.48-7.37 (3H, m, Ar*H*), 4.42 (2H, s, C$H_2$), 3.77 (3H, s, C$H_3$); **$^{13}$C NMR** $\delta$ (126 MHz, $CDCl_3$) 170.60 (C), 165.50 (CH), 135.55 (C), 131.29 (CH), 128.64 (2 × CH), 128.51 (2 × CH), 61.98 ($CH_2$), 52.15 ($CH_3$); ***m/z*** (ESI+) 200 ($[M+Na]^+$, 58 %), 178 ($[M+H]^+$, 100), 118 (7).

All spectroscopic data were in good agreement with the literature.[227]

**(Benzhydrylidene-amino)-acetic acid methyl ester 248a**

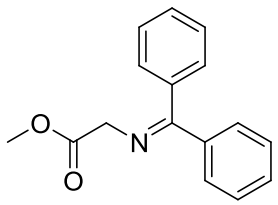

To a slurry of glycine methyl ester hydrochloride (5.00 g, 40.0 mmol) in DCM (40 ml) was added benzophenone imine (6.71 ml, 40.0 mmol) in DCM (40 ml), and the reaction was stirred overnight (~18 h) at RT. The milky mixture was washed with $H_2O$ (2 × 15 ml) and NaCl (15 ml, sat. aq.). The organic layer was separated and dried over $MgSO_4$. The crude product was recrystallised from hexane/DCM to obtain glycine iminoester **248** as a pale yellow solid (8.76 g, 88% yield); $\mathbf{R_f}$ (30% EtOAc in hexane) = 0.51; $\boldsymbol{\nu_{max}}$ (neat)/$cm^{-1}$ 1746 (CO), 1626 (CN); **$^1$H NMR** (500 MHz, $CDCl_3$) δ 7.66 (2H, d, *J* = 7.5 Hz, Ar*H*), 7.50-7.37 (4H, m, Ar*H*), 7.33 (2H, t, *J* = 7.5 Hz, Ar*H*), 7.18 (2H, d, *J* = 7.5 Hz, Ar*H*), 4.22 (2H, s, C$H_2$), 3.75 (3H, s, C$H_3$); **$^{13}$C NMR** *δ* (126 MHz, $CDCl_3$) 172.10 (C), 171.27 (C), 139.35 (C), 136.06 (C), 130.64 (CH), 129.00 (CH), 128.91 (2 × CH), 128.85 (2 × CH), 128.22 (2 × CH), 127.78 (2 × CH), 55.75 ($CH_2$), 52.16 ($CH_3$); ***m/z*** (ESI+) 529 ($[2M+Na]^+$, 17%), 276 ($[M+Na]^+$, 27), 254 ($[M+H]^+$, 100).

All spectroscopic data were in good agreement with the literature.[234,257]

**(Benzhydrylidene-amino)-acetic acid ethyl ester 248b**

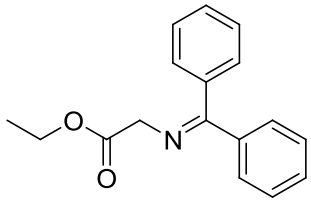


To a slurry of glycine ethyl ester hydrochloride (5.00 g, 36.0 mmol) in DCM (40 ml) was added benzophenone imine (6.04 ml, 36.0 mmol) in DCM (40 ml), and the reaction was stirred overnight (~18 h) at RT. The milky mixture was washed with $H_2O$ (2 × 15 ml) and NaCl (15 ml, sat. aq.). The organic layer was separated and dried over $MgSO_4$. The crude product was recrystallised from hexane/DCM to obtain glycine iminoester **248b** as a colourless solid (8.20 g, 85% yield); $\mathbf{R_f}$ (30% EtOAc in hexane) = 0.56; $\boldsymbol{\nu_{max}}$ (neat)/$cm^{-1}$ 1739 (CO), 1625 (CN); **$^1$H NMR** δ (500 MHz, $CDCl_3$) 7.69 (2H, d, *J* = 7.5

Hz, Ar*H*), 7.53-7.40 (4H, m, Ar*H*), 7.36 (2H, t, *J* = 7.5 Hz, Ar*H*), 7.21 (2H, d, *J* = 7.5 Hz, Ar*H*), 4.23 (2H, q, *J* = 7.1 Hz, C*H*$_2$CH$_3$), 4.22 (2H, s, C*H*$_2$CO), 1.30 (3H, t, *J* = 7.1 Hz, C*H*$_3$); **$^{13}$C NMR** $\delta$ (126 MHz, $CDCl_3$) 171.99 (C), 170.79 (C), 139.34 (C), 136.12 (C), 130.51 (CH), 128.95 (CH), 128.89 (2 × CH), 128.81 (2 × CH), 128.19 (2 × CH), 127.80 (2 × CH), 61.00 ($CH_2$), 55.85 ($CH_2$), 14.34 ($CH_3$); ***m/z*** (ESI+) 557 ($[2M+Na]^+$, 26%), 290 ($[M+Na]^+$, 25), 268 ($[M+H]^+$, 100), 254 (18).

All spectroscopic data were in good agreement with the literature.[234,257]

**(Benzhydrylidene-amino)-acetic acid *tert*-butyl ester 148**

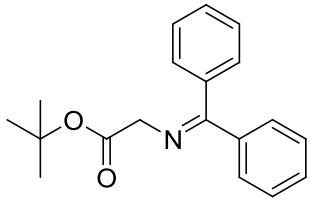


To a slurry of glycine *tert*-butyl ester hydrochloride (5.00 g, 30.0 mmol) in DCM (40 ml) was added benzophenone imine (5.03 ml, 30.0 mmol) in DCM (40 ml), and the reaction was stirred overnight (~18 h) at RT. The milky mixture was extracted with $H_2O$ (2 × 15 ml) and NaCl (15 ml, sat. aq.). The organic layer was separated, dried over $MgSO_4$ and the solvent removed *in vacuo*. The crude product was obtained as a colourless solid which was recrystallised from hexane to obtain iminoester **148** as colourless crystals (8.10 g, 91% yield); $\mathbf{R_f}$ (30% EtOAc in hexane) = 0.70; $\boldsymbol{\nu_{max}}$ (neat)/cm$^{-1}$ 1734 (CO), 1634 (CN); **$^1$H NMR** $\delta$ (500 MHz, $CDCl_3$) 7.69 (2H, d, *J* = 7.5 Hz, Ar*H*), 7.53-7.39 (4H, m, Ar*H*), 7.36 (2H, t, *J* = 7.5 Hz, Ar*H*), 7.21 (2H, d, *J* = 7.5 Hz, Ar*H*), 4.14 (2H, s, C*H*$_2$), 1.49 (9H, s, 3 × C*H*$_3$); **$^{13}$C NMR** $\delta$ (126 MHz, $CDCl_3$) 171.64 (C), 170.00 (C), 139.53 (C), 136.29 (C), 130.49 (CH), 128.88 (3 × CH), 128.74 (2 × CH), 128.16 (2 × CH), 127.86 (2 × CH), 81.20 (C), 56.45 ($CH_2$), 28.24 (3 × $CH_3$); ***m/z*** (ESI+) 613 ($[2M+Na]^+$, 100%), 318 ($[M+Na]^+$, 25), 296 ($[M+H]^+$, 53), 240 (34).

All spectroscopic data were in good agreement with the literature.[234,257]

**Carbonic acid ethyl ester 2-methyl-allyl ester 217**

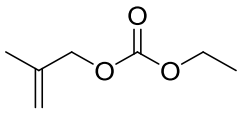

To a stirred solution of 2-methylallyl alcohol (14.4 g, 200 mmol) in DCM (100 ml) cooled to 0 ºC, pyridine (15.8 g, 200 mmol) and ethyl chlorocarbonate (21.7 g, 200 mmol) were added. The reaction mixture was allowed to reach RT and stirred overnight (~18 h). The mixture was quenched with $NH_4Cl$ (100 ml, sat. aq.). The organic layer was separated and the aqueous layer extracted with $Et_2O$ (2 × 100 ml). The combined organic layers were washed with $H_2O$ (100 ml) and dried over $Na_2SO_4$. The solvent was removed *in vacuo* to give the crude allylic carbonate. Flash chromatography (10% EtOAc in hexane) gave the desired allylic carbonate as a colourless oil (23.2 g, 80% yield); $\mathbf{R_f}$ (20% EtOAc in hexane) = 0.80; $\mathbf{\nu_{max}}$ (neat)/$cm^{-1}$ 1742 (CO) 1660 (C=C); **NMR** $\delta$ (500 MHz, $CDCl_3$) 5.00 (s, 1H, C=C$H_a$H$_b$), 4.93 (s, 1H, C=CH$_a$$H_b$), 4.52 (s, 2H, C$H_2$O), 4.19 (2H, q, $J$ = 7.1 Hz, C$H_2$CH$_3$), 1.76 (s, 3H, C$H_3$), 1.30 (3H, t, $J$ = 7.1 Hz, CH$_2$C$H_3$); **$^{13}$C NMR** $\delta$ (126 MHz, $CDCl_3$) 155.18 (C), 139.54 (C), 113.53 ($CH_2$), 71.03 ($CH_2$), 64.12 ($CH_2$), 19.43 ($CH_3$), 14.36 ($CH_3$); ***m/z*** (ESI+) 311 ([2M+Na]$^+$, 8%), 145 ([M+H]$^+$, 10), 101 (5).

All spectroscopic data were in good agreement with the literature.[228,258]

**4-Methyl-2-{[1-phenyl-meth-(*E*)-ylidene]-amino}-pent-4-enoic acid methyl ester 219**

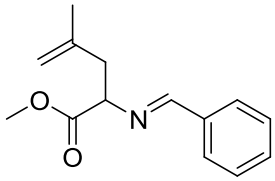

To a solution of Schiff base **218** (35.4 g, 200 mmol) and allyl carbonate **217** (43.2 g, 300 mmol) in dry THF (200 ml), $Pd(PPh_3)_4$ (10.0 g, 8.00 mmol) was added. The reaction mixture was stirred at RT until the starting material was consumed (~6 h). The mixture was poured onto $Et_2O$ and filtered through Celite. The solvent was removed *in vacuo* to yield the product as pale yellow oil with minor triphenyl phosphine impurities (33.5 g, 72% yield); $\mathbf{R_f}$ (20% EtOAc in hexane) = 0.60; $\mathbf{\nu_{max}}$ (neat)/$cm^{-1}$ 1736 (CO), 1641 (C=N); **$^1$H NMR** $\delta$ (500 MHz, $CDCl_3$) 8.24 (1H, s, ArC*H*N), 7.80 (2H, dd, *J* = 7.5 & 1.6 Hz, Ar*H*), 7.52-7.37 (3H, m, Ar*H*), 4.84 (1H, br s, $CCH_aH_b$), 4.76 (1H, br s, $CCH_aH_b$), 4.19 (1H, dd, *J* = 8.3 & 5.6 Hz, C*H*N), 3.78 (3H, s, OMe), 2.78 (1H, dd, *J* = 13.8 & 5.6 Hz, $CHCH_cH_d$), 2.58 (1H, ddd, *J* = 13.8 & 8.3 & 0.7 Hz, $CHCH_cH_d$), 1.77 (3H, s, Me); **$^{13}$C NMR** $\delta$ (126 MHz, $CDCl_3$) 172.46 (C), 163.41 (CH), 141.18 (C), 135.77 (C), 131.27 (CH), 128.73 (2 × CH), 128.69 (2 × CH), 114.13 ($CH_2$), 72.21 (CH), 52.36 ($CH_3$), 41.74 ($CH_2$), 22.93 ($CH_3$); ***m/z*** (ESI+) 254 ($[M+Na]^+$, 7%), 232 ($[M+H]^+$, 76).

All spectroscopic data were in good agreement with the literature.[229,230]

**2-(Benzhydrylidene-amino)-4-methyl-pent-4-enoic acid *tert*-butyl ester 232**

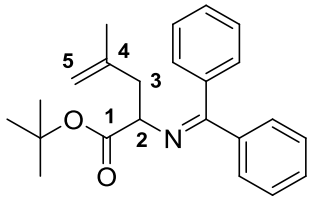


To a solution of Schiff base **148** (1.00 g, 3.83 mmol) and allyl ethyl carbonate **217** (0.730 g, 5.07 mmol) in dry THF (5 ml), $Pd(PPh_3)_4$ (0.195 g, 0.169 mmol) was added. The reaction mixture was stirred at RT until the starting material was consumed (~7 h). The mixture was poured onto $Et_2O$ and filtered through Celite. The solvent was removed *in vacuo*. Flash chromatography (dry loaded basic silica, 1% EtOAc in hexane) gave the product as a colourless solid (1.09 g, 92% yield); $\mathbf{R_f}$ (20% EtOAc in hexane) = 0.71;

**$\nu_{max}$** (neat)/$cm^{-1}$ 1708 (CO), 1624 (CN); **$^{1}$H NMR** $\delta$ (400 MHz, $CDCl_3$) 7.69 (2H, d, *J* = 7.0 Hz, Ar*H*), 7.50-7.27 (6H, m, Ar*H*), 7.24-7.17 (2H, m, Ar*H*), 4.76 (1H, br s, $C_5H_aH_b$), 4.74 (1H, br s, $C_5H_aH_b$), 4.12 (1H, dd, *J* = 8.3 & 5.2 Hz, $C_2H$), 2.67 (1H, dd, *J* = 13.6 & 5.2 Hz, $C_3H_cH_d$), 2.60 (1H, dd, *J* = 13.6 & 8.3 Hz, $C_3H_cH_d$), 1.54 (3H, s, $C_4CH_3$), 1.47 (9H, s, 3 × $CH_3$); **$^{13}$C NMR** $\delta$ (101 MHz, $CDCl_3$) 171.25 (C), 169.92 (C), 141.89 (C), 139.83 (C), 136.55 (C), 130.15 (CH), 128.86 (2 × CH), 128.57 (CH), 128.35 (2 × CH), 128.12 (2 × CH), 127.99 (2 × CH), 113.39 ($CH_2$), 81.02 (C), 64.85 (CH), 41.96 ($CH_2$), 28.10 (3 × $CH_3$), 22.65 ($CH_3$); ***m/z*** (ESI+) 722 ($[2M+Na]^+$, 18%), 372 ($[M+Na]^+$, 13), 350 ($[M+H]^+$, 100), 130 (48).

All spectroscopic data were in good agreement with the literature.[229,230]

**2-Amino-4-methyl-pent-4-enoic acid methyl ester 220**

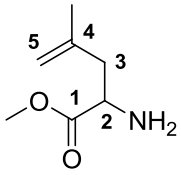


Alkylated Schiff base **219** (33.0 g, 140 mmol) was stirred with HCl (186 ml, 1.5 M aq., 280 mmol) at RT (~2 h). The reaction was monitored for the consumption of the starting material (LC-MS). After washing with $Et_2O$, solid $NaHCO_3$ was added to the aqueous phase until pH 8 was reached. After saturation with solid NaCl, the aqueous phase was extracted with $CHCl_3$ (3 × 100 ml) and dried over $MgSO_4$. The solvent was removed *in vacuo* affording the product as yellow oil (17.0 g, 85% yield); **$R_f$** (20% EtOAc in hexane) = 0.10; **$\nu_{max}$** (neat)/$cm^{-1}$ 1735 (CO), 1648 (C=C); **$^{1}$H NMR** $\delta$ (500 MHz, $CDCl_3$) 4.87 (1H, br s, $C_5H_aH_b$), 4.78 (1H, br s, $C_5H_aH_b$), 3.73 (3H, s, OMe), 3.63 (1H, dd, *J* = 8.9 & 5.1 Hz, $C_2H$), 2.50 (1H, dd, *J* = 13.7 & 5.1 Hz, $C_3H_cH_d$), 2.24 (1H, dd, *J* = 13.7 & 8.9 Hz, $C_3H_cH_d$), 1.75 (3H, s, Me); **$^{13}$C NMR** $\delta$ (126 MHz, $CDCl_3$) 176.11 (C), 141.39 (C), 114.22 ($CH_2$), 52.66 (CH), 52.14 ($CH_3$), 43.67 ($CH_2$), 22.03 ($CH_3$); ***m/z*** (ESI+) 166 ($[M+Na]^+$, 37%), 144 ($[M+H]^+$, 100), 102 (7).

All spectroscopic data were in good agreement with the literature.[229]

**2-Amino-4-methyl-pent-4-enoic acid *tert*-butyl ester 233**

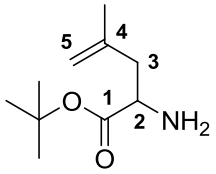


Alkylated Schiff base **232** (1.00 g, 2.86 mmol) was stirred for 2-3 h with an aqueous solution of HCl (20.0 ml, 1 M aq., 20.0 mmol) and THF (20 ml) at RT. The reaction was monitored for the consumption of the starting material (LC-MS). The mixture was diluted with $H_2O$ (40 ml). The aqueous phase was basified with solid $NaHCO_3$, extracted with DCM (3 × 20 ml) and dried over $Na_2SO_4$. The solvent was removed *in vacuo*. Flash chromatography (40 to 60% EtOAc in hexane) afforded the desired amine as a colourless oil (0.495 g, 93% yield); $\mathbf{R_f}$ (50% EtOAc in hexane) = 0.20; $\boldsymbol{\nu_{max}}$ (neat)/$cm^{-1}$ 1728 (CO) 1647 (C=C); **$^1$H NMR** $\delta$ (400 MHz, $CDCl_3$) 4.77 (1H, br s, $C_5H_aH_b$), 4.70 (1H, br s, $C_5H_aH_b$), 3.40 (1H, dd, $J$ = 8.6 & 5.4 Hz, $C_2H$), 2.38 (1H, dd, $J$ = 13.7 & 5.4 Hz, $C_3H_cH_d$), 2.12 (1H, ddd, $J$ = 13.7 & 8.6 & 0.5 Hz, $C_3H_cH_d$), 1.68 (3H, s, Me), 1.43 (2H, br s, $NH_2$), 1.38 (9H, s, 3 × $CH_3$); **$^{13}$C NMR** $\delta$ (101 MHz, $CDCl_3$) 174.79 (C), 141.60 (C), 113.73 ($CH_2$), 81.00 (C), 52.99 (CH), 43.75 ($CH_2$), 28.01 (3 × $CH_3$), 21.90 ($CH_3$); ***m/z*** (ESI+) 208 ($[M+Na]^+$, 17%), 186 ($[M+H]^+$, 10), 102 (7).

All spectroscopic data were in good agreement with the literature.[236,257]

**2-Amino-4-methyl-pent-4-enoic acid *tert*-butyl ester hydrochloride 266**

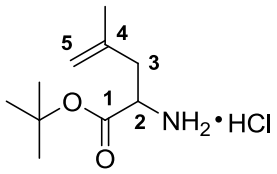

To a stirred solution of alkylated Schiff base **232** (45 mg, 0.12 mmol) in $Et_2O$ (0.30 ml) at 0 ºC, HCl (0.15 ml, 1 M aq., 0.15 mmol) was added dropwise. The reaction mixture was allowed to reach RT and stirred overnight (~18 h). The layers were separated, and the aqueous phase was concentrated *in vacuo* to yield the desired amino ester hydrochloride as a colourless solid (20 mg, 90% yield); $\mathbf{R_f}$ (50% EtOAc in hexane) = 0.10; $\mathbf{\nu_{max}}$ (neat)/$cm^{-1}$ 1741 (CO); **$^1$H NMR** $\delta$ (400 MHz, $D_2O$) 5.06-5.04 (1H, m, $C_5H_aH_b$), 4.95-4.93 (1H, m, $C_5H_aH_b$), 4.21-4.12 (1H, m, $C_2H$), 2.80-2.72 (1H, m, $C_3H_cH_d$), 2.63-2.56 (1H, m, $C_3H_cH_d$), 1.79 (3H, s, Me), 1.51 (s, 9H, 3 × $CH_3$); ***m/z*** (ESI+) 208 ($[M+Na]^+$, 17%), 185 ($[M]^+$, 42), 102 (7); **HRMS** (ESI+) $[M+Na]^+$ found 209.1381, $C_{10}H_{20}O_2NNa$ requires 209.1386.

**2-[Benzyloxycarbonyl-((*E*)-buta-1',3'-dienyl)-amino]-4-methyl-pent-4-enoic acid methyl ester 224**

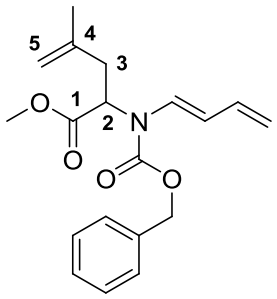


To a solution of amine **220** (40 mg, 0.28 mmol) in DCM (1 ml) crotonaldehyde (24 µl, 0.28 mmol) and molecular sieves (~50 mg) were added at RT. The reaction mixture was stirred overnight (~18 h), then filtered. The filtrate was concentrated *in vacuo* to give the desired imine as a pale yellow oil as confirmed by LC-MS. The imine was dissolved in toluene (1 ml) and added dropwise to a flask containing diethylaniline (45 µl, 0.33 mmol) and benzyl chloroformate (67 µl, 0.42 mmol) at 0 ºC. The reaction mixture was allowed to reach RT and stirred overnight (~18 h). The resulting precipitate was removed by filtration, washed with $Et_2O$ and the filtrate was concentrated *in vacuo*. Flash chromatography (dry loaded silica column, 2% EtOAc in hexane) gave the desired

enamide **224** as a pale yellow oil (27 mg, 30% yield) and amide **230** as a colourless solid (38 mg, 49% yield); $\mathbf{R_f}$ (20% EtOAc in hexane) = 0.42; $\boldsymbol{\nu_{max}}$ (neat)/cm$^{-1}$ 1707 (CO) 1645 (CO); **$^1$H NMR** $\delta$ (400 MHz, 323 K, $CDCl_3$) 7.36-7.34 (5H, m, Ar*H*), 6.96 (1H, d, *J* = 14.6 Hz, NC*H*C), 6.27 (1H, dt, *J* = 17.0 & 10.2 Hz, C*H*=$CH_{cis}H_{trans}$), 5.62 (1H, dd, *J* = 14.3 & 10.2 Hz, CH=C*H*CH), 5.27-5.13 (2H, m, C$H_2$O), 5.06 (1H, d, *J* = 17.0 Hz, $CHCH_{cis}H_{trans}$) 4.93 (1H, d, *J* = 10.2 Hz, $CHCH_{cis}H_{trans}$), 4.90-4.80 (1H, m, $C_2H$), 4.77 (1H, br s, $C_5H_aH_b$), 4.68 (1H, br s, $C_5H_aH_b$), 3.67 (3H, br s, OMe), 2.78-2.75 (2H, m, $C_3H_2$), 1.71 (3H, s, Me); ***m/z*** (ESI+) 681 ([2M+Na]$^+$, 6%), 352 ([M+Na]$^+$, 100), 107 (47); **HRMS** (ESI+) [M+Na]$^+$ found 352.1518, $C_{19}H_{23}O_4NNa$ requires 352.1519.

**2-Benzyloxycarbonylamino-4-methyl-pent-4-enoic acid methyl ester 230**

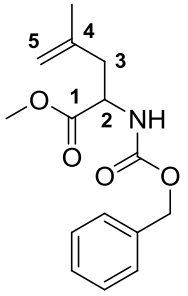


$\mathbf{R_f}$ (20% EtOAc in hexane) = 0.32; $\boldsymbol{\nu_{max}}$ (neat)/cm$^{-1}$ 3340 (NH), 1716 (CO) 1651 (CO); **$^1$H NMR** $\delta$ (400 MHz, $CDCl_3$) 7.48-7.21 (5H, m, Ar*H*), 5.21-5.20 (1H, m, N*H*) 5.11 (2H, s, C$H_2$O), 4.85 (1H, br s, $C_5H_aH_b$), 4.75 (1H, br s, $C_5H_aH_b$), 4.49 (1H, dd, *J* = 13.8 & 8.2 Hz, $C_2H$), 3.74 (3H, s, OMe), 2.55 (1H, dd, *J* = 13.8 & 5.4 Hz, $C_3H_cH_d$), 2.39 (1H, dd, *J* = 13.8 & 8.2 Hz, $C_3H_cH_d$), 1.74 (3H, s, Me); **$^{13}$C NMR** $\delta$ (101 MHz, $CDCl_3$) 172.88 (C), 155.92 (C), 140.38 (C), 136.36 (C), 128.64 (2 × CH), 128.30 (CH), 128.21 (2 × CH), 114.92 ($CH_2$), 67.12 ($CH_2$), 52.43 ($CH_3$), 52.32 (CH), 40.83 ($CH_2$), 21.94 ($CH_3$); ***m/z*** (ESI+) 300 ([M+Na]$^+$, 100%), 278 ([M+H]$^+$, 7), 102 (6); **HRMS** (ESI+) [M+H]$^+$ found 278.1387, $C_{15}H_{20}O_4N$ requires 278.1387.

**2-[Benzyloxycarbonyl-((*E*)-buta-1,3-dienyl)-amino]-4-methyl-pent-4-enoic acid *tert*-butyl ester 235**

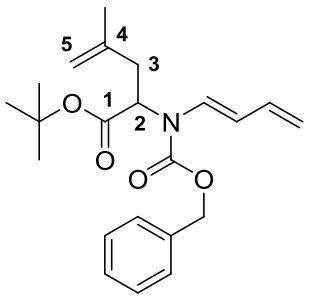


To a solution of amine **233** (254 mg, 1.37 mmol) in DCM (5 ml) crotonaldehyde (0.113 ml, 1.36 mmol) and molecular sieves (~200 mg) were added at RT. The reaction mixture was stirred overnight (~18 h), then filtered. The filtrate was concentrated *in vacuo* to give the desired imine as a pale yellow oil as confirmed by LC-MS. The imine was dissolved in toluene (5 ml) and added dropwise to a flask containing diethylaniline (0.273 ml, 1.72 mmol) and benzyl chloroformate (0.219 ml, 1.56 mmol) at 0 ºC. The reaction mixture was allowed to reach RT and stirred overnight (~18 h). The resulting precipitate was filtered off, washed with $Et_2O$ and the filtrate was concentrated *in vacuo*. Flash chromatography (dry loaded silica column, 2% EtOAc in hexane) gave the desired enamide **235** as a pale yellow oil (341 mg, 67% yield) and amide **237** as a colourless solid (85 mg, 20% yield); $\mathbf{R_f}$ (20% EtOAc in hexane) = 0.40; $\mathbf{\nu_{max}}$ (neat)/$cm^{-1}$ 1718 (CO) 1645 (CO); **$^1$H NMR** $\delta$ (400 MHz, 323 K, $CDCl_3$) 7.42-7.28 (5H, m, Ar*H*), 7.04-6.88 (1H, m, NC*H*=C + C*H*=$CH_{cis}H_{trans}$), 6.27 (0.4H, dt, *J* = 17.0 & 10.3 Hz, C*H*=$CH_{cis}H_{trans}$), 5.62 (0.4H, dd, *J* = 14.3 & 10.3 Hz, CH=C*H*CH), 5.27-5.17 (2H, m, C$H_2$O), 5.03 (0.4H, d, *J* = 17.0 Hz, CH=$CH_{cis}H_{trans}$), 4.92 (0.4H, d, *J* = 10.3 Hz, CH=C$H_{cis}$$H_{trans}$), 4.86-4.79 (1H, m, $C_2H$), 4.75 (1H, s, $C_5H_aH_b$), 4.68 (1H, br s, $C_5H_aH_b$), 4.40 (0.6H, d, *J* = 17.0 Hz, CH=$CH_{cis}H_{trans}$), 4.36 (0.6H, d, *J* = 10.3 Hz, CH=C$H_{cis}$$H_{trans}$) 2.73 (2H, m, $C_3H_2$), 1.71 (3H, s, Me), 1.40 (9H, s, 3 × $CH_3$); **$^{13}$C NMR** $\delta$ (101 MHz, 323 K, $CDCl_3$) 169.54 (C), 169.49 (C), 154.15 (C), 154.10 (C), 141.79 (C), 141.57 (C), 136.24 (C), 136.14 (C), 135.32 (CH), 132.52 (CH), 130.04 (CH), 128.68 (2 × CH), 128.66 (2 × CH), 128.43 (CH), 128.37 (CH), 128.21 (CH), 128.19 (CH), 113.80 ($CH_2$), 113.78 ($CH_2$), 113.68 (CH), 113.65 (CH), 94.46 (CH), 82.15 (C), 81.95 (C), 68.38

($CH_2$), 68.18 ($CH_2$), 57.27 ($CH_2$), 56.55 ($CH_2$), 36.51 ($CH_2$), 36.27 ($CH_2$), 28.03 (3 × $CH_3$), 28.01 (3 × $CH_3$), 22.37 ($CH_3$), 22.33 ($CH_3$); ***m/z*** (ESI+) 394 ($[M+Na]^+$, 47%), 102 (100); **HRMS** (ESI+) $[M+Na]^+$ found 394.1989, $C_{22}H_{29}O_4NNa$ requires 394.1988.

**2-Benzyloxycarbonylamino-4-methyl-pent-4-enoic acid *tert*-butyl ester 237**

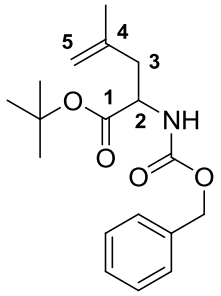


**$R_f$** (20% EtOAc in hexane) = 0.22; **$\nu_{max}$** (neat)/$cm^{-1}$ 3342 (NH), 1714 (CO), 1651 (CO); **$^1$H NMR** $\delta$ (400 MHz, $CDCl_3$) 7.40-7.28 (5H, m, Ar*H*), 5.20-5.18 (1H, m, N*H*), 5.11 (2H, s, C$H_2$O), 4.83 (1H, br s, $C_5H_aH_b$), 4.75 (1H, br s, $C_5H_aH_b$), 4.36 (1H, dd, *J* = 14.0 & 7.8 Hz, $C_2H$), 2.51 (1H, dd, *J* = 14.0 & 6.0 Hz, $C_3H_cH_d$), 2.37 (1H, dd, *J* = 14.0 & 7.8 Hz, $C_3H_cH_d$), 1.76 (3H, s, Me) 1.45 (9H, s, 3 × $CH_3$); **$^{13}$C NMR** $\delta$ (101 MHz, $CDCl_3$) 171.48 (C), 155.89 (C), 140.81 (C), 136.52 (C), 128.62 (3 × CH), 128.25 (CH), 128.20 (CH), 114.66 ($CH_2$), 82.24 (C), 66.98 ($CH_2$), 52.79 (CH), 41.23 ($CH_2$), 28.11 (3 × $CH_3$), 22.04 ($CH_3$); ***m/z*** (ESI+) 661 ($[2M+Na]^+$, 40%), 342 ($[M+Na]^+$, 100), 102 (6); **HRMS** (ESI+) $[M+Na]^+$ found 342.1682, $C_{18}H_{25}O_4NNa$ requires 342.1675.

**4-Methyl-2,3-dihydro-pyrrole-1,2-dicarboxylic acid 1-benzyl ester 2-*tert*-butyl ester**

**Typical procedure for RCM on enamide 235**

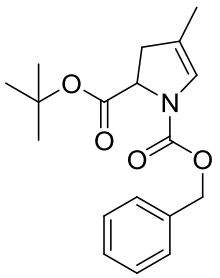

To a solution of enamide **235** (10 mg, 0.027 mmol) in dry DCM (1 ml), Hoveyda-Grubbs II (1.8 mg, 0.0020 mmol) was added. The mixture was stirred and heated to reflux (~40 °C) overnight (~18 h). To the reaction mixture, DMSO (10 µl) was added and the solvent removed *in vacuo*. Flash chromatography (dry loaded silica, 1% EtOAc in hexane) yielded starting material **235** (4.2 mg, 42% yield) and by-product aldehyde **238** as a colourless oil (3.5 mg, 34% yield).

**2-[Benzyloxycarbonyl-((*E*)-3-oxo-propenyl)-amino]-4-methyl-pent-4-enoic acid *tert*-butyl ester 238**

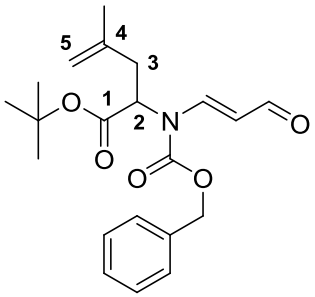


**$R_f$** (20% EtOAc in hexane) = 0.27; **$\nu_{max}$** (neat)/$cm^{-1}$ 1732 (CO), 1676 (CO), 1622 (CO); **$^1$H NMR** $\delta$ (400 MHz, 323 K, $CDCl_3$) 9.38 (1H, d, *J* = 7.4 Hz, C*H*O), 7.92 (1H, d, *J* = 14.5 Hz, NC*H*C), 7.38 (5H, s, Ar*H*), 5.60 (1H, dd, *J* = 14.5 & 7.4 Hz, CH=C*H*CHO), 5.30 (2H, ABq, *J* = 12.1 Hz, C$H_2$O), 4.82 (1H, t, *J* = 7.4 Hz, $C_2H$), 4.74 (1H, s, $C_5H_aH_b$), 4.61 (1H, s, $C_5H_aH_b$), 2.72 (2H, d, *J* = 7.4 Hz, $C_3H_2$), 1.68 (3H, s, Me), 1.40 (9H, s, 3 × $CH_3$); **$^{13}$C NMR** $\delta$ (101 MHz, 323 K, $CDCl_3$) 191.44 (C), 167.80 (C), 153.07 (C), 149.65 (CH), 140.75 (C), 134.95 (C), 129.05 (CH), 128.92 (2 × CH), 128.66 (2 ×

CH), 114.62 ($CH_2$), 112.33 (CH), 83.10 (C), 69.79 ($CH_2$), 57.54 (CH), 36.50 ($CH_2$), 28.00 (3 × $CH_3$), 22.20 ($CH_3$); ***m/z*** (ESI+) 396 ($[M+Na]^+$, 13%), 373 ($[M]^+$, 7), 130 (100); **HRMS** (ESI+) $[M+Na]^+$ found 396.1777, $C_{21}H_{27}O_5NNa$ requires 396.1781.

**2(*S*)-(5-Ethyl-1-aza-bicyclo[2.2.2]oct-2-yl)-quinolin-4-yl-methanol 255**

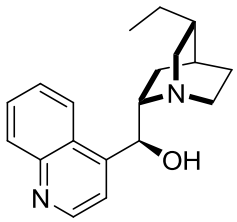


A mixture of (+)-cinchonidine **253** (1.0 g, 3.4 mmol) and 10% Pd/C (0.20 g) in dry MeOH (30 ml) was stirred under hydrogen (1 atm, balloon) at RT overnight (~18 h). The crude reaction mixture was then filtered through Celite as follows: a filter cup filled with Celite was placed over a flask and bathed in DCM. The crude reaction mixture was then added to the top of the Celite and vacuum-filtered through the Celite, with DCM being added to the top to prevent air from being introduced into the filter cup. Periodic samples with capillary tubes were taken as the liquid passed through the filter. Each sample was monitored under UV light for luminescence, indicating the presence of the hydrocinchonidine product. When the luminescent color had dissipated under UV, the filtration was stopped. The solvent was removed *in vacuo* and the resulting colourless solid was suspended in hexane and stirred at RT for 1 h. The resulting precipitate, hydrocinchonidine, was then filtered, concentrated *in vacuo*, and collected as a colourless solid (0.80 g, 80% yield); $\mathbf{R_f}$ (MeOH) = 0.15; **mp** = 110-113 °C, lit.[259] 107-108 °C; $\boldsymbol{\nu_{max}}$ (neat)/$cm^{-1}$ 3305 (OH); **$^1$H NMR** $\delta$ (500 MHz, $CD_3OD$) 8.83 (1H, d, *J* = 4.6 Hz, Ar*H*), 8.19 (1H, d, *J* = 8.4 Hz, Ar*H*), 8.06 (1H, d, *J* = 8.4 Hz, Ar*H*), 7.78 (1H, t, *J* = 7.7 Hz, Ar*H*), 7.73 (1H, d, *J* = 4.6 Hz, Ar*H*), 7.66 (1H, t, *J* = 7.7 Hz, Ar*H*), 5.68 (1H, d, *J* = 3.9 Hz, C*H*OH), 3.29-3.22 (1H, m, C*H*), 3.07 (1H, m, C*H*N), 2.94-2.83 (2H, m, CHC$H_2$N), 2.81-2.72 (1H, m, C*H*), 2.17-2.09 (1H, m, C*H*), 1.72 (1H, br s, C*H*$CH_2CH_3$), 1.67-1.42 (5H m, C$H_2CH_2$N + C$H_2CH_3$ + C*H*), 1.16-1.07 (1H, m, C*H*), 0.94 (3H, t, *J* =

7.2 Hz, $CH_2CH_3$); **$^{13}$C NMR** $\delta$ (126 MHz, $CD_3OD$) 152.22 (C), 150.91 (CH), 148.81 (C), 130.68 (CH), 130.01 (CH), 128.13 (CH), 127.18 (C), 124.52 (CH), 119.90 (CH), 72.30 (CH), 61.38 (CH), 51.77 ($CH_2$), 50.95 ($CH_2$), 38.51 (CH), 27.86 ($CH_2$), 27.51 (CH), 26.17 ($CH_2$), 21.53 ($CH_2$), 12.29 ($CH_3$); ***m/z*** (ESI+) 297 ($[M+H]^+$, 100%), 157 (38).

All spectroscopic data were in good agreement with the literature.[248,184]

**2,7-Bis-bromomethyl-naphthalene 256**

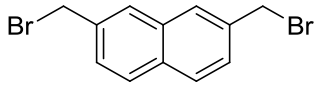


To a stirred solution of 2,7-dimethylnaphthalene **254** (200 mg, 1.28 mmol) in benzene (25 ml), *N*-bromosuccinimide (506 mg, 2.84 mmol) was added, followed by benzoyl peroxide (16.7 mg, 0.0700 mmol). This suspension was stirred and heated to reflux (~120 °C) for 2 h. The reaction was monitored for consumption of the starting material by TLC. The reaction mixture was cooled to 0 °C and filtered. The filtrate was concentrated *in vacuo* and the residue was recrystallized from $CHCl_3$/hexane as follows: warm $CHCl_3$ was added until the crude solid was dissolved; then a generous amount of hexane at RT was added until precipitation occurred; the resultant suspension was cooled in the freezer overnight. The next morning the solvent was filtered off to give 2,7-Bis(bromomethyl)naphthalene as a colourless solid (310 mg, 77% yield); **$R_f$** (5% EtOAc in hexane) = 0.34; **mp** = 150-155 °C, lit.[260] 147-148 °C; **$\nu_{max}$** (neat)/cm$^{-1}$ 842 (CBr); **$^1$H NMR** $\delta$ (400 MHz, $CDCl_3$) 7.84-7.78 (4H m, Ar*H*), 7.52 (2H, dd, *J* = 8.4 & 1.8 Hz, Ar*H*), 4.65 (s, 4H, 2 × $CH_2$) **$^{13}$C NMR** $\delta$ (126 MHz, $CDCl_3$) 136.00 (2 × C), 133.13 (C), 132.85 (C), 128.75 (2 × CH), 128.03 (2 × CH), 127.66 (2 × CH), 33.86 (2 × $CH_2$).

All spectroscopic data were in good agreement with the literature.[248,184]

**(*S*)-(5-Ethyl-1-{7-[5-ethyl-2-((*S*)-hydroxy-quinolin-4-yl-methyl)-1-aza-bicyclo[2.2.2]oct-1-ylmethyl]-naphthalen-2-ylmethyl}-1-aza-bicyclo[2.2.2]oct-2-yl)-quinolin-4-yl-methanol dibromide 257**

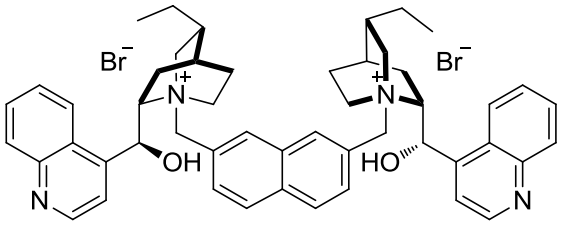


Bis(bromomethyl)naphthalene **256** (220 mg, 0.700 mmol) and (+)-hydrocinchonidine **255** (424 mg, 1.43 mmol) were suspended in a mixture of EtOH (1 ml), DMF (2.50 ml), and $CHCl_3$ (423 μl). This suspension was heated to reflux (100-120 ºC) and stirred vigorously for 2 h. The reaction was monitored by TLC for consumption of the starting material bis(bromomethyl) naphthalene **256**. The reaction mixture was allowed to cool to RT and MeOH (4.30 ml) and $Et_2O$ (12.80 ml) were added. This suspension was stirred at room temperature for 1 h. The crude, light-pink precipitate, was removed by filtration, rinsed with $Et_2O$ (3 × 10 ml) and the product **257** was isolated as a pink solid (450 mg, 71% yield); $\mathbf{R_f}$ (MeOH) = 0.10; **mp** = 170 °C (decomp); $\mathbf{[\alpha]_D}$ = +115 (c 1.00, MeOH), lit.[184] ent-**257** −127 (c 0.57, MeOH) $\mathbf{\nu_{max}}$ (neat)/$cm^{-1}$ 3101 (OH); **$^1$H NMR** $\delta$ (500 MHz, $(CD_3)_2CO$) 9.02 (2H, d, *J* = 4.5 Hz, Ar*H*), 8.49 (2H, s, Ar*H*), 8.37 (2H, d, *J* = 8.5 Hz, Ar*H*), 8.24 (2H, d, *J* = 8.5 Hz, Ar*H*), 8.13 (2H, d, *J* = 8.5 Hz, Ar*H*), 8.00 (2H, d, *J* = 8.5 Hz, Ar*H*), 7.90 (2H, d, *J* = 4.5 Hz, Ar*H*), 7.87 (2H, t, *J* = 7.2 Hz, Ar*H*), 7.75 (2H, t, *J* = 7.2 Hz, Ar*H*), 6.88 (2H, d, *J* = 3.5 Hz, 2 × C*H*OH), 6.59 (2H, s, 2 × O*H*), 5.31 (2H, d, *J* = 12.5 Hz, ArC$H_2$N), 5.12 (2H, d, *J* = 12.5 Hz, ArC$H_2$N), 4.15-4.01 (2H, m, 2 × C*H*), 3.97 (2H, t, *J* = 10.0 Hz, CHC$H_a$H$_b$N), 3.61 (2H, t, *J* = 10.0 Hz, CHCH$_a$$H_b$N), 3.11-2.92 (2H, m, 2 × C*H*N), 2.39-2.22 (2H, m, C$H_2$), 1.87 (2H, br s, 2 × C*H*C$H_2$C$H_3$), 1.85-1.62 (8H, m, 4 × C$H_2$), 1.60-1.44 (4H, m, 2 × C$H_2$C$H_3$), 1.16-0.98 (2H, m, C$H_2$), 0.86 (6H, t, *J* = 7.2 Hz, 2 × $CH_3$); **$^{13}$C NMR** $\delta$ (126 MHz, $(CD_3)_2CO$) 150.22 (2 × CH), 147.66 (2 × C), 145.07 (2 × C), 134.54 (2 × CH), 133.52 (C), 132.28 (C), 131.70 (2 ×

CH), 129.86 (2 × CH), 129.45 (2 × CH), 128.32 (2 × CH), 127.23 (2 × CH), 126.51 (2 × C), 124.40 (2 × C), 123.87 (2 × CH), 120.21 (2 × CH), 67.35 (2 × CH), 64.85 (2 × CH), 62.20 (2 × $CH_2$), 56.25 (2 × $CH_2$), 55.96 (2 × $CH_2$), 34.76 (2 × CH), 24.11 (2 × CH), 23.83 (2 × $CH_2$), 23.55 (2 × $CH_2$), 20.40 (2 × $CH_2$), 11.30 (2 × $CH_3$); ***m/z*** (ESI+) 373 ($[M/2\text{-}2Br]^{2+}$, 100%), 157 (63).

All spectroscopic data were in good agreement with the literature.[248,184]

**(*S*)-(1-{7-[2-((*S*)-Allyloxy-quinolin-4-yl-methyl)-5-ethyl-1-aza-bicyclo[2.2.2]oct-1-ylmethyl]-naphthalen-2-ylmethyl}-5-ethyl-1-aza-bicyclo[2.2.2]oct-2-yl)-quinolin-4-yl- Allyloxy-methanol dibromide 258**

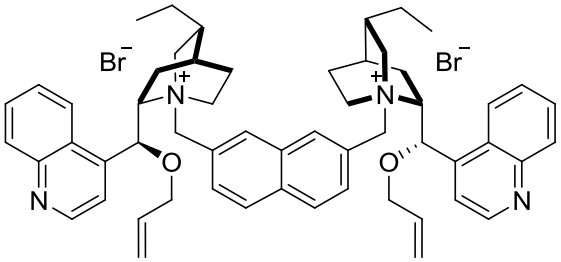


To a suspension of 2,7-bis(hydro-cinchonidinium-N-methyl) naphthalene dibromide (400 mg, 0.440 mmol) in DCM (1.26 ml) allyl bromide (224 μl, 2.65 mmol) was added, followed by KOH (4.41 ml, 50% aq., 84.0 mmol). The reaction was monitored for the consumption of the starting material by LC-MS. The reaction was quenched by addition of $H_2O$ (20 ml). The suspension was then extracted with DCM (3 × 50 ml). The combined organic layers were dried over $MgSO_4$, filtered and concentrated *in vacuo*. The residue was purified by recrystallization thusly: the crude solid was dissolved in a minimal amount of warm DCM; then hexane at RT was added generously until precipitation occurred. This precipitate was filtered immediately to yield the allylated product **258** as a light-orange solid (400 mg, 92% yield); $\mathbf{R_f}$ (100% MeOH) = 0.15; **mp** = 175 °C (decomposition); $\mathbf{[\alpha]_D}$ = +139 (c 1.00, $CHCl_3$), lit.[184] ent-**258** −196 (c 0.62, $CHCl_3$) $\mathbf{\nu_{max}}$ (neat)/$cm^{-1}$ 1058 (CO); **$^1$H NMR** $\delta$ (500 MHz, $(CD_3)_2CO$) 9.04 (2H, d, *J* = 4.5 Hz, Ar*H*), 8.44 (2H, s, Ar*H*), 8.33 (2H, d, *J* = 8.5 Hz, Ar*H*), 8.25 (2H, d, *J* = 8.5 Hz,

Ar*H*), 8.16 (2H, d, *J* = 8.5 Hz, Ar*H*), 7.97 (2H, d, *J* = 8.5 Hz, Ar*H*), 7.89 (2H, t, *J* = 7.3 Hz, Ar*H*), 7.78 (2H, t, *J* = 7.3 Hz, Ar*H*), 7.74 (2H, d, *J* = 4.5 Hz, Ar*H*), 6.53 (2H, s, 2 × C*H*O), 6.21 (2H, ddt, *J* = 17.1 & 10.6 & 5.3 Hz, 2 × C*H*$CH_{cis}H_{trans}$), 5.51 (2H, dd, *J* = 17.1 & 1.6 Hz, 2 × $CHCH_{cis}H_{trans}$), 5.36 (2H, d, *J* = 13.0 Hz, Ar$CH_2$N), 5.33 (2H, dd, *J* = 10.6 & 1.6 Hz, 2 × $CHCH_{cis}H_{trans}$), 5.14 (2H, d, *J* = 13.0 Hz, Ar$CH_2$N), 4.45 (2H, dd, *J* = 12.7 & 5.1 Hz, $CH_2$), 4.16 (2H, br t, *J* = 11.5 Hz, $CH_2$), 4.12-3.98 (4H, m, $CH_2$ + 2 × C*H*), 3.63-3.53 (2H, m, $CH_2$), 3.46-3.35 (4H, m, 2 × $CHCH_2$N), 2.37-2.25 (2H, m, $CH_2$), 2.19-2.08 (2H, m, $CH_2$), 2.00 (2H, br s, 2 × C*H*$CH_2CH_3$), 1.80-1.75 (4H, m, $CH_2$ + 2 × C*H*), 1.52 (2H, br t, *J* = 11.5 Hz, $CH_2$), 1.32-1.11 (4H, m, 2 × $CH_2CH_3$), 0.71 (6H, t, *J* = 7.3 Hz, 2 × $CH_3$); **$^{13}$C NMR** $\delta$ (126 MHz, $(CD_3)_2CO$) 150.27 (2 × CH), 148.07 (2 × C), 141.27 (2 × C), 134.51 (2 × CH), 134.33 (2 × CH), 133.58 (C), 132.17 (C), 131.81 (2 × CH), 129.98 (2 × CH), 129.67 (2 × CH), 128.33 (2 × CH), 127.46 (2 × CH), 126.33 (2 × C), 125.12 (2 × C), 123.76 (2 × CH), 119.73 (2 × CH), 117.47 (2 × $CH_2$), 72.11 (2 × CH), 69.28 (2 × $CH_2$), 67.74 (2 × CH), 63.43 (2 × $CH_2$), 61.49 (2 × $CH_2$), 51.23 (2 × $CH_2$), 34.98 (2 × CH), 25.21 (2 × $CH_2$), 24.82 (2 × $CH_2$), 23.66 (2 × CH), 20.63 (2 × $CH_2$), 11.27 (2 × $CH_3$); ***m/z*** (ESI+) 413 ($[M/2-2Br]^{2+}$, 37%), 157 (90), 130 (100).

All spectroscopic data were in good agreement with the literature.[248,184]

**1-Anthracen-9-ylmethyl-2-((*R*)-methoxy-quinolin-4-yl-methyl)-5-vinyl-1-azonia-bicyclo[2.2.2]octane iodide 267**

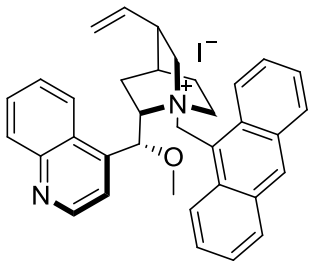


To a suspension of *N*-(9-anthracenylmethyl)cinchonidium chloride (2.20 g, 4.22 mmol) in DCM (30 ml) were added methyl iodide (1.69 g, 21.2 mmol) and NaOH (0.660 ml,

50% aq., 12.7 mmol). The resulting mixture was stirred at RT for 4-5 h, during which time all of the solids were dissolved. The mixture was diluted with $CHCl_3$ (300 ml), washed with water (3 × 20 ml) and NaCl (20 ml, sat. aq.). The combined organic layers were dried over $MgSO_4$, filtered and concentrated *in vacuo*. The residue was poured onto $Et_2O$ (50 ml) and the mixture was stirred at RT for 1 h. The suspension was filtered and the dark orange solid was collected and used for the next step without further purification (2.30 g, 86% yield); **$R_f$** (20% MeOH in DCM) = 0.21; **mp** = 180-185 °C; **$[\alpha]_D$** = –294 (c 1.0, DCM), lit.[247] –288 (c 1.0, DCM); **$\nu_{max}$** (neat)/$cm^{-1}$ 1640 (CN); **$^1$H NMR** $\delta$ (500 MHz, $CDCl_3$) 9.67 (1H, d, *J* = 9.1 Hz, Ar*H*), 9.06 (1H, d, *J* = 4.4 Hz, Ar*H*), 8.67 (1H, s, Ar*H*), 8.36-8.31 (1H, m, Ar*H*), 8.20 (1H, d, *J* = 9.1 Hz, Ar*H*), 8.15 (1H, d, *J* = 8.4 Hz, Ar*H*), 8.06 (1H, d, *J* = 8.4 Hz, Ar*H*), 7.99-7.91 (1H, m, Ar*H*), 7.92-7.81 (2H, m, Ar*H*), 7.75-7.68 (2H, m, Ar*H*), 7.62-7.55 (3H, m, Ar*H*), 7.07 (1H, d, *J* = 14.0 Hz), 6.53 (1H, brs, C*H*O), 6.05-5.84 (1H, m, C*H*$CH_{cis}H_{trans}$), 5.19 (1H, d, *J* = 17.1 Hz, $CHCH_{cis}H_{trans}$), 5.07 (1H, d, *J* = 10.5 Hz, $CHCH_{cis}H_{trans}$), 4.98-4.87 (1H, m), 4.54-4.40 (1H, m), 3.82 (3H, s, OMe), 3.13-3.02 (2H, m), 2.73-2.65 (1H, m), 2.42-2.33 (1H, m), 2.04-1.87 (2H, m), 1.59-1.36 (4H, m); **$^{13}$C NMR** $\delta$ (126 MHz, $CD_3OD$) 151.09 (CH), 149.38 (C), 142.96 (C), 138.52 (CH), 134.79 (C), 134.66 (C), 133.99 (CH), 133.11 (C), 133.08 (C), 131.50 (CH), 131.30 (CH), 131.21 (CH), 130.66 (CH), 129.46 (CH), 129.39 (2 × CH), 127.23 (C), 126.65 (CH), 126.63 (CH), 125.32 (CH), 124.79 (2 × CH), 124.32 (CH), 121.66 (CH), 118.94 (C), 117.79 ($CH_2$), 70.31 (CH), 63.46 ($CH_2$), 57.52 (CH), 57.51 ($CH_2$), 53.82 ($CH_2$), 39.53 ($CH_3$), 27.29 (CH), 26.22 ($CH_2$), 23.09 ($CH_2$); ***m/z*** (ESI+) 499 ($[M\text{-}I]^+$, 100%), 309 (7), 191 (10).

All spectroscopic data were in good agreement with the literature.[247]

**(*S*)-2-(Benzhydrylidene-amino)-4-methyl-pent-4-enoic acid *tert*-butyl ester 252**

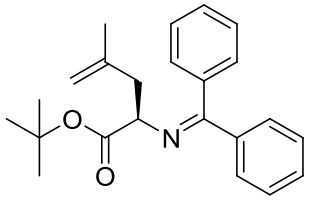

**Method A**

To a suspension of Schiff base **148** (50.0 mg, 0.169 mmol), chiral catalyst **267** (10.6 mg, 0.0169 mmol), $[PdCl(\pi\text{-}C_3H_5)]_2$ (5.2 mg, 0.0140 mmol) and DDPE (7.00 mg, 0.0169 mmol) in toluene (0.56 ml) were added allyl carbonate **217** (49.0 mg, 0.340 mmol) then KOH (44.0 µl, 50% aq., 0.850 mmol), at 0 °C. The reaction mixture was stirred at 0 °C until the starting material had been consumed (~7 h), and then the mixture was diluted with $Et_2O$ (15 ml). The organic phase was washed with $NaHCO_3$ (3 × 5 ml, sat. aq.) and NaCl (5 ml, sat. aq.). The organic layer was dried over $Na_2SO_4$, filtered, and concentrated *in vacuo*. Flash chromatography (dry loaded basic silica*, 1% EtOAc in hexane) gave the product as a colourless solid (51.0 mg, 85% yield, 5 to 15 % ee, see table **6**).The enantioselectivity was determined by chiral HPLC Agilent 1100 (Chiralcel OD-H column, 1% 2-propanol in hexane, 0.8 ml $min^{-1}$, 254 nm). $R_t$ (S-major) = 4.91 min, $R_t$ (R-minor) = 5.58 min.

**Method B**

To a suspension of Schiff base **148** (50.0 mg, 0.169 mmol) and chiral catalyst **258** (1.70 mg, 0.00169 mmol) in a mixture of toluene/$CHCl_3$ (3/1, 1 ml) methallyl bromide **251** (85.0 µl, 0.850 mmol) was added. The reaction mixture was then cooled to 0 °C and KOH (0.25 ml, 50% aq., 4.75 mmol) was added. The reaction mixture was stirred at 0 °C until the starting material had been consumed (~10 h). The suspension was diluted with Et2O (20 ml), washed with water (2 × 5 ml), dried over MgSO4, filtered and concentrated in vacuo. Flash chromatography (dry loaded basic silica*, 1% EtOAc in hexane) gave the product as a colourless solid (55.0 mg, 92% yield, 91 % ee). The enantioselectivity was determined by chiral HPLC (Chiralcel OD-H column, 1% 2-

propanol in hexane, 1.0 ml $min^{-1}$, 254 nm). $R_t$ (S-minor) = 4.96 min, $R_t$ (R-major) = 5.70 min. (Fig. **53**)

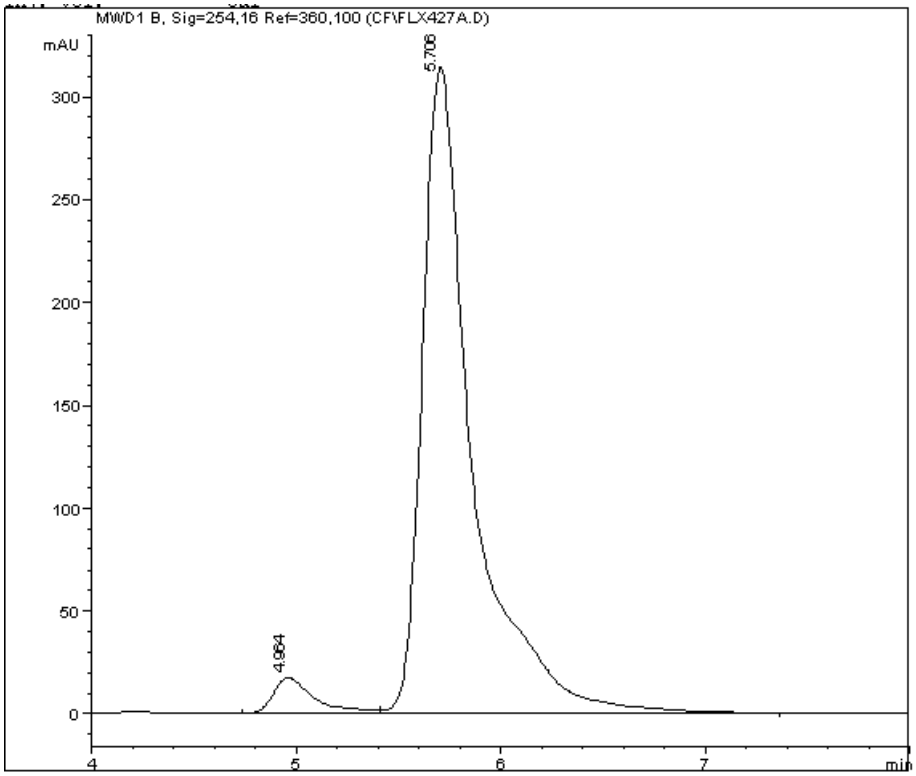


| Meas. R | Area % | Width | Symmetr |
|---|---|---|---|
| 4.964 | 4.341 | 0.207 | 0.513 |
| 5.706 | 95.659 | 0.249 | 0.499 |

**Figure 53**: HPLC traces for enantioselective alkylation of **148**.

**Appendix 1**: Spectroscopic data of biotinylated anisomycin **28**

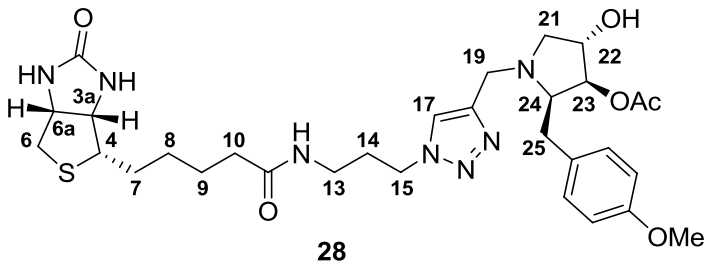


**28**

| **$^1$H** | **Bio−$N_3$** | **Ani−≡** | **Bio-Ani** |
|---|---|---|---|
| $C_{3a}H$ | 4.30 **dd**, 7.8, 4.6 | | 4.30 **dd**, 7.8, 4.5 |
| $C_4H$ | 3.23-3.19 **m** | | 3.21-3.18 **m** |
| $C_{6a}H$ | 4.49 **dd**, 7.8, 4.6 | | 4.52-4.48 **m** |
| $C_6H_aH_b$ | 2.93 **dd**, 12.7, 5.0 | | 2.93 **dd**, 13.1, 5.0 |
| $C_6H_aH_b$ | 2.71 **d**, 12.7 | | 2.73 **d**, 13.0 |
| $C_7H_2$ | 1.70-1.54 **m** | | 1.84-1.55 **m** |
| $C_8H_2$ | 1.49-1.38 **m** | | 1.49-1.38 **m** |
| $C_9H_2$ | 1.70-1.54 **m** | | 1.84-1.55 **m** |
| $C_{10}H_2$ | 2.21 **t**, 7.3 | | 2.23 **t**, 7.3 |
| $C_{13}H_2$ | 3.25 **d**, 6.7 | | 3.23 **t**, 6.7 |
| $C_{14}H$ | 1.75 **qn**, 6.7 | | 2.13 **qn**, 6.7 |
| $C_{15}H_2$ | 3.36 **t**, 6.7 | | 4.47 **t**, 7.0 |
| $C_{17}H$ | | | 7.97 **s** |
| $C_{19}H_cH_d$ | | 3.58 **d**, 2.3 | 4.06 **d**, 14.2 |
| $C_{19}H_cH_d$ | | 3.58 **d**, 2.3 | 3.84 **d**, 14.2 |
| $C_{21}H_eH_f$ | | 3.34 **dd**, 9.8, 7.0 | 3.41-3.35 **m** |
| $C_{21}H_eH_f$ | | 2.61 **dd**, 9.8, 7.0 | 2.52 **dd**, 10.7, 4.2 |
| $C_{22}H$ | | 4.13 **t**, 7.0 | 4.04-3.99 **m** |
| $C_{23}H$ | | 4.47 **dd**, 5.7, 1.60 | 4.66 **dd**, 5.0, 1.5 |
| $C_{24}H$ | | 3.21 **dt**, 10.2, 5.2 | 3.16 **dd**, 9.4, 4.5 |
| OAc | | 2.14 **s** | 2.12 **s** |
| $C_{25}H_gH_h$ | | 2.85 **dd**, 13.4, 4.5 | 3.05 **dd**, 13.1, 5.0 |
| $C_{25}H_gH_h$ | | 2.70 **dd**, 13.4, 10.2 | 2.74 **dd**, 13.4, 10.2 |
| OMe | | 3.78 **s** | 3.77 **s** |

**Table 8:** NMR data ($^1$H) of compound **28** and its starting materials **28** and **264**.

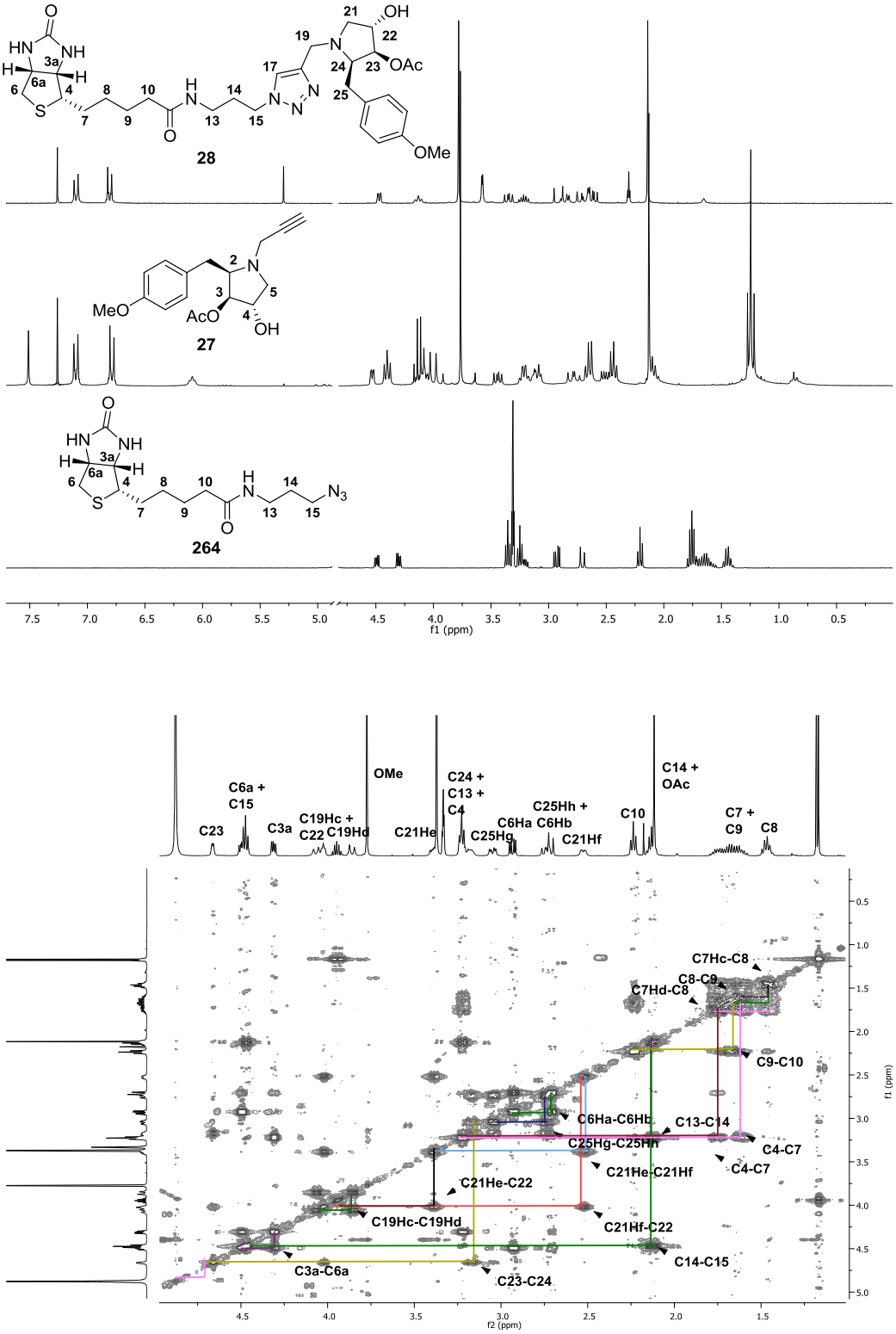


**Figure 54**: $^{1}$H spectra of compound **28** and its starting materials **27** and **264** and COSY spectrum of **28.**

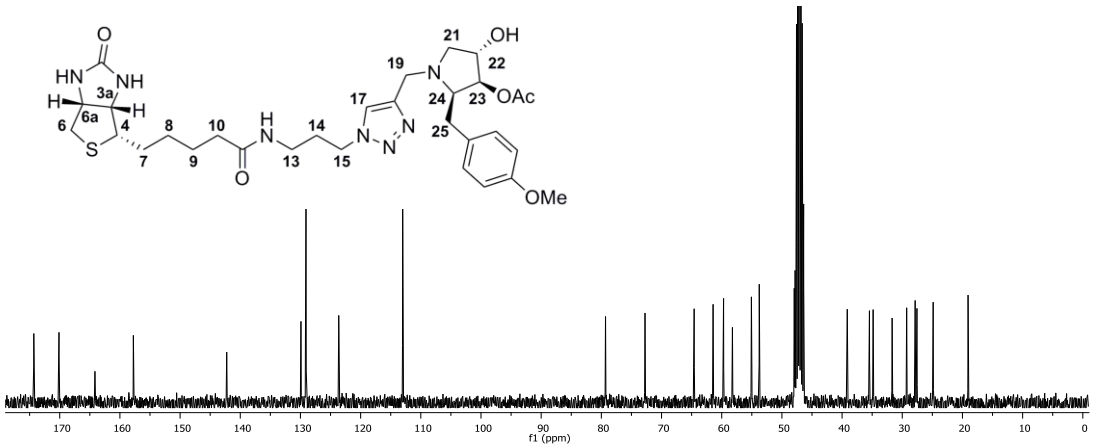


**Figure 55**: $^{13}C$ spectrum of compound **28**.

| $^{13}C$ | **Bio-Ani** |
|---|---|
| $C_1$ | 166.05 |
| $C_{3a}H$ | 63.33 |
| $C_4H$ | 56.97 |
| $C_{6a}H$ | 61.60 |
| $C_6H_2$ | 41.04 |
| $C_7H_2$ | 29.46 |
| $C_8H_2$ | 29.76 |
| $C_9H_2$ | 26.77 |
| $C_{10}H_2$ | 36.74 |
| $C_{11}$ | 176.21 |
| $C_{13}H_2$ | 37.35 |
| $C_{14}H$ | 31.17 |
| $C_{15}H_2$ | 48.76 |
| $C_{17}H$ | 125.54 |
| $C_{18}$ | 144.16 |
| $C_{19}H_2$ | 48.30 |
| $C_{21}H_2$ | 60.12 |
| $C_{22}H$ | 74.65 |
| $C_{23}H$ | 81.21 |
| $C_{24}H$ | 66.48 |
| C, OAc | 172.02 |
| $CH_3$, OAc | 20.97 |
| $C_{25}H_2$ | 33.58 |
| C, Ar | 131.82 |
| C, Ar | 159.67 |
| $CH_3$, OMe | 55.66 |

**Table 9**: $^{13}C$ spectrum of compound **28** and its $^{13}C$ data.

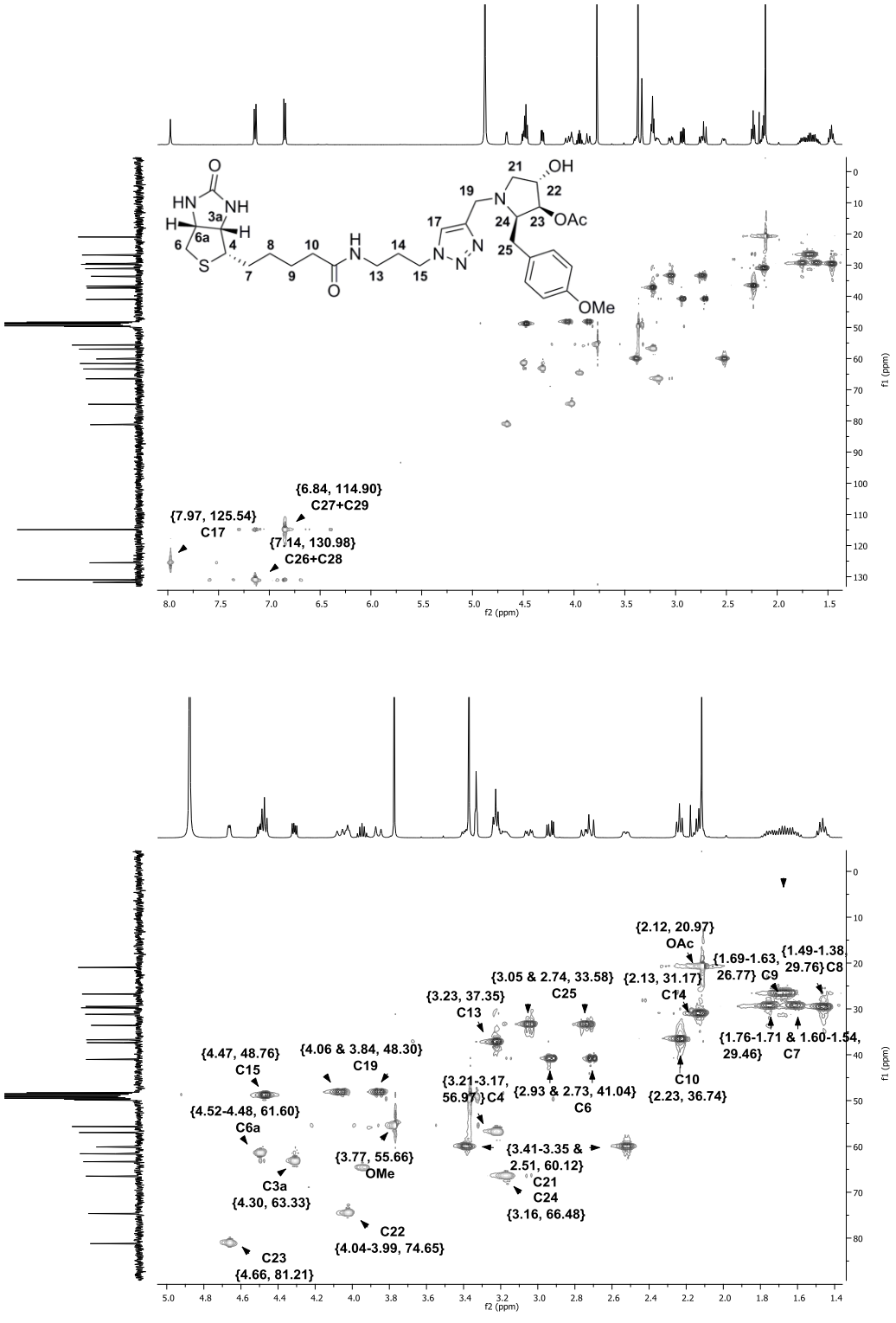


**Figure 56**: HSQC spectrum of compound **28**.

## Abbreviations

| | |
|---|---|
| Å | Angstrom |
| ABPP | Activity-based probe profiling |
| Ac | Acetyl |
| Ag | Antigen |
| AIBN | Azobisisobutyronitrile |
| ATP | Adenosine triphosphate |
| aq | Aqueous |
| Ar | Aryl |
| Boc | Di-tert-butyl dicarbonate |
| Bn | Benzyl |
| BODIPY | Dipyrromethene boron difluoride |
| BOP | Benzotriazol-1-yloxy tris (dimethylamino)-phosphonium hexafluorophosphate |
| BSA | Bovine serum albumin |
| CbzCl | Benzyl chloroformate |
| CID | Collision-induced dissociation |
| CML | Chronic myeloid leukemia |
| CCCP | Compound-centric chemical proteomics |
| COSY | Correlation spectroscopy |
| CSA | Camphorsulfonic acid |
| CuAAC | Copper-catalysed azide-alkyne cycloaddition |
| DCM | Dichloromethane |
| DIBAL | Diisobutylaluminium hydride |
| DIPEA | *N*,*N*-Diisopropylethylamine |
| DEPBT | 3-(Diethoxy-phosphoryloxy)-3H-benzo[d][1,2,3] triazin-4-one |
| DEPT | Distortionless enhancement polarisation transfer |
| 2D-GE | Two-dimensional gel electrophoresis |
| DIC | Diisopropylcarbodiimide |

| | |
|---|---|
| DUB | Deubiquitinating |
| DMAP | 4-Dimethylaminopyridine |
| DME | Dimethyl ether |
| DMF | Dimethylformamide |
| DMP | Dess-Martin periodinane |
| DNA | Deoxyiribonucleic acid |
| DPPE | 1,2-Bis(diphenylphosphino)ethane |
| DSC | Disuccinimidyl carbonate |
| ee | enantiomeric excess |
| EDC | Ethyl (dimethylaminopropyl) carbodiimide |
| EDTA | Ethylenediaminetetraacetic acid |
| ERK | Extracellular signal regulated protein kinase |
| ELISA | Enzyme-linked immunosorbent assay |
| EM | Electron microscopy |
| ESI | Electrospray ionization |
| Et | Ethyl |
| EtOH | Ethanol |
| Fab | Fragment antigen-binding |
| FAB | Fast atom bombardment |
| FBS | Fetal bovine serum |
| FDA | Food and Drug Administration |
| FKBP | FK506 binding protein |
| Fmoc | Fluorenylmethoxycarbonyl |
| FRET | Forster resonance energy transfer |
| h | Hours |
| HABA | 2-(4-hydroxyphenylazo)-benzoic acid |
| HATU | 2-(7-Aza-1H-benzotriazole-1-yl)-1,1,3,3-tetramethyluronium hexafluorophosphate |
| HCV | Hepatitis C virus |
| HEK | Human embryonic kidney |

| | |
|---|---|
| HEPES | 4-(2-hydroxyethyl)-1-piperazineethanesulfonic acid |
| HIV | Human immunodeficiency virus |
| HOAT | 1-Hydroxy-7-Azabenzotriazole |
| HOBt | Hydroxybenzotriazole |
| HPIAC | High performance immunoaffinity chromatography |
| HPLC | High performance liquid chromatography |
| HRMS | High Resolution Mass Spectrometry |
| HSQC | Heteronuclear Single Quantum Coherence |
| IBs | Inclusion bodies |
| ICAT | Isotope-coded affinity tag |
| iTRAQ | Isobaric tag for relative and absolute quantification |
| Ig | Immunoglobulin |
| IMAC | Immobilised metal ion affinity chromatography |
| IR | Infra red |
| JNK | c-Jun N-terminal kinase |
| kDa | Kilodalton |
| LC-MS | Liquid chromatography-mass spectrometry |
| LDI | Laser desorption ionization |
| LRMS | Low Resolution Mass Spectrometry |
| MAGL | Monoacylglycerol lipase |
| MALDI-TOF | Matrix assiste laser/desorption ionization-time of flight |
| MAPK | Mitogen activated protein kinase |
| MAPKK | Mitogen activated protein kinase kinase |
| MAPKKK | Mitogen activated protein kinase kinase kinase |
| MAS | Magic angle spinning |
| Me | Methyl |
| Mes | 2,4,6-trimethylphenyl |
| MHz | Megahertz |
| mp | Melting point |
| MTBE | Methyl tertiary butyl ether |

| | |
|---|---|
| MTD | Maximum tolerated dose |
| NBS | *N*-Bromosuccinimide |
| NMM | *N*-Methyl morpholine |
| NOBA | m-nitrobenzyl alcohol |
| μ-BACC | microbead-based affinity chromatography |
| min | Minutes |
| MRC PPU | Medical research council protein phosphorilation unit |
| MS | Mass spectrometry |
| NAD | Nicotinamide adenine dinucleotide |
| NADP | Nicotinamide adenine dinucleotide phosphate |
| NBD | Nitrobenz-2-oxa-1,3-diazole |
| NHS | *N*-hydroxy succinimide |
| NMA | Methoxy-(1-naphthyl) acetic acid |
| nm | nanometer |
| NMR | Nuclear magnetic resonance |
| 3-NOBA | 3-nitro benzyl alcohol |
| PDGF | Platelet-derived growth factor |
| PBS | Phosphate Buffered Saline |
| Peg | Polyethylene glycol |
| Ph | Phenyl |
| p*I* | Isoelectric point |
| ppm | Parts per million |
| PTC | Phase transfer catalyst |
| PTMs | Post-translational modifications |
| PTSA | p-Toluenesulfonic acid |
| RCM | Ring closing metathesis |
| RNP | Ribonucleoprotein |
| qNIRFABPs | Quenched near-infrared fluorescent activity based probes |
| RCC | Renal cell carcinoma |
| RNA | Ribonucleic acid |

| | |
|---|---|
| $R_f$ | Retention factor |
| RT | Room temperature |
| SAPK | Stress activated protein kinase |
| SAR | Structure activity relationship |
| SDS-PAGE | sodium dodecyl sulfate polyacrylamide gel electrophoresis |
| SILAC | Stable isotope labelling by amino acids |
| SPA | Solution phase analogue |
| *t*-BuOH | *tert*-butanol |
| TBDMSCl | Tert-Butyldimethylchlorosilane, |
| TBTA | Tris-(1-benzyl-1*H*-[1,2,3]triazol-4-ylmethyl)-amine |
| TEDOR | Transferred-echo double resonance |
| TEMPO | 2,2,6,6-Tetramethylpiperidin-1-yloxyl |
| TFA | Trifluroacetic acid |
| THF | Tetrahydrofuran |
| THIOG | thioglycerol |
| TLC | Thin layer chromatography |
| UV | Ultra violet |
| VPP | Vancomycin photoaffinity probe |

## References


(1) Cuatrecasas, P.; Anfinsen, C. B. *Annu. Rev. Biochem.* **1971**, *40*, 259-278.

(2) *Affinity Chromatography Principles and methods*; Amersham Biosciences, GE Healthcare 2003 (18-1022-29).

(3) Hage, D. S. *Clin. Chem.* **1999**, *45*, 593-615.

(4) Phillips, T. M. *J. Chromatogr., A* **1991**, *550*, 741-749.

(5) Firer, M. A. *J. Biochem. Biophys. Methods* **2001**, *49*, 433-442.

(6) Narayanan, S. R.; Crane, L. J. *Trends Biotechnol.* **1990**, *8*, 12-16.

(7) Azarkan, M.; Huet, J.; Baeyens-Volant, D.; Looze, Y.; Vandenbussche, G. *J. Chromatogr., B* **2007**, *849*, 81-90.

(8) Zamolo, L.; Salvalaglio, M.; Cavallotti, C.; Galarza, B.; Sadler, C.; Williams, S.; Hofer, S.; Horak, J.; Lindner, W. *J. Phys. Chem. B* **2010**, *114*, 9367-9380.

(9) Schiel, J. E.; Joseph, K. S.; Hage, D. S. *Advances in Chromatography*; CRC Press, 2010.

(10) Campbell, D. H.; Luescher, E.; Leonard Lerman S. *Proc. Nat. Acad. Sci.* **1951**, *37*, 575-578.

(11) Kojima, K. *J. Biochem. Biophys. Methods* **2001**, *49*, 241-251.

(12) Leitner, A.; Lindner, W. *J. Chromatogr., B* **2004**, *813*, 1-26.

(13) Rix, U.; Superti-Furga, G. *Nat. Chem. Biol.* **2009**, *5*, 616-624.

(14) Choudhary, C.; Mann, M. *Nat. Rev. Mol. Cell. Biol.* **2010**, *11*, 427-439.

(15) Domon, B.; Aebersold, R. *Science* **2006**, *312*, 212 -217.

(16) Ahrens, C. H.; Brunner, E.; Qeli, E.; Basler, K.; Aebersold, R. *Nat. Rev. Mol. Cell. Biol.* **2010**, *11*, 789-801.

(17) Aebersold, R.; Mann, M. *Nature* **2003**, *422*, 198-207.

(18) Gygi, S. P.; Rist, B.; Gerber, S. A.; Turecek, F.; Gelb, M. H.; Aebersold, R. *Nat. Biotechnol.* **1999**, *17*, 994-999.

(19) Ong, S.; Mann, M. *Nat. Chem. Biol.* **2005**, *1*, 252-262.

(20) Geiger, T.; Cox, J.; Ostasiewicz, P.; Wisniewski, J. R.; Mann, M. *Nat. Meth.* **2010**, *7*, 383-385.

(21) Ross, P. L.; Huang, Y. N.; Marchese, J. N.; Williamson, B.; Parker, K.; Hattan, S.; Khainovski, N.; Pillai, S.; Dey, S.; Daniels, S.; Purkayastha, S.; Juhasz, P.; Martin, S.; Bartlet-Jones, M.; He, F.; Jacobson, A.; Pappin, D. J. *Mol. Cell. Proteomics* **2004**, *3*, 1154 -1169.

(22) Ghoreschi, K.; Laurence, A.; O'Shea, J. J. *Nat. Immunol.* **2009**, *10*, 356-360.

(23) Zhang, J.; Yang, P. L.; Gray, N. S. *Nat. Rev. Cancer* **2009**, *9*, 28-39.

(24) Bantscheff, M.; Eberhard, D.; Abraham, Y.; Bastuck, S.; Boesche, M.; Hobson, S.; Mathieson, T.; Perrin, J.; Raida, M.; Rau, C.; Reader, V.; Sweetman, G.; Bauer, A.; Bouwmeester, T.; Hopf, C.; Kruse, U.; Neubauer, G.; Ramsden, N.; Rick, J.; Kuster, B.; Drewes, G. *Nat. Biotechnol.* **2007**, *25*, 1035-1044.

(25) Rix, U.; Hantschel, O.; Durnberger, G.; Remsing Rix, L. L.; Planyavsky, M.; Fernbach, N. V.; Kaupe, I.; Bennett, K. L.; Valent, P.; Colinge, J.; Kocher, T.; Superti-Furga, G. *Blood* **2007**, *110*, 4055-4063.

(26) Wang, G.; Shang, L.; Burgett, A. W. G.; Harran, P. G.; Wang, X. *Proc. Nat. Acad. Sci.* **2007**, *104*, 2068 -2073.

(27) Sadaghiani, A. M.; Verhelst, S. H.; Bogyo, M. *Curr. Opin. Chem. Biol.* **2007**, *11*, 20-28.

(28) Patricelli, M. P.; Giang, D. K.; Stamp, L. M.; Burbaum, J. J. *Proteomics* **2001**, *1*, 1067-1071.

(29) Berkers, C. R.; Verdoes, M.; Lichtman, E.; Fiebiger, E.; Kessler, B. M.; Anderson, K. C.; Ploegh, H. L.; Ovaa, H.; Galardy, P. J. *Nat. Meth.* **2005**, *2*, 357-362.

(30) Schmidinger, H.; Birner-Gruenberger, R.; Riesenhuber, G.; Saf, R.; Susani-Etzerodt, H.; Hermetter, A. *ChemBioChem* **2005**, *6*, 1776-1781.

(31) Greenbaum, D.; Baruch, A.; Hayrapetian, L.; Darula, Z.; Burlingame, A.; Medzihradszky, K. F.; Bogyo, M. *Mol. Cell. Proteomics* **2002**, *1*, 60 -68.

(32) Chan, E. W. S.; Chattopadhaya, S.; Panicker, R. C.; Huang, X.; Yao, S. Q. *J. Am. Chem. Soc.* **2004**, *126*, 14435-14446.

(33) Kato, D.; Boatright, K. M.; Berger, A. B.; Nazif, T.; Blum, G.; Ryan, C.; Chehade, K. A. H.; Salvesen, G. S.; Bogyo, M. *Nat. Chem. Biol.* **2005**, *1*, 33-38.

(34) Kessler, B. M.; Tortorella, D.; Altun, M.; Kisselev, A. F.; Fiebiger, E.; Hekking, B. G.; Ploegh, H. L.; Overkleeft, H. S. *Chem. Biol.* **2001**, *8*, 913-929.

(35) Borodovsky, A.; Ovaa, H.; Kolli, N.; Gan-Erdene, T.; Wilkinson, K. D.; Ploegh, H. L.; Kessler, B. M. *Chem. Biol.* **2002**, *9*, 1149-1159.

(36) Saxon, E.; Bertozzi, C. R. *Science* **2000**, *287*, 2007-2010.

(37) Rostovtsev, V. V.; Green, L. G.; Fokin, V. V.; Sharpless, K. B. *Angew. Chem. Int. Ed.* **2002**, *41*, 2596-2599.

(38) Speers, A. E.; Adam, G. C.; Cravatt, B. F. *J. Am. Chem. Soc.* **2003**, *125*, 4686-4687.

(39) Nomura, D. K.; Dix, M. M.; Cravatt, B. F. *Nat. Rev. Cancer* **2010**, *10*, 630-638.

(40) Jessani, N.; Niessen, S.; Wei, B. Q.; Nicolau, M.; Humphrey, M.; Ji, Y.; Han, W.; Noh, D.; Yates, J. R.; Jeffrey, S. S.; Cravatt, B. F. *Nat. Meth.* **2005**, *2*, 691-697.

(41) Jessani, N.; Liu, Y.; Humphrey, M.; Cravatt, B. F. *Proc. Nat. Acad. Sci.* **2002**, *99*, 10335 -10340.

(42) Chiang, K. P.; Niessen, S.; Saghatelian, A.; Cravatt, B. F. *Chem. Biol.* **2006**, *13*, 1041-1050.

(43) Nomura, D. K.; Long, J. Z.; Niessen, S.; Hoover, H. S.; Ng, S.; Cravatt, B. F. *Cell* **2010**, *140*, 49-61.

(44) Greenbaum, D.; Medzihradszky, K. F.; Burlingame, A.; Bogyo, M. *Chem. Biol.* **2000**, *7*, 569-581.

(45) Joyce, J. A.; Baruch, A.; Chehade, K.; Meyer-Morse, N.; Giraudo, E.; Tsai, F.; Greenbaum, D. C.; Hager, J. H.; Bogyo, M.; Hanahan, D. *Cancer Cell* **2004**, *5*, 443-453.

(46) Blum, G.; von Degenfeld, G.; Merchant, M. J.; Blau, H. M.; Bogyo, M. *Nat. Chem. Biol.* **2007**, *3*, 668-677.

(47) Edgington, L. E.; Berger, A. B.; Blum, G.; Albrow, V. E.; Paulick, M. G.; Lineberry, N.; Bogyo, M. *Nat. Med.* **2009**, *15*, 967-973.

(48) Fretz, H.; Albers, M. W.; Galat, A.; Standaert, R. F.; Lane, W. S.; Burakoff, S. J.; Bierer, B. E.; Schreiber, S. L. *J. Am. Chem. Soc.* **1991**, *113*, 1409-1411.

(49) Koteva, K.; Hong, H.; Wang, X. D.; Nazi, I.; Hughes, D.; Naldrett, M. J.; Buttner, M. J.; Wright, G. D. *Nat. Chem. Biol.* **2010**, *6*, 327-329.

(50) Leclercq, R.; Derlot, E.; Duval, J.; Courvalin, P. *N. Engl. J. Med.* **1998**, *319*, 157–161.

(51) Hutchings, M. I.; Hong, H.; Buttner, M. J. *Mol. Microbiol.* **2006**, *59*, 923-935.

(52) Stinson, S. C. *Chem. Eng. News* **1993**, *71*, 38-65.

(53) Lough, W. J. *J. High Resol. Chromatogr.* **1993**, *16*, 120-120.

(54) Porath, J. *Protein Expression Purif.* **1992**, *3*, 263-281.

(55) Hidalgo, A.; Betancor, L.; Mateo, C.; Lopez-Gallego, F.; Moreno, R.; Berenguer, J.; Guisan, J.; Fernandez-Lafuente, R. *Biotechnol. Prog.* **2004**, *20*, 1578-1582.

(56) Feng, G.; Hu, D.; Yang, L.; Cui, Y.; Cui, X.; Li, H. *Sep. Purif. Technol.* **2010**, *74*, 253-260.

(57) Harlow, E.; Lane, D. *Antibodies: a laboratory manual*; Cold spring harbor laboratory, 1988.

(58) Santala, V.; Saviranta, P. *J. Immunol. Methods* **2004**, *284*, 159-163.

(59) Cho, S.; Lee, S.; Chung, W.; Kim, Y.; Lee, Y.; Kim, B. *Electrophoresis* **2004**, *25*, 3730-3739.

(60) Sturm, M. G.; PhD thesis; University of Vienna **2010**.

(61) Sturm, M.; Leitner, A.; Lindner, W. *Bioconjugate Chem.* **2011**, *22*, 211-217.

(62) Vultur, A.; Buettner, R.; Kowolik, C.; Liang, W.; Smith, D.; Boschelli, F.; Jove, R. *Mol. Cancer Ther.* **2008**, *7*, 1185 -1194.

(63) Fernbach, N. V.; Planyavs ller, A.; Breitwieser, F. P.; Colinge, J.; Rix, U.; Bennett, K. L. *J. Proteome Res.* **2009**, *8*, 4753-4765.

(64) Rix, U.; Remsing Rix, L. L.; Terker, A. S.; Fernbach, N. V.; Hantschel, O.; Planyavsky, M.; Breitwieser, F. P.; Herrmann, H.; Colinge, J.; Bennett, K. L.; Augustin, M.; Till, J. H.; Heinrich, M. C.; Valent, P.; Superti-Furga, G. *Leukemia* **2010**, *24*, 44-50.

(65) Sobin, B. A.; Tanner, F. W. *J. Am. Chem. Soc.* **1954**, *76*, 4053.

(66) Lynch, J. E.; English, A. R.; Bauck, H.; Deligianis, H. *Antibiot. Chemother.* **1954**, *4*, 844-8.

(67) Hansen, J. L.; Moore, P. B.; Steitz, T. A. *J. Mol. Biol.* **2003**, *330*, 1061-1075.

(68) Schwardt, O.; Veith, U.; Gaspard, C.; Jager, V. *Synthesis* **1999**, 1473-1490.

(69) Nishina, H.; Wada, T.; Katada, T. *J. Biochem.* **2004**, *136*, 123 -126.

(70) Johnson, G. L.; Lapadat, R. *Science* **2002**, *298*, 1911-1912.

(71) Tibbles, L. A.; Woodgett, J. R. *Cell. Mol. Life Sci.* **1999**, *55*, 1230-1254.

(72) Mitsios, N.; Gaffney, J.; Kumar, P.; Krupinski, J.; Kumar, S.; Slevin, M. *Pathobiology* **2006**, *73*, 159-175.

(73) Chen, Y.; Tan, T. *Int. J. Oncol.* **2000**, *16*, 651-662.

(74) Zhu, X.; Raina, A. K.; Lee, H.; Casadesus, G.; Smith, M. A.; Perry, G. *Brain Res.* **2004**, *1000*, 32-39.

(75) Bayer, E. A.; Wilchek, M. *J. Chromatogr., A* **1990**, *510*, 3-11.

(76) Inverarity, I. A.; Viguier, R. F. H.; Cohen, P.; Hulme, A. N. *Bioconjugate Chem.* **2007**, *18*, 1593-1603.

(77) Inverarity, I. A.; PhD thesis; The University of Edinburgh **2007**.

(78) Landi, F.; Johansson, C. M.; Campopiano, D. J.; Hulme, A. N. *Org. Biomol. Chem.* **2010**, *8*, 56.

(79) Verhelst, S.; Fonović, M.; Bogyo, M. *Angew. Chem. Int. Ed.* **2007**, *46*, 1284-1286.

(80) Murphy, H. R.; Harris, H. W. *Anal. Biochem.* **1987**, *165*, 88-95.

(81) Hooker, J. M.; Kovacs, E. W.; Francis, M. B. *J. Am. Chem. Soc.* **2004**, *126*, 3718-3719.

(82) Nessen, M. A.; Kramer, G.; Back, J.; Baskin, J. M.; Smeenk, L. E. J.; de Koning, L. J.; van Maarseveen, J. H.; de Jong, L.; Bertozzi, C. R.; Hiemstra, H.; de Koster, C. G. *J. Proteome Res.* **2009**, *8*, 3702-3711.

(83) Gubbens, J.; Ruijter, E.; de Fays, L. E.; Damen, J. M. A.; de Kruijff, B.; Slijper, M.; Rijkers, D. T.; Liskamp, R. M.; de Kroon, A. I. *Chem. Biol.* **2009**, *16*, 3-14.

(84) Best, M. D. *Biochemistry* **2009**, *48*, 6571-6584.

(85) Moses, J. E.; Moorhouse, A. D. *Chem. Soc. Rev.* **2007**, *36*, 1249.

(86) Yu, Y.; Maeda, T.; Mamiya, J.; Ikeda, T. *Angew. Chem. Int. Ed.* **2007**, *46*, 881-883.

(87) Sagi, K.; Nakagawa, T.; Yamanashi, M.; Makino, S.; Takahashi, M.; Takayanagi, M.; Takenaka, K.; Suzuki, N.; Oono, S.; Kataoka, N.; Ishikawa, K.; Shima, S.; Fukuda, Y.; Kayahara, T.; Takehana, S.; Shima, Y.; Tashiro, K.; Yamamoto, H.; Yoshimoto, R.; Iwata, S.; Tsuji, T.; Sakurai, K.; Shoji, M. *J. Med. Chem.* **2003**, *46*, 1845-1857.

(88) Yamada, N.; Okuyama, K.; Serizawa, T.; Kawasaki, M.; Oshima, S. *J. Chem. Soc., Perkin Trans. 2* **1996**, 2707.

(89) Ono, Y.; Nakashima, K.; Sano, M.; Kanekiyo, Y.; Inoue, K.; Shinkai, S.; Sano, M.; Hojo, J. *Chem. Commun.* **1998**, 1477-1478.

(90) Debaene, F.; Da Silva, J. A.; Pianowski, Z.; Duran, F. J.; Winssinger, N. *Tetrahedron* **2007**, *63*, 6577-6586.

(91) Ghosh, A. K.; Doung, T. T.; McKee, S. P.; Thompson, W. J. *Tetrahedron Lett.* **1992**, *33*, 2781-2784.

(92) Benalil, A.; Carboni, B.; Vaultier, M. *Tetrahedron* **1991**, *47*, 8177-8194.

(93) Montalbetti, C. A.; Falque, V. *Tetrahedron* **2005**, *61*, 10827-10852.

(94) Hong, V.; Presolski, S.; Ma, C.; Finn, M. *Angew. Chem. Int. Ed.* **2009**, *48*, 9879-9883.

(95) Hein, J. E.; Fokin, V. V. *Chem. Soc. Rev.* **2010**, *39*, 1302.

(96) Himo, F.; Lovell, T.; Hilgraf, R.; Rostovtsev, V. V.; Noodleman, L.; Sharpless, K. B.; Fokin, V. V. *J. Am. Chem. Soc.* **2005**, *127*, 210-216.

(97) Chan, T. R.; Hilgraf, R.; Sharpless, K. B.; Fokin, V. V. *Org. Lett.* **2004**, *6*, 2853-2855.

(98) Ahlström, L.; Sparr Eskilsson, C.; Björklund, E. *TrAC, Trends Anal. Chem.* **2005**, *24*, 49-56.

(99) Voyksner, R. D.; Straub, R.; keever, J. T. *Environ. Sci. Technol.* **1993**, *27*, 1665–1672.

(100) Andrew, E. R.; Bradbury, A.; Eades, R. G. *Nature* **1958**, *182*, 1659.

(101) Lowe, I. J. *Phys. Rev. Lett.* **1959**, *2*, 285.

(102) McDermott, A.; Polenova, T. *Solid State NMR Studies of Biopolymers*; John Wiley & Sons, Inc., 2010.

(103) Alia, A.; Ganapathy, S.; Groot, H. J. M. *Photosynth. Res.* **2009**, *102*, 415-425.

(104) Wasmer, C.; Benkemoun, L.; Sabaté, R.; Steinmetz, M.; Coulary-Salin, B.; Wang, L.; Riek, R.; Saupe, S.; Meier, B. *Angew. Chem. Int. Ed.* **2009**, *48*, 4858-4860.

(105) van der Wel, P. C. A.; Lewandowski, J. R.; Griffin, R. G. *Biochemistry* **2010**, *49*, 9457-9469.

(106) Jehle, S.; Falb, M.; Kirkpatrick, J. P.; Oschkinat, H.; Rossum, B. V.; Althoff, G.; Carlomagno, T. *J. Am. Chem. Soc.* **2010**, *132*, 3842-3846.

(107) Bayer, E.; Albert, K.; Reiners, J.; Nieder, M.; Müller, D. *J. Chromatogr., A* **1983**, *264*, 197-213.

(108) Zumbrink, T.; Demiroglou, A.; Jennissen, H. P. *J. Mol. Recognit.* **1995**, *8*, 363-373.

(109) Pal, B.; Pradhan, P. K.; Jaisankar, P.; Giri, V. S. *Synthesis* **2003**, 1549-1552.

(110) Le, Z.; Chen, Z.; Hu, Y.; Zheng, Q. *Synthesis* **2004**, 208-212.

(111) Molina Pinilla, I.; Bueno Martínez, M.; Galbis, J. A. *Macromolecules* **2002**, *35*, 2985-2992.

(112) Matsumoto, H.; Kimura, T.; Hamawaki, T.; Kumagai, A.; Goto, T.; Sano, K.; Hayashi, Y.; Kiso, Y. *Bioorganic & Medicinal Chemistry* **2001**, *9*, 1589-1600.

(113) Somei, M.; Yamada, F.; Kurauchi, T.; Nagahama, Y.; Hasegawa, M.; Yamada, K. *Chem. Pharm. Bull.* **2001**, *49*, 87-96.

(114) Laitinen, O. H.; Hytönen, V. P.; Nordlund, H. R.; Kulomaa, M. S. *Cell Mol. Life Sci.* **2006**, *63*, 2992-3017.

(115) Plażuk, D.; Zakrzewski, J.; Salmain, M. *Org. Biomol. Chem.* **2011**, *9*, 408.

(116) Bogusiewicz, A.; Mock, N. I.; Mock, D. M. *Anal. Biochem.* **2004**, *331*, 260-266.

(117) N, M.; N, A.; J, G. *Chromatography* **2003**, *24*, 19-34.

(118) Dea, M. K.; Hamilton-Wessler, M.; Ader, M.; Moore, D.; Schäffer, L.; Loftager, M.; Vølund, A.; Bergman, R. N. *Diabetes* **2002**, *51*, 762 -769.

(119) Budin, G.; Moune-Dimala, M.; Leriche, G.; Saliou, J.; Papillon, J.; Sanglier-Cianférani, S.; Van Dorsselaer, A.; Lamour, V.; Brino, L.; Wagner, A. *ChemBioChem* **2010**, *11*, 2359-2361.

(120) Hartmann, I.; Hollweck, T.; Haffner, S.; Krebs, M.; Meiser, B.; Reichart, B.; Eissner, G. *J. Immunol. Methods* **2010**, *363*, 80-89.

(121) Narayan, V.; Eckert, M.; Zylicz, A.; Zylicz, M.; Ball, K. L. *Journal of Biological Chemistry* **2009**, *284*, 25889 -25899.

(122) Teruya, T.; Sasaki, H.; Fukazawa, H.; Suenaga, K. *Org. Lett.* **2009**, *11*, 5062-5065.

(123) Gao, X.; Liu, Y.; Kwong, S.; Xu, Z.; Ye, T. *Org. Lett.* **2010**, *12*, 3018-3021.

(124) Tan, L. T. *Phytochemistry* **2007**, *68*, 954-979.

(125) Roberts, P. J.; Der, C. J. *Oncogene* **2007**, *26*, 3291-3310.

(126) Boys, S. K.; PhD thesis; The University of Edinburgh **2011**.

(127) Wellbrock, C.; Karasarides, M.; Marais, R. *Nat. Rev. Mol. Cell. Biol.* **2004**, *5*, 875-885.

(128) Schreck, R.; Rapp, U. R. *Int. J. Cancer* **2006**, *119*, 2261-2271.

(129) Yoon, S.; Seger, R. *Growth Factors* **2006**, *24*, 21-44.

(130) Schulze, A.; Nicke, B.; Warne, P. H.; Tomlinson, S.; Downward, J. *Mol. Biol. Cell* **2004**, *15*, 3450-3463.

(131) Zuber, J.; Tchernitsa, O. I.; Hinzmann, B.; Schmitz, A.; Grips, M.; Hellriegel, M.; Sers, C.; Rosenthal, A.; Schafer, R. *Nat. Genet.* **2000**, *24*, 144-152.

(132) Wan, P. T.; Garnett, M. J.; Roe, S.; Lee, S.; Niculescu-Duvaz, D.; Good, V. M.; Project, C. G.; Jones, C.; Marshall, C. J.; Springer, C. J.; Barford, D.; Marais, R. *Cell* **2004**, *116*, 855-867.

(133) Murphy, A. C.; Mitova, M. I.; Blunt, J. W.; Munro, M. H. G. *J. Nat. Prod.* **2008**, *71*, 806-809.

(134) Pattenden, G.; Thom, S. M.; Jones, M. F. *Tetrahedron* **1993**, *49*, 2131-2138.

(135) Boger, D. L.; Yohannes, D. *J. Org. Chem.* **1988**, *53*, 487-499.

(136) Tung, R. D.; Rich, D. H. *J. Am. Chem. Soc.* **1985**, *107*, 4342-4343.

(137) De Luca, L.; Giacomelli, G.; Taddei, M. *J. Org. Chem.* **2001**, *66*, 2534-2537.

(138) Gardelli, C.; Nizi, E.; Muraglia, E.; Crescenzi, B.; Ferrara, M.; Orvieto, F.; Pace, P.; Pescatore, G.; Poma, M.; Rico Ferreira, M. D. R.; Scarpelli, R.; Homnick, C. F.; Ikemoto, N.; Alfieri, A.; Verdirame, M.; Bonelli, F.; Gonzalez Paz, O.; Taliani, M.; Monteagudo, E.; Pesci, S.; Laufer, R.; Felock, P.; Stillmock, K. A.; Hazuda, D.; Rowley, M.; Summa, V. *J. Med. Chem.* **2007**, *50*, 4953-4975.

(139) Li, W.; Yu, S.; Jin, M.; Xia, H.; Ma, D. *Tetrahedron Lett.* **2011**, *52*, 2124-2127.

(140) Deguest, G.; Bischoff, L.; Fruit, C.; Marsais, F. *Tetrahedron: Asymmetry* **2006**, *17*, 2120-2125.

(141) Charrier, J.; Duffy, J. E. S.; Hitchcock, P. B.; Young, D. W. *J. Chem. Soc., Perkin Trans. 1* **2001**, 2367-2371.

(142) Zlatopolskiy, B. D.; Loscha, K.; Alvermann, P.; Kozhushkov, S. I.; Nikolaev, S. V.; Zeeck, A.; de Meijere, A. *Chem. Eur. J.* **2004**, *10*, 4708-4717.

(143) Conrow, R.; Portoghese, P. S. *J. Org. Chem.* **1986**, *51*, 938-940.

(144) Bergeron, R. J.; Wiegand, J.; McManis, J. S.; McCosar, B. H.; Weimar, W. R.; Brittenham, G. M.; Smith, R. E. *J. Med. Chem.* **1999**, *42*, 2432-2440.

(145) Garfunkle, J.; Kimball, F. S.; Trzupek, J. D.; Takizawa, S.; Shimamura, H.; Tomishima, M.; Boger, D. L. *J. Am. Chem. Soc.* **2009**, *131*, 16036-16038.

(146) De Luca, L.; Giacomelli, G.; Porcheddu, A. *Org. Lett.* **2001**, *3*, 1519-1521.

(147) Singh, S.; Rao, S. J.; Pennington, M. W. *J. Org. Chem.* **2004**, *69*, 4551-4554.

(148) Harrigan, G. G.; Goetz, G. H.; Luesch, H.; Yang, S.; Likos, J. *J. Nat. Prod.* **2001**, *64*, 1133-1138.

(149) Okino, T.; Qi, S.; Matsuda, H.; Murakami, M.; Yamaguchi, K. *J. Nat. Prod.* **1997**, *60*, 158-161.

(150) Fujii, K.; Sivonen, K.; Adachi, K.; Noguchi, K.; Shimizu, Y.; Sano, H.; Hirayama, K.; Suzuki, M.; Harada, K. *Tetrahedron Lett.* **1997**, *38*, 5529-5532.

(151) Chen, C.; Lang, G.; Mitova, M. I.; Murphy, A. C.; Cole, A. L. J.; Din, L. B.; Blunt, J. W.; Munro, M. H. G. *J. Org. Chem.* **2006**, *71*, 7947-7951.

(152) Barlow, D. J.; Thornton, J. M. *J. Mol. Biol.* **1988**, *201*, 601-619.

(153) Holmgren, S. K.; Taylor, K. M.; Bretscher, L. E.; Raines, R. T. *Nature* **1998**, *392*, 666-667.

(154) Schlechtingen, G.; Zhang, L.; Maycock, A.; DeHaven, R. N.; Daubert, J. D.; Cassel, J.; Chung, N. N.; Schiller, P. W.; Goodman, M. *J. Med. Chem.* **2000**, *43*, 2698-2702.

(155) Ruchala, P.; Picur, B.; Lisowski, M.; Cierpicki, T.; Wieczorek, Z.; Siemion, I. *Biopolymers* **2003**, *70*, 497-511.

(156) Heindl, C.; Hübner, H.; Gmeiner, P. *Tetrahedron: Asymmetry* **2003**, *14*, 3153-3172.

(157) Heindl, C.; Hübner, H.; Gmeiner, P. *Tetrahedron: Asymmetry* **2003**, *14*, 3141-3152.

(158) Iwanami, S.; Takashima, M.; Hirata, Y.; Hasegawa, O.; Usuda, S. *J. Med. Chem.* **1981**, *24*, 1224-1230.

(159) Mishra, R. K.; Chiu, S.; Chiu, P.; Mishra, C. P. *Methods Finds Exp. Clin. Pharmacol.* **1983**, *5*, 203-233.

(160) Del Valle, J. R.; Goodman, M. *J. Org. Chem.* **2003**, *68*, 3923-3931.

(161) Aoyagi, Y.; Williams, R. M. *Tetrahedron* **1998**, *54*, 13045-13058.

(162) Rajeev, K. G.; Sanjayan, G. J.; Ganesh, K. N. *J. Org. Chem.* **1997**, *62*, 5169-5173.

(163) De Luca, L.; Giacomelli, G.; Porcheddu, A. *Org. Lett.* **2001**, *3*, 3041-3043.

(164) Del Valle, J. R.; Goodman, M. *Angew. Chem. Int. Ed.* **2002**, *41*, 1600-1602.

(165) Crabtree, R. H.; Felkin, H.; Morris, G. E. *J. Organomet. Chem.* **1977**, *141*, 205-215.

(166) Zhao, M.; Li, J.; Mano, E.; Song, Z.; Tschaen, D. M.; Grabowski, E. J. J.; Reider, P. J. *J. Org. Chem.* **1999**, *64*, 2564-2566.

(167) Brown, J. M.; Hall, S. A. *J. Organomet. Chem.* **1985**, *285*, 333-341.

(168) Chirgadze, N. L.; Schacht, A. L.; Smith, G. F.; Willey, M. R. *Eli Lilly and Co.* **1995**, U.S. Patent 9,523,608.

(169) Petasis, N. A.; Bzowej, E. I. *J. Am. Chem. Soc.* **1990**, *112*, 6392-6394.

(170) Marfey, P. *Carlsberg Res. Comm.* **1984**, *49*, 591-596.

(171) Fehr, C.; Farris, I. *Angew. Chem. Int. Ed.* **2006**, *45*, 6904-6907.

(172) Jew, S.; Park, H. *Chem. Commun.* **2009**, 7090.

(173) Hashimoto, T.; Maruoka, K. *Chem. Rev.* **2007**, *107*, 5656-5682.

(174) Hentges, S. G.; Sharpless, K. B. *J. Am. Chem. Soc.* **1980**, *102*, 4263-4265.

(175) Dolling, U. H.; Davis, P.; Grabowski, E. J. J. *J. Am. Chem. Soc.* **1984**, *106*, 446-447.

(176) Maruoka, K. *Chem. Record* **2010**, *10*, 254-259.

(177) O'Donnell, M. J.; Bennett, W. D.; Wu, S. *J. Am. Chem. Soc.* **1989**, *111*, 2353-2355.

(178) Lygo, B.; Wainwright, P. G. *Tetrahedron Lett.* **1997**, *38*, 8595-8598.

(179) Corey, E. J.; Xu, F.; Noe, M. C. *J. Am. Chem. Soc.* **1997**, *119*, 12414-12415.

(180) Jew, S.; Lee, Y.; Lee, J.; Kang, M. J.; Jeong, B.; Lee, J.; Yoo, M.; Kim, M.; Choi, S.; Ku, J.; Park, H. *Angew. Chem. Int. Ed.* **2004**, *43*, 2382-2385.

(181) Kolb, H. C.; VanNieuwenhze, M. S.; Sharpless, K. B. *Chem. Rev.* **1994**, *94*, 2483-2547.

(182) Jew, S.; Jeong, B.; Yoo, M.; Huh, H.; Park, H. *Chem. Commun.* **2001**, 1244-1245.

(183) Park, H.; Jeong, B.; Yoo, M.; Park, M.; Huh, H.; Jew, S. *Tetrahedron Lett.* **2001**, *42*, 4645-4648.

(184) Park, H.; Jeong, B.; Yoo, M.; Lee, J.; Park, M.; Lee, Y.; Kim, M.; Jew, S. *Angew. Chem. Int. Ed.* **2002**, *41*, 3036.

(185) Lee, J.; Jeong, B.; Ku, J.; Jew, S.; Park, H. *J. Org. Chem.* **2006**, *71*, 6690-6692.

(186) Jew, S.; Yoo, M.; Jeong, B.; Park, I. Y.; Park, H. *Org. Lett.* **2002**, *4*, 4245-4248.

(187) Jew, S.; Jeong, B.; Lee, J.; Yoo, M.; Lee, Y.; Park, B.; Kim, M. G.; Park, H. *J. Org. Chem.* **2003**, *68*, 4514-4516.

(188) Wang, X.; Yin, L.; Yang, T.; Wang, Y. *Tetrahedron: Asymmetry* **2007**, *18*, 108-114.

(189) Bozkurt, S.; Durmaz, M.; Yilmaz, M.; Sirit, A. *Tetrahedron: Asymmetry* **2008**, *19*, 618-623.

(190) Patel, P.; Huang, S.; Fisher, S.; Pirnik, D.; Aklonis, C.; Dean, L.; Meyers, E.; Fernandes, P.; Mayerl, F. *J. Antibiot.* **1995**, *48*, 997-1003.

(191) Butcher, R. A.; Schroeder, F. C.; Fischbach, M. A.; Straight, P. D.; Kolter, R.; Walsh, C. T.; Clardy, J. *Proc. Nat. Acad. Sci.* **2007**, *104*, 1506 -1509.

(192) *J. Chem. Soc., Perkin Trans. 1* **2002**, 69-79.

(193) Huang, Y.; Iwama, T.; Rawal, V. H. *J. Am. Chem. Soc.* **2000**, *122*, 7843-7844.

(194) Friedrich, A.; Jainta, M.; Nising, C. F.; Bräse, S. *Synlett* **2008**, *4*, 589-591.

(195) Oppolzer, W.; Bieber, L.; Francotte, E. *Tetrahedron Lett.* **1979**, *20*, 981-984.

(196) Oppolzer, W.; Fröstl, W. *Helv. Chim. Acta* **1975**, *58*, 590-593.

(197) Oppolzer, W.; Bieber, L.; Francotte, E. *Tetrahedron Letters* **1979**, *20*, 4537-4540.

(198) Oppolzer, W.; Fröstl, W. *Helv. Chim. Acta* **1975**, *58*, 587-589.

(199) Nguyen, S. T.; Johnson, L. K.; Grubbs, R. H.; Ziller, J. W. *J. Am. Chem. Soc.* **1992**, *114*, 3974-3975.

(200) Conrad, J.; Fogg, D. *Curr. Org. Chem* **2006**, *10*, 185-202.

(201) Schwab, P.; France, M. B.; Ziller, J. W.; Grubbs, R. H. *Angew. Chem. Int. Ed. Engl.* **1995**, *34*, 2039-2041.

(202) Schwab, P.; Grubbs, R. H.; Ziller, J. W. *J. Am. Chem. Soc.* **1996**, *118*, 100-110.

(203) Schrock, R. R. *Tetrahedron* **1999**, *55*, 8141-8153.

(204) Kingsbury, J. S.; Harrity, J. P. A.; Bonitatebus, P. J.; Hoveyda, A. H. *J. Am. Chem. Soc.* **1999**, *121*, 791-799.

(205) Garber, S. B.; Kingsbury, J. S.; Gray, B. L.; Hoveyda, A. H. *J. Am. Chem. Soc.* **2000**, *122*, 8168-8179.

(206) Malcolmson, S. J.; Meek, S. J.; Sattely, E. S.; Schrock, R. R.; Hoveyda, A. H. *Nature* **2008**, *456*, 933-937.

(207) Grubbs, R. H.; Miller, S. J.; Fu, G. C. *Acc. Chem. Res.* **1995**, *28*, 446-452.

(208) Yee, N. K.; Farina, V.; Houpis, I. N.; Haddad, N.; Frutos, R. P.; Gallou, F.; Wang, X.; Wei, X.; Simpson, R. D.; Feng, X.; Fuchs, V.; Xu, Y.; Tan, J.; Zhang, L.; Xu, J.; Smith-Keenan, L. L.; Vitous, J.; Ridges, M. D.; Spinelli, E. M.; Johnson, M.; Donsbach, K.; Nicola, T.; Brenner, M.; Winter, E.; Kreye, P.; Samstag, W. *J. Org. Chem.* **2006**, *71*, 7133-7145.

(209) Badjić, J. D.; Cantrill, S. J.; Grubbs, R. H.; Guidry, E. N.; Orenes, R.; Stoddart, J. F. *Angew. Chem. Int. Ed.* **2004**, *43*, 3273-3278.

(210) Waldmann, H. *Nat. Chem. Biol.* **2009**, *5*, 76-77.

(211) Jakubec, P.; Cockfield, D. M.; Dixon, D. J. *J. Am. Chem. Soc.* **2009**, *131*, 16632-16633.

(212) Kobayashi, J.; Watanabe, D.; Kawasaki, N.; Tsuda, M. *J. Org. Chem.* **1997**, *62*, 9236-9239.

(213) Aïssa, C. *J. Org. Chem.* **2006**, *71*, 360-363.

(214) Hynes, P. S.; Stupple, P. A.; Dixon, D. J. *Org. Lett.* **2008**, *10*, 1389-1391.

(215) Martin, D. B. C.; Vanderwal, C. D. *Angew. Chem. Int. Ed.* **2010**, NA-NA.

(216) Kinderman, S. S.; van Maarseveen, J. H.; Schoemaker, H. E.; Hiemstra, H.; Rutjes, F. P. J. T. *Org. Lett.* **2001**, *3*, 2045-2048.

(217) Wang, H.; Goodman, S. N.; Dai, Q.; Stockdale, G. W.; Clark, W. M. *Org. Process Res. Dev.* **2008**, *12*, 226-234.

(218) Kuhn, K. M.; Champagne, T. M.; Hong, S. H.; Wei, W.; Nickel, A.; Lee, C. W.; Virgil, S. C.; Grubbs, R. H.; Pederson, R. L. *Org. Lett.* **2010**, *12*, 984-987.

(219) Toumi, M.; Couty, F.; Evano, G. *J. Org. Chem.* **2008**, *73*, 1270-1281.

(220) Moïse, J.; Arseniyadis, S.; Cossy, J. *Org. Lett.* **2007**, *9*, 1695-1698.

(221) Hoye, T. R.; Jeffrey, C. S.; Tennakoon, M. A.; Wang, J.; Zhao, H. *J. Am. Chem. Soc.* **2004**, *126*, 10210-10211.

(222) Krompiec, S.; Pigulla, M.; Krompiec, M.; Baj, S.; Mrowiec-Bialon, J.; Kasperczyk, J. *Tetrahedron Lett.* **2004**, *45*, 5257-5261.

(223) Blaser, H. *Top. Catal.* **2010**, *53*, 997-1001.

(224) Baldwin, J. E.; Fryer, A. M.; Spyvee, M. R.; Whitehead, R. C.; Wood, M. E. *Tetrahedron* **1997**, *53*, 5273-5290.

(225) Kondo, T.; Sugimoto, I.; Nekado, T.; Ochi, K.; Ohtani, T.; Tajima, Y.; Yamamoto, S.; Kawabata, K.; Nakai, H.; Toda, M. *Bioorg. Med. Chem.* **2007**, *15*, 2715-2735.

(226) Kondo, T.; Nekado, T.; Sugimoto, I.; Ochi, K.; Takai, S.; Kinoshita, A.; Hatayama, A.; Yamamoto, S.; Kawabata, K.; Nakai, H.; Toda, M. *Bioorg. Med. Chem.* **2008**, *16*, 190-208.

(227) Wang, C.; Liang, G.; Xue, Z.; Gao, F. *J. Am. Chem. Soc.* **2008**, *130*, 17250-17251.

(228) Matsuhashi, H.; Asai, S.; Hirabayashi, K.; Hatanaka, Y.; Mori, A.; Hiyama, T. *Bull. Chem. Soc. Jpn.* **1997**, *70*, 1943-1952.

(229) Blaauw, R.; Kingma, I. E.; Laan, J. H.; van der Baan, J. L.; Balt, S.; de Bolster, M. W. G.; Klumpp, G. W.; Smeets, W. J. J.; Spek, A. L. *J. Chem. Soc., Perkin Trans. 1* **2000**,

1199-1210.

(230) Ferroud, D.; Genet, J. P.; Kiolle, R. *Tetrahedron Lett.* **1986**, *27*, 23-26.

(231) Bird, J.; De Mello, R. C.; Harper, G. P.; Hunter, D. J.; Karran, E. H.; Markwell, R. E.; Miles-Williams, A. J.; Rahman, S. S.; Ward, R. W. *J. Med. Chem.* **1994**, *37*, 158-169.

(232) Cossey, K. N.; Funk, R. L. *J. Am. Chem. Soc.* **2004**, *126*, 12216-12217.

(233) Bach, T.; Schroder, J. *J. Org. Chem.* **1999**, *64*, 1265-1273.

(234) Pintér, Á.; Haberhauer, G. *Eur. J. Org. Chem.* **2008**, *2008*, 2375-2387.

(235) Nakoji, M.; Kanayama, T.; Okino, T.; Takemoto, Y. *J. Org. Chem.* **2002**, *67*, 7418-7423.

(236) Ohshima, T.; Gnanadesikan, V.; Shibuguchi, T.; Fukuta, Y.; Nemoto, T.; Shibasaki, M. *J. Am. Chem. Soc.* **2003**, *125*, 11206-11207.

(237) Wagner, J.; Martin Cabrejas, L. M.; Grossmith, C. E.; Papageorgiou, C.; Senia, F.; Wagner, D.; France, J.; Nolan, S. P. *J. Org. Chem.* **2000**, *65*, 9255-9260.

(238) Denmark, S. E.; Yang, S. *J. Am. Chem. Soc.* **2002**, *124*, 2102-2103.

(239) Jin, J.; Chen, Y.; Li, Y.; Wu, J.; Dai, W. *Org. Lett.* **2007**, *9*, 2585-2588.

(240) Garber, S. B.; Kingsbury, J. S.; Gray, B. L.; Hoveyda, A. H. *J. Am. Chem. Soc.* **2000**, *122*, 8168-8179.

(241) Krämer, K.; Kazmaier, U. *J. Org. Chem.* **2006**, *71*, 8950-8953.

(242) Glorius, F.; Neuburger, M.; Pfaltz, A. *Helv. Chim. Acta* **2001**, *84*, 3178-3196.

(243) Evans, P. A.; Kennedy, L. J. *J. Am. Chem. Soc.* **2001**, *123*, 1234-1235.

(244) Bondzic, B. P.; Farwick, A.; Liebich, J.; Eilbracht, P. *Org. Biomol. Chem.* **2008**, *6*, 3723.

(245) Lloyd-Jones, G. C.; Pfaltz, A. *Angew. Chem. Int. Ed. Engl.* **1995**, *34*, 462-464.

(246) Genet, J. -.; Juge, S.; Achi, S.; Mallart, S.; Ruiz Montes, J.; Levif, G. *Tetrahedron* **1988**, *44*, 5263-5275.

(247) Nakoji, M.; Kanayama, T.; Okino, T.; Takemoto, Y. *J. Org. Chem.* **2002**, *67*, 7418-7423.

(248) Andrus, M. B.; Christiansen, M. A.; Hicken, E. J.; Gainer, M. J.; Bedke, D. K.; Harper, K. C.; Mikkelson, S. R.; Dodson, D. S.; Harris, D. T. *Org. Lett.* **2007**, *9*, 4865-4868.

(249) Hoye, T. R.; Jeffrey, C. S.; Tennakoon, M. A.; Wang, J.; Zhao, H. *J. Am. Chem. Soc.*

**2004**, *126*, 10210-10211.

(250) Wallace, D. J. *Angew. Chem. Int. Ed.* **2005**, *44*, 1912-1915.

(251) Schlummer, B.; Scholz, U. *Adv. Synt. Catal.* **2004**, *346*, 1599-1626.

(252) Mayer, T.; Maier, M. E. *Eur. J. Org. Chem.* **2007**, *2007*, 4711-4720.

(253) Zhao, X. Z.; Semenova, E. A.; Liao, C.; Nicklaus, M.; Pommier, Y.; Burke Jr., T. R. *Bioorg. Med. Chem.* **2006**, *14*, 7816-7825.

(254) Cooper, R. J.; Camp, P. J.; Gordon, R. J.; Henderson, D. K.; Henry, D. C. R.; McNab, H.; De Silva, S. S.; Tackley, D.; Tasker, P. A.; Wight, P. *Dalton Trans.* **2006**, 2785.

(255) Ohkanda, J.; Katoh, A. *Tetrahedron* **1995**, *51*, 12995-13002.

(256) Bräse, S.; Gil, C.; Knepper, K.; Zimmermann, V. *Angew. Chem. Int. Ed.* **2005**, *44*, 5188-5240.

(257) O'Donnell, M. J.; Polt, R. L. *J. Org. Chem.* **1982**, *47*, 2663-2666.

(258) Tsuji, J.; Shimizu, I.; Minami, I.; Ohashi, Y.; Sugiura, T.; Takahashi, K. *J. Org. Chem.* **1985**, *50*, 1523-1529.

(259) Fiedziuszko, J.; Suszko, J. *Acad. Pol. Sci., Ser. Sci. Chim.* **1934**, 413-420.

(260) Katz, T. J.; Slusarek, W. *J. Am. Chem. Soc.* **1979**, *101*, 4259-4267.